CHARACTERISATION OF SPRAY-DRIED TREHALOSE/ALKALINE PHOSPHATASE FORMULATIONS

Amina Khalid
MSc.Pharm.

Submitted for the degree of Doctor of Philosophy
The School of Pharmacy, University of London

September 2006

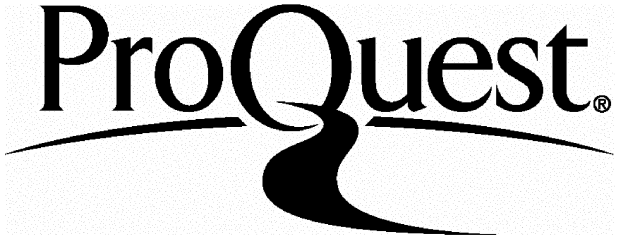

Plagiarism Statement

This thesis describes research conducted in the School of Pharmacy, University of London, between 2002 and 2006 under the supervision of Prof. S. Brocchini and Prof. G. Buckton. I certify that the research described is original and that any parts of the work that have been conducted by collaboration are clearly indicated. I also certify that I have written all the text written herein and have clearly indicated by suitable citation any part of this dissertation that has already appeared in publication.

Signature

3/10-06

Date

ABSTRACT

Despite the advances in biotechnology the formulation of protein based medicine is limited. This is because proteins are not stable molecules. Generally protein formulations are produced from freeze drying but solid formulations can also be obtained through spray drying. These processes can have detrimental effects on protein stability. Disaccharides, particularly trehalose, are common excipients that are examined in protein formulations, as they may act as protectants for proteins in the solid state. The aim of this thesis was to prepare spray-dried trehalose/alkaline phosphatase particles and investigate the properties of trehalose in the presence of a protein. Furthermore, the influences of acetone and surfactants on the properties of trehalose are also examined.

The tendency of trehalose to convert into different physical forms was studied by differential scanning calorimetry (DSC), as it is believed to be a key property in its ability to stabilise proteins. Transformation pathways were determined depending on heating rates and sample size and indicated that these could occur concurrently at varying degrees. The spray dryer, SDMicro^{TM} was commissioned and evaluated by processing amorphous trehalose. Amorphous trehalose samples were studied with regard to morphology and water sorption behaviour. The NIR data collected during the water sorption studies were compared to the different physical forms of trehalose. It could be concluded that regardless of the spray drying process, all amorphous trehalose batches crystallised to the dihydrate form when exposed to increased humidity. The NIR spectra also revealed that some batches proceeded to the dihydrate form via the anhydrous forms and confirmed the finding of the DSC study.

Spray-dried samples of trehalose were prepared with alkaline phosphatase and surfactants. These formulations showed significant differences in particle morphology as a function of protein concentration, acetone and surfactants. The stability of the samples was investigated by exposure to increased humidity and NIR spectra were also recorded to study the changes in trehalose during storage. The crystallisation process of trehalose in the spray-dried samples could be observed but no band could be assigned for protein degradation. This was due to the low protein content in the formulations. The degradation was followed by activity assays. The morphology of the spray-dried AP particles could be correlated to the surface properties. The surface properties of these particles were studied with regards to their morphology, glass transitions and surface energies. The AP particles prepared with surfactant, showed correlation between protein degradation and the crystallisation of trehalose.

He has taught you, which you knew not (before)

(Quran verse 2:239)

For Aimal, Muizz & Arzu with all my love

Acknowledgements

I would like to acknowledge my supervisors, Professor Steve Brocchini and Professor Graham Buckton for their support and optimism. I would also like to thank the EPSRC for funding this work.

I would like to thank David McCarthy for the SEM images of my samples, Dr. Sune Andernson for his help with the SDMicro™ and Dr. Nicola Wilson for her help and expertise with the NIR data. Thanks are also due to Keith Barnes who was always willing to help and was indispensable when things broke down. A special thanks to Steve for his continuous help and enthusiasm throughout this project, especially during the tough times.

The PhD was hard but would have been near impossible without the support of my colleagues in SOP. I would like to acknowledge Dima, Jaz, Abi, Emma, John, Rita, Ameet, Matt, Ray, Antony, Elisa, Sibu, Stefan, Brij, Ash, Ketan, Bal, Viraj, Kshipra, Pav, Suzie, & Sukh for their help, support and encouragement. The daily chats, tea breaks, and lunch breaks were a welcomed distraction from the endless lab work. I would also like to thank my friends from "college hall", the girls (Fi, Deepti, Maria, Sangeeta, Asma & Ambuja) and P.J., for all of the wonderful memories and for keeping me sane. During this PhD, I have met some wonderful people and without their friendship the four years would not have been as memorable. I would like to thank you all for your continued love and support.

I would like to thank Bal for his friendship and for being there each time I had to move (every year!!). I would also like to thank Ambuja for her wonderful madness and support throughout these four years. I would also like to thank Sukh for his friendship, encouragement and optimism when it was most needed.

The memories of the long, late night walks in Paris, the pumpkin and pancakes in Barcelona, the constant banter in the study room, the never ending chats in college hall and the periodic nervous breakdowns cured by food, will always stay with me. To all my friends, I just need to say that I appreciate your friendships and love you all.

Last but not least I would like to thank my family, Khalid, Salma, Fawad, Jawad, Aisha and Nadiya, for their continued love, support and understanding. To Mama & Papa, all my accomplishments in life are due to your love and support. I would like to acknowledge the three most wonderful "little people", Aimal, Muizz and Arzu, who have always managed to make me happy no matter how difficult things were. I would like to take this opportunity to express my love for you all.

TABLE OF CONTENTS

LIST OF FIGURES

CHAPTER 1

CHAPTER 2

CHAPTER 3

CHAPTER 4

CHAPTER 5

CHAPTER 6

LIST OF TABLES

CHAPTER 1

CHAPTER 2

CHAPTER 3

CHAPTER 4

CHAPTER 5

CHAPTER 6

LIST OF ABBREVIATIONS

A	Absorbance
a	Surface area of one probe molecule
AIDS	Acquired immune deficiency syndrome
AP	Alkaline phosphate
BCA	Bicinchoninic acid
BSA	Bovine serum albumin
C	Adsorption energy constant
ca.	Approximately
D	Denatured form of protein
DSC	Differential scanning calorimetry
DVS	Dynamic vapour sorption
F	Flow rate
FID	Flame ionisation detector
FTIR	Fourier transform infrared
ΔG	Change in Gibbs free energy
ΔG_A^0	Free energy of adsorption
ΔG_A^{SP}	Specific free energy of adsorption
H	Enthalpy
h	Hours
HPLC	High performance liquid chromatography
IGC	Inverse gas chromatography
J	Compression factor
K	Kelvin
k	Equilibrium constant
l	Path length
LDH	Lactate dehydrogenase
MG	Molten globule
N	Avogardo's constant
NMR	Nuclear magnetic resonance
NIRS	Near infrared spectroscopy
NEB	Nonenzymatic browning

P	Sample pressure
Pa	Pascal
PCA	Principal component analysis
PEG	Polyethylene glycol
pH	$-\log [H^+]$
PhD	Doctorate of philosophy
P_i	Inlet pressure
pKa	-log [Ka]
PMMA	Poly(methyl methacrylate)
PNPP	Para-nitrophenyl phosphate
P_o	Atmospheric pressure
P_{sg}	Adsorbate vapour pressure in the gaseous standard state
PVP	Polyvinyl pyrrolidone
P_0	Saturation vapour pressure of adsorbate
R	Gas constant
RH	Relative humidity
s	Seconds
Sa	Surface area of adsorbent
SD	Standard deviation
SDS	Sodium dodecyl sulfate
SEM	Scanning electron microscopy
SNV	Standard normal variance
T	Temperature of column
T_{am}	Amorphous Trehalose
TCD	Thermal conductivity detector
T_{DB}	Dry bulb temperature
T_{DP}	Dew point temperature
Tg	Glass transition temperature
TGA	Thermogravimetric analysis
T_K	Kauzmann temperature
Tm	Melting temperature
t_n	Net retention time
t_o	Delay time
t_r	Retention time

t_α	α-Trehalose
t_β	β-Trehalose
t_γ	γ-Trehalose
t_h	Trehalose dihydrate
t_κ	κ-Trehalose
T_{WB}	Wet bulb temperature
U	Unfolded form of protein
V	Volume
Vads	Volume adsorbed
Vm	Monolayer volume
V_N	Retention volume
w	Weight of adsorbent in column
W_a	Work of adhesion
XRPD	X-Ray powder diffraction
π	Standard surface pressure
γ^D_S	Solid surface energy
γ^D_L	Surface energy of the non-polar liquid
ε	Molar absorption coefficient

CHAPTER 1

Introduction

1. INTRODUCTION

1.1 NEW TECHNOLOGIES AND OLD PROBLEMS

In recent years, there have been a lot of innovations arising from biotechnology and related recombinant techniques, which have led to an increase in the proposed use of macromolecular drugs inducing protein pharmaceuticals. The availability of therapeutic proteins has been increasing due to advances in protein purification from a number of different sources. In comparison to other macromolecular drugs, protein pharmaceuticals have high specificity and activity at relatively low concentrations. These features have made protein pharmaceuticals indispensable in combating human diseases. In a recent survey 324 biotechnological medicines were listed, which are in either human clinical trials or under review by regulatory agencies. These medicines cover over 150 diseases including cancer, infectious diseases, autoimmune diseases, AIDS/HIV and related diseases. A substantial number of these substances are proteins (Holmer, 2004).

The basic challenge associated with protein pharmaceuticals is the physical and the chemical stability of proteins. Since proteins degrade in solution, protein formulations commonly produced are solid forms that are reconstituted into solutions by adding the required diluents prior to administration. These solid formulations are often obtained through processes such as freeze drying or spray drying where proteins are subjected to conditions that can have a detrimental effect on protein stability, such as pH, temperature, hydration/dehydration, humidity, etc. (Wang, 1999). Although conventional formulations have the same focus, the unique structure of protein molecules makes protein formulations more complex and challenging. Hence, the pharmaceutical scientist is faced with a significant formulation challenge regarding proteins as products with optimal therapeutic effects.

In order to understand the mechanisms of protein stability attention has been drawn to nature where anhydrobiotic organisms are known to show desiccation tolerance. The common factor in these organisms are the presence of disaccharides (Crowe et al., 1998; Crowe, 2002). The most common disaccharides to be found in these organisms are

sucrose and trehalose. In general, sucrose seems to be favoured by seeds and higher plants, while lower plants and small animals and microorganisms utilise trehalose. The complete mechanism by which disaccharides can produce stabilising effects has not yet been established but a few plausible theories exist.

These theories and the subject are still under debate and are the focus of this PhD thesis. This chapter aims to provide a general overview of the issues surrounding protein stability with disaccharides, specifically with trehalose as a focal point, which will be further investigated in chapters 3-6.

1.2 ANHYDROBIOSIS

Certain organisms are found in nature that exhibit a form of latency in which all or some of the metabolic processes come to a standstill due to extreme conditions (cold, heat or drought). These organisms rapidly resume normal activity when more favourable conditions are introduced. Such extreme latency has been referred to as "anabiosis" by Preyer in 1891 and as "abiosis" by Schmidt in 1948 (Crowe, 1971). Later, the term "cryptobiosis" was introduced by Keilin in 1959 (Crowe, 1971). Anhydrobiosis was a further development of all of the terms mentioned above and has been investigated extensively by Crowe and colleagues. According to these researchers, anhydrobiotic organisms are capable of surviving with as little as 0.1 % water content in their tissue. When water is introduced to these dry dormant organisms, they swell and resume active life. Cysts of brine shrimp, *Artemia*, and several nematodes and some fungal spores demonstrate these anhydrobiotic qualities (Crowe et al., 1992). Other examples include the "resurrection plants", *Craterostigma plantagineum* and *Selaginella lepidophylle*, which can remain dry for up to fifty years, during which no metabolic processes are detected. However upon rehydration their metabolic activity restarts and they revert rapidly into the state they were in prior to dehydration (Roser, 1991). A common feature in all of these organisms is an increased intracellular concentration of disaccharides, particularly trehalose (Crowe et al., 1992).

The presence of sugars and sugar alcohols in these anhydrobiotic organisms has been known for quite some time. The efficacy order for the biostabilising properties of sugars is reported to be trehalose followed by lactose, maltose, sucrose and then glucose in a

decreasing order (Crowe et al., 1984; Mouradian et al., 1984). Several studies have investigated the plausible mechanisms for the biostabilising qualities of trehalose and other sugars. These sugars become amorphous under conditions leading to dehydration, which was considered fundamental to the mechanism of anhydrobiosis (Crowe et al., 1992). It has been suggested that the glass forming characteristics were directly related to the biostabilising activity (Green et al., 1989). Green and Angell tested the glass transition (Tg) for some of the carbohydrates and the order of the Tg was the efficacy order of the carbohydrates as seen by other researchers. Trehalose proved to have the highest Tg followed by maltose, sucrose and glucose. Other groups have concurred with these findings (Crowe et al., 1992).

The abundance of trehalose in nature, specifically in the anhydrobiotic organisms, has caused a particular interest in this carbohydrate and its biostabilising mechanisms. Despite the advances in biotechnology and wide availability of potentially therapeutic proteins, their formulation is limited due to stability problems and hence trehalose has gained particular interest in the pharmaceutical industry. The mechanisms behind protein stability during and after processing are discussed in this chapter.

1.3 CRYSTALLINE FORM

The crystalline state involves a three-dimensional periodic arrangement of units (atoms, ions, molecules) in a spatial lattice. Crystalline solids have well-defined thermodynamic properties (e.g. melting temperature, vapour pressure, solubility) and a lower free energy than observed in the amorphous state. The lower free energy results in reduced molecular motion within the crystal lattice and hence the crystalline materials are physically and chemically more stable than their amorphous counterparts (Hancock et al., 1997).

Many drugs can exist in more than one crystalline form and organic molecules frequently crystallise to different forms depending on the crystallisation or precipitation conditions to which they are exposed. This phenomenon is known as "polymorphism", whereby the same compound can exist in two or more crystalline forms. These forms have different arrangements and/or conformations of the molecules in the crystal lattice and thus have different physical properties. This results in different lattice energies,

which again leads to different melting points. The impact of polymorphism extends to solubility, dissolution rate, bioavailability and compression properties. The most stable polymorph has the lowest free energy and thus the highest melting point and slowest dissolution rate (Grant, 1999; Vippagunta et al., 2001). Polymorphs can exist as either enantiotropes or monotropes. In an enantiotropic system, the two polymorphs are stable (i.e. have the lower free energy content and solubility) at different temperature ranges and are therefore reversible. In a monotropic system, only one polymorph is stable at all temperatures below the melting point, making the process irreversible (Grant, 1999).

Solvates are known as pseudopolymorphs and are crystalline solid adducts containing solvent molecules within the crystal structure in either stoichiometric or non-stoichiometric proportions. This gives rise to unique differences in the physical and pharmaceutical properties of drugs. If the solvate within the crystal structure is water, then the solvate is termed a hydrate (Vippagunta et al., 2001).

The differences in the physical properties of the various solids have a great impact on the processing of these materials into products, which can affect drug activity among other things (Vippagunta et al., 2001). Hence, it is important to study the polymorphic qualities of the substances before processing, which is also the focus of chapter 3.

1.4 AMORPHOUS FORM

The amorphous state does not exhibit the three-dimensional long-range order associated with the crystalline state. As a result, the position of molecules relative to one another is random and is often compared to the liquid state. Amorphous solids do display short-range order over a few molecular dimensions but are chemically and physically less stable than their corresponding crystalline state. Due to the increased internal energy and molecular motion of the amorphous solids they have better dissolution properties and can retain some free water within the less ordered structure (Hancock et al., 1997; Yu, 2001). During development of a product, the pharmaceutical processes can influence the crystalline state of the final dosage form. This could alter the desired effects of the end product and also lead to variations in batches and properties. The amorphous character can be induced in a pharmaceutical system in the following ways (Hancock et al., 1997):

- Condensation from the vapour state.
- Supercooling of a liquid below the melt.
- Mechanical activation of a crystalline material (e.g. milling, grinding, micronisation).
- Rapid precipitation from solution (e.g. freeze drying and spray drying).

Processes such as freeze drying, spray drying, granulation and anything else involving prolonged exposure to water vapour from the atmosphere can chemically and physically alter the properties of a solid state. Water has a greater impact on amorphous solids than on crystalline solids (assuming there is no hydrate formation), as amorphous solids dissolve more readily. Water uptake by crystalline materials is termed "adsorption" and for amorphous materials is termed "absorption", while sorption is used as a general term referring to both adsorption and absorption. Water exerts its effects on crystalline solids via adsorption of the monolayers, which is limited by the available surface area. However the uptake of water in amorphous solids is greatly determined by the total mass of the solids (Hancock et al., 1998).

Amorphous materials have been of pharmaceutical interest as they show better dissolution properties over their respective counterparts (Hancock et al., 2000). The amorphous or glassy state has been a subject of interest due to its ability to stabilise proteins and peptides in the pharmaceutical industry, where the drying of proteins is required for the necessary shelf life of the product (Franks et al., 1991).

1.5 GLASS TRANSITION TEMPERATURE

The essential differences between the formation of amorphous and crystalline systems are described by various researchers and can be illustrated by Figure 1.1 (Craig et al., 1999; Hancock et al., 1997). When a liquid is "cooled" rather than "supercooled", crystallisation occurs at the melting temperature (Tm). During cooling the molecules within the liquid state have adequate time to evolve into an ordered lattice. This exothermic crystallisation leads to a dramatic reduction in volume (V) due to contraction and simultaneously decreases the enthalpy (H). The material reduces the volume and enthalpy at a slower rate when cooled further.

Conversely, when a liquid is "supercooled" (rapid cooling rate) below the melting temperature, no discontinuity in volume or enthalpy is seen and a "supercooled" liquid is formed. During this process the molecules do not have sufficient time to orientate into a lattice. This amorphous state is also known as the "rubbery state" and can be characterised by a molecular mobility of less than 100 s, and a viscosity between 10^{-3}-10^{12} Pa·s. Both these properties are highly dependent on the temperature. Upon further cooling a change in the slope is seen at the glass transition temperature (Tg). Here the molecular mobility is so slow that it may be termed as fixed in a glassy state and is thermodynamically unstable. The viscosity is usually greater than 10^{12} Pa·s and any further reduction in temperature has only a small effect on the structure (Angell, 1995).

The glass transition can thus be seen as a thermodynamic requirement for a "supercooled" liquid as without this transition the amorphous material could attain a lower enthalpy than the crystalline state at some critical temperature. This critical temperature is known as the Kauzmann temperature (T_K) and is thought to represent the lower limit of Tg, where the entropy of the system reaches zero. T_K is thought to generally occur 20 K below Tg (Angell, 1995; Hancock et al., 1997). When water is dissolved in an amorphous solid it can act as a "plasticiser". This is due to the very low Tg of water (- 135 °C), which lowers the overall Tg of the system (Crowe et al., 1996). This leads to increased intermolecular space (free volume) of the solid by reduction of the hydrogen bonding between adjoining molecules with a corresponding reduction in the glass transition temperature. Hence, the local viscosity is decreased and simultaneously the mobility is increased. The amorphous material is in a "glassy state" below the Tg but above the Tg the molecules are free to move around (rubbery state). Hence, crystallisation occurs after the material undergoes structural collapse if the experimental temperature is below the Tg (Franks et al., 1991; Hancock et al., 2001).

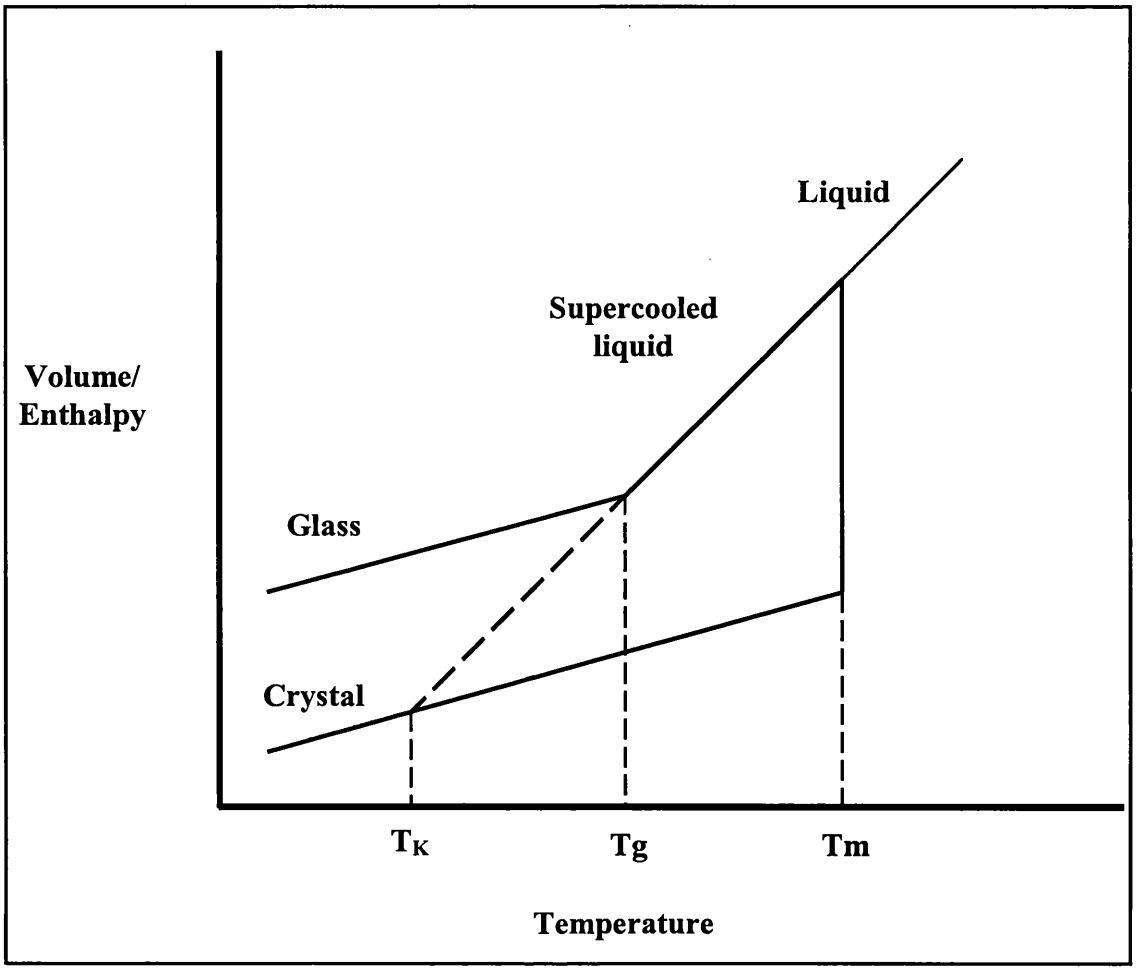

Figure 1.1. *Schematic representation of the variation of volume/enthalpy with temperature (Hancock et al., 1997).*

1.5.1 PHARMACEUTICALLY ADVANTAGEOUS PROPERTIES OF AMORPHOUS MATERIAL

Amorphous substances are generally kept under their Tg value in order to enhance stability. As described in the previous section, below the Tg value the molecular mobility of the system is decreased, which prevents destabilisation. However there is evidence of molecular mobility below the Tg (Angell, 1995). Streefland and colleagues investigated the chemical reactivity of water soluble glasses and concluded that the storage of therapeutic agents in glassy matrix below Tg did not confer indefinite stability (Duddu et al., 1997; Streefland et al., 1998). This was highly influenced by the stabilising properties of the individual excipients.

Yoshioka and Hancock have studied the molecular mobility of amorphous substances below their Tg value (Hancock et al., 1995; Yoshioka et al., 1994; Yoshioka et al., 1995). They concluded that the stability of the amorphous substances required a storage temperature at least 50 K below the Tg value of each substance. The studies conducted, included three commercially used compounds in the pharmaceutical industry, indomethacin, polyvinyl pyrrolidone (PVP) and sucrose. All three compounds were stored below their known Tg values at various temperatures and for various periods of time. Similar studies have been conducted using sucrose and trehalose (Duddu et al., 1997; Elamin et al., 1995). The studies concluded that the storage temperatures far below the Tg value of the substances provided negligible molecular motion over the product shelf life.

Amorphous materials have certain properties that can be of advantage in drug formulation (e.g. dissolution properties). The difference in physical properties of an amorphous material to its crystalline counterpart is due to the high-energy state and the disordered nature. Hence, thermodynamically the stable crystalline form is favoured and the amorphous form will always try to revert to this state (Hancock et al., 1997). Many of the advantages and disadvantages of this system are based on this concept. In the pharmaceutical industry amorphous materials are produced regularly, either deliberately or as a side effect of the processes used for powder production (spray drying, freeze-drying, milling, grinding etc.). These processes can produce amorphous regions in otherwise crystalline samples, which tend to be on the surface of the material, causing interaction with other components in the formulation. These can have detrimental effects on the final product. Hence the detection and quantification of the amorphous content has been the subject of much interest in the pharmaceutical industry and a number of different techniques have been evolved in order to investigate this phenomena (Al Hadithi et al., 2004; Buckton et al., 1995; Buckton et al., 1998; Hogan et al., 2000).

Spray drying is commonly used to produce amorphous powder. Figure 1.2 shows how amorphous materials are generally obtained via spray drying, regardless of the spray dryer used. It might for example be beneficial to deliver a sparingly soluble drug as amorphous, as it will have a lower energetic barrier to overcome when entering a solution than the crystalline counterpart. This can result in increased solubility,

dissolution rate and bioavailability (Yu, 2001). However, the disadvantages are the increased chemical and physical instabilities due to an increase in moisture uptake (Yu, 2001). It has also been shown that amorphous sugars provide stability to proteins in spray-dried formulations (Hatley et al., 1999; Hinrichs et al., 2001).

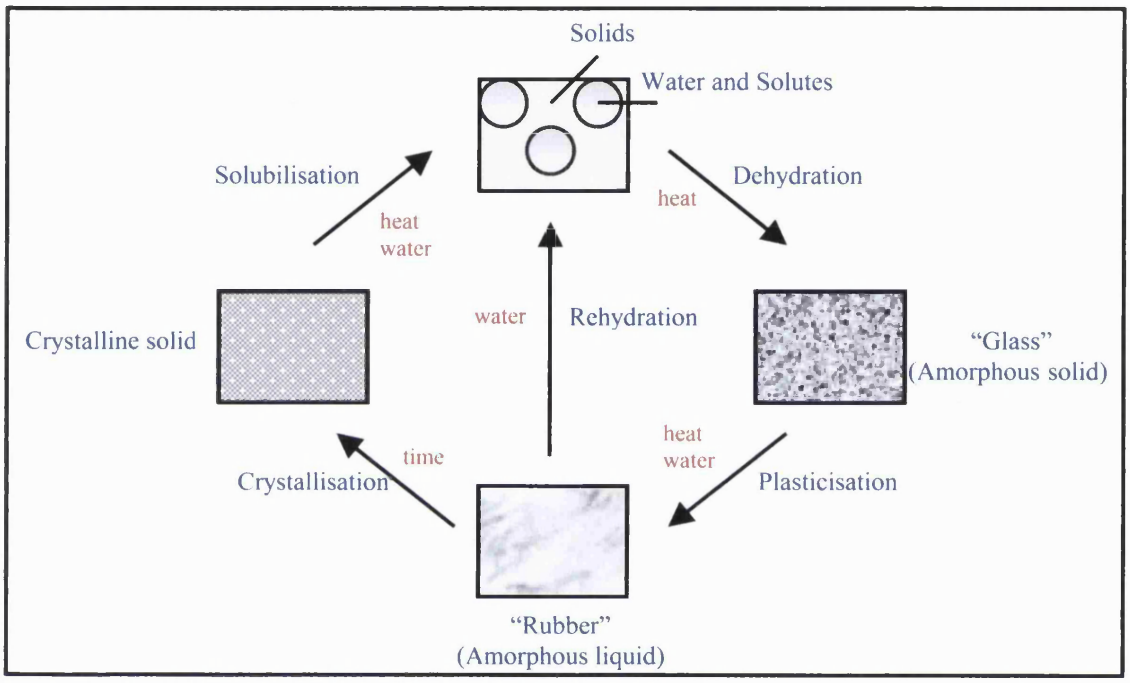

Figure 1.2. *Representation of amorphous formation during dehydration caused by spray drying. Depicting the relationship between equilibrium (solution, crystalline solid) and nonequilirium (amorphous solid and liquid state) (Roos, 2002).*

The amorphous state of sugars is believed to play an important role in the stabilisation of macromolecules. The amorphous carbohydrates have the ability to hold proteins rigid in their glassy matrix (vitrification theory), thus retaining their tertiary structure (Crowe et al., 1998). Furthermore, upon drying, carbohydrates are capable of replacing the hydrogen bonds (water replacement theory), which are present in solution between proteins and water, yet again helping to protect the tertiary structure (Crowe et al., 1993a; Crowe et al., 1993b). Aldous and colleagues have suggested that the ability of some carbohydrates (e.g. trehalose) to stabilise protein formulations during the drying process is due to the formation of hydrates upon crystallisation and removing water

from the remaining amorphous phase (Aldous et al., 1995). The mechanisms behind these remarkable abilities of trehalose will be discussed in more details later in this chapter and in chapter 3.

Biotechnological products such as proteins are generally produced by freeze dying and more recently spray drying. The understanding of the amorphous form is crucial for the stability of the final product. The effect of these processes on protein stability during production and storage has been investigated by a number of groups (Arakawa et al., 2001; Carpenter et al., 1997; Craig et al., 1999; DePaz et al., 2002; Fitzpatrick, 2003; Franks et al., 1991; Maa et al., 1997; Maa et al., 1998a; Troung, 2004). Though these studies have provided a great insight into the relationship between biostability, processing and Tg value, the results depend to a certain extent on the substances being used. The findings and the theories behind them will be discussed in more detail later in this chapter.

1.6 SPRAY DRYING VERSUS FREEZE DRYING

Freeze drying is a relatively gentle way of removing solvents from solutions in the frozen state. It is a well-established process and has been used in the pharmaceutical industry since the 1930`s. During the Second World War this method was used for drying of blood plasma and serum (Pakowski et al., 1995). This process involves three stages (Liapis et al., 1995):

- The freezing stage
- The primary drying stage
- The secondary drying stage

In the freezing stage, the solvent and solutes are completely frozen. The integrity formed during freezing must be maintained at drying to get the right physical characteristics of a freeze-dried product. After freezing is achieved primary drying removes frozen solvent under vacuum through sublimation. During primary drying, a receding boundary is observed in the vial when the thickness of dry solids increases as the sublimation interface and the thickness of frozen solution decreases. Due to the small dimensions of the pores in a typical dried product, flow in the dried product

contributes to most of the total product resistance. This in turn, determines the economics of the freeze drying process. Once all water is removed, the apparently "dry" product still contains some solvent, which did not freeze (the sorbed or bound solvent). Secondary drying removes this unfrozen bound water through the pores of the material being dried (Liapis et al., 1995).

As far as the pharmaceutical industry is concerned spray drying is not a novel technology either as they have been successfully using it since the early 1940`s (Broadhead et al., 1992). Important industrial applications of spray drying occurred in the 1920`s where it was used in the milk and detergent industries (Masters, 2002). Spray drying has the advantage of being a simple one-stage process, and due to the rapid drying process, it is particularly suitable for formulating biotechnological products such as proteins. Spray drying is discussed in more detail in chapter 2.

Due to the high temperatures needed to dry the feed solutions it was previously believed that spray drying could not be exploited for heat sensitive pharmaceuticals. Hence lyophilisation (freeze drying) was the preferred method for drying highly sensitive materials. Comparative studies of the two drying methods have not concluded which would be the superior technique as both have certain advantages and disadvantages as listed in Table 1.1.

Cepeda and colleagues evaluated the two techniques using the flour of Vicia faba protein (Cepeda et al., 1998). First of all a difference in powder appearance was observed as spray drying produced a whitish colour powder with spherical agglomerates of diverse sizes. The protein concentrate obtained by freeze drying was a darker colour powder in the form of strands. The particle size showed that smaller particles with less distribution were obtained by spray drying. This fact has an impact on the hygroscopicity of both protein powders. Furthermore, the spray-dried protein powder did not show any denaturation compared to the freeze-dried protein where 10 % denaturation could be experienced. The solubility of the protein concentrate was dependent on the protein concentration.

Table 1.1. *An overview comparing the advantages and the disadvantages of spray drying and freeze drying (Liapis et al., 1995; Maa et al., 1997; Maa et al., 2000).*

Method	Advantages	Disadvantages
Spray drying	Easy and convenient operation Rapid production of dry powder Good particle size control Spherical-shaped particles Aseptic process Organic and aqueous feed solutions Large surface area Free flowing powder	Expensive process Yield dependent on formulation and processing Heat inactivation Surface denaturation
Freeze-drying	Convenient operation High final product yield Aseptic process Large surface area	Expensive process Relatively slow production of dry powder Poor particle size control Irregular shaped particles Broad particle size distribution Caking Some organic solutions are incapable of freezing

In 2002 Seville and colleagues successfully prepared dry powder dispersions for non-viral gene delivery by spray drying. The researchers concluded that spray-dried powder was generally superior than the freeze-dried powder (Seville et al., 2002). Other researchers believe that the underlying mechanism by which a protein is stabilised is also dependent on the drying method used (Liao et al., 2004). Miao and Roos studied the nonenzymatic browning (NEB, maillard reaction) in respect to the two drying techniques (Miao et al., 2004). NEB is an amino-carbonyl reaction and is one of the most important chemical phenomena that may affect food quality in processing and storage. The NEB reaction can be affected by a number of factors, such as time, temperature, water activity, pH etc. Although the research did not conclude which process caused the greatest amount of NEB reaction it was shown that the crystallisation of component sugars in the freeze-dried samples was slightly more delayed than in spray-dried samples. Furthermore the glass transition temperatures in spray-dried samples were higher than those of the freeze-dried samples at the same water activity.

It seems that both techniques have their advantages and disadvantages and the properties of the final dried product are dependent on the method used. Hence it is important to consider the qualities that are required of the dried powder in order to choose the most efficient drying method. Furthermore, the previously assumed notion that spray drying is detrimental for the thermolabile macromolecules does not hold true.

1.7 PROTEIN STRUCTURE

There are 20 naturally occurring amino acids and these are the "building blocks" of proteins. The human body needs all 20 amino acids but is not capable of synthesising some of the amino acids, known as the "essential" amino acids. Essential amino acids are obtained through the diet. By definition, an amino acid contains at least one amino group ($-NH_2$) and one carboxyl group (-COOH). Proteins can be thought of as amino acid derived polymers. The formation of a protein molecule involves a reaction between the amino group of one amino acid and the carboxyl group of another amino acid. The molecule formed by the two amino acids is called a dipeptide, and the bond joining them is a peptide bond. The reaction can continue to form the complete polypeptide chain. Peptides contain typically less than twenty amino acids while proteins contain at

least fifty amino acids. Polypeptides contain between twenty and fifty amino acids. Polypeptides and peptides make up the primary structure of proteins (Banga, 1995c).

The structure of proteins is customarily divided into four levels of organisation. The "primary structure" refers to the unique amino acid sequence of the polypeptide chain. These amino acids are often referred to as residues in a protein chain. The "secondary structure" describes the spatial arrangement of the amino acids in the polypeptide chain and the repetitive conformation of the polypeptide. The common conformations of the secondary structures are the α-helices and the β-sheets, while β-bends, small loops and random coils also exist. Proteins are arranged in both the α-helix and the β-sheet to varying degrees, for example the α-helix is maintained by the hydrogen bonds. Therefore, if the size or charge of the amino acids in the polypeptide chain is changed it could prevent the formation of an α-helix and instead produce a β-conformation (Banga, 1995c).

The term "tertiary structure" is given to the three-dimensional structure stabilised by the disulfide bonds between cysteine residues, as well as to such noncovalent forces as Van der Waals forces, hydrogen bonding, and electrostatic forces. The hydrogen bonds in the tertiary structure join residues that are far apart in the polypeptide chain but are brought into proximity as a result of the folding of the chain. This is the main difference between the tertiary and the secondary structure (Banga, 1995c).

The "quaternary structure", like the tertiary structure, describes the overall arrangement of all atoms comprising the arrangement of the polypeptide chains into three-dimensional complexes. These polypeptide chains are held together by interaction including noncovalent forces such as hydrophobic interactions, hydrogen bonds, or Van der Waals forces (Banga, 1995c).

Generally, proteins are divided into two categories, globular and fibrous depending on their tertiary structure. Globular proteins are characterised by their compactness. In these molecules, the polypeptide chain is folded up to fill most of the space within its domain, leaving relatively little empty volume. Therapeutic proteins are generally globular proteins (Banga, 1995c). The polypeptide chains in fibrous proteins on the

other hand are generally folded into strands and sheets and are present in wool, hair and silk.

In principle, a protein has many possible conformations. In the native state, the protein can possess a maximum number of noncovalent interactions and disulfide linkages. In the other extreme, the completely denatured state, most of the noncovalent interactions and the dislufide bonds are broken, and the molecule has the shape of a random coil. Depending on the protein and the environmental conditions, the protein may also have other intermediate conformations (Banga, 1995b; Hovgaard et al., 2000). Biologically active proteins are properly folded and the most stable conformation is usually the native state. The native structure of the protein exists in a water rich environment which seems critical for both the protein structure and function (Shamblin et al., 1998).

1.8 PROTEIN FORMULATION AND STABILITY CONCERNS

Only a few clinically used proteins (e.g. NovoRapid®, Humulin S® etc.) have adequate stability to be marketed as solutions with a desirable shelf life. Most protein products on the market are freeze-dried powders that are reconstituted into solution just before administration. It seems to be important to dry proteins in order to prevent degradation. Proteins are sensitive to elevated temperatures and therefore drying is commonly done using freeze drying (lyophilisation) (Akers et al., 2000; Franks et al., 1991). Freeze drying results in products with high specific surface area contributing to fast and complete dissolution during reconstitution. This allows the formulation of injectable products. The freeze-dried materials are generally not suitable in the formulation of inhalation products due to characteristics such as static and low flowability.

Spray drying is a well-established drying process and has been explored as an alternative to lyophilisation of biotechnological products. Spray drying is currently being used in production of protein powders for inhalation as the shape and size of the dried product can be controlled (Bosquillon et al., 2001; Maa et al., 1998b). Spray drying of proteins for clinical application is limited due to concerns that the more temperature-labile proteins would not be able to withstand the heat and may be destroyed during the process (Banga, 1995a). Common for both processes is the rapid removal of water, which can cause materials that ordinarily exist in a crystalline form to

become partially or fully amorphous. Amorphous materials compared to crystalline materials, have the ability to absorb water vapour from the atmosphere into their bulk structure. This can lead to conformational changes and hence influence biological activity of the protein formulation (Franks et al., 1991; Shamblin et al., 1998) .

The mechanism behind protein stability/instability depends on a number of different factors, which among other things include the choice of the stabilising agents and the stresses imposed during processing and then during storage. These factors will be highlighted in the next few sections by reviewing the relevant literature.

1.9 BIOSTABILISING EXCIPIENTS

Different research groups have used various excipients in various combinations in order to find the ideal protection for proteins during spray drying and freeze drying. Although disaccharides have been investigated the most due to their inherent biostabilising properties (especially trehalose), other additives are also used regularly for this purpose and the most common ones will be highlighted in sections 1.9.1, 1.9.2 and 1.9.3. Polymers have been used successfully for stabilising proteins during processing and storage (Anchordoquy et al., 1996; Hinrichs et al., 2001; Izutsu et al., 1995). Some practical advice regarding issues and excipients, which need to be considered for stabilisation of proteins during and after lyophilisation has been published (Carpenter et al., 1997; Wang, 2000).

1.9.1 SALTS

The effect of salts on protein stability is complex due to the ionic interactions. Salts may stabilise, destabilise, or have no effect on protein stability depending on the type and concentration of salt, nature of ionic interaction and charged residues in proteins (Kohn et al., 1997).

Miller and colleagues investigated the effect of trehalose and trehalose/sodium tetraborate mixtures on the recovery of lactate dehydrogenase (LDH) activity following freeze thawing and vacuum drying. The Tg values of freeze-dried trehalose borate mixtures were considerably higher than trehalose alone. This resulted in better storage stability under high temperatures and high relative humidity for mixtures containing

borate (Miller et al., 1998). Mazzobre and colleagues conducted a similar study investigating the combined effects of trehalose and cations on the preservation of β-galactosidase in freeze-dried systems. When samples prepared from trehalose were subjected to conditions leading to crystallisation they quickly inactivated upon heating at 70 °C. On the other hand, the samples containing CsCl (caesium chloride), NaCl (sodium chloride) and particularly KCl (potassium chloride) and $MgCl_2$ (magnesium chloride) showed improved protein stability compared to trehalose samples (Mazzobre et al., 2001).

Vogel examined the influence of salts on different properties of the protein, rhodpsin. The stability of the protein was found to be controlled by two counteracting effects – a salt dependent unfolding of protein domains and a salt dependent stabilisation of the protein. This was considered a direct result of the shift in pKa values of the protein groups caused by the salts affecting the conformational equilibrium of the protein (Vogel, 2004).

The use of salts in protein stability has potential but during the drying of a protein formulation, stabilisers and bulking agents are needed. Low salt contents are generally used in protein formulation and hence salts cannot be used as a bulking agent. Thus other bulking agents, which also can enhance protein stability, such as carbohydrates, are preferred.

1.9.2 SURFACTANTS

In two reviews by Wang, the general role and impact of surfactants are outlined in liquid proteins and in solid proteins (Wang, 1999; Wang, 2000). They work by dropping surface tension of protein solutions and reducing the driving force of protein adsorption and/or aggregation at hydrophobic surfaces. Surfactants are basically non-ionic or ionic though non-ionic surfactants are generally preferred in protein stabilisation (Hussain et al., 2004; Wang, 1999). In another review absorption enhancers in pulmonary protein delivery were listed and contained a number of surfactants (Hussain et al., 2004).

Adler and colleagues examined the combined effect of trehalose and a surfactant (polysorbate 80 or sodium dodecyl sulfate (SDS)) on the stability of BSA (bovine serum albumin) upon spray drying. They characterised the spray-dried particles via electron

spectroscopy for chemical analysis in order to quantify the components on the surface of the particles. The addition of polysorbate 80 to a spray solution containing trehalose and BSA resulted in a concentration-dependent hindrance of protein adsorption at the surface of the spray-dried particles. The addition of SDS showed that an increase in the surfactant concentration in the particle surface results in a decrease of protein concentration (Adler et al., 2000). The researchers proposed that the surfactants reduce protein adsorption at the water/air-interface due to a complex formation with the surfactant within the bulk spray solution.

Hillgren and colleagues investigated the effect of non-ionic surfactant, Tween 80 (polyethyelene 20 sorbitan monooleate) on LDH upon freeze thawing. The researchers proposed that Tween 80 exhibited protection by preventing interaction of LDH with ice. Low concentrations of the surfactant resulted in reduced coverage of the surface of ice crystals, which allowed increased protein and ice contact and protein degradation (Hillgren et al., 2002).

Surfactants are being used regularly in the medicinal industry as antimicrobial agents and solubilisers and have their place in biostabilisation, as highlighted in this section. They cannot be used as bulking agents in a protein formulation and hence other excipients are needed when preparing product for clinical use. Further discussion of the biostabilising abilities of the surfactants will continue in chapter 6.

1.9.3 CARBOHYDRATES

The role of carbohydrates in biostabilisation has been highlighted through out this chapter. This section provides a general overview of a few carbohydrates but trehalose is discussed in more detail in chapter 3.

High molecular weight carbohydrates have also been investigated for their biostabilising qualities. Hinrichs and colleagues investigated inulin molecules with various degree of polymerisation and found that a high degree of polymerisation exhibited high Tg values. These inulins proved to be better stabilisers than trehalose and hence highlighted the importance of the glass transition values in protein stabilisation (Hinrichs et al., 2001).

Allison et al. (1998) investigated the level of actin activity after air-drying or freeze drying They used dextran, which is known for its high Tg value. These researchers concluded that dextran could not provide any protection on its own but with the addition of another sugar, sucrose, improved the recovery of protein activity (Allison et al., 1998). The common notion that a high Tg value could provide protection against protein degradation is thus proved wrong and highlights the importance of disaccharides and reverts the attention to nature.

Disaccharides have shown remarkable biostabilisation qualities though the mechanisms involved remain a matter of debate and will be discussed in section 1.10. Trehalose has received particular attention in anhydrobiosis (section 1.2) and the properties are further described in chapter 3. Even though the biostabilising qualities of trehalose remain disputed a few different concepts seem to be involved, high Tg and high molecular weight (Sun et al., 1998).

1.10 MECHANISMS OF PROTEIN STABILISATION BY DISACCHARIDES

In 1990 Crowe and colleagues investigated the similarities between the stress imposed upon protein during freezing and dehydration. These researchers concluded that these stresses were in fact fundamentally different (Crowe et al., 1990). Carpenter et al. (1993) also demonstrated that the selection of stabilising additives specific to the stresses imposed on the protein (freezing and drying) could optimise the stability of protein following storage and rehydration. In another study polyethylene glycol (PEG) was used in combination with trehalose to protect protein (lactate dehydrogenase (LDH) and phosphofructokinase) (Prestrelski et al., 1993a). It was proposed that during the spray drying process, the ideal combination of stabilising additives would include a compound to prevent degradation in solution, another compound to protect the protein upon drying and a compound to raise the Tg of the formulation to improve product shelf life. Liao and colleagues have also corroborated the idea of different mechanisms being involved during the different stages of protein formulation (from solution to dry powder) (Liao et al., 2004).

Hence it is important to understand the various mechanisms involved in protein stability. In a review by Arakawa et al. (2001) the factors affecting the short-term and the long-term stability of proteins are described. This paper provides a useful separation of the various mechanisms and stages involved and are discussed in sections 1.10.1 to 1.10.4.

1.10.1 PROTEINS IN SOLUTION

Denaturation of proteins in solution can be caused by changes in the environment such as pH, temperature or chemical instability due to e.g. oxidation, hydrolysis, deamidation etc. (Wang, 1999). The tendency of proteins to aggregate or precipitate in solution also causes denaturation and loss of activity (Franks et al., 1991). To produce an amorphous product containing protein requires the compounds to be dissolved in a solvent regardless of the drying method (freeze-drying or spray drying) and hence protein degradation in solution must be considered. Timasheff and colleagues have developed a single universal mechanism for stabilisation of any protein in aqueous solution by numerous different solutes e.g. sugars (Timasheff, 1992).

Protein stability can be explained in terms of the thermodynamic stability of a protein that unfolds and refolds rapidly, reversibly, cooperatively, and with a simple, two-state mechanism. N and D represent the native and the denatured forms of a protein, respectively and the equilibrium constant is K (= D/N). This is referred to as the Wyman theory (Arakawa et al., 2001; Timasheff, 1992). The native state of a protein has a minimum Gibbs energy. The conformation of the native protein is determined by its overall intramolecular interactions, which in turn depend on the primary structure, that is, its amino acid sequence. The denaturation process is generally cooperative, that is, the transition from the native state, to random coil conformation occurs over a narrow range of temperature, pH, or denaturant concentration. In these cases, the stability of the protein is simply the difference in Gibbs free energy, ΔG, between the folded (native) G_N and the unfolded (denatured) G_D states:

$$- RT \ln K = \Delta G = G_D - G_N \qquad \text{[Equation 1.1]}$$

The larger the ΔG the more stable the protein. The folded state of proteins is only marginally more stable than the unfolded state since its ΔG is small. The ΔG for proteins has been reported in the range 5-20 Kcal/mol (Timasheff, 1992; Wang, 1999). An important problem in biology centres on protein folding, the mechanism by which the linear information in the amino acid sequence of an unfolded polypeptide gives rise to the unique three-dimensional structure of the native protein. In reality most proteins fold to their native conformations in a matter of seconds or less (Dobson et al., 1998; Wang, 1999). Therefore, they must fold in a highly directed and cooperative manner (Banga, 1995b; Brange, 2000). In many cases, studies have shown that there is an intermediate state called molten globule (MG), which contains secondary but not tertiary structure. It is important that any such state is not too stable. Otherwise, the large activation barrier would prevent it from reaching the native conformation. Unfolded proteins or molten globules contain many hydrophobic regions exposed to water. Consequently, they have a great tendency to aggregate, either among themselves or with other components, leading to precipitation, incorrectly folded structures or both (Figure 1.3).

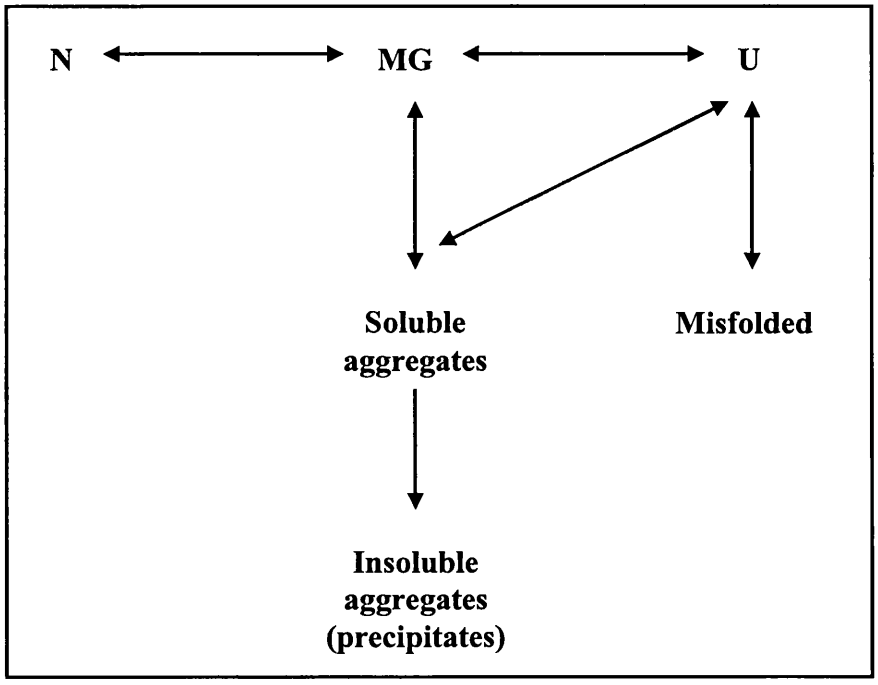

Figure 1.3. *The transition pathway of proteins. Adapted from Brange et al. (2000).*

The proteins after unfolding can form insoluble aggregates, which tend to be high in molecular weight. Aggregation is a two-step process. The first step involves unfolding of the protein thus exposure of buried hydrophobic amino acids residues to the aqueous solvent. In the second step the hydrophobic residues of the unfolded protein molecules undergo association leading to protein aggregation. If proteins are to be delivered they must be in the folded form and therefore they must be stabilised to retain their activity (Banga, 1995b; Brange, 2000).

In the two state-model explained above the native state is favoured because it has lower free energy than the denatured state. The degree of the difference in free energy (ΔG) between the native and denatured state dictates the relative stability of the native state. If the ligand binds to either the native or the denatured state the free energy is lowered. If more ligands bind to the native than the denatured state, the free energy of the denaturation will increase leading to the stabilisation of the native state. Due to thermodynamically favoured process, the ligand only binds to the protein if the ligand-protein complex has a lower free energy value than the protein alone. Considering this in the case of stabilising agents (e.g. disaccharides) Timasheff and colleagues introduced "preferential interaction" (Timasheff, 1992).

Preferential interaction means that a protein prefers to interact with either water or an excipient. In the presence of stabilising additives, the protein prefers to interact with water (preferential hydration) and the excipient/additive is preferentially excluded from the protein domain (preferential exclusion). In this case, proportionally more water molecules and fewer excipient molecules are found at the surface of the protein than in the bulk (Figure 1.4) (Crowe et al., 1990).

Thermodynamically, this means that the excipient (ligand) has negative binding to the protein and thus there is an increase in the free energy in the preferentially hydrated state. The degree of exclusion is greater for the denatured state than for the native state because unfolding leads to a greater surface area of protein exposed to the solvent. Thus even though there is an increase in the free energy of the native state, there is a greater increase in the free energy of the denatured state resulting in the stability of the native state. Hence protein stabilisation arises from destabilisation of the denatured state by the excipient leading to a larger free energy change.

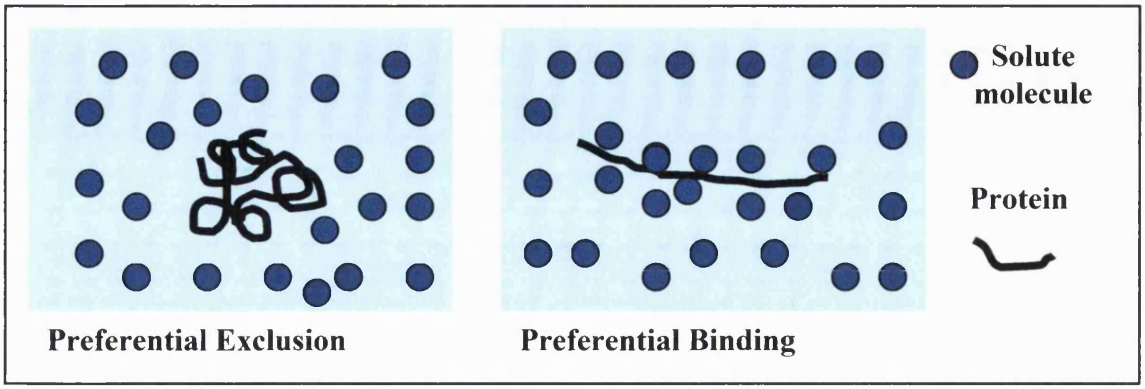

Figure 1.4. *Illustration of preferential exclusion and binding. Preferential exclusion of solutes from the vicinity of a protein in its stable native form. Preferential binding of the solute to the protein leading to unfolding (denaturation). Adapted from Crowe et al. (1990).*

Disaccharides and other stabilising additives have demonstrated the above described protection mechanism during the primary stage of drying when bulk water and the hydration layer of the protein are still present (Crowe et al., 1998).

1.10.2 DRIED PROTEINS

Protein dehydration can be seen as a two stage drying process. In the initial stage the bulk water is removed from the system. But even prior to the removal of protein's hydration shell caused by the removal of the bulk water, denaturation can occur (Crowe et al., 1998). This can be caused by the following conditions:

- increased solute concentration
- exposure to air-water interface
- intermolecular interaction with protein molecules that have become unfolded

The mechanism of protein stabilisation during this initial stage of drying is the same as described for proteins in solution (section 1.10.1). The hydration layer surrounding the protein is completely lost in the final stage of drying and the levels of moisture retained within the dry protein are not sufficient to maintain a full hydration layer. Interactions of the protein with water are critical for formation of the native folded structure. It is hypothesised that preservation of the native conformation is the mechanism by which

several stabilising additives retain activity. Thus, the recovery of protein activity upon rehydration is dependent on preventing drying-induced conformational changes (Prestrelski et al., 1993b). Stabilisation additives that are used for proteins in solution do not necessarily confer any protection to proteins during desiccation. Disaccharides are hence special as they are capable of achieving stabilisation upon complete removal of water (Arakawa et al., 2001).

Two theories are widely recognised in relation to the stabilising mechanisms of disaccharides. Though the research is still ongoing and the complete mechanism of this protection is under debate. "Water replacement" and "glass formation (vitrification)" theories provide explanations for the plausible mechanisms. Many researchers now agree that both theories are possible and indeed necessary in order for disaccharides to protect proteins.

1.10.3 THE GLASSY MATRIX THEORY

The rationale for "vitrification" is the formation of a glassy matrix upon drying which prevents molecular mobility and thus prevents unfolding or intermolecular interactions. Disaccharides are one of the most important glass formers as they have high Tg values correlating to their high molecular weight and for them water is a poor plasticiser. In conclusion to this if an excipient with a high intrinsic Tg is selected to stabilise protein formulation a glassy product with relatively high water content will be achieved. All these qualities may lead to stabilisation of the protein formulation (Franks et al., 1991).

Previously other researchers had proposed that the high Tg of trehalose was related to its biostabilising abilities (Green et al., 1989). This proposal was supported by Crowe et al. (1996) when they observed that amorphous trehalose had a high Tg at all water contents compared to sucrose. In another study the mannitol content during freeze drying was manipulated to see its effect on the protein denaturation (Izutsu et al., 1994). The increased amount of mannitol resulted in crystallisation that denatured the protein, whereas the low amounts of mannitol remained amorphous and protected the protein.

The argument against this concept is that many proteins already exist in the glassy state as proteins form an amorphous phase in the dried solid. They do not easily crystallise but still are not stable upon drying (Angell, 1996). If the molecular weight of the

carbohydrate is increased, the glassy state is formed more readily and should according to the vitrification theory, provide the protein with greater stability. Tanaka and colleagues discarded this hypothesis as they investigated the effect of increasing chain length of saccharides and dextrans (Tanaka et al., 1991). In their study they found no significant differences in the protective activities of glucose, maltose and maltriose on the basis of their weight. The protecting ability of these saccharides decreased with chain length (glucoside residues) greater than 3. It was suggested that this reduction was due to steric hindrance of the larger saccharide molecules prohibiting hydrogen bonding to the polar groups of the protein. The percentage of protein denaturation was also increased with increasing molecular weights of dextran. As described in section 1.9.3, Allison and colleagues also found that amorphous dextran failed to protect protein on its own (Allison et al., 1998). In studies investigating the biostabilising properties of raffinose it was also concluded that the high Tg value was not enough to protect the protein (Chatterjee et al., 2005a; Chatterjee et al., 2005b). These studies are described in chapter 3.

Crowe and colleagues have also reviewed the glassy matrix theory and concluded that the glassy state of the stabilising excipient was not sufficient in stabilising organisms under extreme dehydrating conditions (Crowe et al., 1998). These researchers proposed that a combination of vitrification and interaction (water replacement, described in section 1.10.4) is needed to stabilise proteins by amorphous carbohydrates. These findings support the concept that the glassy state alone is not responsible for protein stabilisation by disaccharides. Another study conducted by Prestrelski and colleagues suggested that high molecular weight and hence higher Tg is ideal in stabilising additives in regards to long term storage of proteins, but they do not prevent dehydration induced unfolding (Prestrelski et al., 1995).

These findings suggest that though it is necessary for the stabilising additives to remain amorphous in order to provide protection during dehydration, glass formation alone is not sufficient for protein stabilisation when the hydration shell is removed.

1.10.4 THE WATER REPLACEMENT THEORY

Several studies provide evidence of another stabilisation mechanism termed "water replacement hypothesis". According to this hypothesis the carbohydrate and the protein

are in the glassy state and the carbohydrate hydrogen binds to the polar and charged residues as water is removed and thus prevents drying induced denaturation of the protein (Crowe, 1971; Crowe et al., 1993a; Crowe et al., 1993b). Carpenter et al. (1989) used FTIR spectroscopy to explore carbohydrate and protein interactions. It was shown that when carbohydrates are dried with proteins, the hydrogen bonding between the carbohydrate molecules is reduced due to bonding between the carbohydrate and protein molecules. A band representing hydrogen bonding of water to carboxylate groups was located when the protein was dried in the presence of a carbohydrate, suggesting a stabilising interaction between carbohydrate and protein. The band was not seen when the protein was dried alone. Belton and Gil (1994) investigated the interaction of protein and carbohydrate as proposed by Carpenter et al. (1989) and were unable to concur with these researchers. Although they observed changes in the FTIR spectrum of the protein and trehalose samples, they could not find any evidence of interaction and concluded that the changes were due to the presence of water in the sample.

Prestrelski and colleagues provided compelling evidence for the water replacement hypothesis while investigating lyophilisation of poly-l-lysine (Prestrelski et al., 1993b). Poly-l-lysine assumed three different conformational forms depending on the solution conditions. At neutral pH it existed as an unordered peptide and at pH 11.2 it adopted a α-helical conformation. A pH 12 solution of poly-l-lysine resulted in formation of a β-sheet. Regardless of the initial conformation in the aqueous solution poly-l-lysine assumed an intermolecular β-sheet conformation in the dried state. The preferred β conformation of the dried protein allowed more intermolecular bonding within the protein structure, thus replacing those hydrogen bonds that were lost through the removal of the hydration layer. When poly-l-lysine was lyophilised in the presence of a carbohydrate, the original solution structure was retained in the dried state because of the carbohydrate hydrogen bonds in the place of water and hence β-sheet formation is unnecessary.

In another study conducted using calorimetric techniques the protein/carbohydrate interactions were investigated in the amorphous state (Souillac et al., 2002). These researchers were able to observe direct interaction between protein and sucrose and trehalose. The interaction according to the group was most likely due to hydrogen

bonding. Liao et al. (2004) also related the stabilising capacity of the excipients (glycerol, trehalose and sucrose) to their ability to form hydrogen bonds with the protein. These researchers also stated that the glassy state could be useful to prevent aggregation and dissociation of the protein.

It is evident from all of the studies that the importance of the amorphous state of a stabilising additive is to allow effective hydrogen bonding between the protein and the additive. A glassy additive, which is not capable of providing this interaction, will not retain protein activity during dehydration. Other mechanisms have also been investigated in order to explain the biostabilising abilities of carbohydrates. These theories do not undermine the other mechanisms but work together in order to explain the complexity in which carbohydrates protect protein denaturation. Chapter 3 concentrates on the biostabilising abilities of trehalose and gives a short overview of the plausible mechanisms.

1.11 AIMS OF THE THESIS

The overall aims of this PhD thesis are:

1. To further understand the properties of trehalose in the dry state.

2. To examine how trehalose can be used as an excipient to spray dry alkaline phosphatase.

3. To determine the correlations that influence the morphology of spray-dried trehalose/alkaline phosphatase particulates.

These aims were achieved by meeting the following objectives:

- Characterise the polymorphic properties of trehalose for the purpose of protein stabilisation in the dried state and to study the processing parameters of the SDMicro^{TM} systematically.

- Investigate the impact of acetone as the organic solvent for processing and its impact on particle formation and characteristics.

- Determine the role of surface-active compounds (surfactants) in protein compositions and their impact on particle formation and characteristics.

- Correlate the nature and surfaces of the spray-dried protein particles when probed with polar and non-polar solvents by inverse gas chromatography (IGC).

- Utilise the combined techniques of dynamic vapour sorption (DVS) and near infrared spectroscopy (NIR) for the purposes of the solid-state analysis of spray-dried protein formulations.

CHAPTER 2

Materials and Methods

2. MATERIALS AND METHODS

2.1 MATERIALS

Table 2.1. *Sources and specific information for materials used in the studies described in chapters 3-6.*

Material	Source	Specific Information
α,α-Trehalose dihydrate	Sigma Aldrich, St. Louis, USA	(D)-(+) Trehalose Product code T-5251 From *Saccharomyces cerevisiae* $C_{12}H_{22}O_{11}$ $2H_2O$ Mwt: 378.3 g/mol
Alkaline Phosphatase	Sigma Aldrich, St. Louis, USA	Orthophosphoric-monoester phosphohydrolase Product code P-7640 From bovine intestinal mucosa 10-30 DEA units/mg solid homodimer Mwt ~160 kDa
para-Nitrophenyl phosphate	Sigma Aldrich, St. Louis, USA	Sigma 104® phosphatase substrate Product code 104-0 $C_6H_4NNa_2O_6P$, $6H_2O$ Mwt: 371.14 g/mol
Bicinchoninic Acid (BCA) Kit	Sigma Aldrich, St. Louis, USA	1 L of Bicinchoninic Acid Solution 25 mL of 4% (w/v) $CuSO_4$, $5H_2O$ Solution Product code BCA-1
Magnesium Chloride	Sigma Aldrich, St. Louis, USA	Magnesium chloride hexahydrate Product code M-2670 $MgCl_2$, $6H_2O$ Mwt: 203.30 g/mol
Diethanolamine	Sigma Aldrich, St. Louis, USA	2,2'-Iminodiethanol / Bis (2-hydroxyethyl)amine Product code D885 $NH(CH_2CH_2OH)_2$ Mwt: 105.14 g/mol
Tween 20	Sigma Aldrich, St. Louis, USA	Product code P-1379
Span 85	Sigma Aldrich, St. Louis, USA	Product code S-7135
Sodium taurocholate	Sigma Aldrich, St. Louis, USA	Product code T-0750
Benzalkonium chloride	Sigma Aldrich, St. Louis, USA	Product code B-6295
Phosphorus pentoxide 98 %	Acros Organics, Geel, Belgium	P_2O_5 C.A.S 1314-56-3

The materials used during the experimental studies are listed in Table 2.1. All other materials used were of analytical grade.

2.2 SPRAY DRYING

2.2.1 GENERAL PRINCIPLES OF SPRAY DRYING

Spray drying is a commonly used and established industrial process involving particle formation from aqueous or organic solutions, pumpable suspensions and emulsions, which are sprayed into a hot dry air stream to obtain a dry product. It is highly suited for the continuous production of dry solids in either powder, granulate or agglomerate. Spray drying is an ideal process where the end product must comply with precise quality standards regarding particle size distribution, residual moisture content, bulk density, and particle shape (Broadhead et al., 1992; Masters, 2002b). The resulting dried product depends to a certain extent on the physical and chemical properties of the feed, the dryer design and operation. Spray drying is widely used in the pharmaceutical industry as well as food industry. The applications in the pharmaceutical/biochemical industry include synthetic drugs (e.g. antibiotics), proteins, excipients, vitamins and more. The principal advantage of spray drying is the ability to manipulate and control properties such as particle size, distribution, shape, density, porosity, moisture content, flowability etc. (Masters, 2002c) (section 1.6). Spray drying of proteins could provide an important alternative to lyophilisation in that the end product can be generated with the desired characteristics.

There are many different types of spray dryers, however they generally consist of a feed solution delivery system, an atomiser, an air heater, an air dispenser, a drying chamber, and systems for exhaust air cleaning and powder recovery (Corrigan, 1995). The selection of the atomiser, the most suitable airflow pattern and the design of the drying chamber influence the drying characteristics and the quality of the spray dried product. Spray drying consists of four fundamental stages, which are carried out irrespective of the dryer design (Maa et al., 1998; Masters, 2002b):

- Atomisation of feed into a spray of droplet.
- Spray-air contact, mixing and droplet/particle flow.
- Evaporation of volatiles from droplets, particle formation and drying.
- Separation of particles from drying air and dried product discharge.

2.2.1.1 Atomisation

Atomisation is the process of transforming the liquid feed material into small droplets. This is the fundamental process around which a spray drying operation is based. The main purpose of atomisation is to generate a spray, which has a high surface area to mass ratio, resulting in high evaporation rates. The final product characteristics can be affected by a number of different parameters at this stage. First of all a homogenous spray is required to ensure that optimum evaporation occurs and that the final product has the desired particle size, shape and residual moisture. The type of nozzle used to create the atomised solution also has an impact on the above mentioned particle characteristics (Masters, 2002a). There are a number of different types of nozzles but the nozzle used during the experiments performed through chapters 4-6 is the two-fluid pneumatic nozzle.

In a two-fluid pneumatic nozzle system the liquid feed and the atomisation gas (nitrogen) are passed separately to the nozzle head. High nitrogen velocities are generated for effective feed contact, which breaks up the liquid into a spray of fine droplets. This liquid disintegration occurs in two phases. The first phase involves the tearing of the liquid into filaments and large droplets. The second phase completes the atomisation by breaking these liquid forms into smaller and smaller droplets. The spray droplets, formed by the feed atomisation follow the subsequent contact with drying gas in the chamber (nitrogen), creating ideal conditions for heat and mass transfer (moisture evaporation). This results in the formation and drying of particles. Dried particles are allowed to settle out of the drying medium and fall to the base of the drying chamber and are retained in the exhaust drying air (nitrogen) leaving the drying chamber for recovery in the dry particulate collectors (Masters, 2002a). In general, spray-air movement in spray dryers suggest that fine sprays can be considered to move under the complete influence of the gas flow throughout the dryer volume (Masters, 2002d). It is believed that the small droplets attain the velocity of the surrounding air in the proximity of the atomiser whereas the large droplets can travel several metres before achieving the same conditions (Masters, 2002d). Hence, moisture content, particle morphology and particle size can all be affected by the droplets.

2.2.1.2 Spray-air contact

The atomised solutions come into contact with the drying gas, typically air, but in the closed system used here, it is nitrogen. Spray-air contact is determined by the position of the atomiser in relation to the drying air/gas inlet. Hence, depending on the design of the spray dryer, it is possible to achieve different flow patterns. Fine sprays are generally influenced more by the surrounding air/gas flow than coarse dense sprays, thus affecting the residence time of the particle in the drying chamber. The system used in the spray dryer, SDMicro^{TM}, is a co-current system in which the spray and air come from the same side. In this system the particles usually reach a temperature of ca. 10-15 °C below the inlet temperature for a short period of time (approximately 30 s) Therefore heat sensitive systems can be dried as the evaporation is very rapid (Masters, 2002d).

2.2.1.3 Evaporation-drying

During atomisation the surface area of the material is increased, aiding the vaporisation of the droplet, which begins immediately upon contact with hot air/gas. As soon as the droplet of the spray comes into contact with the drying air (nitrogen), evaporation takes place from the saturated vapour film, which is established at each droplet surface.

Evaporation takes place in two stages. In the first stage of drying the evaporation takes place at a constant rate. This is due to diffusion of moisture in liquid form from within the droplet maintaining saturated surface conditions. When the moisture content becomes too low to maintain saturated conditions, a critical point is reached and a dried shell forms at the droplet surface. Evaporation is now dependent on the rate of moisture diffusion through the dried shell. The thickness of the dried shell increases with time, causing a decrease in the rate of evaporation. This is termed the second period of drying (Masters, 2002d).

There have been various proposals regarding the drying of the droplets. Recently a new model has been evolved and is portrayed in Figures 2.1 and 2.2. According to this recent model the droplet undergoes four different phases in order to dry, A-B, B-C, C-D-E and E-F (Farid, 2003).

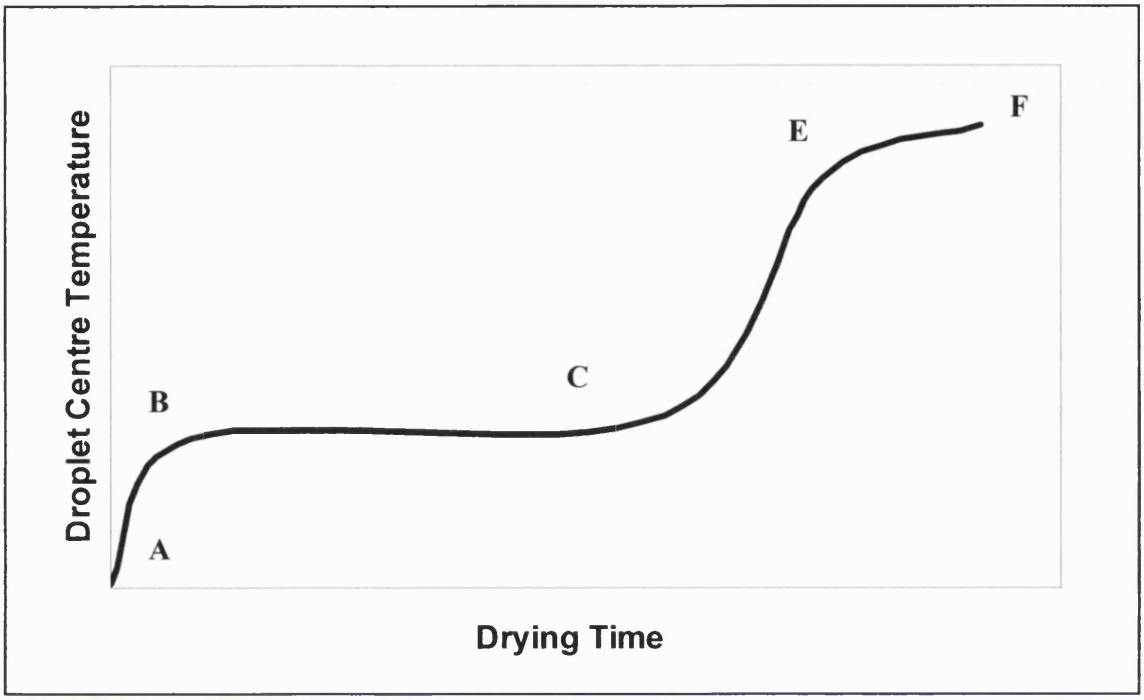

Figure 2.1. *The drying of a single droplet and its core temperature. Adapted from (Farid, 2003).*

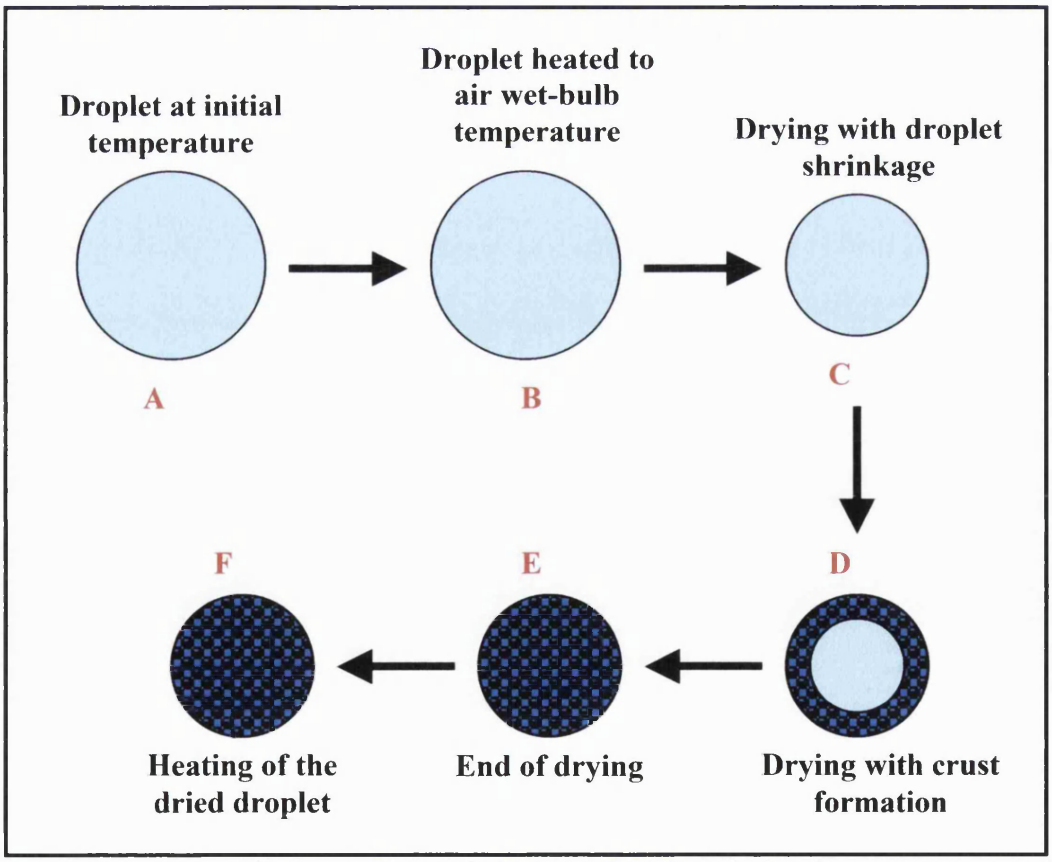

Figure 2.2. *The different stages of drying of a liquid droplet containing solid. Adapted from (Farid, 2003).*

Before discussing these four different stages, the terms, wet bulb temperature (T_{WB}), dry bulb temperature (T_{DB}) and dewpoint temperature (T_{DP}) need to be explained. The wet bulb temperature, T_{WB}, is the lowest temperature the droplet can be cooled to by evaporation. The moisture in the air affects T_{WB}: if the amount of moisture present in the air is high, the evaporation rate reduces. The dew point temperature (T_{DP}) is the temperature a parcel of air must be cooled to in order to reach saturation. Cooling past the T_{DP} normally results in condensation. The dry bulb temperature (T_{DB}) is the actual temperature while T_{WB} is the temperature air will cool to when water is evaporated into unsaturated air. When the air is saturated, T_{DP} is equal to T_{WB} and T_{DB}. In unsaturated air, T_{DP} is always lower than T_{WB} because as air is saturated, the temperature decreases while at the same time T_{DP} increases.

In the first stage, A-B, the droplet is heated by the drying air with no significant evaporation until the droplet surface reaches T_{WB}. At this point there is no change in droplet size or shape. In the second stage, B-C, the droplet starts to shrink with negligible temperature change. During this shrinkage, the temperature of the droplet remains at T_{WB}. The shrinkage continues until the solid helps the droplet maintain a fixed rigid shape. In the third stage, C-D-E, the evaporation on the droplet continues but with a formation of a moving interface, which is assumed to remain at T_{WB}. The interface is assumed to move inwards, separating the droplet into two regions: the dry crust and the inner wet core. The inner core keeps decreasing while the dry crust keeps increasing. In the final stage, E-F, after the drying of the droplet is completed, either because there is no solvent present or the solvent is locked in the core, slight heating of the droplet continues (Farid, 2003).

The drying of the product along with other factors will govern the final powder properties of a material such as particle shape, particle size distribution, moisture content and density (Masters, 2002d).

2.2.1.4 Product separation and recovery

The final stage in spray drying involves the separation of the solid product from the air stream and collecting in the product recovery vessel attached to the cyclone. The air and the product pass through the cyclone after exiting the drying chamber. The separation of the product is then made at the base of the drying chamber. However this does not result

in 100 % product recovery, as a fraction of the spray-dried particles are lost through the exhaust and a fraction adsorbs to the inner surfaces of the spray dryer. Some systems such as the SDMicro™ have a secondary filter system to catch some of the fines that do not reach the cyclone (Masters, 2002b).

2.2.2 CHARACTERISTICS OF THE SDMICRO™

The SDMicro™ is the smallest spray dryer produced by Niro (GEA Powder Technology Division, Søborg, Denmark) and the intrinsically safe operation makes the dryer suitable for use with nitrogen for products dissolved in organic solvents. Other unique features include the ability to collect powder from the cyclone as well as from the bag filters (< 5 μm). The design also includes a glass chamber, which makes it easy to follow the atomisation of the solute into a fine spray. The two-fluid nozzle atomiser (pneumatic nozzle) is designed for fine particles (5-20 μM) and high capacity production (Masters, 2002b). All of these characteristics make the SDMicro™ a desirable dryer for evaluating the early stages of product development and hence an attractive instrument in a pharmaceutical research laboratory (Figure 2.3.). The SDMicro™ is a relatively new and expensive machine due to its design that allows it to be used with organic solvents.

The SDMicro™ comprises of several components as can be seen in Figure 2.3. The nitrogen generator is an important and necessary feature that permits the use of flammable feeds. However it requires a lot of space, which is limited in a university. This did not allow for the generator to be placed in a separate room to the spray dryer, which is generally the norm due to the noise and heat generation. This has resulted in a very different set up than what would perhaps be seen in the pharmaceutical industry but at the same time has created an innovative academic research environment.

Currently less than ten SDMicro™ units are in use in the UK, providing an excellent opportunity to study and comprehend the full use and advantages of the spray dryer and generate new data. The SDMicro™ has two main advantages over many pilot-plant spray dryers, nitrogen generator and pneumatic nozzle. The nitrogen generator permits the use of flammable feeds, and the fluid dynamics mimic those of an industrial scale plant, therefore scale up is not an issue. The system operates with a two pneumatic nozzle atomiser that produces a liquid film of spray with a high velocity gas.

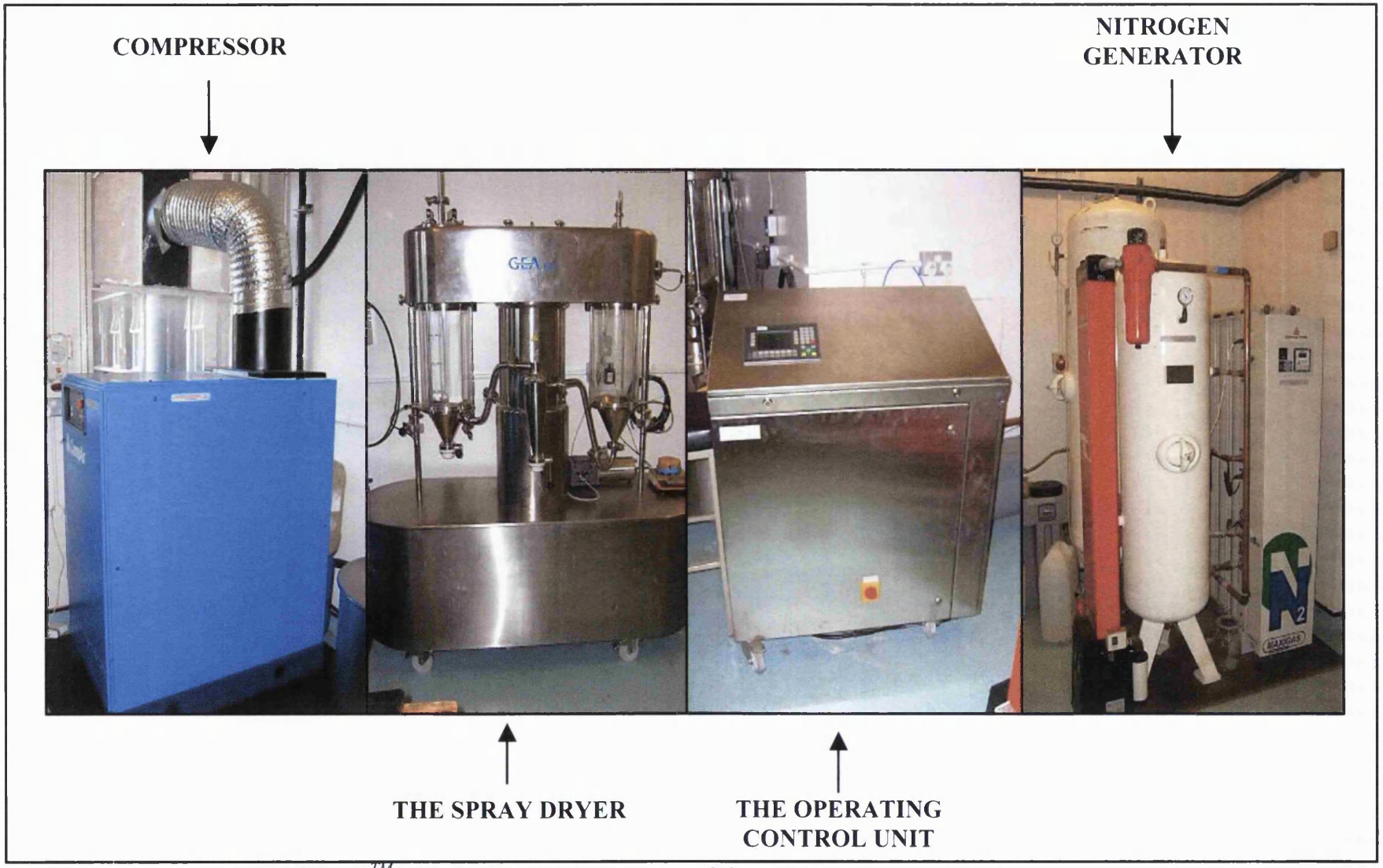

Figure 2.3. *A picture of the SDMicro™ with the nitrogen generator and the compressor.*

The main disadvantage of the spray dryer is its exclusiveness, which makes the entire process (from set up to continuous dried particle production) more challenging. The solutions to the problems encountered during the entire process were generally a little more difficult to find due to a lack of expertise in the area. A classic example of this was a sudden change in the feed pump air pressure, seen as E102 on the control panel (Figure 2.4. and Table 2.2.).

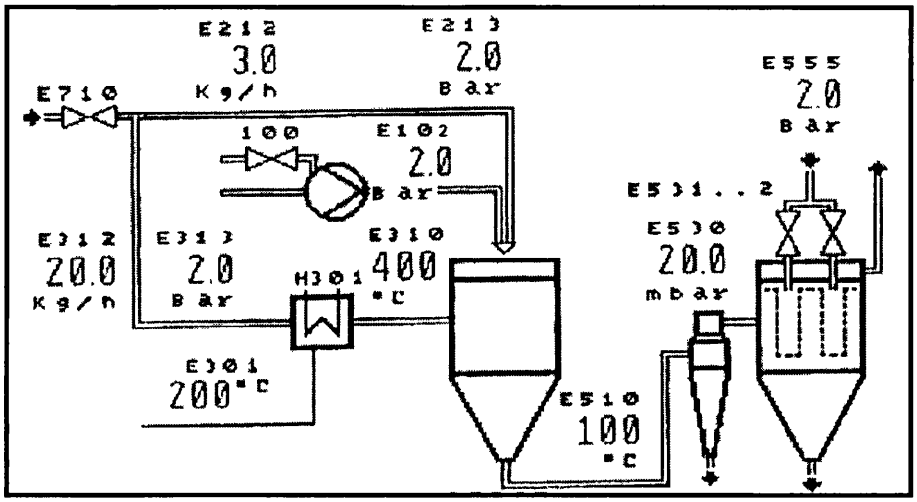

Figure 2.4. *Overview of the control panel of the SDMicro™ (the values shown do not represent the actual values).*

This change was unexpected as all the parameters used were the same but the air pressure of the feed pump (bar) was much lower, which resulted in very different powder morphology. The SEM (Scanning electron microscopy) pictures showed particles that were fused together and this phenomena was seen with all the formulations produced. The feed pump air pressure is related to the feed rate and the outlet temperature. Further investigations showed that neither the feed rate nor the outlet temperature had changed and yet a decrease of feed pump air pressure was being observed. This jeopardised the research that was being carried out on the SDMicro™. The feed pump air pressure could be increased to that previously observed by increasing the outlet temperature by at least 10 °C. This however had implications on the formulations being produced especially for the thermally labile solutions.

Table 2.2. *Explanation of the tags seen in the control panel of the SDMicro™.*

TAGS	EXPLANATIONS
V710	Nitrogen main valve
V100	Feed pump main valve
H301	Process gas heater
E102	Feed pump air pressure control (Bar)
E212	Nozzle atomizer gas flow control (Kg/h)
E213	Nozzle atomizer gas pressure (Bar)
E312	Process gas chamber inlet flow control (Kg/h)
E313	Process gas chamber inlet pressure (bar)
E310	Process gas chamber inlet temperature (°C)
E510	Process gas chamber outlet temperature (°C)
E530	Bag filter pressure differential (mbar)
E555	Bag filter jet pulse cleaning air pressure control (bar)

The Niro engineers were contacted and other options such as a nitrogen leak were considered though none were found. This brought the entire process to a dead end and resulted in a complete halt in the use of the spray dryer. Finally, as last resort the spray dryer was dismantled and a melt of the gasket surrounding the centre of the spray dryer where the heater is contained was observed. The melt of the gasket was resulting in heat loss and once that was replaced the air pressure of the feed pump increased, resulting in free flowing powder production. The encountered problems have provided hands on knowledge of the spray dryer and an expertise of the SDMicro™ has been gained.

Another important aspect of the SDMicro™ is its capacity to produce large amounts of powder, which although is a desirable quality, does not have much use in an academic research laboratory where generally only small amounts of materials are available. The production of amorphous trehalose was conducted as process validation (chapter 4). This was to be used later in more complex formulations containing protein (chapters 5 and 6). Proteins are usually expensive making it difficult to process large amounts of

this material. Hence it is essential that the reproducibility of the equipment be established using small amounts of solution (50 – 100 ml) that can also easily be used in more conventional laboratory scaled spray dryers (e.g. Buchi).

2.2.3 SDMICRO™ VERSUS BUCHI

Spray drying on a laboratory scale is employed using a variety of instruments but the Buchi mini spray dryer (Buchi Laboratory – Techniques Ltd., Switzerland) is most commonly used in research laboratories for the preliminary study of formulations. In comparison to the SDMicro™ the Buchi is more compact, requires less space and is easier to install. Most importantly due to the fact it is so universally used a lot of information regarding the frequently encountered problems and their solutions are available. The published works to date provide with an extensive library containing parameters used for spray drying with the Buchi. Problems with product yield and reproducibility are encountered with all types of spray dryers, including the SDMicro™. Hence it is important to validate a spray dryer in order to produce reproducible data.

The data published are usually on the small laboratory scale spray dryers and cannot be transferred to the industrial scale spray dryers. This is not the case with the SDMicro™ even though it is still a fairly new instrument with no reported data in the literature. Hence an extensive study exploring the operating variables of the SDMicro™ is necessary. Buchi have also explored the merits of spray drying with organic solvents in a safe manner and have recently developed a mini spray dryer that can be used under inert conditions.

Table 2.3 gives an overview of the operating variables for the in house Buchi-191 and SDMicro™. There are fewer parameters to be set when using the Buchi-191 compared to the SDMicro™, making it much simpler and easier to use. In contrast, due to the ability to control more parameters directly, the SDMicro™ provides an excellent opportunity to influence and study the properties of the spray-dried powder that may be affected by these parameters (e.g. appearance, density, particle size and distribution). The main advantage of the SDMicro™ is the ability to spray dry from organic solutions in a safe manner. Both instruments have their advantages and disadvantages and these should be considered and explored in order to optimise the usage.

Table 2.3. *An overview of the operating variables of the Buchi and the SDMicro™.*

Parameters	Buchi	SDMicro™
Inlet Temperature (°C)	Input of an exact value.	Input of an exact value or the desirable heater output (%).
Outlet Temperature (°C)	Indirectly controlled by the inlet temperature and the feed rate.	Input of an exact value or set the desirable pump setting (%). AND Indirectly controlled by the inlet temperature and the feed rate.
Atomising air flow	Set as NL/h. Compressed air flow rate.	Set as Kg/h for the nozzle flow (atomiser gas flow).
Drying air flow pressure	Set as an exact value (bar).	Set as exact values (Kg/h) for: ▪ nitrogen flow (chamber inlet flow) These values establish the pressure (bar).
Feed rate	Pump setting (%) set as an exact value.	Pump setting (%) set as an exact value. OR Indirectly controlled by the settings for the outlet temperature.
Aspirator	Set as an exact value (%).	Not applicable.

2.3 DIFFERENTIAL SCANNING CALORIMETRY (DSC)

2.3.1 INTRODUCTION

Differential scanning calorimetry (DSC) measures the amount of energy (heat) absorbed or released by a sample as it is heated, cooled or held at a constant temperature. Two types of DSC measurements are possible, power-compensation DSC and heat-flux DSC (Brittain, 1999). In power compensation DSC, the sample and reference materials are kept at the same temperature by separate heaters. The observed parameter recorded is the difference in power inputs to the two heaters. In heat-flux DSC, the differential heat between the sample and reference materials is monitored. A power-compensation DSC was employed for the experiments conducted in chapter 3-6.

The types of the transition and reaction, that can be measured using this technique, include fusion, sublimation and vaporisation, crystallinity and glass transitions. Figure 2.5 shows a hypothetical DSC trace. The endotherms represent a process in which heat is absorbed, such as solvent loss or melting. The exotherms represent processes where heat is evolved such as crystallisation or chemical reactions. The area under the peaks is proportional to the heat change involved.

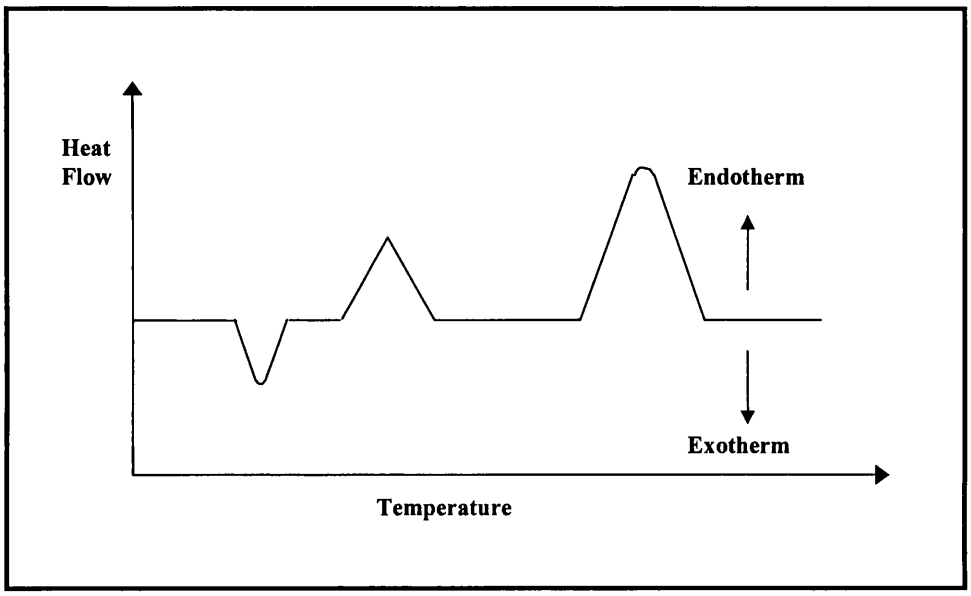

Figure 2.5. *Hypothetical DSC trace showing possible changes of a sample upon heating.*

Consequently DSC can be used to accurately measure the melting point and the associated variation of enthalpy of a sample at any heat rate. Generally slow scanning rates improve peak resolution, while faster scanning rates improve the sensitivity of the technique. High scanning rates also tend to shift the peaks to higher temperatures. Several factors can affect the DSC output, including heating rate, atmosphere and particle size. The sample being studied is placed in a pan and the types of sample pans used can also influence the DSC trace.

Modulated DSC allows the use of low scan rates. The advantages of such a system are an increased sensitivity and resolution as well as the ability to separate thermal events (Hohne et al., 1997). One of the major uses of modulated DSC is the study of glass

transition temperatures (Tg), which are often masked by other thermal events when conventional DSC is used.

The merits of using very fast scan rates in DSC experiments (HyperDSC™, Trademark of Perkin-Elmer) have been explored in recent years using scan rates of 100 °C/min to 500 °C/min (Pijpers et al., 2002; Saunders et al., 2004). A major advantage of HyperDSC™ is the fact that certain transitions are not able to occur in the time available and as such the DSC trace will tend to reflect the constituents of the starting material.

2.3.2 INSTRUMENTATION

The differential scanning calorimetry measurements were carried out using a Perkin-Elmer DSC, Pyris 1 (Perkin-Elmer Instruments, Beaconsfield, Bucks, UK). Pyris software 3.81 was used for all the measurements. During the measurements the calorimeter head was flushed with pure nitrogen at 20 ml/min. Temperature and enthalpy readings were calibrated using pure indium (156.60 °C, 28.45 J/g) and lead (419.47 °C) at the same scan rates as used in the experiments. DSC scans were run on accurately weighed samples. Pyris 1 was used at a low scan rate, 10°C/min, and as a HyperDSC™ with a scan rate of 100°C/min. The experiments were carried out using either crimped aluminium pans or hermetically sealed pans.

Modulated DSC was also used in order to detect the glass transition temperatures (Tg) of the spray-dried products. Exposing the samples to a cycle of heating and cooling periods removed any absorbed moisture within the sample, presenting the true Tg of the samples. A scan rate of 2 °C/min along with an isothermal hold time of 0.5 min was used on samples in crimped aluminium pans. Unless otherwise stated, the temperature range of 80-130 °C was employed.

2.4 THERMOGRAVIMETRIC ANALYSIS (TGA)

2.4.1 INTRODUCTION

Thermogravimetric analysis (TGA) is a measure of the thermally induced weight loss of a material as a function of the applied temperature. TGA is restricted to transitions that involve either a gain or loss of mass. It is a useful method for the quantitative

determination of the total volatile content of a solid and can be used in comparison to Karl Fischer titrations for the determination of moisture (Brittain, 1999).

A thermogravimetic instrument is generally made up of a microbalance, a compartment where the sample is placed, situated in a small oven and a computer that operates the instrument. The TGA consists of a null position balance, which is kept horizontal by an optically controlled meter movement. A small flag on the top of the balanced arm blocks an equal amount of light from reaching the two photo diodes. The position of the balance arm and flag moves in response to any weight changes in the sample pan. This causes an unequal amount of light to reach the photo diodes. This unbalanced signal is nulled by the control circuitry, which causes the meter movement to bring the balance arm back to the horizontal position. The consequent change in the current is directly proportional to the change in mass and is recorded as a weight signal.

Mass loss is only seen due to the loss of solvent (typically water), which may be free (≤ 100 °C) or bound (> 100 °C) (Darcy et al., 1997). The sample could also be undergoing degradation and in order to minimise this the experiments are typically carried out in an oxygen free environment, under dry nitrogen flow.

2.4.2 INSTRUMENTATION

Thermogravimetric analysis was performed using a TA Instruments Hi-Res TGA 2950 ThermoGravimetric Analyser and analysed using Thermal Analyst 2000 v1.0 (both TA Instruments, Inc. Leatherhead, Surrey UK). Weight calibration, using 100 mg and 1 g standards and temperature calibration, using indium were performed. During the measurements the samples were placed in open aluminium pans and flushed with pure nitrogen gas. Approximately 10-15 mg of sample was loaded on the pan and before subjecting the sample to a heating rate of 10 °C/min at a temperature range of 20 – 200 °C.

2.5 X-RAY POWDER DIFFRACTION (XRPD)

2.5.1 INTRODUCTION

The structure of solids can be investigated by power X-Ray diffraction (XRPD). X-rays are scattered by the sample creating a pattern of the scattered radiation, unique to each

crystal structure. The XRPD tube contains a copper anode. This anode is bombarded with electrons under high potential to produce X-rays. The X-rays then pass out of the tube through a beryllium window. The diverging X-ray beam is focused by a series of divergence slits within the goniometer on to the flat surface of the sample. The rays are diffracted at Bragg angle θ by suitable orientated crystallites within the sample coverage approximately to a single line where the receiving split is placed. The X-ray beam then passes through a second parallel slit system, a scatter slit and a monochromator, to the detector. The signal from the detector gives an output of intensity versus scan angle 2θ (Brittain, 1999).

The degree of crystallinity of a sample can be described by the diffraction pattern it produces.

- Crystalline*:* The baseline is flat between 3° and 40° 2θ and the peaks are sharp and well defined.

- Partially amorphous*:* The baseline rises to a broad hump at around 20° 2θ before decreasing again and has superimposed peaks.

- Amorphous*:* A smooth hump without peaks.

2.5.2 INSTRUMENTATION

In this study a Philips PW 3710 X-ray powder diffractometer (Cambridge, UK) with PC-APD control and analysis software (version 3.6) was used. The powdered samples were placed in the 27 mm diameter cavity of the sample holder. XRPD was carried out with a diffraction angle of 2θ from 5-45° at 35kV and 23mA using 0.02° step size and 0.5 seconds for each step.

2.6 SCANNING ELECTRON MICROSCOPY (SEM)

2.6.1 INTRODUCTION

Scanning electron microscopy (SEM) is a technique that gives insight into the particle morphology, an estimation of the particle size and can differentiate between amorphous and crystalline structures. Surface structures as small as 1 μm can be visualised by this

technique. However, the observations can be subjective and rely on homogeneity of the sample.

2.6.2 INSTRUMENTATION

Scanning electron microscopy (SEM) was carried out on the samples using carbon cement and coated in gold. This was performed using an EMETECK K550 (Emitech, Kent, UK) set at 30 mA for 4 min. Scanning electron micrographs were obtained using a Philips L20 SEM (Philips, Eindhoven, Netherlands).

2.7 NEAR INFRARED SPECTROSCOPY (NIRS)

2.7.1 INTRODUCTION

The near infrared (NIR) region of the electromagnetic spectrum is found between 750 nm to 2500 nm. Absorptions in the NIR spectrum originate from overtones and combinations of fundamental vibrations (Bugay, 2001; Ciurczak, 2001). NIR spectroscopy is based upon the concept of vibrational spectroscopy, in which atom-atom bonds within molecules vibrate at specific frequencies. The frequency of vibration is determined by the properties of the atoms contributing to the band. Bond strengths and lengths may vary due to atom characteristics and thus affect the frequency at which the absorption band may appear. This absorption band is frequently referred to as a peak.

Bonds between atoms in molecules vibrate at specific frequency with the absorption of light resulting in excitations to a higher energy level. Different energy level transitions for vibrations of different bonds give rise to different types of transitions. Figure 2.6 illustrates the potential energy curve for a simple diatomic molecule. The excitation from ground state to vibrational energy level 1 ($v = 0$ to $v = 1$) illustrates a fundamental frequency in the mid IR region whereas excitation from $v = 0$ to $v = 2$ corresponds to the first overtone of the fundamental frequency in the NIR region (Jee, 2004).

Overtone peaks usually arise from X-H stretching vibrations, as these overtones are generally much weaker than fundamental transitions. The weaker bond vibrations, such as bending or rotating would be in the third or fourth overtone in the NIR spectrum. Combination peaks arise from the combination of two or more (additive or subtractive)

vibrations to give a single band. These are also much weaker than the original fundamental vibration (Ciurczak, 2001).

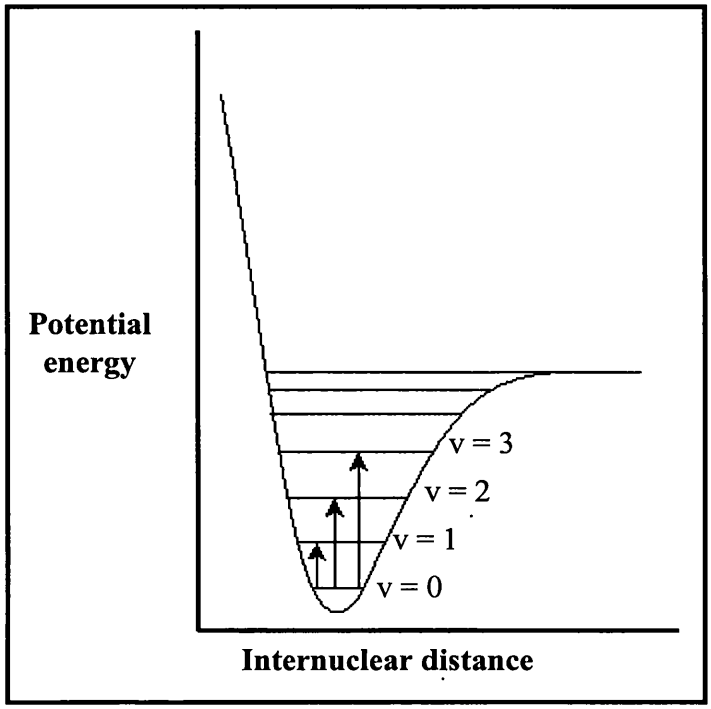

Figure 2.6. *Vibrational energy level for a diatomic molecule (Reproduced from Jee, 2004).*

NIR spectroscopy is becoming more popular in the pharmaceutical industry due to the non-destructive nature of data collection. It has been considered difficult to work with the NIR spectrum due to the innate variability of peaks caused by overtones and combinations. The development of better computer softwares (e.g. Chemometrics and Principal component analysis, PCA) designed to deal with mathematical manipulation of the data.

2.7.2 INSTRUMENTATION

Foss NIRSystems rapid content sampler (Foss NIRSystems, Maryland, USA) and a Foss NIRSystems model 6500 spectrophotomer (Foss NIRSystems, Maryland, USA) connected to a computer running Vision® for Windows version 2.51 (Foss NIRSystems, Maryland, USA) was used to collect the NIR data of the samples. Samples were placed in a 4 ml Waters vial, which was gently sealed with a pierced plastic lid. The samples were incubated at either 0 % RH at 50 °C or 75 % RH at ambient temperatures. The

vials filled with the samples were shaken and tapped before being placed on the sampling unit and an average of 32 spectra were taken. This was repeated three times to produce an average spectrum and confirm homogeneity of the sample within the vial. Calibration was performed on a ceramic reference disc that was used to produce a background against which the samples could be run. This was done every time at the start of the experiments being performed on the day. Vision software was used to produce to standard normal variance (SNV) 2^{nd}-derivative spectra. The spectra were also imported into a chemometric software, Unscrambler® version 7.6.

2.8 DYNAMIC VAPOUR SORPTION AND NEAR INFRARED SPECTROSCOPY (DVS-NIRS)

2.8.1 INTRODUCTION

Dynamic Vapour Sorption (DVS) and Near Infrared Spectroscopy (NIRS) are used in a combined technique. DVS is a gravimetric technique used to investigate the water sorption behaviour of samples at controlled relative humidities. This combined technique was described by Lane et al. 2000. It has predominantly been used to investigate crystallisation behaviour and solid-state transitions (Buckton et al., 1995; Hogan et al., 2001; Vora et al., 2004).

The DVS apparatus consists of a humidity controlled ultra sensitive microbalance within an accurately controlled temperature chamber. The system consists of two identical sample and reference pans, which are suspended from the microbalance. The humidity control is achieved by the regulation of the flow of dry nitrogen gas into the system. The desired relative humidity (RH) is attained through the mixing of dry and wet gas into the sample compartment. Switching valves are used to alternate the flow of nitrogen either directly to the sample and reference pans (0 % RH) or through a glass humidification vessel, containing a solvent reservoir (typically water). By mixing the gas from the dry and/or wet inlets in the correct proportions, the relative humidity is achieved. An NIR probe is positioned approximately 4 mm below the base of the sample pan, and an average of 32 spectra are taken at regular intervals.

2.8.2 INSTRUMENTATION

The experiments were performed on an adapted DVS-1 system (Surface Measurement Systems, London, United Kingdom). The NIR spectra was collected by the optical reflectance near infrared probe (Foss NIRSystems, Maryland, USA) connected to the Vision® software version 2.21. The samples were evenly spread on the pan in such a way that no cracks on the surface could be seen, which allowed the NIR spectra to be collected. NIR calibration was performed as described in section 2.7.2. The DVS microbalance calibration was performed monthly using a 100 mg calibration weight. A service engineer validated relative humidity on a yearly basis. Saturated salt solutions of sodium chloride were used to validate the relative humidity every three months.

2.9 INVERSE GAS CHROMATOGRAPHY (IGC)

2.9.1 INTRODUCTION

Gas chromatography methods are used to study adsorption, diffusion and the reaction kinetics of the stationary phase (Williams et al., 1991). In analytical chromatography the identification and quantification of unknown compounds is achieved by comparing the retention behaviour of the unknown adsorbate introduced into the mobile phase with the behaviour of a known adsorbate for a standard reference stationary phase. Inverse gas chromatography (IGC) is a gas phase technique used for characterising surfaces and bulk properties (Papirer et al., 1988). IGC has many advantages over conventional adsorption techniques as it is rapid, accurate and allows studies of temperature and humidity effects. In IGC known vapours are eluted through the stationary phase revealing fundamental chemical information about the solid surface. A glass column is normally packed with test powder, then extremely small amounts of vapour probes, such as alkanes (e.g. hexane, heptane, octane etc.) or polar probes (e.g. acetone, ethyl acetate etc.) are injected and their retention time is measured. This is then used to calculate the retention volume (V_N), which is the fundamental quantity measured and is directly related to partitioning of the adsorbate between the mobile and stationary phases. The retention volume thus defines chromatographic behaviour for a vapour with a particular stationary phase and is a function of the temperature and pressure of the column as well the adsorbate concentration.

2.9.1.1 IGC and dispersive surface energy

Vapour probes are injected at infinite dilution into the material packed in the column (the stationary phase). Each probe binds to the solid phase (the material surface) with varying degrees. Therefore the adsorbed probe molecules can be separated from each other as the probes are eluted at different speeds. This is referred to as the retention time (t_r).

The carrier gas for the probes is either helium or nitrogen. A delay period is required for the flow of these gases, referred to as the delay time (t_o). A reference elution time is calculated to account for the delay by using an inert probe (e.g. methane). The net retention time (t_n) is defined as:

$$\mathbf{t_n = t_r - t_o} \qquad \text{[Equation 2.1]}$$

To normalise conditions, such as flow rate, the retention time can be converted into total retention volume, which is then further converted to the net retention volume (V_N) by subtracting the column void space:

$$\mathbf{V_N = JF\,(t_r - t_o)} \qquad \text{[Equation 2.2]}$$

- F is the flow rate (ml/min) of the carrier gas.
- J is the compression factor for the pressure drop due to the compressibility of the gas over the column:

$$\mathbf{J = \frac{3}{2}\,\frac{[(P_i/P_o)^2 - 1]}{[(P_i/P_o)^3 - 1]}} \qquad \text{[Equation 2.3]}$$

- P_i is the pressure at the inlet of the column.
- P_o is the atmospheric pressure.

The free energy of adsorption (ΔG_A^0) for a gaseous probe can be calculated from V_N (De Boer, 1953):

$$\mathbf{\Delta G_A^0 = - RT \ln (V_N P_{sg} / \pi w Sa)} \qquad \text{[Equation 2.4]}$$

- R is the gas constant.
- T is the temperature of the column (K).
- P_{sg} is the adsorbate vapour pressure in the gaseous standard state (1.013×10^5 Pa) – (arbitrary standard from De Boer, 1953).
- π is the standard surface pressure (3.37×10^{-4} N/m^2) – (De Boer, 1953).
- w is the weight of the adsorbent in the column (g).
- Sa is the surface area of the adsorbent (m^2/g).

Sa, P_{sg}, π and w are all constant, these terms can be reduced to a constant, K` (Schultz et al., 1987):

$$\Delta G_A^0 = - RT \ln V_N K` \qquad \text{[Equation 2.5]}$$

High values of ΔG_A^0 usually demonstrate a particularly favourable adsorption of the probes, which implies a highly energetic surface. ΔG_A^0 is related to the work of adhesion (W_a) per unit surface area between an adsorbate and adsorbent:

$$\Delta G_A^0 = - N a W_a \qquad \text{[Equation 2.6]}$$

- N is Avogado`s number.
- a is the surface area of one probe molecule.

The dispersive energy component of the surface of a compound can be calculated by the interaction of non-polar probes (alkanes), with regard to their free energy adsorption. This interaction is dominated by dispersive Van der Waal`s surface forces. The dispersive components of the solid surface energy (γ^D_S) and the surface energy of the non-polar liquid (γ^D_L) can be used to determine W_a (Fowkes, 1964):

$$W_a = 2 (\gamma^D_S \gamma^D_L)^{1/2} \qquad \text{[Equation 2.7]}$$

By combining equations 2.5, 2.6 and 2.7 the following equation can be obtained:

$$RT \ln V_N = 2N (\gamma^D_S)^{0.5} a(\gamma^D_L)^{0.5} + K` \qquad \text{[Equation 2.8]}$$

If a plot of the surface energy of adsorption of liquid probes onto solids "RT ln V_N" is drawn as a function of the dispersion components of the alkanes, a straight line is obtained (Figure 2.7). From the slope of the line the dispersive component of the solid can be calculated, $2N (\gamma^D_S)^{0.5}$. Values for "a" and "γ^D_L" are obtained from literature (Table 2.4) (Schultz et al., 1987; Nardin et al., 1990).

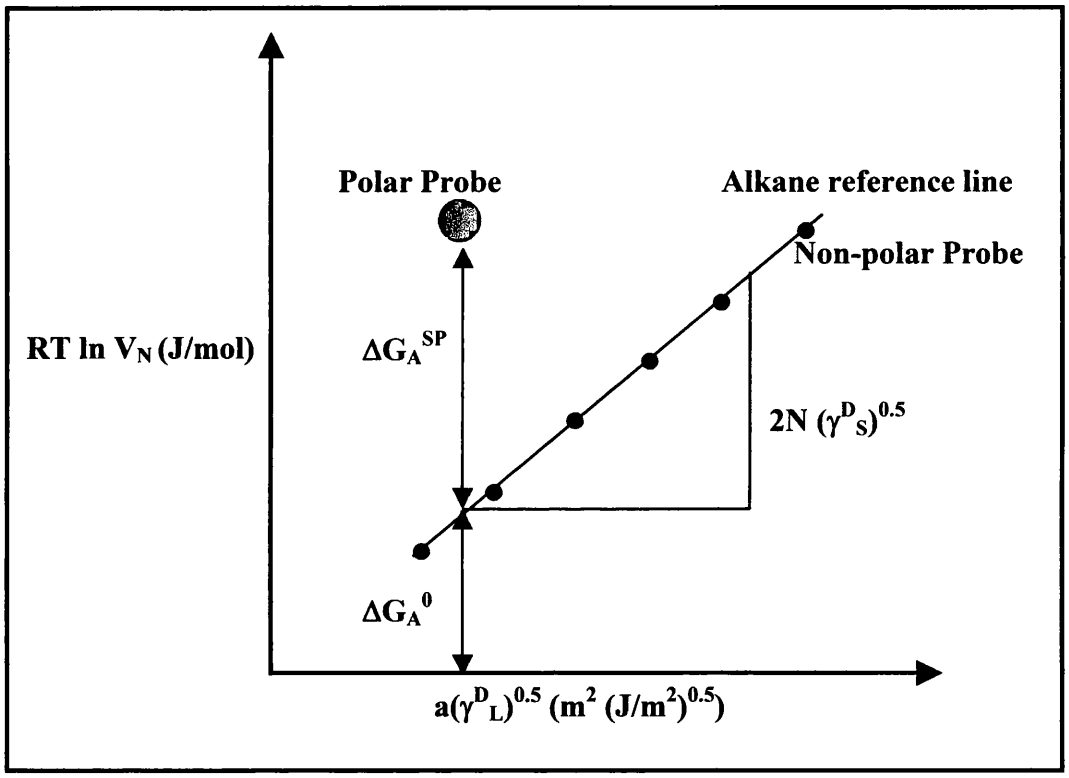

Figure 2.7. *Illustration of the free energy of adsorption of alkanes and polar probes.*

2.9.1.2 Specific polar interactions (acid/base)

Interactions of polar probes with a solid involve both Van der Waals forces (dispersive component) and polar interactions (specific or acid-base interactions). As a result of this interaction, polar probes would provide higher energies of adsorption than non-polar probes. Thus the polar probe lies above the alkane line and the specific free energy of adsorption of the probe (ΔG_A^{SP}) is the vertical distance between the point and the alkane reference line (Figure 2.7).

The acid-base properties of each probe can be determined from ΔG_A^{SP}. These specific interactions are essentially Lewis acid-base interactions or electron acceptor-donor interactions (Gutmann, 1978). According to Gutmann (1978), each probe is given two values, describing the probe's electron donating (base) and accepting (acid) properties, DN and AN, respectively. Gutmann suggested that strong interactions only develop between an acid and a base. Therefore materials of a similar nature, both being acids and or bases, even with high surface polarities will exchange nearly zero specific interaction. Some probes possess high AN values due to contribution from Van der Waals forces. AN* was developed, being solely due to polar interaction forces (Fowkes, 1978). The acid and base values and other properties of the solvents are listed in Table 2.4.

Table 2.4. *Properties of vapour probes required for IGC analysis (γ^D_L represents the surface tension of the probes as liquids).*

Vapour probe	Molecular Area (m^2 x 10^{-19})	γ^D_L (mJ/m^2)	AN* (kcal/mol)	DN (kcal/mol)
Decane	7.5	23.4	0	0
Nonane	6.9	22.7	0	0
Octane	6.3	21.3	0	0
Heptane	5.7	20.3	0	0
Hexane	5.2	18.4	0	0
Acetone	3.4	16.5	2.5	17.0
Chloroform	4.4	25.0	5.4	0
Ethanol	3.5	21.1	10.3	19.6
Ethyl Acetate	3.3	19.6	1.6	17.1

The acid-base parameters (K^A and K^D) of the material surface can be calculated by the specific free energy of adsorption

$$\Delta G_A^{SP} = K^A DN + K^D AN^* \qquad \text{[Equation 2.9]}$$

A plot of $\Delta G_A^{SP}/AN^*$ against DN/AN^* for the various probes, provides the K^A (acid) and K^D (base) values. The result is a straight line with a gradient of K^A and an intercept of K^D.

The acid-base characteristics can also be calculated using other properties of the injected probes. Alternate properties can be plotted against $RTlnV_N$ to determine the free energy of adsorption values.

2.9.2 INSTRUMENTATION

Experiments were performed using IGC (Surface Measurement Systems Ltd, UK). The IGC instrument contains mass flow controllers (MKS instruments) to accurately control the flow of gas within the system. Helium is the carrier gas. It powers the thermal conductivity detector (TCD), which detects the alkanes and the humidity. The flame ionisation detector (FID – measures all probes) is powdered by hydrogen and air gases.

Glass columns used were of 6 mm outer diameter, 4 mm internal diameter and 30 cm in length. The columns were treated with dimethyldichlorosilane (DMCS, Replecote®, BDH) to ensure the surface of the columns would not interact with any gaseous probe. The columns were then thoroughly washed with absolute alcohol and purified water and allowed to dry (Mohammed et al., 1982). Silated glass wool was used at both ends to hold the sample within the column.

The columns were equilibrated in the oven for 2 hours before starting the experiment at 25 °C and 0 % RH. This allowed the removal of any weakly adsorbed surface contaminants, such as moisture. The column was then injected with probes at infinite dilution (0.04 % v/v). At infinite dilution, the probe molecules will have minimal lateral interactions with each other, thus maximising the interaction of the probes with the material surface. The probes used are listed in Table 2.4. The solvents used were all of HPLC grade. Methane gas (BOC grade) was used for the reference probe. The probes were held at 37 °C, while the column was held at 25 °C. The helium gas flow was at 10 ml/min.

The SMS engineers routinely serviced the IGC. Although there is no standard material for testing the surface energy, poly (methyl methacrylate) (PMMA) was used as an indicator. The dispersive surface energy of PMMA is expected to have a value between 35 to 40 mJ/m^2 according to the instrument manufacturers.

2.10 SPECIFIC SURFACE AREA ANALYSIS

2.10.1 INTRODUCTION

The specific surface area (m^2/g) of the solids can be measured using the BET equation. The BET theory was developed in 1938 by Brunauer, Emmett and Teller (Brunauer et al., 1938). It is a mathematical model based on three specific assumptions:

- There is a difference between the energy evolved by a nitrogen molecule adsorbing on a sample surface and a nitrogen molecule adsorbing onto a previously adsorbed nitrogen molecule.

- The surface of the sample has uniform attraction to nitrogen molecules, as it is homogeneous.

- Neighbouring nitrogen molecules already adsorbed do not affect each other as the attractive forces are assumed to be vertical.

However, the BET theory is not a complete theory as it can only be implemented on samples that produce "Type II" and "Type IV" isotherms. There are six different types of isotherms, with specific characteristics associated with each one of them (Figure 2.8). Other isotherms show deviation from BET predictions.

Type I isotherms are indicative of microporous adsorbents. This Langumir type isotherm is obtained when adsorption is restricted to a monolayer (Langumir, 1916; Langumir, 1918). Type II represents strong fluid-solid interactions where the adsorbents are nonporous or macroporous. Type III isotherms are also due to nonporous or macroporous adsorbents but the fluid-solid interactions is weak. Type IV and V isotherms are seen for mesoporous adsorbents. The hysteresis loops are associated with capillary condensation in the mesopores. The only difference between the two isotherms

is that strong fluid-solid interactions are associated with Type IV, whereas Type V represents weak fluid-solid interactions. The adsorbents are nonporous or macroporous for Type VI isotherms with stepwise multiplayer adsorption (Sing et al., 1985).

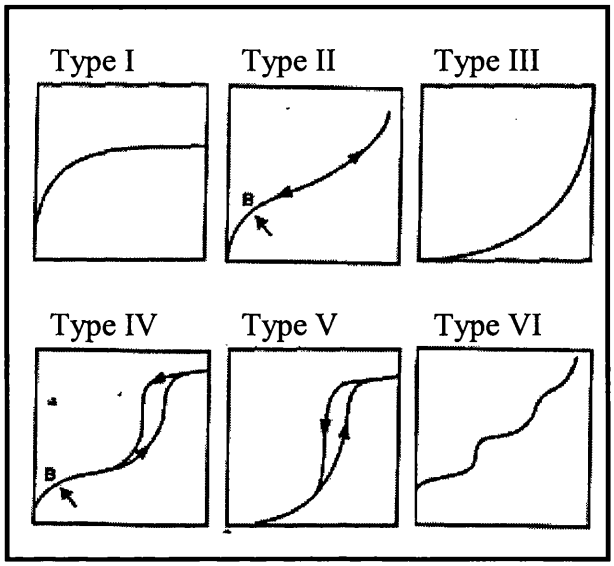

Figure 2.8. *Types of adsorption isotherms.*

Nitrogen is considered the most suitable adsorptive for surface area measurements. The BET theory permits calculation of monolayer capacity from an adsorption isotherm using only mass of a sample as the dependent input as seen by equation 2.10 (Brunauer et al., 1938):

$$\frac{P}{V_{ads}(P_0 - P)} = \frac{C-1}{V_m C} \times \frac{P}{P_0} + \frac{1}{V_m C}. \quad \text{[Equation 2.10]}$$

- Vads is volume adsorbed.
- Vm is the monolayer volume.
- C is the adsorption energy constant.
- P is sample pressure.
- P_0 is saturation vapour pressure of adsorbate.

The BET equation can only be applied for coverage that does not exceed the monolayer too greatly. This is only possible when the surfaces are homogenous. Type II isotherms

are the most common isotherms produced and hence the BET equation was used to measure the surface area of the spray dried particles.

2.10.2 INSTRUMENTATION

The surface area measurements were conducted using the Coulter SA3100. The sample is contained in a sample tube and each particle of the sample is coated with a layer of condensed gas (helium). This "outgassing" takes place under vacuum at a constant temperature. The tube is then immersed into liquid nitrogen (–195 °C). At this stage, the sample is under high vacuum and its surface, having previously outgassed, is ready to attract gas molecules (nitrogen) onto it the moment they are admitted to the sample tube. Nitrogen is used to measure the surface area and helium covers the sample so nothing else can attach to it. Heat and vacuum cleans the sample.

The gas enters the tube in a known volume. The sample attracts this gas and retains at its surface a percentage of the total admitted to the tube. The SA3100 measures this surface retention of gas in terms of volume retained (adsorbed) and the final remaining gas exerting pressure in the sample tube. Gas molecules that are adsorbed cannot exert a pressure, but molecules from any one dose that are not adsorbed are free to express themselves as a gas and hence exert a pressure. As more doses of gas are added, the amount adsorbed increases, as does the overall pressure in the sample tube.

If the data is plotted as pressure in the sample tube on the X-axis and the volume of gas adsorbed at that pressure on the Y-axis an isotherm is produced. Surface area is measured from the amount of gas required to form a monolayer and this amount is derived directly from the isotherm. The Coulter™ SA-VIEW™ software 1.01 was used to analyse the data. Calibration was performed using a known sample supplied by the manufacturers with a known specific surface area and was conducted every three months.

2.11 PROTEIN QUANTIFICATION BY BICINCHONINIC ACID (BCA) ASSAY

2.11.1 INTRODUCTION

Protein determination is one of the most common operations performed in the biochemical research laboratory. The principle of the bicinchoninic acid (BCA) assay is based on the formation of a Cu^{2+}-protein complex under alkaline conditions, followed by reduction of the Cu^{2+} to Cu^{1+}. The amount of reduction is proportional to the protein present. It has been shown that cysteine, tryptophan, tyrosine, and the peptide bond are able to reduce Cu^{2+} to Cu^{1+}. BCA forms a purple-blue complex with Cu^{1+} in alkaline environments, thus providing a basis to monitor the reduction of alkaline Cu^{2+} by proteins at absorbance maximum 562 nm (Smith et al., 1985).

2.11.2 METHODOLOGY

A protein assay was used to quantify the concentration of alkaline phosphatase (AP) solution made in distilled water. 1mg/ml standard stock solution of AP was made in distilled water and serial dilutions were done to prepare different concentrations of AP. A 96 well plate was used and 20 µl of these standards were added to the plate. As a control 20 µl of distilled water was used. An assay reagent consisting of 2 % (w/v) copper II sulphate in bicinchoninic acid solution (BCA) (1:50 ratio) was added to all of the wells containing the controls, standards and protein samples, using a multipipette. The samples were incubated for 30 minutes at room temperature. Absorption readings were recorded in each well spectrophotometrically at 562 nm. The absorbance is directly proportional to the protein concentration and a standard curve was prepared for pure alkaline phosphatase (Figure 2.9). This alkaline phosphatase concentration could be determined by linear regression in the spray-dried samples (Smith et al., 1985). The assay was performed in three replicates and alkaline phosphatase concentration was determined by linear regression.

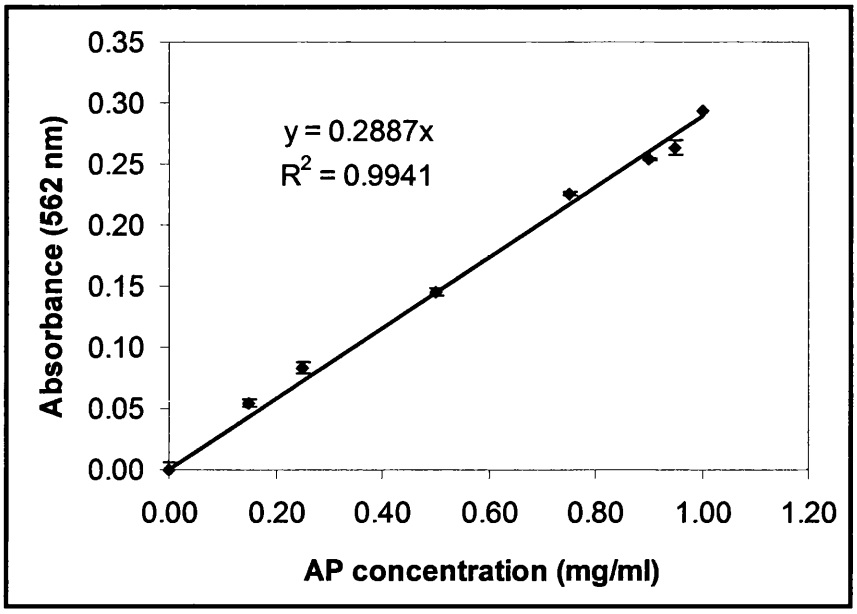

Figure 2.9. An example of a calibration curve of alkaline phosphatase (AP) (mg/ml) against absorbance (562 nm) used in the calculation of AP content in the spray-dried samples.

Interference of the absorbance due to trehalose, acetone and surfactants was also considered and "blank" samples (with no alkaline phosphatase) were prepared and measured as described above. If any of the blank samples gave an absorbance reading it was subtracted from the readings of corresponding samples (containing alkaline phosphatase). Hence a "true" reading for alkaline phosphatase could be achieved.

2.12 PROTEIN QUANTIFICATION AT 280 NM

2.12.1 INTRODUCTION

Proteins in solution absorb ultraviolet light with absorbance maxima at 280 nm (Pace et al., 1995). Amino acids with aromatic rings are the primary reason for the absorbance peak at 280 nm. Secondary, tertiary, and quaternary structure all affect absorbance, therefore factors such as pH, ionic strength, etc. can alter the absorbance spectrum. This absorbance assay is fast and convenient, since no additional reagents or incubations are required. The relationship of absorbance to protein concentration is linear. Because different proteins and nucleic acids have widely varying absorption characteristics, there may be considerable error, especially for unknowns or protein mixtures. Any non-protein component of the solution that absorbs ultraviolet light will interfere with the

assay. The concentration of a protein solution can be determined by measuring the absorbance near 280 nm and by using the Beer-Lambert law (Pace et al., 1995):

$$A = \varepsilon l C \qquad \text{[Equation 2.11]}$$

- A is the absorbance (280 nm).
- l is the path length (1 cm).
- ε is the molar absorption coefficient (M^{-1} cm^{-1}).
- C is the protein concentration (M).

A known concentration of protein is measured at 280 nm at known concentrations. A standard curve is prepared and linear regression is used to measure the protein content in the unknown samples.

2.12.2 METHODOLOGY

This assay was performed using the same protocols as described for BCA assay. A standard curve was prepared using pure alkaline phosphatase in water. The linear relationship between the absorbance readings and the concentrations was used to measure the AP content in the spray-dried samples. This was performed in three replicates for each sample. This method was used to confirm the results obtained by the BCA assay.

2.13 ALKALINE PHOSPHATASE (AP) ACTIVITY ASSAY

2.13.1 INTRODUCTION

The measurement of alkaline phosphatase activity is based upon the hydrolysis of para-nitrophenyl phosphate (PNPP). PNPP, which is colourless, is hydrolysed by alkaline phosphatase at pH 10 to form free para-nitrophenol, which is coloured yellow (see Equation 2.12). The rate of hydrolysis can be determined by following the increase in absorbance at 405 nm at 37 °C (Walter et al., 1974).

$$\text{p-Nitrophenyl Phosphate} + H_2O \xrightarrow{\text{AP}} \text{p-Nitrophenyl} + \text{Pi} \qquad \text{[Equation 2.12]}$$

- Pi is inorganic phosphate.

Once a standard curve of the protein is prepared the activity of the protein in the unknown samples can be determined using linear regression.

2.13.2 METHODOLOGY

Alkaline phosphatase activity was measured in 1.0 M Diethanolamine Buffer with 0.50 mM magnesium chloride and adjusted to pH 9.8 using 5 M hydrochloric acid (HCl). This buffer was kept cold during the experiment. 150 mM p-NPP solution is prepared in distilled water. AP activity was determined by preparing AP solutions in buffer containing 0.1 – 0.2 units/mL AP. The specific units of AP are stated by the supplier, Sigma. Two different batches of alkaline phosphatase were used containing 17 unit/mg solid and 24 units/mg solid, respectively. Hence the standard curve was established for each batch.

2.80 ml of buffer is added into a cuvette (1 cm) followed by 0.30 mL of p-NPP solution. The buffer and p-NPP solution are quickly mixed in the cuvette and measured in the spectrophotometer at 37 °C for 5 minutes. Absorbance readings at the start (t = 0 min) and at the end (t = 5 min) are noted. These are used to determine the blank/background reading. Then 2.70 mL of buffer is added into the cuvette followed by 0.30 mL p-NPP and 0.1 mL of the AP solution. The increase in the absorbance reading is measured for 5 minutes. The protein activity can thus be determined using Equation 2.13:

$$\text{Units/mL enzyme} = \frac{(\Delta A_{405}/\text{min Test} - \Delta A_{405}/\text{min Blank})\ 3.1}{18.5 \times 0.1} \qquad \text{[Equation 2.13]}$$

- 3.1 = the total volume of the assay in mL
- 18.5 = the mM extinction coefficient of p-Nitrophenyl at 405 nm
- 0.1 = the amount of enzyme used in the assay

The active units of AP measured by Equation 3.13 are then compared to the expected active units of AP (as stated by the supplier) and hence AP activity can be expressed as a percentage. The absorption readings of AP are concentration dependent as seen in Figure 2.10. Hence AP solutions prepared in buffer were all between 0.2 and 0.02

mg/mL. The activity of the spray-dried samples was measured by using the AP content determined by the BCA assay and by quantification at 280 nm. The measured active units were then compared to the expected active units at that particular concentration of AP.

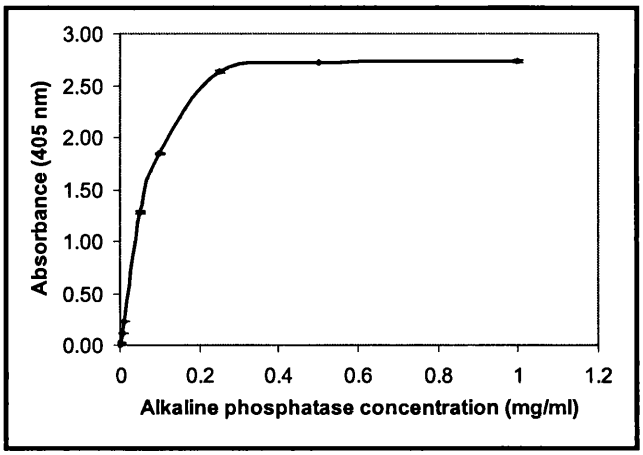

Figure 2.10. *An example of a calibration curve of alkaline phosphatase (AP) (mg/ml) against absorbance (405 nm).*

2.14 SALT SOLUTION

Saturated salt solutions can be determined to maintain specified relative humidities in closed chambers for stability studies. Sodium chloride solution was used to provide a relative humidity of 75 % within desiccators at 25 °C. The salt solution was prepared by mixing the salt in distilled water at 60 °C for 30 hours (Nyqvist, 1983).

CHAPTER 3

The polymorphic properties of trehalose

3. THE POLYMORPHIC PROPERTIES OF TREHALOSE

3.1 INTRODUCTION

The main purpose of this chapter is to determine what may happen to amorphous trehalose when it is crystallised. This chapter describes the polymorphic properties of the α,α-trehalose and gives an overview of the transformation pathways of trehalose using differential scanning calorimetry (DSC) and exploring the merits of hyper-DSC. The study was undertaken in order to understand and clarify the interconversion between crystalline and amorphous trehalose, which could provide some background information for the more complex studies that followed such as the impact of trehalose crystallisation on protein stability. The different metastable morphologies of trehalose may be a key property in its ability to stabilise proteins and as such it is vital that the potential transitions are understood.

3.1.1 POLYMORPHISM AND TREHALOSE

Polymorphism is the tendency of a substance to crystallise into different crystalline states. These crystalline states have different arrangements and/or conformations of the molecules in the crystal lattice and thus have different physical properties, as described in sections 1.2 and 1.3. The pharmaceutical industry is always confronted by these polymorphs and their impact on melting temperature, heat capacity, viscosity, stability, solubility, dissolution rate, bioavailability and compression properties. The process of transformation of one polymorph into another is referred to as a phase transition, which may also occur during processing or storage (Grant, 1999; Vippagunta et al., 2001).

α,α-Trehalose (α-D-glucopyranosyl α-D-glucopyranoside), a non-reducing disaccharide of glucose, has gained much attention due to its importance in nature and has been proclaimed as the most effective carbohydrate in providing protection during dehydration and storage of protein formulations (Ding et al., 1996; Crowe et al., 1998; Crowe, 2002). Different pathways for thermally induced conversions of the amorphous and crystalline forms of this disaccharide have been observed (Reisener et al., 1962; Shafizadeh et al., 1973; Sussich et al., 1998; Nagase et al., 2002; Furuki et al., 2005).

Organisms are found in nature that have evolved the remarkable ability to desiccate at ambient temperatures, remain metabolically dormant under harsh environmental conditions for a long period of time and yet regain full metabolic activity when rehydrated (Crowe, 1971; Franks et al., 1993; Crowe, 2002). This phenomena is referred to as cryptobiosis or anhydrobiosis and is found in both the plant and animal kingdom (Sussich et al., 2001; Crowe, 2002). Studies of yeast, *Saccharomyces cerevisiae*, have shown that the synthesis of trehalose is both necessary and sufficient to account for the protection of all the biomolecules in the organism during drying (Gadd et al., 1987; Coutinho et al., 1998). In 1994 Colaco and colleagues showed that trehalose was a better stabilising excipient than other carbohydrates with respect to long-term stability of the restriction enzyme, *PstI*. The study was carried out on a number of different carbohydrates such as sorbitol, maltose and trehalose. These sugars were dried in vacuum with the restriction enzyme and stored for a month at temperatures 37 °C to 70 °C. Although some of the excipients stabilised the enzyme during drying and on storage at 37 °C, only the samples stabilised using trehalose retained activity when stored at higher temperatures (Colaco et al., 1994). It is frequently claimed that α,α-trehalose is unique in its ability to stabilise biomolecules even though the mechanism behind this property is still unclear. The plausible theories are still being discussed (Chapter 1). One of these theories highlights the lack of an intramolecular hydrogen bond in the crystalline trehalose dihydrate, although the relevance of this to the properties of the sugar in a supersaturated aqueous solution is still unclear (Aldous et al., 1995). In a study by Levine the uniqueness of trehalose was questioned but it was still considered one of the most effective stability enhancing disaccharides (Levine et al., 1992).

In a study by Aldous and colleagues it was suggested that the desiccant protection qualities of α,α-trehalose were not unique and that other saccharides such as β,β-trehalose and raffinose would have similar stabilising qualities (Aldous et al., 1995). In this study partially dried solutions of α,α-trehalose dihydrate and raffinose pentahydrate were prepared. The solutions were subjected to a variety of cooling and heating protocols and the time-temperature curves were recorded using DSC. Their observations indicated that trehalose crystallises and phase separates when it is stored above its glass transition temperature (Tg). Hence the crystallised trehalose is separated from the

amorphous trehalose, which contains the biological product. The crystallisation of the trehalose provides additional desiccation by removing water from the amorphous phase and thereby increasing the Tg and storage stability. It was argued that if this was the case then trehalose cannot be unique in its ability to stabilise biological products (Saleki-Gerhardt et al., 1994; Aldous et al., 1995). Aldous et al. (1995) suggest that other sugars with the ability to crystallise to stoichiometric hydrates from the amorphous state would exhibit the same biostabilising properties as α,α-trehalose. In fact the degree of such desiccation would depend on the molar ratio sugar:water and would therefore be expected to increase as the number of moles of water per mole of sugars increased (Table 3.1) (Aldous et al., 1995).

Saleki-Gerhardt and colleagues investigated the properties of raffinose pentahydrate (Saleki-Gerhardt et al., 1994; Saleki-Gerhardt et al., 1995). They established that it displayed very interesting hydration and dehydration properties in both the amorphous and crystalline state. This is partially due to its ability to form a trihydrate without any appreciable change in lattice structure. Recently Chatterjee and colleagues have investigated raffinose as a potential biostabilising excipient (Chatterjee et al., 2005a; Chatterjee et al., 2005b). They chose lactate dehydrogenase (LDH) as a model to study the effect of phase separation on protein activity and showed that raffinose crystallisation during freeze drying is accompanied by a significant loss of protein activity. The properties of raffinose and other saccharides (Table 3.1) still need to be characterised further and investigated in comparison to α,α-trehalose with regards to the biostabilising properties of these sugars. In contrast, maybe due to the appearance of α,α-trehalose in nature, much has been done to characterise this sugar.

Reisner and colleagues reported the complicated polymorphism exhibited by trehalose in 1962. Articles regarding the different transformation pathways of trehalose have appeared in the literature ever since to elucidate its mechanism of anhydrobiotic action. Figure 3.1 presents the different polymorphic forms of trehalose and their interconverting pathways. These polymorphic forms and pathways will be described in more detail in the next few sections.

Table 3.1. *Overview of the theoretically increasing order of biostabilisation provided by saccharides as a result of the increase in water molecules (Aldous et al., 1995).*

Saccharides	mol H_2O / mol sugar
α,α-trehalose	2
melibiose	2
melezitose	2
mannotriose	3
β,β-trehalose	4
stachyose	4
raffinose	5

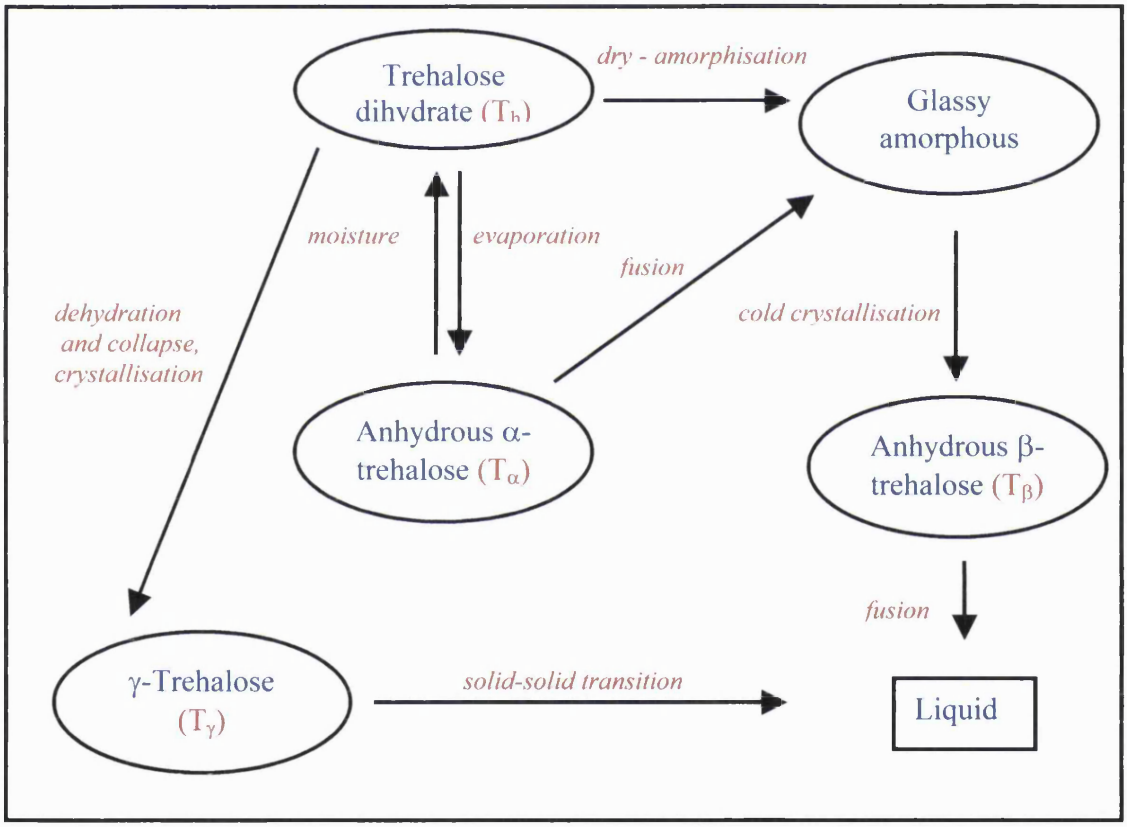

Figure 3.1. *Schematic representation of the transfomation pathways of α,α-trehalose presented by Sussich et al. (2002).*

3.1.2 α,α-TREHALOSE DIHYDRATE (T_h)

Trehalose was first discovered in rye in 1832 by Wiggers. The name trehalose was derived later from the desert trehala, where the French chemist Berthelot found this sugar (Sussich et al., 1999). α,α-Trehalose (α-D-glucopyranosyl α-D-glucopyranoside)

is a non-reducing disaccharide of glucose. The structure of the native crystalline form, α-α-trehalose dihydrate is shown in Figure 3.2.

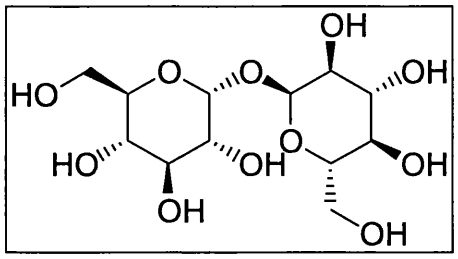

Figure 3.2. *Structure of α,α-trehalose.*

Although the isomeric α,β-trehalose and β,β-trehalose have been synthesised only the α,α isomer occurs naturally (Brown, 1972). This form is found in a variety of plants and insects. Ding et al. (1996) showed that trehalose dihydrate converted to the amorphous form when dehydrated at temperatures between 70-95 °C in vacuum. In a study by Sussich et al. (1998) the dehydration process of T_h was highlighted in respect to its impact on the formation of the different polymorphic forms of trehalose. They showed that using different DSC heating rates could produce different polymorphs. With the use of slow heating rates (1 K/min) the hydrate was lost with the formation of an amorphous material, which then crystallised to an anhydrous material (at 180 °C) followed by a melt (200 °C). At faster scan rates a crystallisation was observed after the dehydration (100 °C) followed by a melt around 140 °C. The difference in the thermal events occurring above 100 °C as a function of the scanning rates is due to the rate of water loss, which seems to be a key factor in the formation of anhydrous trehalose (Sussich et al., 1998).

It is important to remember that the process of anhydrobiosis in nature is much slower than anything described in the studies discussed above. The plants, organisms etc are desiccated for years and hence the techniques used to study trehalose are not capable of mimicking that time frame.

3.1.3 ALPHA ANHYDROUS TREHALOSE (T_α)

The alpha anhydrous form, T_α, can be produced by holding a sample of T_h at 85 °C for 4 h under vacuum (Reisener et al., 1962). Under these conditions the rate of water loss does not allow the α,α-trehalose to relax into a more compact form (Sussich et al., 1998). T_α can be fully rehydrated back to T_h by exposing it to 50 % relative humidity at 25 °C for about 24 h, indicating that T_α has the same molecular morphology as T_h (Sussich et al., 2001). This reversible dehydration-hydration mechanism may be one of the key features in the biostabilising properties of trehalose in nature. DSC thermograms of T_α show a melt of this anhydrous crystal around 125 °C producing an amorphous phase (Sussich et al., 1998). Depending on the scan rate this event is followed by a recrystallisation, indicating the conversion to T_β, which again is followed by a melt around 200 °C (Sussich et al., 1998; Sussich et al., 2000).

3.1.4 BETA ANHYDROUS TREHALOSE (T_β)

The beta anhydrous form, T_β, can be produced by holding a sample of T_h at 130 °C for 4 h (Reisener et al., 1962). This anhydrous form is believed to be the most stable anhydrous forms of α,α-trehalose. This is due to its high melting point around 210 °C (Sussich et al., 2000). Regardless of the scan rates used and the various intermediates that can be produced, the melt of the β-form is always present when trehalose dihydrate (T_h) is heated above 200 °C (Reisener et al., 1962; Shafizadeh et al., 1973; Sussich et al., 2000; Sussich et al., 2002).

3.1.5 GAMMA TREHALOSE (T_γ)

Sussich and colleagues first observed the γ-form of T_h in 1997 (Sussich et al., 1997). This is the only group that has reported the Tγ and it has only been produced in a DSC through a process of cold crystallisation (Sussich et al., 1998). The formation of T_γ was induced by heating T_h at scan rates of 5-10 K / min and could be seen by the presence of an exothermic peak right after the dehydration (~ 100 °C). This was followed by a melt (120-130 °C) proving that this was not a stable polymorph. By comparing the XRPD diffraction patterns (X-ray powder diffraction) of T_α and T_γ, Sussich et al. (1998) concluded that these are two different forms. However, in 1999, they suggested that rather than being a new form, this was in fact a mixture of the hydrate and the beta

anhydrate (presumed to be a hydrate core and an anhydrate surface) (Sussich et al., 1999).

The rationale behind the formation of T_γ, according to Sussich et al. (1998), is that at low scan rates the water from T_h is only partially removed and an amorphous solid with a Tg lower than the Tg of the anhydrous form is formed containing the small amount of water remaining from the original dihydrate. Cold crystallisation occurs in the solid, which is plasticised by the presence of a small amount of water. When the temperature is raised above the Tg, the amorphous state transforms from its metastable form to a more stable form, undergoing cold crystallisation (~ 120 °C) producing T_γ (Sussich et al., 1998). When subjected to further heating T_γ undergoes solid-solid transition where the hydrated part of the T_γ transforms to T_β (~ 125 °C) followed by the melt of T_β (~ 210 °C) (Sussich et al., 2000).

3.1.6 FORM II

Form II was introduced by Belton and Gil as an anhydrous form of α,α-trehalose (Belton et al., 1994). They describe three forms of α,α-trehalose. The term Form I was denoted to α,α-trehalose (T_h). Form III was produced by heating up the dihydrate to 358 K and refers to the commonly known β-anhydrous form. Form II was obtained by leaving Form I in vacuum for 48 h, at 323 K. This was considered a new anhydrous form of α,α-trehalose and further studies were carried out to characterise Form II using vibrational and solid-state NMR spectroscopy (Gil et al., 1996). Taylor et al (1998) disputed the novelty of Form II as they produced a FT-Raman spectrum almost identical to that obtained for Form II by Gil and Belton (Gil et al., 1996; Taylor et al., 1998a). By dehydrating α,α-trehalose with a particle size fraction of less than 45 μm at 80 °C the researchers could mimic the spectrum of Form II. They concluded that Form II was clearly a disordered product of the dehydrated dihydrate. Further studies conducted by Akao and colleagues on Form II also concluded that Form II was likely to be the same as T_α (Akao et al., 2001).

3.1.7 KAPPA ANHYDROUS TREHALOSE (T_κ)

Nagase et al. (2002) reported T_κ as another anhydrous polymorphic form of α,α-trehalose, which was obtained from T_h by vacuum heating and also by heating in hot air.

Similarities to the T_α and Form II could be seen as the calorimetric study showed a transformation of T_κ to an amorphous form around 127 °C. They also showed that T_κ was very hygroscopic as it readily converted to the dihydrate form when exposed to 43 % relative humidity at 25 °C, similar to the qualities of T_α as seen by Sussich et al. (2001). Nagase et al. (2002) suggested that the biostabilising effect of trehalose was due to the production of T_κ and amorphous trehalose in the organisms under conditions of dehydration. They showed that when the amorphous form and T_κ were mixed and exposed to humidity, T_κ would transform to T_h more rapidly than water adsorption to the amorphous form. This was in agreement with the hypothesis of Aldous et al. (1995) who proposed that trehalose has the ability to crystallise and phase separate above its Tg in order to protect the remaining amorphous phase (section 3.2). This would explain the unique properties of trehalose and its effect on the plants and insects during the dehydration periods. This could also explain the significance of this particular form during the entire process but the researchers could still not give clear evidence that this was in fact a different form than T_α and/or Form II. The XRPD diffraction patterns and the DSC thermograms showed similarities to the previously published data (Gil et al., 1996; Sussich et al., 1997; Sussich et al., 1998; Sussich et al., 1999; Sussich et al., 2000).

3.1.8 AMORPHOUS TREHALOSE (T_{am})

Ding et al. (1996) proposed the possibility that glassy amorphous anhydrous trehalose could be produced by dehydration of its dihydrate crystalline form. The glassy properties of the dehydrated α,α-trehalose remains unsettled as researchers argue that the dehydration of the dihydrate directly produces an amorphous phase, and not the glassy form, which can be prepared only if the under-cooled liquid is quenched at temperatures below the glass transition (Sussich et al., 1998) (Figure 1.1).

Shafizadeh et al. (1973) reported a Tg of the amorphous trehalose around 133 °C. Other reported glass transitions of the amorphous phase have varied from around 80 °C onwards (Green et al., 1989; Levine et al., 1992; Roos, 1993; Ding et al., 1996; Sussich et al., 1998). Amorphous trehalose has a remarkably high Tg compared to other saccharides, which is believed to contribute to its biostabilising properties (Crowe et al.,

1998). The difference in the reported Tg values has been due to the difference in water content of the tested samples as shown by Crowe et al. (1996).

3.1.9 Td ANHYDROUS TREHALOSE

This anhydrous from has so far only been reported by Moran (2004). This form was produced by holding α,α-trehalose at 0 % relative humidity (under nitrogen pure gas) at 25 °C for 28 h in the Dynamic Vapour Sorption (DVS) analyser. Near infrared (NIR) spectra was recorded during the dehydration to compare the changes in the spectra to other polymorphic forms. The anhydrous form, T_d showed the ability to readily rehydrate back to the dihydrate form. Moran concluded that this was consistent with the description of an isomorphic desolvate by Stephenson et al. (1998). The term isomorphic desolvate defines a desolvate that retains the structure of its parent solvate form, i.e. the desolvate structure retains the three-dimensional order of the original crystal as defined by space group symmetry and the lattice parameters. The lattice produced by dehydration is less stable than the respective hydrated form. This makes the dehydrate extremely hygroscopic and rapid rehydration can be seen when the dehydrate is re-exposed to elevated humidity (Stephenson et al., 1998). Moran concluded that the Td form was different to T_α and T_β by comparing the XRPD patterns of these anhydrous forms. DSC thermograms obtained of Td were similar to that for T_α, however a Tg value was observed around 80 °C indicating amorphous content in the sample. There is a clear need to elucidate the crystal structures of all of the anhydrous forms in order to determine their similarities and/or differences.

3.1.10 PARTICLE SIZE DEPENDENT MOLECULAR REARRANGEMENT

The dehydration of the dihydrate seems to be a key factor in the formation of the various anhydrous forms (Sussich et al., 1998). Sussich et al. (1998) describe the escape of water from the crystalline structure and the subsequent collapse as a very delicate kinetic balance. This balance depends on the time and/or amount of water encapsulated in the trehalose molecules, which would allow the molecules to structurally reorganise themselves after the initial water removal. The formation seen after the dehydration reflects the effusion of water from the crystalline structure, which leads to the collapse of the structure or symmetric displacement. The depletion of water can be influenced by factors such as temperature and by the period of time in which water is removed.

Taylor and colleagues have also studied the dehydration behaviour of α,α-trehalose dihydrate (Taylor et al., 1998a; Taylor et al., 1998b; Taylor et al., 1998c). They did not debate on the various anhydrous forms of trehalose and made no attempt to characterise these forms but they disputed the idea of Form II being an anhydrous form of trehalose (Taylor et al., 1998a). They focused on the dihydrate form, the "anhydrate" and the amorphous forms (Taylor et al., 1998b). They compared the formation of the anhydrate and the amorphous forms to the particle size of the dihydrate. They demonstrated that small particles (< 45 μm) formed an amorphous form, which liquefied above its Tg (< 80 °C) temperature and formed an anhydrate through crystallisation. This was due to the large surface area-to-volume ratio of these small particles, which resulted in dehydration commencing prior to reaching the threshold temperature for rearrangement. However, the large particles (> 425 μm) underwent a solid-solid conversion from the dihydrate to the anhydrate (> 80 °C). This was due to the catalytic effect of the water released from the dihydrate on the rearrangement of the dehydrated phase to the anhydrate (Taylor et al., 1998a; Taylor et al., 1998b).

3.2 EXPERIMENTAL PROTOCOLS

3.2.1 DIFFERENTIAL SCANNING CALORIMETRY (DSC)

Differential scanning calorimetry (DSC) measurements were carried out using a Perkin-Elmer DSC Pyris 1 as described in section 2.3. The dehydration process of trehalose dihydrate (T_h) was examined at two different scanning rates introducing "HyperDSC" using a scan rate of 100 °C/min and a regular DSC scan rate of 10 °C/min. The effect of sample size (either 1 or 5 mg) was also examined as an important factor in the understanding of the DSC profiles. Each experiment was repeated four times in order to confirm the reproducibility. The experiments were carried out using both crimped aluminium pans and hermetically sealed pans

3.2.2 THERMOGRAVIMETRIC ANALYSIS (TGA)

The TGA experiments were performed using Hi-Res TGA 2950 from TA instruments as described in section 2.4. The experiments were repeated three times in order to confirm the reproducibility.

3.3 RESULTS AND DISCUSSION

The dehydration of α,α-trehalose was performed using differential scanning calorimetry to study the influence of sample size (section 3.3.1.), heating rate (section 3.3.2.) and water vapour (section 3.3.3.). The polymorphic properties are believed to play an important role in biostabilisation and an understanding of its solid state transitions could allow better formulations of protein pharmaceuticals.

3.3.1 SAMPLE SIZE DEPENDENT DEHYDRATION BEHAVIOUR OF α,α-TREHALOSE DIHYDRATE

The effects of sample size on the dehydration of trehalose dihydrate are apparent in the DSC profiles represented in Figures 3.3 and 3.4. With a small sample size (1 mg) after the initial dehydration (large endotherm at just below 100°C) there is another small endotherm at around 130°C (insert in Figure 3.3). The data for this small endotherm (1.5 J/g) are reproducible and are presented in Table 3.2. This small endothermic peak is described in the literature as the melting of the anhydrous T_α crystalline form (Sussich et al., 2000; Sussich et al., 2002). Upon further heating a large crystallisation is seen around 180°C. This is described in the literature as the formation of the β-crystalline form followed by the melt of the anhydrous T_β above 200°C (Sussich et al., 2000; Sussich et al., 2002).

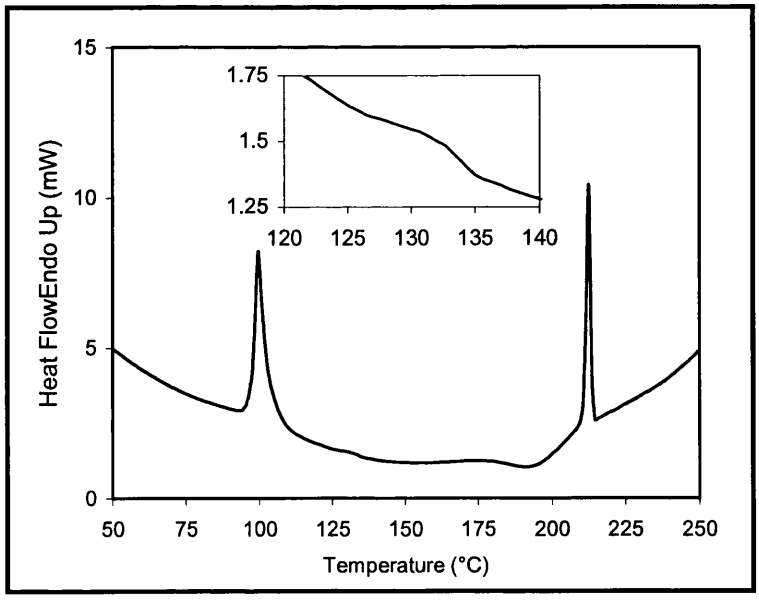

Figure 3.3. *Typical DSC profile of 1 mg trehalose dihydrate using standard crimped pans at 10 °C/min.*

When a larger sample mass (5 mg) was used the sharp dehydration peak was followed immediately by a crystallisation which in turn followed an immediate endothermic peak around 114 °C (ca. 125 J/g). According to Sussich et al. (2002) the presence of an exothermic peak right after the initial water depletion is in keeping with an amorphous form crystallising into the γ-crystal form (section 3.1.4). T_γ is thought to be formed by the partial removal of water with the formation of an external layer of anhydrous crystals with the core still made of α,α-trehalose dihydrate (Sussich et al., 1998; Sussich et al., 2000; Sussich et al., 2002). Sussich et al (2002) report that the γ-form melts in the range from 102-130 °C. More realistically this can be expected to be the further and slow dehydration of the (largely) encapsulated core of the particles (section 3.1.4). This dehydration has been observed as an exotherm. There should simultaneously be the formation of some amorphous material and crystallization of that material to the β-form. All of these events are thought to contribute to the protracted net exotherm seen in the region from 105-110 °C in Figure 3.4. Consequently it is almost certainly a misnomer to say this is a crystal form (T_γ), but rather a mixture of the T_β and the dihydrate. This mixed system is able to form in situations where the hydrate does not have time to fully dehydrate, as would be the case with a large sample mass, for which the rate of heat transfer will be more limited than for a small sample.

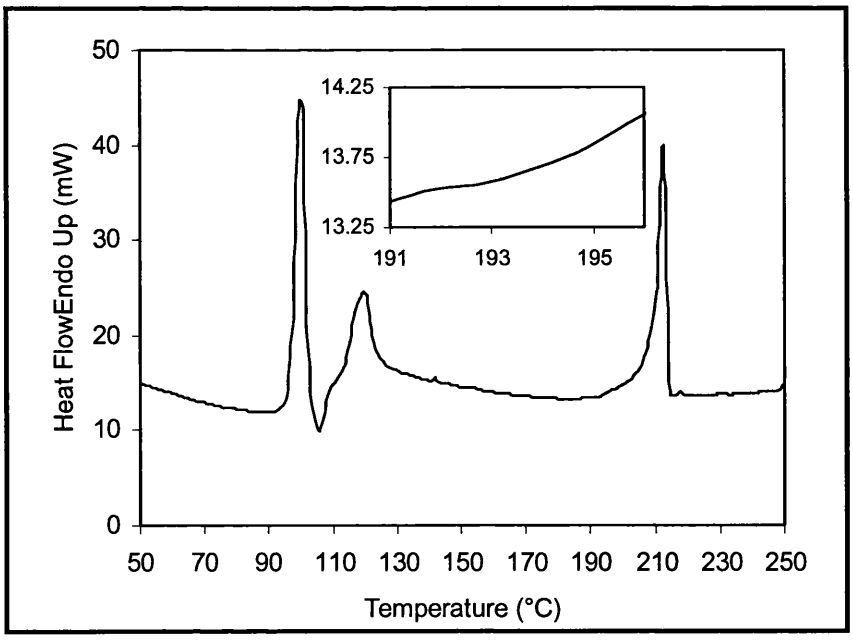

Figure 3.4. *Typical DSC profile of 5 mg trehalose dihydrate using standard crimped pans at 10 °C/min.*

Hence the 1 mg sample primarily follows the transition mechanism labelled "B" in Figure 3.5 and 5 mg sample primarily follows route "A". The transition scheme shown in Figure 3.5 is different from that reported in the literature in that it does not show the formation of any γ-form (Figure 3.1). The reason these routes are referred to as the primary routes is the fact that a sample is capable of using more than one transition pathway simultaneously, which is evident in this study. Table 3.2 gives the exact values of these transitions and it can be seen that the 1 mg sample shows a small melt of the α-form (~127 °C; ~1.5 J/g), which means that a small part of the sample must be going through route "A".

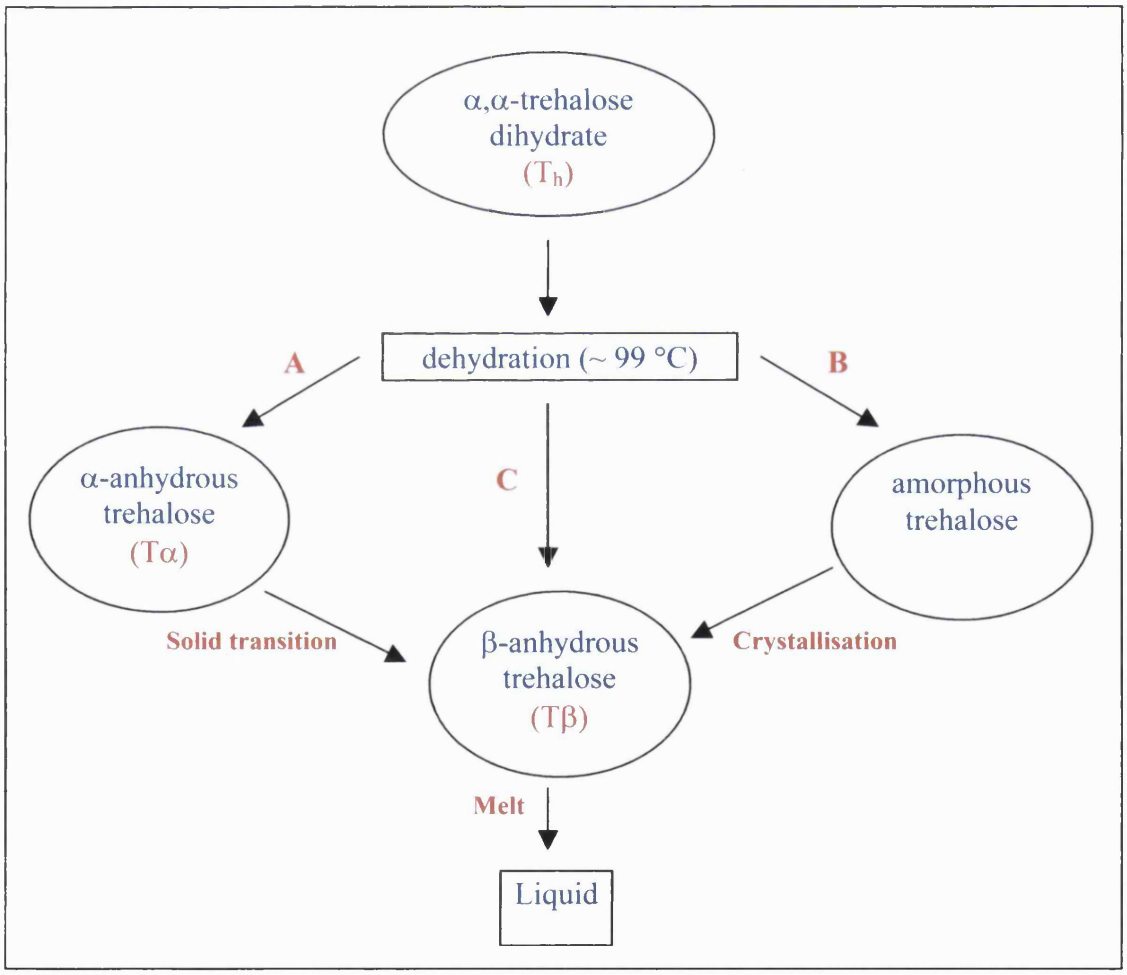

Figure 3.5. *Schematic representation of transformation pathways of trehalose.*

In contrast, a 5 mg sample undergoes a small crystallisation event around 196 °C (-8.9 J/g), which is the result of a small amount of sample following route "B" the rest of the sample undergoes transitions through route "A". According to Taylor et al. (1998) trehalose forms an amorphous phase and transforms into the anhydrate through crystallisation only when the dehydration is commenced prior to attaining the threshold temperature for rearrangement of the dehydrated phase (section 3.1.10). This could explain why a small sample size mainly reaches the β-anhydrous form through crystallisation (route "B") and a large sample size primarily transforms in to the β-from through solid transition.

Table 3.2. *Thermal transitions of trehalose dihydrate in standard crimped pans.*

Sample size; Scan rate	**Onset temperature (°C) (SD); Enthalpy (J/g) (SD)**			
1 mg, 10 °C/min	97.8 (0.1); 144.0 (9.1)	127.0 (0.7); 1.5 (0.9)	182.8 (2.7); -38.2 (20.0)	211.2 (0.2); 73.2 (14.9)
5 mg, 10 °C/min	96.5 (1.3); 159.1 (9.7)	113.6 (0.9); 125.4 (9.8)	196.5 (1.1); -8.9 (4.7)	209.6 (0.2); 110.7 (4.7)
1 mg, 100 °C/min	99.6 (0.7); 156.5(10.5)	130.0 (2.3); 17.0 (6.9)	168.7 (3.0); -0.9 (0.7)	210. 7 (0.3); 95.9 (3.4)
5 mg, 100 °C/min	99.3 (0.4); 149.3 (5.1)	126.2 (0.9); 174.2 (37.9)		208.6 (0.8); 125.8 (2.9)

3.3.2 RATE DEPENDENT DEHYDRATION BEHAVIOUR OF α,α-TREHALOSE DIHYDRATE

In Figures 3.6 and 3.7 typical HyperDSC profiles of trehalose dihydrate (using standard crimped pans at rate 100°C/min) are presented. For the small sample mass (1 mg) after the initial dehydration of T_h there is a broad endothermic event taking place around 130°C. This is attributed to the melt of the anhydrous T_α crystalline form, which could also be seen using this sample size at the lower scan rate (Figure 3.3). The transition is more evident at the higher scan rate. It is generally thought that HyperDSC is so fast that the sample will be unable to transform into new entities during the experiment (Pijpers et al., 2002). However we observed some evidence of the sample undergoing

the T_α form and clear evidence of the melt of the T_β. In contrast crystallisation is not easily detectable but was reproducibly measured around 170°C (Table 3.2). This exothermic event takes place at a lower temperature than seen with the slower scan rate (Figure 3.6 compared with Figure 3.3). The transitions show limited solid transition and limited crystallisation, hence, either the sample crystallises slowly (not detected by DSC) or some material converts to the β- form directly following loss of the dihydrate, route "C" in Figure 3.5.

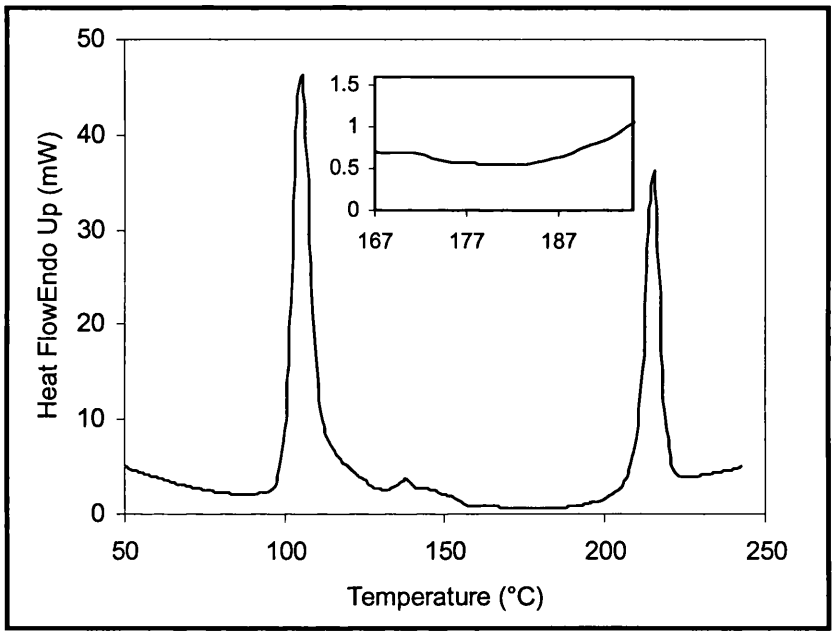

Figure 3.6. *Typical DSC profile of 1 mg trehalose dihydrate using standard crimped pans at 100 °C/min.*

For the 5 mg sample at 100 °C/min (Figure 3.7) a clear melt of the α-form is seen around 126 °C, which then through solid transition forms the β-form (melt around 208 °C). The transitions follow transformation pathway "A" in Figure 3.4. The data reported here differ from the previous literature, which indicates that increasing scan rates result in a loss of a detectable melt of the α-form. Samples either crystallise to the β-form without going through the T_α or crystallise to what Sussich et al. (2002) describe as the formation of the γ-form. These data indicate that within each sample some of the

material follows route "A", some route "B" and some route "C". The multiple pathways seem a better way to understand the complexity of the thermal transitions of trehalose.

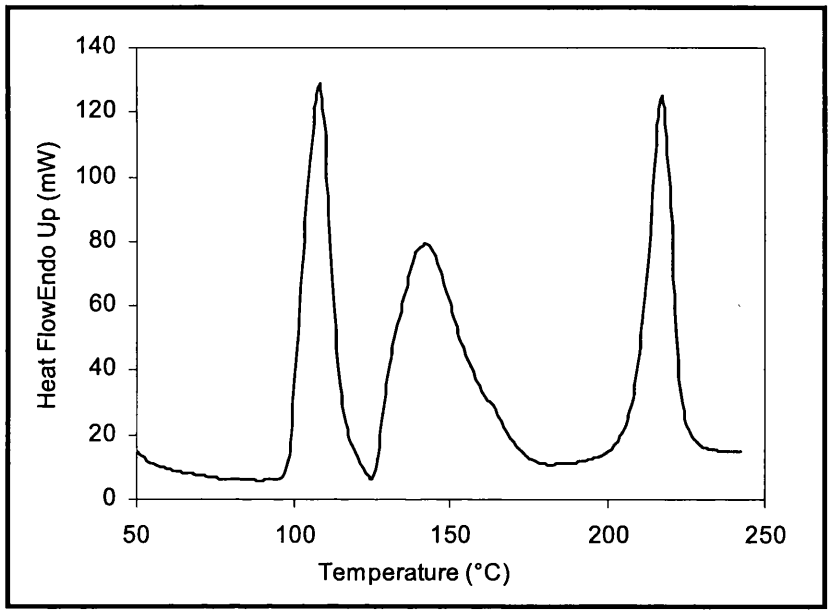

Figure 3.7. *Typical DSC profile of 5 mg trehalose dihydrate using standard crimped pans at 100 °C/min.*

When compared to the results obtained using a lower scan rate (10 °C/min) the findings do not support the same hypothesis. With a higher scan rate (100 °C/min) the dehydration process would be commencing earlier and hence an amorphous phase followed by a crystallisation to the anhydrate should be evident as suggested by Taylor et al. (1998). However, this does not seem to be the case, as we did not observe any significant crystallisation. Taylor et al. (1998) did not use such high dehydration rates in their study so these findings cannot be compared to their data. They did however establish that the dehydration process was dependent on the scanning rate. These researchers concentrated on the impact of particle size fractions whereas in the current study un-fractionated samples of trehalose dihydrate were used. The in house thermogravimetric analyser could not be used at high scan rates so the dehydration profile for 100 °C/min could not be produced and compared to the TGA profiles obtained at 10 °C/min. The TGA experiments were conducted to complement the

information on the dehydration process. The water loss was 9.58 % (± 0.19 %) from the initial weight using a rate of 10°C/min (Figure 3.8) corresponding to the loss of two water molecules. The maximum loss is seen between 100-120°C but small yet detectable amounts of weight loss can be seen up until 140°C. This differs from the DSC data where the large endothermic event is centred around 100°C.

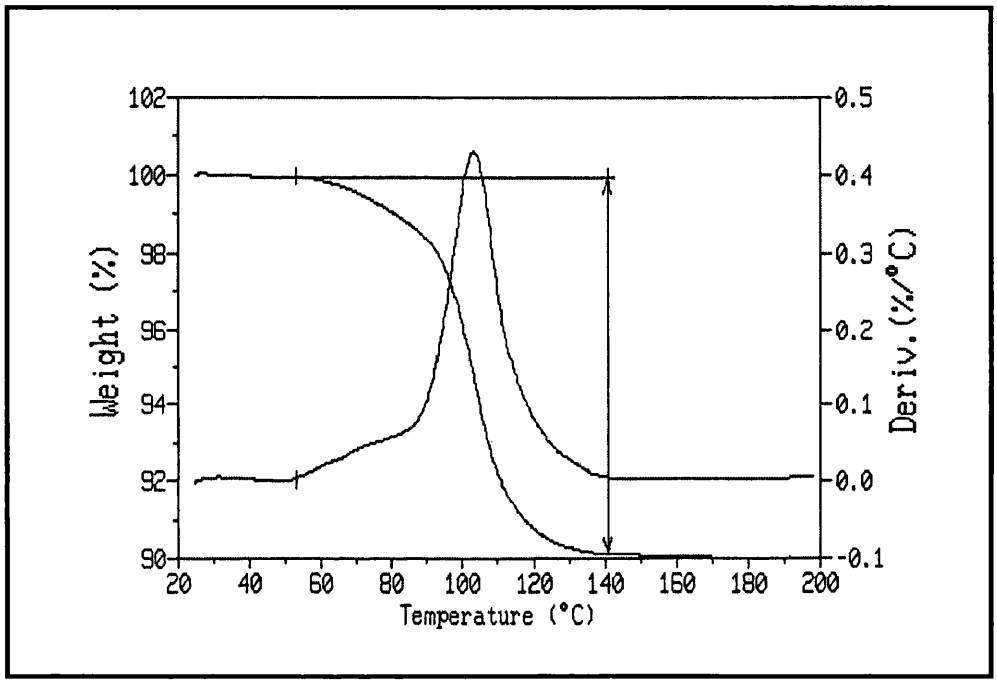

Figure 3.8. *Typical TGA trace of trehalose dihydrate at 10 °C/min.*

This can be explained by the fact that the TGA results do not exactly reproduce the DSC, as the experimental conditions are different. In DSC, the sample pan was crimped whereas in the TGA an open sample pan was used under nitrogen flux. It has been reported that the two water molecules of trehalose are not equivalent, which could explain the partial removal of water (Taga et al., 1972; Brown, 1972). These researchers have shown that molecules of α,α-trehalose and water are held together in the crystal by a complex system of twelve crystallographically independent hydrogen bonds. It is thought that one water molecule is tetrahedrally coordinated with four hydrogen bonds to the glucose ring while the other has a pyramidal coordination with three hydrogen bonds. This could explain the importance of the dehydration of trehalose dihydrate and

its impact on the polymorphic behaviour of trehalose. Although, further studies are required to extend the study of polymorphism of trehalose dihydrate to the hyperDSC region, as the impact of heating and the subsequent dehydration results in a different pattern than observed previously.

3.3.3 THE EFFECT OF WATER VAPOUR

Similar DSC studies were carried out using hermetically sealed pans where the melting of T_h occurs without the effusion of the water from the pans. The major difference to be observed here is the lack of significant peaks above 100 °C (Figure 3.9). Figures 3.9a and 3.9b show typical DSC profiles of the hermetically sealed pans at a rate of 10°C/min. A large endothermic peak is seen for both sample sizes just around 100°C followed by an exothermic event, which cannot be resolved from the first event.

This exothermic event is attributed to the crystallisation of the anhydrate (Taylor et al., 1998b). Taylor et al (1998b) suggest that the presence of water vapour in the DSC pan interacts with the anhydrate and causes some dissolution and prevents a melt (Shafizadeh et al., 1973). However, a broad endothermic event can be seen around 140 °C using a large sample size (Table 3.3), which could be the melt of the β-form. It is difficult to conclude anything about this endothermic event, as this could in fact also be a shift of the baseline. The hermetically sealed pans have a tendency to pop open during the DSC runs due to the increasing water vapour pressure in the pans at higher temperatures.

When a rate of 100°C/min was used (Figure 3.9c and d) the initial endothermic event was moved to a higher temperature and the exothermic event was not present. The large sample size also showed a broad endothermic event around 150°C, which can either be the melt of the β-form or just a baseline shift caused by the increasing vapour pressure of the water. Further studies need to be conducted to explain the behaviour of the released water vapour on the trehalose.

The results from the hermetically sealed pans cannot be compared to the results obtained from the crimped pans, as the water behaves in very different ways in these

two systems. However the differences highlight the importance and impact of water during thermal transitions of trehalose.

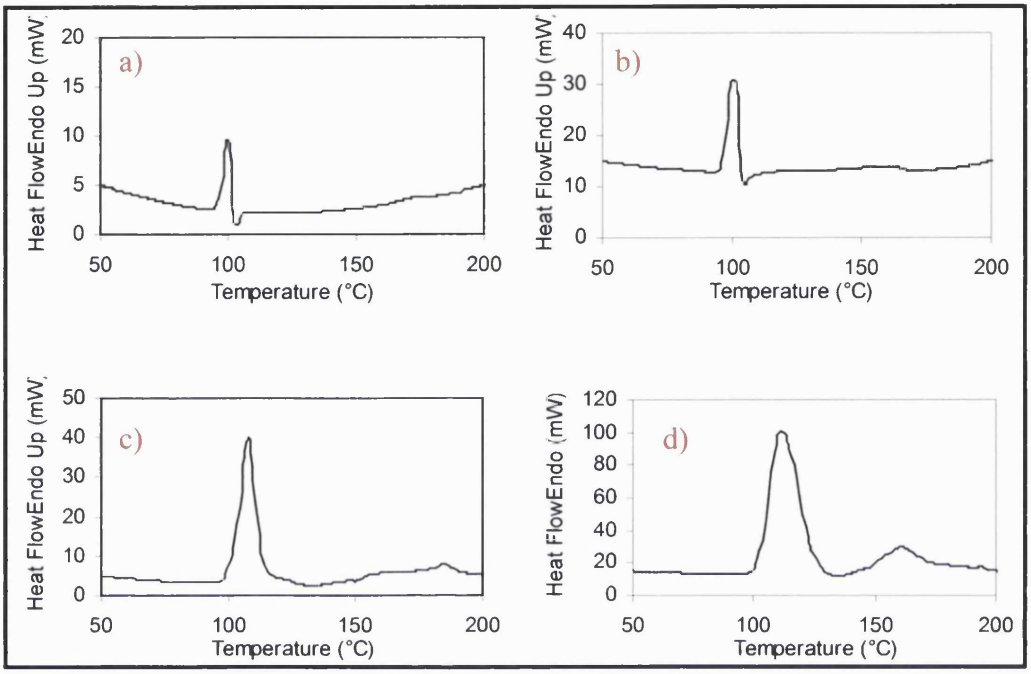

Figure 3.9. *Typical DSC profiles of trehalose dihydrate using hermetically sealed pans. Graphs a and b represent 1 and 5 mg samples at 10 °C/min, respectively. Graphs c and d represent 1 and 5 mg samples at 100 °C/min, respectively.*

Table 3.3. *Thermal transitions of trehalose in hermetically sealed pans.*

Sample size; Scan rate	**Onset temperature (°C) (SD); Enthalpy (J/g) (SD)**	
1 mg, 10 °C/min	97.0 (0.4); 159.5 (19.7)	
5 mg, 10 °C/min	95.7 (0.5); 112.9 (5.6)	141.7 (6.6); 19.6 (1.7)
1 mg, 100 °C/min	102.0 (0.1); 150.1(5.3)	
5 mg, 100 °C/min	103.2 (1.0); 145.9 (9.5)	148.9 (4.2); 23.1 (7.3)

3.4 CONCLUSIONS

This study was conducted to understand the polymorphic properties of trehalose. Trehalose was to be processed to produce spray-dried particles containing protein (chapters 5 and 6). During spray drying and processing of trehalose the different polymorphic forms may emerge and hence it is vital that the potential transitions are understood.

The study has indicated that the different DSC profiles for sample masses of 1 and 5 mg of trehalose dihydrate dehydrate in a similar fashion. However the 5 mg samples convert to the α-anhydrous form and then predominantly proceed through a solid transition (little or no crystallisation) to the β-anhydrous form, which then melts. The smaller sample (1 mg at 10 °C/min) undergoes dehydration to yield an amorphous material with only modest amount of the α-form, which then by solid transition and some crystallisation produces a smaller amount of β-form than is seen with the large sample masses. To summarise, it can be seen that for 1 and 5 mg at both scan rates there was a dehydration at just below 100 °C, however the subsequent transitions varied depending upon sample mass and scan rate. The data also showed that the different pathways could occur simultaneously to varying degrees. This may explain the occurrence of "new" reported forms in the literature (e.g. T_{κ}, Td etc.). These forms may be a result of two transformation pathways occurring at the same time whereby different physical forms of trehalose are being formed. The different physical forms of trehalose need to be re-examined and characterised with the theory of competing pathways in mind to ensure which of these forms are in fact "genuine".

These findings may have implications for the mechanism by which trehalose acts as a biostabiliser. However, from a pharmaceutical regulatory viewpoint it is essential that the physical structure of a formulation remains essentially unchanged over the shelf life of a product. Hence the generation of hydrate forms on storage of a product containing amorphous trehalose is unacceptable regardless of their bioprotective properties. Therefore it is essential to have an understanding of the interconnecting forms of the trehalose in order to comprehend its bioprotective properties and to facilitate in prediction of the solid-state changes that are likely to occur on product storage.

CHAPTER 4

Amorphous trehalose

4. AMORPHOUS TREHALOSE

4.1 INTRODUCTION

The purpose of this study was to evaluate the new spray dryer, SDMicro™ and to characterise amorphous trehalose. The SDMicro™ was especially commissioned for this project and considering that it had never been used in a UK university previously and less than ten units are in use in the UK, the initial commissioning and the evaluation of this unit was critical. As trehalose was to be the major component in the spray-dried protein/trehalose formulations, it was important to characterise spray-dried trehalose. The main purpose was initially to establish the general procedure for spray drying trehalose with the SDMicro™. Once commissioning and initial parameters were established the more complex systems, containing proteins would be examined (chapters 5 and 6).

4.1.1 SPRAY DRYING AND AMORPHOUS TREHALOSE

Spray drying of trehalose solutions produces amorphous material, which may be important for the biostabilisation of proteins. As discussed in chapter 3, the stabilising qualities of trehalose may in part be due to its ability to form hydrates (Aldous et al., 1995). The polymorphic forms of trehalose include the amorphous phase, which is readily converted to the crystalline form (Figures 3.1. and 3.5.). Hence it is important to study amorphous trehalose and its ability to convert into the different anhydrous forms, which may occur upon storage even though that is not a desirable trait from a pharmaceutical regulatory perspective. Furthermore, it is generally believed that the preparation method will affect the physicochemical properties and morphology of the amorphous material produced (Masters, 2002; Corrigan, 1995; Broadhead et al., 1992). Hence it is essential to establish reproducibility when preparing amorphous trehalose and other formulations using the SDMicro™.

The amorphous state of some sugars is believed to play an important role in the stabilisation of macromolecules. As previously highlighted in chapters 1 and 3, the amorphous carbohydrates have the characteristic to keep proteins within their glassy matrix (vitrification theory), thus retaining their tertiary structure (Crowe et al., 1998).

Also carbohydrates are capable of replacing the hydrogen bonds (water replacement theory), which are present in solution between proteins and water, yet again helping to protect the tertiary structure when dried (Crowe et al., 1993a; Crowe et al., 1993b). Aldous and colleagues have suggested that the ability of some carbohydrates (e.g. trehalose) to stabilise protein formulations during the drying process is due to the formation of hydrates upon crystallisation and removal of water from the remaining amorphous phase (Aldous et al., 1995). As discussed in chapter 3, trehalose possesses all of the required qualities needed to stabilise proteins. Hence it is important to study the amorphous form of trehalose separately to understand its role in systems containing protein.

4.2 EXPERIMENTAL PROTOCOLS

4.2.1 PRODUCTION OF SPRAY-DRIED TREHALOSE

Trehalose solutions (10 % w/v) were prepared by dissolving trehalose (10 g) in water (100 mL). Trehalose was spray-dried from purely aqueous solutions or from aqueous acetone. Formulations containing acetone were prepared in two steps. First the entire amount of trehalose was dissolved in water and then the appropriate amount of acetone was slowly added with constant stirring. All of the solutions were made to volume in volumetric flasks (100 ml). The SDMicro^{TM} was used to spray dry all of the batches. The spray-dried powder was collected in 100 ml containers which were stored at 0 % RH in vacuum desiccators containing P_2O_5. The operating parameters were changed in order to evaluate their possible effects on the characteristics of the spray-dried product (yield, morphology, water content etc.). Table 4.1 and 4.2 outline the prepared batches and the applied parameters.

Table 4.1. *The applied processing parameters for spray drying the aqueous trehalose solutions (10 % w/v).*

Batch	Chamber flow (Kg/h)	Nozzle flow (Kg/h)	Inlet temperature (°C)	Outlet temperature (°C)
1	25–	2.5–	95–	60–
2	25–	2↓	95–	60–
3	25–	3↑	95–	60–
4	25–	2.5–	105↑	60–
5	25–	2.5–	85↓	60–
6	25–	2.5–	85↓	50↓
7	25–	2↓	85↓	50↓
8	25–	3↑	85↓	50↓
9	30↑	3↑	95–	60–
10	20↓	2↓	95–	60–
11	30↑	1↓	95–	60–

↑ Increase in the shown parameter
↓ Decrease in the shown parameter
– No change in the parameter.

Table 4.2. *The applied processing parameters for spray drying the aqueous acetone trehalose solutions (10 % w/v).*

Batch	water: acetone ratio	Chamber flow (Kg/h)	Nozzle flow (Kg/h)	Inlet temperature (°C)	Outlet temperature (°C)
12	4:1	25–	2.5–	95–	60–
13	1:1	25–	2.5–	95–	60–
14	4:1	25–	2.5–	90↓	55↓
15	4:1	20↓	2↓	90↓	55↓
16	4:1	27↑	2.7↑	90↓	55↓
17	4:1	30↑	2.5–	70↓	50↓
18	4:1	30↑	2.7↑	60↓	45↓

↑ Increase in the shown parameter
↓ Decrease in the shown parameter
– No change in the parameter.

4.2.2 X-RAY POWDER DIFFRACTION (XRPD)

X-ray diffractions (XRPD) were performed on all of the spray-dried powders as described in section 2.5. This was done in order to ensure that the spray-dried powders were amorphous. The XRPD were performed in three replicates on each batch to confirm reproducibility.

4.2.3 SCANNING ELECTRON MICRSOSCOPY (SEM)

Scanning electron microscopy (SEM) was carried out on all of the spray-dried powders as described in section 2.6. This was done in order to investigate the particle morphology and to get an estimation of the particle size.

4.2.4 THERMOGRAVIMETRIC ANALYSIS (TGA)

Moisture content of the spray-dried powders was measured using thermogravimetric analysis (TGA). The data were collected as described in section 2.4 for each batch in three replicates.

4.2.5 DIFFERENTIAL SCANNING CALORIMETRY (DSC)

The glass transitions of the spray-dried trehalose powders were detected using differential scanning calorimetry (DSC). Pyris 1 was used to collect modulated DSC data as described in section 2.3. The Tg value was measured three times for each batch to ensure reproducibility.

4.2.6 DYNAMIC VAPOUR SORPTION AND NEAR INFRARED SPECTROSCOPY (DVS-NIRS)

The data were collected using the DVS-1 system (dynamic vapour sorption) fitted with an optical reflectance NIR probe (section 2.8). Approximately 30-60 mg of the spray-dried trehalose samples were weighed onto the flat glass sample pan. To study the crystal transitions, the DVS was programmed to run at 0 % RH for 8 h, 75 % RH for 10 h and finally 0 % RH for 6 h. All experiments were run at 25 °C. The fibre optic probe (Foss NIR Systems, Cheshire, UK) was positioned 3-4 mm under the sample pan of the DVS. The spectra were recorded over the infrared wavelength range 1100-2500 nm every 15 min. All measurements were a mean of 32 scans over 40 s (resolution of 2 mm) and the reference signal was obtained from a ceramic tile. NIR data were collated during DVS experiments. NIR data processing and analysis were carried out using

Vision ® for Windows version 2.51. The standard SNV 2nd-derivative NIR spectra were compared visually to identify the occurring changes. Further analysis was carried out by importing the SNV 2nd-derivative spectra into a chemometric software package, Unscrambler® version 7.6, whereby the areas giving rise to the largest amount of changes can be highlighted (section 2.7). The data relating to this change were then presented as a score plot, which showed how different the samples were from one another. A loading plot was also created, which showed where in the data the changes were occurring within each spectrum.

4.3 RESULTS AND DISCUSSION

The influences of the process variables of the SDMicro™ were studied with regards to particle size, particle morphology, moisture content and crystallisation qualities. Process validation of the equipment was conducted by examining the effects of the various parameters (temperatures, nitrogen flow etc.) on the spray-dried powders.

All the batches were spray-dried with the process parameters listed in Tables 4.1 and 4.2. All of the batches were spray-dried at least three times to estimate reproducibility. The yield of the spray-dried powders was the major problem encountered during these experiments. Trehalose proved to be very static and a large portion of the dried powders was adsorbed to the large surface area between the cylinder and collecting vessel within the spray dryer. The yields were not always reproducible and varied from less than 10 % and up to 50 %. Higher amounts of trehalose solutions could have been spray-dried to increase the amount of the final product. However trehalose was later to be used in protein formulations (chapter 5 and 6) where due to cost it would not be practical to spray dry large quantities. It was therefore important to gauge the spray drying process using smaller volumes of trehalose. Once the powders were produced, the collection jars were stored at 0 % RH. Amorphous content was confirmed by XRPD.

The SEM images were obtained to determine if processing parameters influenced particle morphology and to obtain an estimation of the particle size. The SEM images required a small amount of sample and hence provided a practical way to estimate particle morphology and size. It is important to remember that SEM images only illustrate a small part of the batch and thus may not always represent the entire batch. At

the time of the study, the Mastersizer was not available to determine the particle size. Hence SEM images were used to estimate the particle size. TGA measurements were also performed to study the influence of the various processing parameters on the residual moisture content.

Considering the complex and interconverting polymorphic forms of trehalose described in chapter 3, it was necessary to understand the nature of the crystallisation of trehalose from the amorphous spray-dried form of this disaccharide. This was achieved by using DVS/NIR to examine the crystallisation process. The data were compared to the NIR spectra of the various anhydrous forms of trehalose that were provided by Moran (2004).

4.3.1 MORPHOLOGICAL VARIATIONS IN AQUEOUS SYSTEMS

The starting process parameters for spray drying trehalose (Batch 1) were selected on the basis of trial, error and experience. The process parameters were readily achieved on the SDMicro™ and reproducibly gave amorphous powders with a narrow particle size distribution as determined by SEM (Figure 4.1). Smooth surfaced particles of approximately 5 μm were produced using these parameters (Table 4.1). Different batches were prepared to test the reproducibility of spray drying with the SDMicro™ and to ensure that the instrument settings were the most favourable. Once the starting parameters were chosen, the relationship between some of the processing variables (chamber flow, nozzle flow, inlet temperature and the outlet temperature) and the resulting powder characteristics were investigated (Tables 4.1). The effects of variation of process parameters on particle morphology were of primary importance for this study.

Each spray-dried batch was evaluated by XRPD to determine its amorphous content (Figure 4.2). The amorphous nature of the spray-dried trehalose powders was also confirmed by modulated DSC, where a Tg value was observed at approximately 120 °C confirming the literature values (Sussich et al., 2001). Modulated DSC was used in order to see an unambiguous glass transition temperature. This method ensured the removal of water, which could plasticize the sample and change/depress the Tg value (Figure 4.3). The water content was also measured using TGA and a typical thermogram can be seen in Figure 4.4 and the values are listed in Table 4.3.

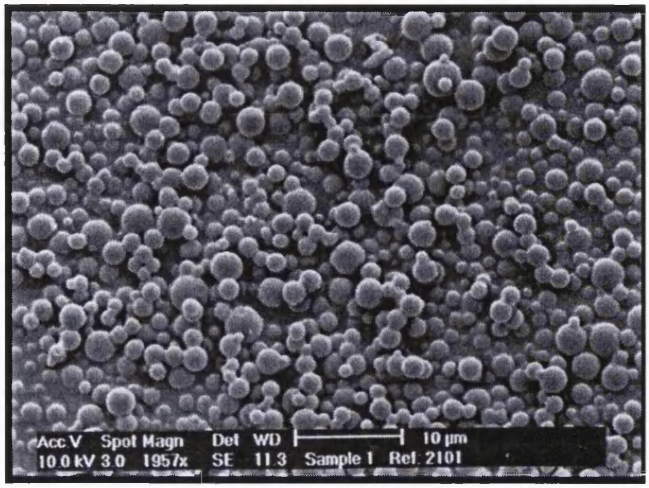

Figure 4.1. *SEM image of spray-dried amorphous trehalose (10 % w/v) (Batch 1).*

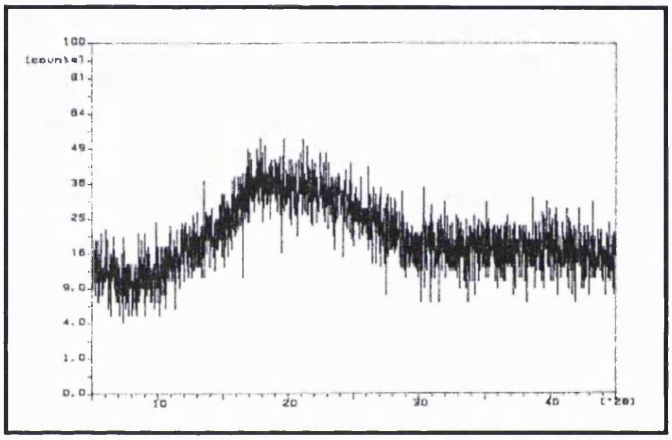

Figure 4.2. *A typical X-ray diffraction pattern of spray-dried amorphous trehalose.*

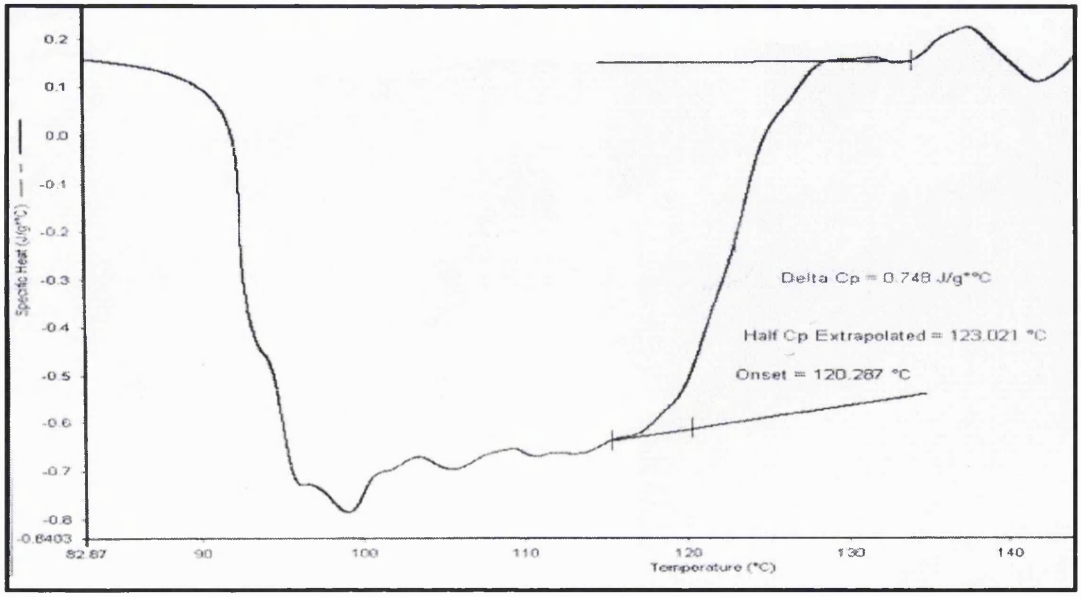

Figure 4.3. *A typical DSC thermogram showing Tg of amorphous trehalose.*

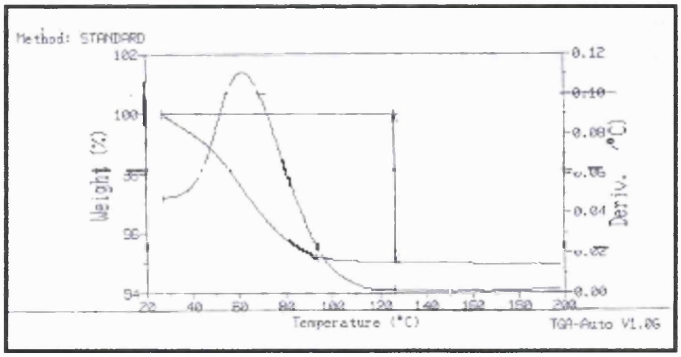

Figure 4.4. *A typical TGA thermogram of spray-dried trehalose.*

Table 4.3. *Water content (%) of the spray-dried Batches presented in Table 4.2 using TGA.*

Batch	Residual water content (%) ± S.D.
1	2.4 (0.42)
2 ↓ nozzle flow	3.3 (0.38)
3 ↑ nozzle flow	4.7 (0.45)
4 ↑ inlet temperature	4.0 (0.54)
5 ↓ inlet temperature	3.1 (0.52)
6 ↓ inlet temperature ↓ outlet temperature	4.6 (0.61)
7 ↓ nozzle flow ↓ inlet temperature ↓ outlet temperature	3.4 (0.48)
8 ↑ nozzle flow ↓ inlet temperature ↓ outlet temperature	3.8 (0.54)
9 ↑ chamber flow ↑ nozzle flow	2.4 (0.46)
10 ↓ chamber flow ↓ nozzle flow	2.2 (0.36)
11 ↑ chamber flow ↓ nozzle flow	4.1 (0.44)

4.3.1.1 Nozzle flow

In order to investigate the influences of nozzle flow (Kg/h), this processing parameter was changed while keeping all other parameters constant. The nitrogen flow through the nozzle was varied in Batches 2 and 3 (Table 4.2). By decreasing the nozzle flow (Batch 2) smooth surfaced particles were produced (Figure 4.5a). In contrast, an increase of the nozzle flow (Batch 3) resulted in particles that appeared almost melted or fused together (Figure 4.5b). This highlights the importance of the nozzle flow as the amount of nitrogen flowing through the nozzle influences the atomisation process and indirectly the solution feed rate.

Decreasing the nitrogen nozzle flow (Batch 2) while keeping all other operating conditions constant resulted in a decrease of the solution feed rate and prolonged the atomisation process time and hence the droplet generation time. Due to the lower nitrogen flow the nitrogen velocity in the nozzle head was lowered resulting in a non-homogenised droplet formation, which in turn results in a wider particle size distribution. An increase of the nitrogen flow (Batch 3) through the nozzle increased the solution feed rate. This created a coarse spray and resulted in insufficient time for the atomisation process to be completed. Hence a wet product due to inadequate drying was produced.

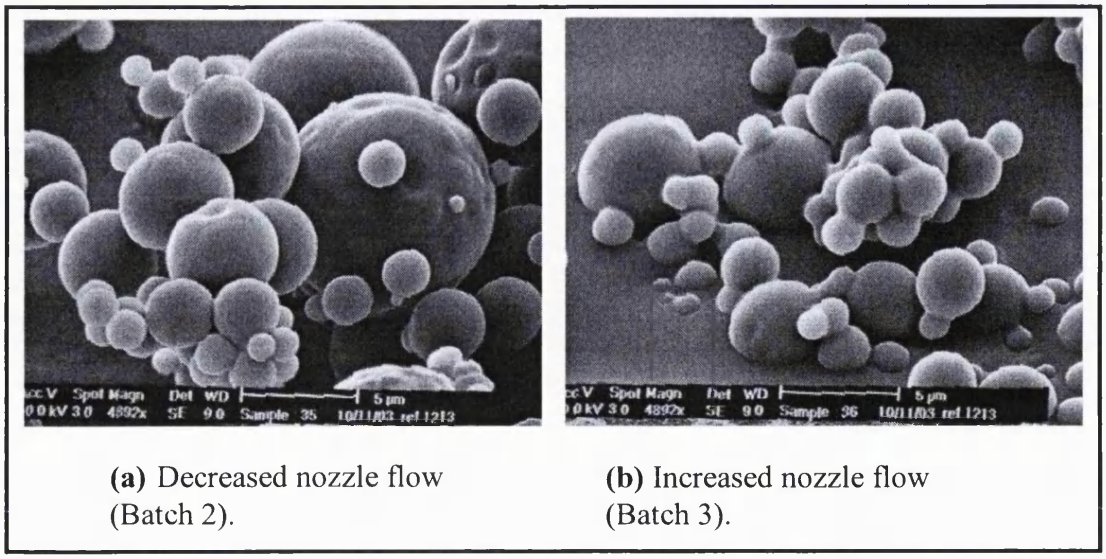

(a) Decreased nozzle flow (Batch 2).

(b) Increased nozzle flow (Batch 3).

Figure 4.5. *SEM images of Batches 2 and 3, portraying the influence of nozzle flow on particle morphology.*

The moisture content of these powders compared to the starting batch (Batch 1) also showed the effects of nozzle flow (Table 4.3). By increasing the nozzle flow (Batch 3) a TGA value of 4.7 % (± 0.45) was observed. This is double the value obtained from Batch 1 (Table 4.3). Hence, moisture content, particle morphology and particle size can all be affected by the nozzle flow and therefore it is an important parameter to control in order to achieve the desired particle characteristics.

4.3.1.2 Inlet temperature

The effects of inlet temperature were investigated while keeping all other processing parameters constant (Figure 4.6). By increasing the inlet temperature (Batch 4), the drying process occurs quickly and the solution feed rate is increased as more solution is pumped through in order to maintain the outlet temperature. The solution feed rate was also increased by the increase in nozzle flow (Batch 3), resulting in fused and wet particles. The increase in the solution feed rate by increasing the inlet temperature (Batch 4) was not enough to produce wet particles. In contrast, a decrease of the inlet temperature (Batch 5) resulted in a slower solution feed rate and moisture content of 3.1 % (± 0.52) (Table 4.3). Hence even though no major difference can be seen in the particle morphology by manipulating the inlet temperature the effect on the moisture content is evident.

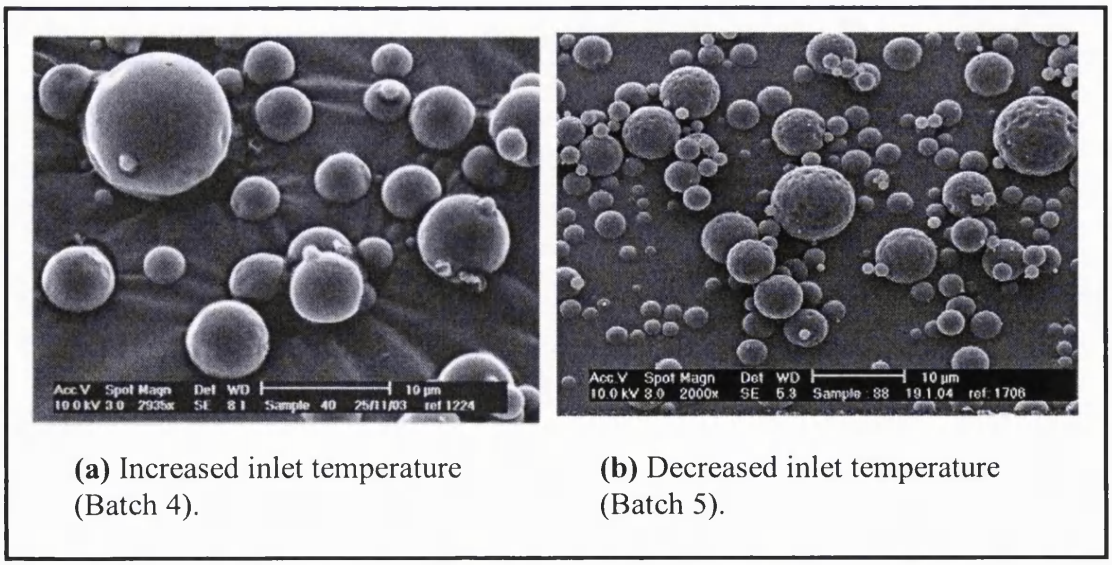

(a) Increased inlet temperature (Batch 4).

(b) Decreased inlet temperature (Batch 5).

Figure 4.6. *SEM images of Batches 4 and 5, portraying the influence of inlet temperature on particle morphology.*

4.3.1.3 Outlet temperature

In spray drying all the processing parameters are either directly or indirectly influenced by each other. As seen in the previous sections, a change in the inlet temperature affected the solution feed rate to maintain the outlet temperature. Thus the outlet temperature was manipulated along with the inlet temperature to investigate their combined influence on the particle morphology (Batch 6). A decrease in both of these temperatures resulted in particles that were fused together even though the solution feed rate remained the same. The fused particles are due to the higher moisture content, 4.6 % (± 0.61) (Table 4.3), caused by the decrease in the outlet temperature (Figure 4.7).

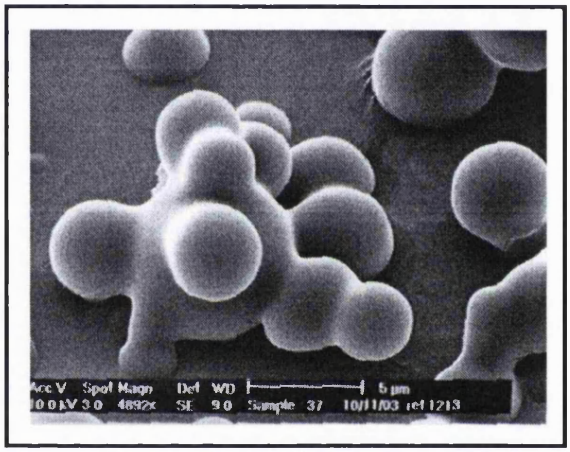

Figure 4.7. *SEM image of Batch 6, portraying the influence of decreased inlet and outlet temperatures, on particle morphology.*

The outlet temperature seems to have a greater influence on particle morphology than the inlet temperature. This was further investigated in Batches 7 and 8 where the impact of temperature and nozzle flow were studied together. The inlet and outlet temperatures were decreased and the nozzle flow was varied (Batches 7 and 8). When the nitrogen flow through the nozzle was decreased while decreasing the inlet and the outlet temperatures (Batch 7), large particles were produced (Figure 4.8a). In comparison an increase of the nitrogen flow through the nozzle combined with decreased inlet and outlet temperatures (Batch 8) resulted in comparatively smaller particles (Figure 4.8b). The TGA values do not show any major differences in the moisture content (Table 4.3).

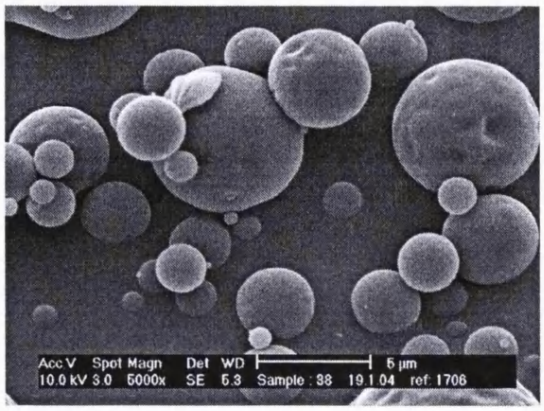

(a) Decreased nozzle flow with decreased inlet and outlet temperatures (Batch 7).

(b) Increased nozzle flow with decreased the inlet and outlet temperatures (Batch 8).

Figure 4.8. *SEM images of Batches 7 and 8, portraying the influence of decreased inlet and outlet temperatures combined with varying nozzle flow on particle morphology.*

4.3.1.4 Chamber flow

The effect of nitrogen flow in the nozzle and the chamber was investigated. The particles produced (Batches 9 and 10) did not display any significant differences in morphology. The ratio between the chamber and nozzle flow was kept constant during both experiments (Table 4.3). This resulted in the same solution feed rate and therefore no major changes can be seen in the particle morphology or moisture content (Figure 4.10a and b and Table 4.3). Hence the particles and moisture content are very similar to the ones produced by Batch 1 (Figure 4.1).

Another experiment was carried out where the nitrogen flow through the chamber was increased while decreasing the nitrogen flow through the nozzle (Batch 11). Comparatively larger particles with a larger distribution were produced using this setting (Figure 4.10c). This highlights the importance of the ratio between the chamber and nozzle flow, which also indirectly controls the solution feed rate.

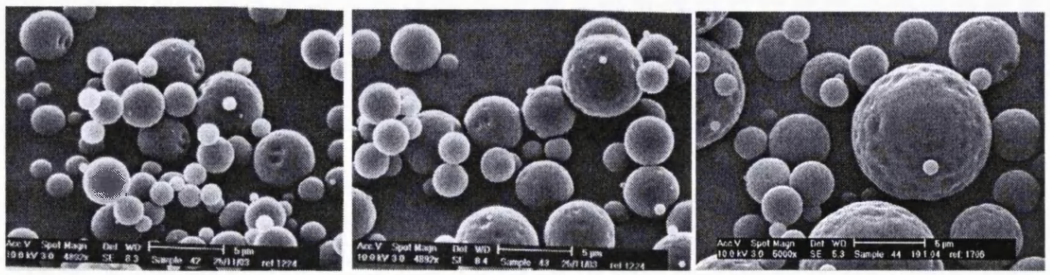

(a) Increased chamber and nozzle flow (Batch 9).

(b) Decreased chamber and nozzle flow (Batch 10).

(c) Increased chamber and decreased nozzle flow (Batch 11).

Figure 4.9. *SEM images of Batches 9, 10 and 11, portraying the influence of the ratio between chamber and nozzle flow, on particle morphology.*

4.3.2 MORPHOLOGICAL VARIATIONS IN AQUEOUS ACETONE SYSTEMS

Trehalose was spray-dried from blends of water and acetone. This was done in order to investigate the influence of acetone on particle morphology and to examine a simple, Class 3, water miscible organic solvent on the SDMicro™. Class 3 solvents do not have any absolute limits on the residual levels in the finished product and are considered safe by the Food and Drug Administration and the European Agency for the Evaluation of Medicinal Products. This was also important with regards to the studies performed later where aqueous acetone was used to spray dry protein formulations (chapters 5 and 6). Batches 12 to 18 were produced using aqueous acetone as described in Table 4.2. The acetone solutions encountered yield problems during preparation. The acetone seemed to contribute to the electrostatic nature of trehalose and hence the yields were extremely low (less than 15 %). Only SEM images and X-ray diffraction data could be obtained due to low yields.

Trehalose was spray-dried from a 4:1 and 1:1 (v/v) ratio of water and acetone (Batches 12 and 13) using the starting parameters for Batch 1 (Tables 4.1 and 4.2). No significant difference was observed due to aqueous acetone ratios. Both Batches were amorphous but the high amounts of acetone seemed to reduce the particle size slightly. The main difference between these particles prepared from aqueous acetone compared to particles spray-dried from water is the almost swollen nature of the particles and among them the

almost collapsed particles. This is associated with the rapid drying process causing "balloon formation" and hardening of the particle surface that subsequently leads to expansion of trapped moisture (Masters, 1991). The rapid drying is caused due to a decrease in the water content of the prepared solutions as compared to the previous study. Large amounts of acetone were not desirable as precipitation could be seen while preparing Batch 13. Hence the rest of the formulations were spray-dried from low acetone content (20 % v/v).

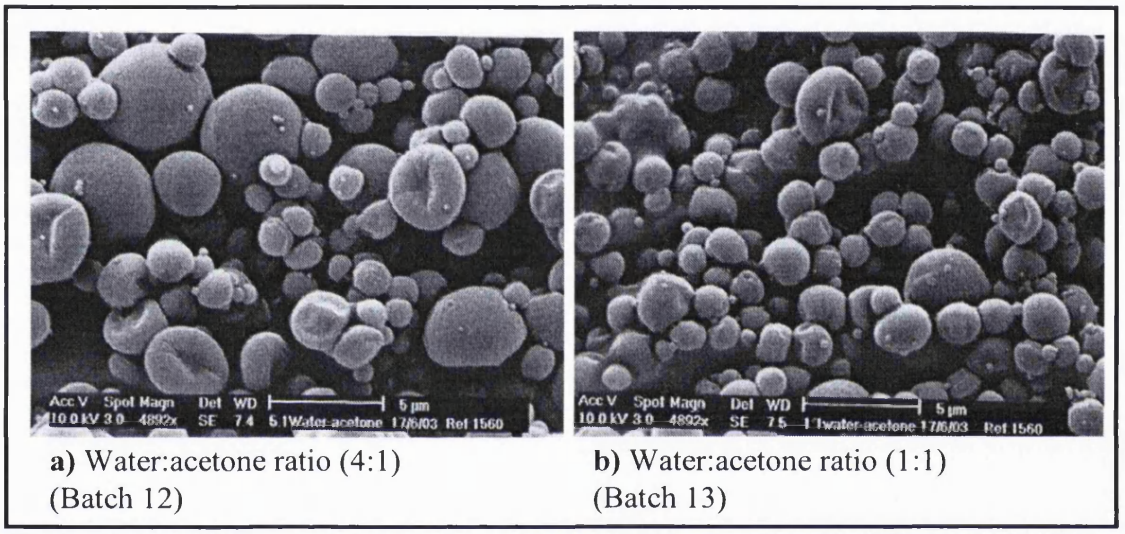

a) Water:acetone ratio (4:1) (Batch 12)

b) Water:acetone ratio (1:1) (Batch 13)

Figure 4.10. *SEM images of Batches 12 and 13, portraying the influence of aqueous acetone on particle morphology.*

4.3.2.1 Temperature and nitrogen flow

As already established in the previous section, all the parameters have an influence on the solution feed rate, which contributes to changes in particle characteristics. Initially the inlet and outlet temperatures were decreased while keeping all other parameters constant (Batch 14). Similar settings used of aqueous solution had produced particles that were fused together and showed high moisture content (Batch 6, Figure 4.7). This was not the case when spray drying from a solution containing acetone (20 % v/v). Here the decrease of the temperature was not enough to increase the moisture content as the formulation contained less water due to the addition of acetone.

Next the nitrogen flow through the chamber and the nozzle were decreased while simultaneously decreasing both the inlet and the outlet temperatures (Batch 15) (Figure 4.11a). The changes in the processing parameters did not have an impact on the solution feed rate. In contrast, by increasing the nitrogen flow through the chamber and nozzle while decreasing the inlet and outlet temperatures (Batch 16) fused particles were produced. This setting provided an adequate increase of the solution feed rate and did not allow sufficient time for the atomisation process to be completed. Hence wet and fused particles were produced (Figure 4.11b).

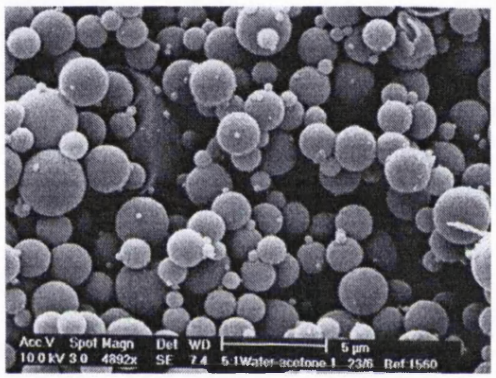

(a) Decreased chamber and nozzle flow along with decreased inlet and outlet temperatures (Batch 15).

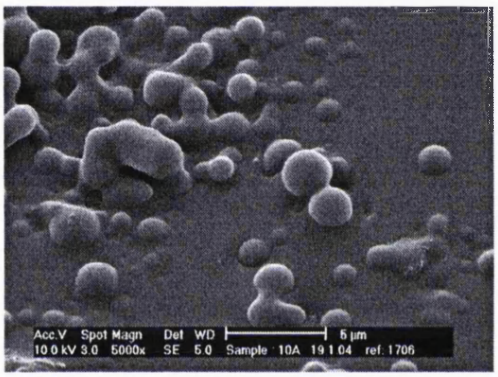

(b) Increased chamber and nozzle flow along with decreased inlet and outlet temperatures (Batch 16).

Figure 4.11. *SEM images of Batches 15 and 16, portraying the influence of nitrogen flow and temperatures on particle morphology.*

The Batches prepared from aqueous acetone contain less water than the Batches prepared from water alone. Hence the temperatures were lowered further while the nitrogen flow was increased. This is the only way the desired temperatures could be achieved. Lowering the inlet and the outlet temperatures to 70°C and 50°, respectively while the nitrogen chamber flow was increased resulted in Batch 17 (Figure 4.12a). The self-binding effects between the very small particles could be the cause of the agglomeration seen in the SEM image. The solution feed rate was decreased due to the low temperatures, which resulted in prolonged atomisation process time and droplet generation time with a wider particle size distribution. When the temperatures were

lowered further while both the nitrogen chamber and nozzle flow were increased smooth surface particles were produced with a wide particle size distribution, (Batch 18) (Figure 4.12b). The increase of the nozzle flow results in a balanced solution feed rate compared to Batch 17 but it also increases the particle size.

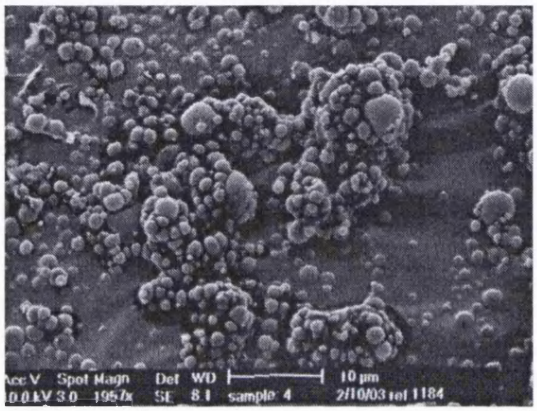

(a) Increased chamber flow along with decreased inlet and outlet temperatures (Batch 17).

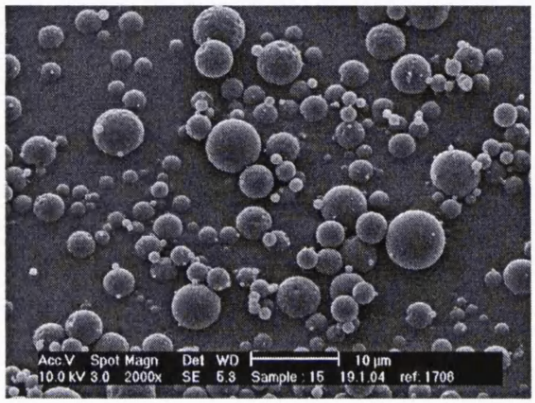

(b) Increased chamber and nozzle flow along with and decreased inlet and outlet temperatures (Batch 18).

Figure 4.12. *SEM images of Batches 17 and 18, portraying the relationship between nitrogen flow and temperatures and their impact on particle morphology.*

Spray drying aqueous acetone compared to water only solutions results in different particle characteristics. The parameters used to manipulate these particle characteristics can also react very differently depending on the solution. Hence it is important to establish what particle characteristics are desired and what settings would provide these particles. It was noted that the most reproducible results were achieved when spray drying with chamber nitrogen flow of 25 Kg/h, nozzle nitrogen flow of 2.5 Kg/h, inlet temperature of 95 °C and outlet temperature of 60 °C. These parameters were used to produce Formulation 1 and 12, resulting in smooth surface particles. The same parameters were used later to spray dry protein formulations (chapters 5 and 6).

4.3.3 CONCLUSIONS: MORPHOLOGICAL VARIATIONS AND PROCESSING PARAMETERS

The following conclusions can be made from the studies conducted in sections 4.3.1 and 4.3.2:

- The processing parameters of the SDMicro^{TM} are influenced in measurable ways.

- The solution feed rate seems to be related directly/indirectly to all of the processing parameters and influences the particle morphology and moisture content the most.

- Acetone can be successfully used to produce amorphous trehalose particles although the yields were reduced due to the presence of acetone in the solution.

4.3.4 ANALYSIS OF THE CRYSTALLISATION TRENDS OF SPRAY-DRIED TREHALOSE

Gravimetric studies on solid trehalose batches that were spray-dried from aqueous solutions, were conducted using a humidity and temperature-controlled microbalance, Dynamic Vapour Sorption (DVS), as described in section 4.2.6. The aim was to investigate the crystallisation of amorphous trehalose at 75% RH to simplify the analysis of the more complicated systems containing protein and surfactants. The crystallisation trends were also studied in regards to the polymorphic forms of trehalose discussed in chapter 3. As already established in the previous chapter there is an intrinsic relationship between the interconversion of the polymorphic forms. Crystallising amorphous trehalose and then comparing the NIR data to the NIR data for the various physical forms of trehalose, was designed to investigate this relationship. Moran (2004) provided the NIR data for the various anhydrous forms (T_α, T_β, and Td), which were then compared to the crystallisation data collected from the gravimetric studies. The NIR data could not be collected for the trehalose solutions containing acetone, as there was not sufficient sample.

4.3.4.1 NIR spectra of the different forms of trehalose

The physical forms of trehalose discussed in this section are the amorphous form, the crystalline form, the α-anhydrous form, the β-anhydrous form and the Td anhydrous form. Near infrared spectra were recorded for the amorphous and dihydrate trehalose forms and were compared to the spectra of the alpha, beta and Td-anhydrous forms provided by Moran (2004).

Figure 4.13 shows the collated spectra for all of the proposed forms of trehalose. It is evident from Figure 4.13 that most regions of these spectra overlap. The spectrum for amorphous trehalose is distinctive for its lack of sharp peaks. The term "peak" when discussing near infrared spectra, is used to describe downward pointing troughs corresponding to mathematically treated SNV normalised, second derivative spectra. The spectrum for amorphous trehalose was then subtracted from all of the different forms of trehalose in order to highlight the differences between the anhydrous/crystalline forms (Figure 4.14).

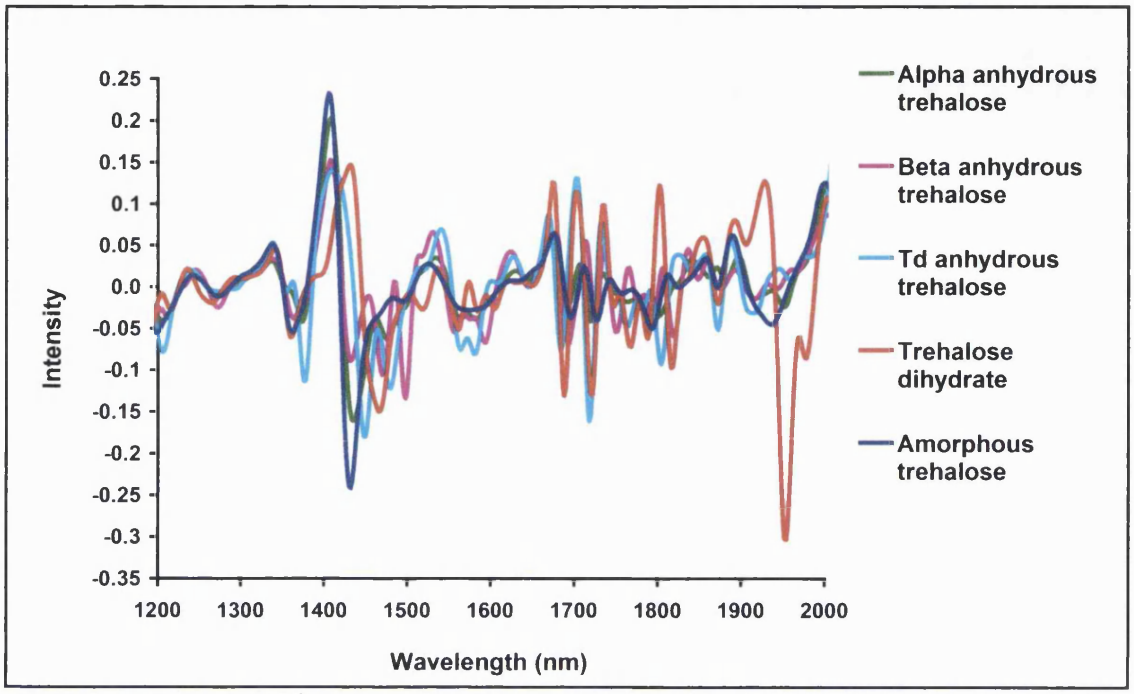

Figure 4.13. *SNV-2nd derivative NIR spectra (between 1200-2000 nm) of the α-anhydrous, β-anhydrous, Td-anhydrous, trehalose dihydrate and amorphous trehalose forms.*

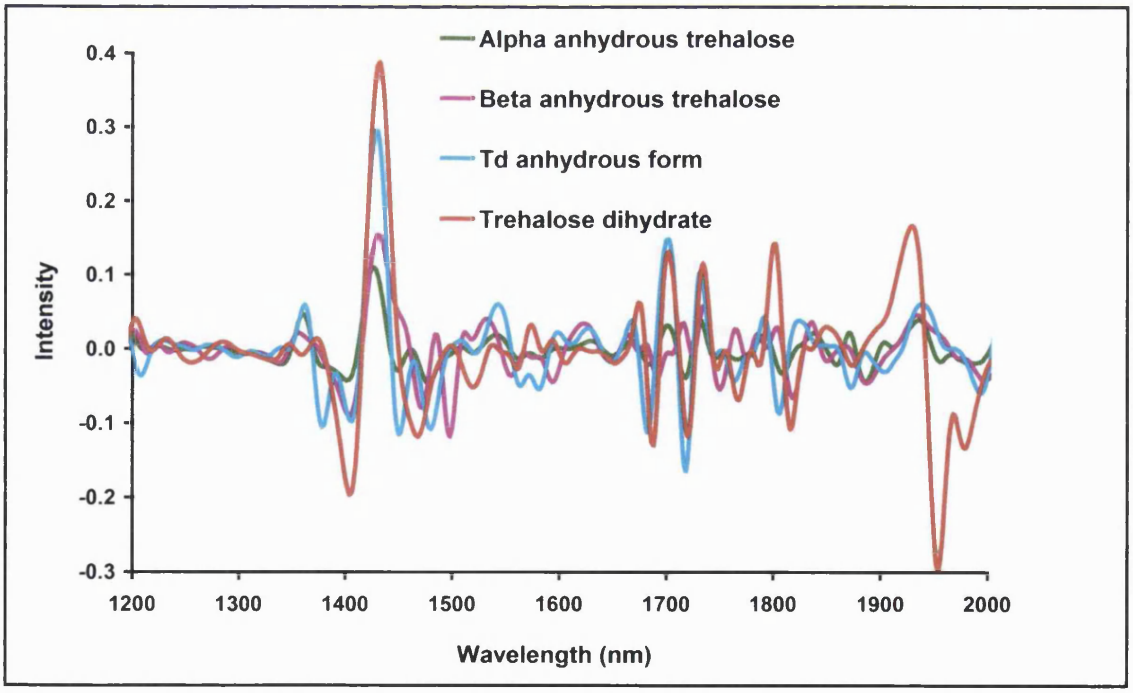

Figure 4.14. *SNV-2nd derivative NIR spectra (between 1200-2000 nm) of the α-anhydrous, β-anhydrous, Td-anhydrous and trehalose dihydrate forms after subtracting the amorphous spectrum from the different forms of trehalose.*

The amorphous and crystalline trehalose forms have overlapping spectra, which makes assignment of the specific identifying peaks very difficult. As a final attempt to determine the specific identifying peaks of the various physical forms the spectra of trehalose dihydrate were subtracted from the alpha, beta and Td forms (Figure 4.15).

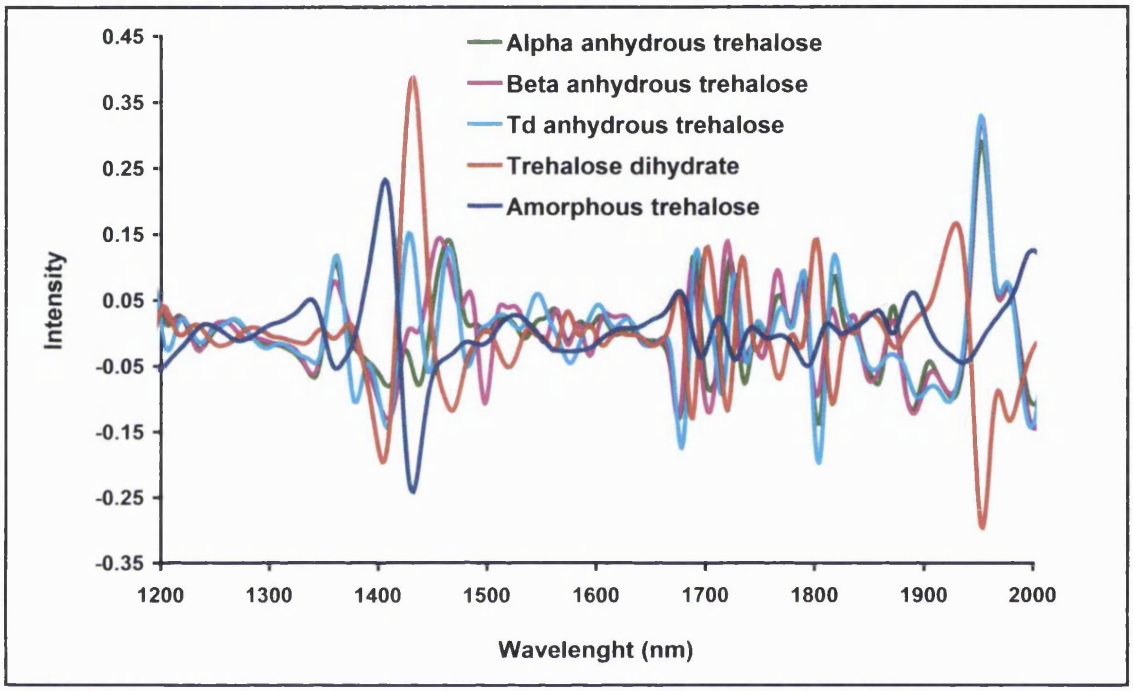

Figure 4.15. *SNV-2nd derivative NIR spectra (between 1200-2000 nm) of the α-anhydrous, β-anhydrous and Td-anhydrous forms subtracted of the amorphous and crystalline spectrum. The dihydrate form presented is subtracted from the amorphous form.*

Moran (2004) studied the various physical forms of trehalose and compiled a table containing the most important wavelengths based on visual differences between the different forms using the Vision® software (Table 4.4). The NIR spectra was only used between 1100 and 2200 nm, as above these wavelength the spectra displayed disturbances. The diagnostic peaks for the various forms obtained here are slightly different than those identified by Moran (2004). This is due to the subtractions conducted on the spectra. The spectra presented in Figure 4.15 have been separated into regions for clarity and are presented through Figures 4.16 to 4.18.

Table 4.4. *Assignment of the diagnostic peaks in the NIR spectrum between 1100-2000 nm for the physical forms of trehalose. The shaded cells contain the identifying peaks assigned by Moran (2004).*

α,α-Trehalose dihydrate (T_h)	α-anhydrous trehalose (T_α)	β-anhydrous trehalose (T_β)	Td anhydrous trehalose	Amorphous trehalose (T_{am})
1954/1980 (Figure 4.19)	No specific peaks could be assigned	**1498** (Figure 4.17) **1552** (Figure 4.18) **1594** (Figure 4.18)	**1380** (Figure 4.16) **1482** (Figure 4.17)	1936 (Figure 4.19)
1954/1978	1860/1882	1556/1594	1376 1480 1804	1936

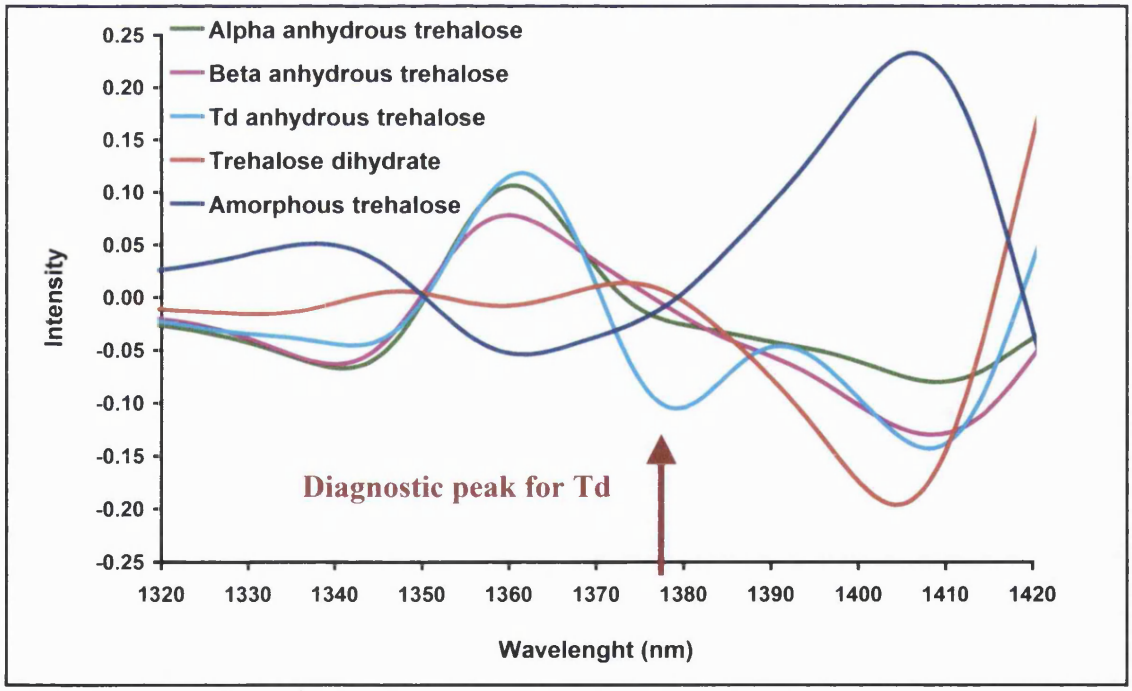

Figure 4.16. *SNV-2nd derivative NIR spectra (between 1320-1420 nm) of the physical forms of trehalose presented in Figure 4.15. The arrow indicates the diagnostic peak for Td around 1380 nm.*

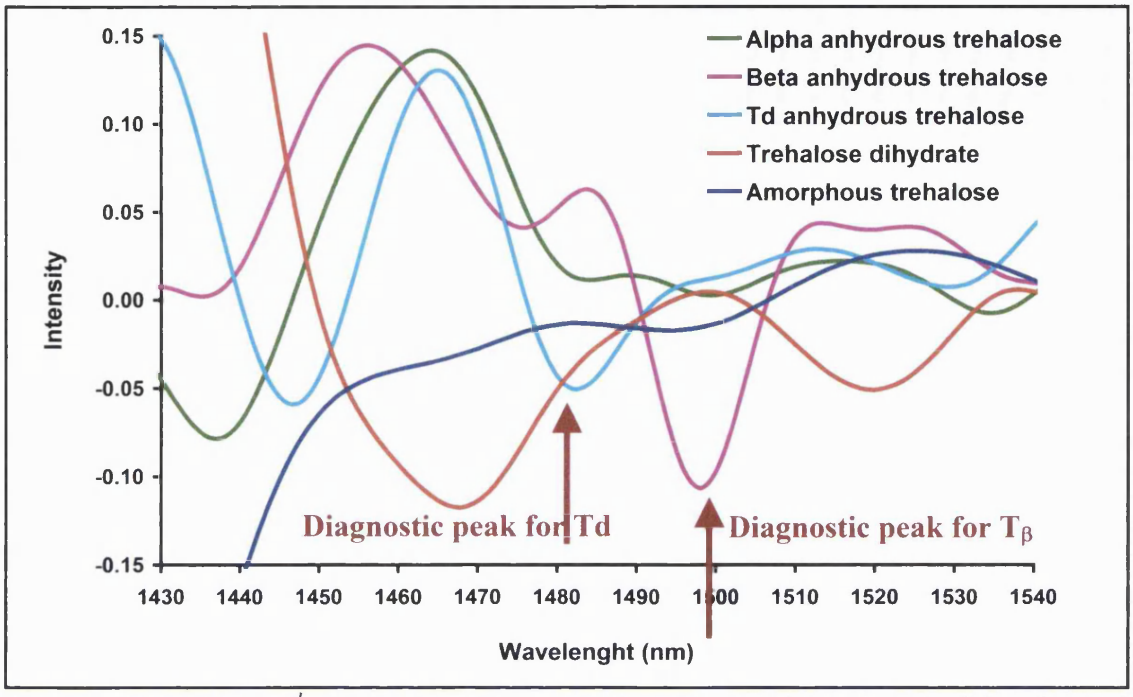

Figure 4.17. *SNV-2nd derivative NIR spectra (between 1430-1540 nm) of the physical forms of trehalose presented in Figure 4.15. The arrows indicate the diagnostic peaks around 1480 nm and 1498 nm for Td and T_β, respectively.*

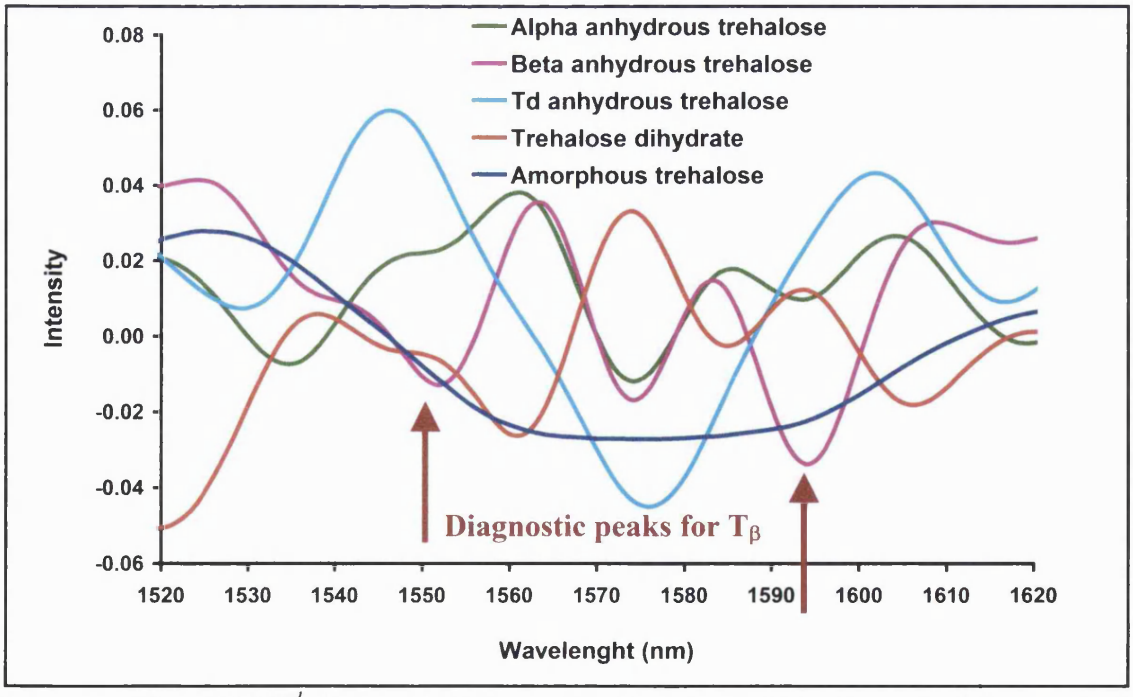

Figure 4.18. *SNV-2nd derivative NIR spectra (between 1520-1620 nm) of the physical forms of trehalose presented in Figure 4.15. The arrows indicate the diagnostic peaks for T_β around 1552 and 1594 nm.*

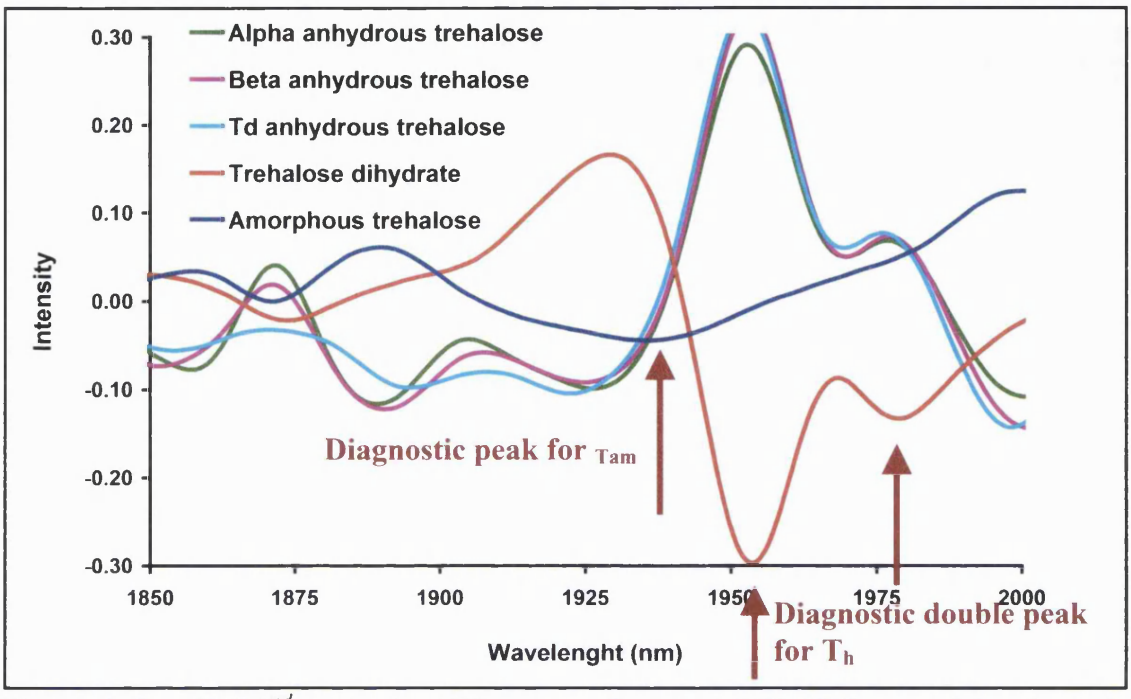

Figure 4.19. *SNV-2nd derivative NIR spectra (between 1850-2000 nm) of the physical forms of trehalose presented in Figure 4.15. The arrows indicate the diagnostic double peak for the dihydrate form at 1954/1980 nm and the diagnostic peak for amorphous trehalose at 1936 nm.*

The peaks for the α-anhydrous form of trehalose could not be assigned as the spectra were overlapping the spectra of the other physical forms of trehalose. The peaks assigned for the α-from by Moran (2004) were seen but were not exclusive for the α-form (Figure 4.24). The overlapping spectra of the different physical forms of trehalose show that the backbone structure of trehalose is retained through the different interconversions. The most distinctive peak could be assigned for the dihydrate form of trehalose as seen in Figure 4.19. This double peak is representative of the dihydrate water (bound water) at 1954 and 1980 nm. These specifically assigned peaks will be used to follow the crystallisation process of the amorphous trehalose during the gravimetric studies in the next section and later during crystallisation of the spray-dried trehalose/protein powders.

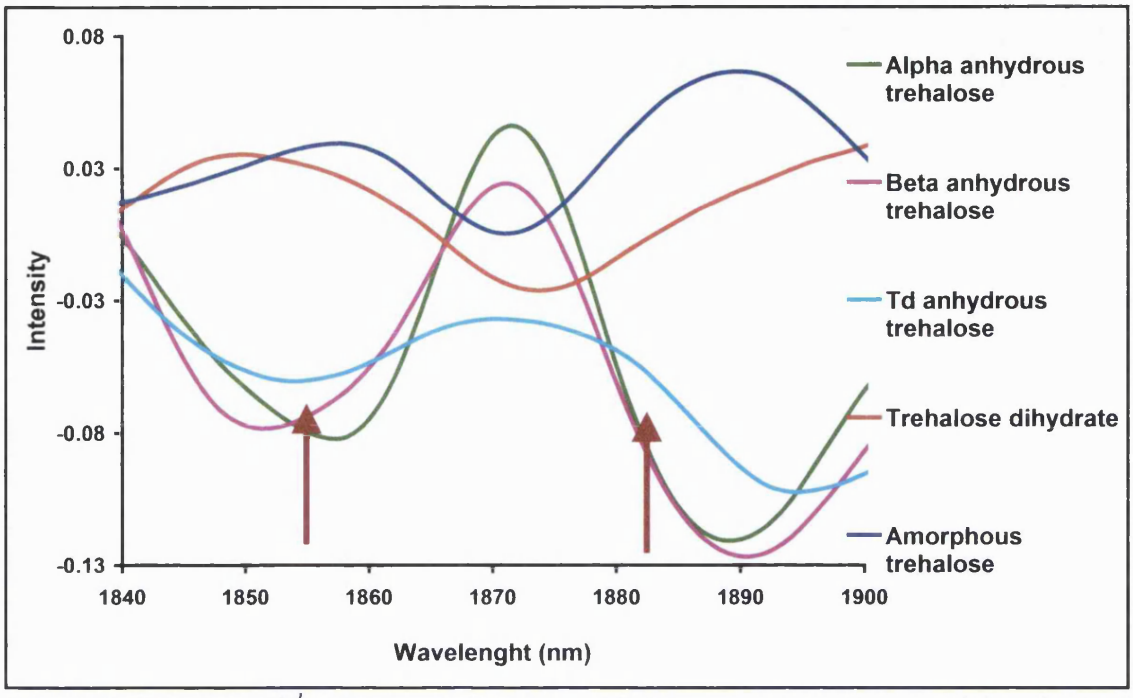

Figure 4.20. *SNV-2nd derivative NIR spectra (between 1840-1900 nm) of the physical forms of trehalose presented in Figure 4.15. No peaks could be allocated in this region exclusively to any of the physical forms of trehalose. The arrow indicates the identifying peaks allocated by Moran, 2004 T_α (1860/1882 nm).*

4.3.4.2 Gravimetric and NIR data for spray-dried trehalose - Batch 1

Batch 1 was spray-dried with processing parameters that were considered to be reproducible (Table 4.1). The DVS plot for Batch 1 is displayed in Figure 4.21. During the initial drying phase (0% RH for 8 h) the excess moisture was removed as evident by no loss of mass after 480 minutes. In the second stage the humidity was increased to 75 % RH resulting in a mass increase associated with moisture absorption. The increase reached a maximum of approximately 15.5 % of the mass change, which was sufficient to lower Tg below the experimental temperature (25 °C) and consequently gave the material sufficient mobility to allow crystallisation to occur (Saleki-Gerhardt et al., 1995; Saleki-Gerhardt et al., 1994). At this point, collapse of the sample occurred expelling water observed by the loss of mass. The mass loss (ca. 4 %) is indicative of excess water being expelled from the system and is followed by the rearrangement of molecules to the crystal form. The sample showed gradual and consistent mass loss,

which continues during the remainder of the exposure to 75 % RH. During the second drying stage (0 % RH, 6 h) the sample mass decreased further to an anhydrous state with eventual loss of any hydrate water associated with the crystal structure. The molecular weight of trehalose is ca. 342 g/mol (378 g/mol minus the two water molecules, ~36). The gain of the two molecules of water per molecule of trehalose to produce the dihydrate crystal form would therefore be equivalent to a mass increase of approximately 10.5 %. Batch 1 gained approximately 10.5 % in weight between the end of the first drying stage and the end of the 75 % RH stage suggesting the presence of the dihydrate form. The continuous mass loss at 75 % RH suggests that the sample was changing to a different physical form of trehalose, perhaps an anhydrous form. If the 75 % RH stage was increased a different form of trehalose may have been produced.

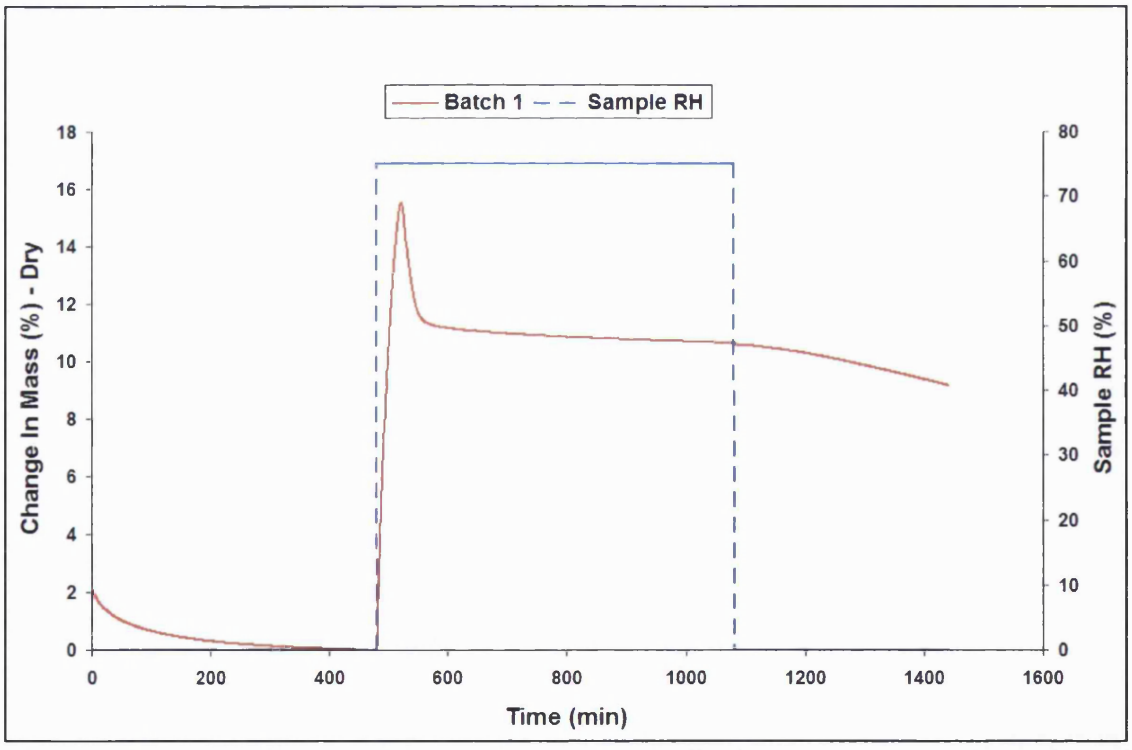

Figure 4.21. *DVS plot for Batch 1exposed to 0 % RH for 8 h, 75 % RH for 10 h and then 0 % RH for a further 6 h (at 25 °C).*

It was hoped that the analysis of the NIR spectra collected during the DVS experiment would provide clarification as to the trehalose form prior, during and after the crystallisation. The SNV, second-derivative NIR spectra of Formulation 1 is displayed

in Figure 4.22 and displays the spectra of the samples at the end of the first drying stage, end of the 75 % RH stage and at the end of the second drying stage collected during the DVS experiment. The spectra collected at the end of the first drying stage differ from the other two stages. The spectra displays the double peak associated with the dihydrate form of trehalose (1954/1980 nm).

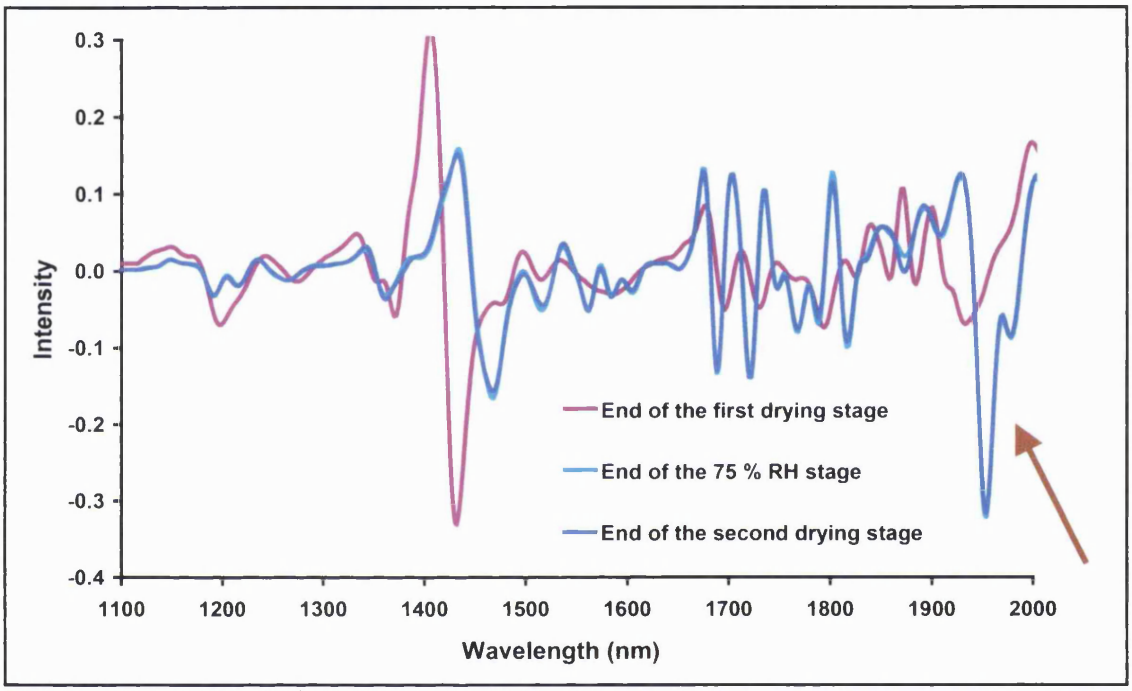

Figure 4.22. *SNV-2nd derivative NIR spectra (between 1100-2000 nm) of Batch 1 during three different stages of the DVS experiment shown in Figure 4.21. The arrow identifies the diagnostic double peak for T_h (1954/1980 nm).*

The spectra of the dry form produced at the end of the first drying stage were further investigated by comparing it to the various physical forms of trehalose displayed in Figures 4.15. The spectra of the dry sample were very similar to that of amorphous trehalose with some discrepancies (Figure 4.23), which generally could not be related to any of the anhydrous forms of trehalose (α, β or Td). However it was evident from Figure 4.23 that the dry sample contained some anhydrous form of trehalose due to the double peak around 1860/1884 nm. This double peak was assigned by Moran (2004) as the identifying peak for the α-anhydrous form of trehalose. However Figure 4.20

illustrated that this particular peak is present in all of the anhydrous forms (α, β and Td). Hence it seem that the amorphous trehalose crystallises to the dihydrate form via one or more of the anhydrous forms. This corresponds to the findings in chapter 3, showing that the different polymorphic pathways of trehalose often occur simultaneously at varying degrees.

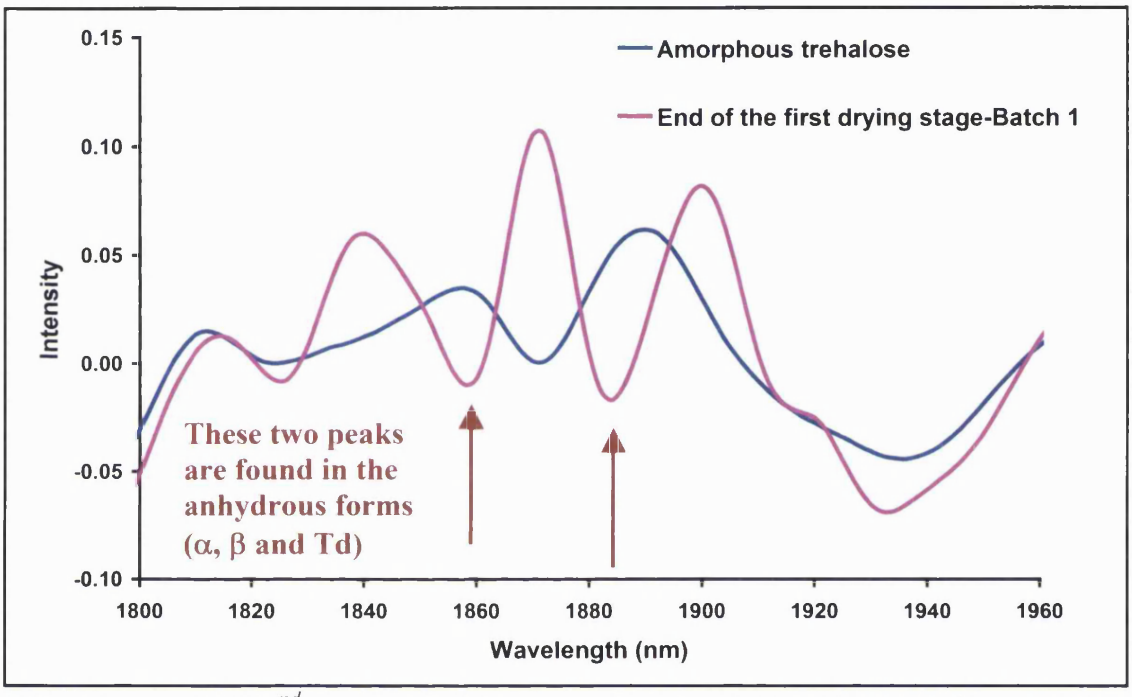

Figure 4.23. *SNV-2nd derivative NIR spectra (between 1300-2000 nm) of Formulation 1, at the end of the first drying stage and the amorphous form of trehalose. The arrows indicate the double peak present in all of the anhydrous form as seen in Figure 4.20.*

The other trehalose Batches were also investigated under the same conditions in order to see whether the spray drying conditions would influence the crystallisation event of these amorphous samples. The differences in morphology may cause differences in the diffusion rates. The NIR data for these Batches were compared with the NIR data for the different forms of trehalose to investigate the possibility of the amorphous form crystallising in to one of the anhydrous forms instead of the dihydrate trehalose. The gravimetric data shown for Batches differed from the Batch prepared by the starting processing parameters (Batch 1) (Figure 4.21).

4.3.4.3 Gravimetric and NIR data for spray-dried trehalose - Batch 6

Decreasing the inlet and the outlet temperatures while keeping all other parameters constant produced Batch 6 (Table 4.1). This produced particles that were fused together (Figure 4.7) as opposed to the smooth surfaced particles produced by Batch 1. The TGA data showed that the decrease in the inlet and outlet temperatures resulted in higher moisture content (Table 4.3). The effect of this elevated moisture content was further investigated by DVS (Figure 4.24).

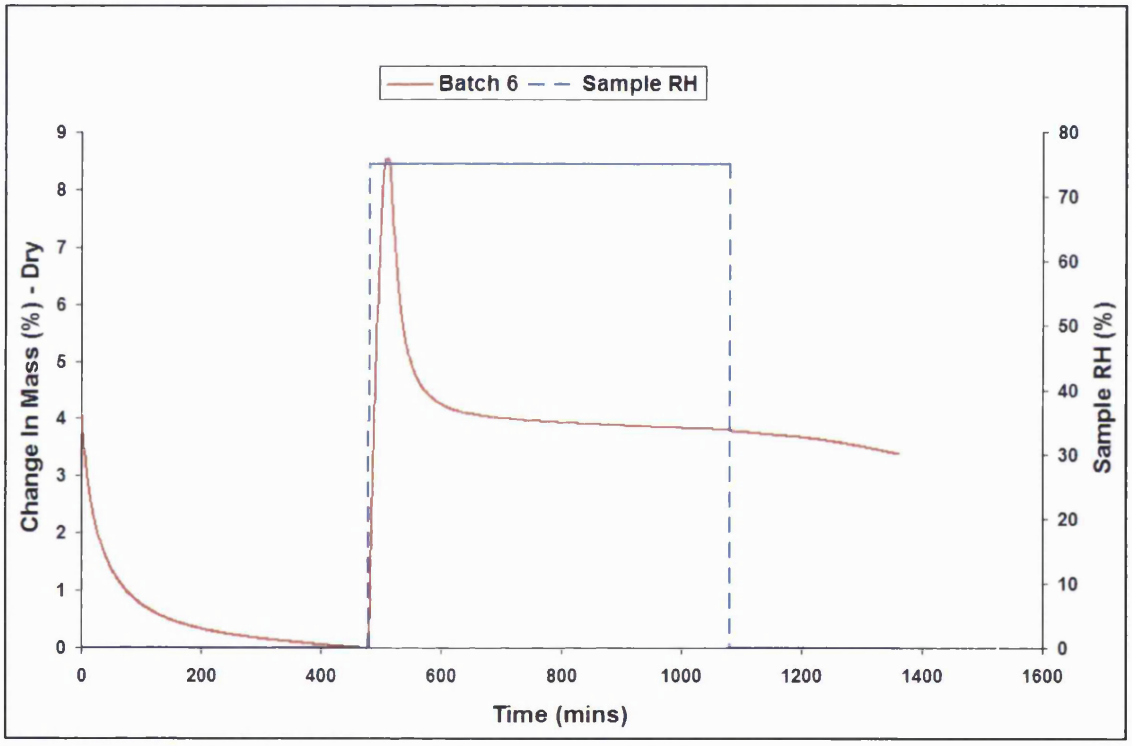

Figure 4.24. *DVS plot for Batch 6 exposed to 0 % RH for 8 h, 75 % RH for 10 h and then 0 % RH for a further 6 h (at 25 °C).*

The first drying stage for this Batch shows a mass decrease of 4 %, which can also be confirmed by the TGA data (Table 4.3). The main difference compared to Batch 1 could be seen when the humidity was increased to 75 % RH and the uptake of moisture caused the weight gain of approximately 8.5 %, which is almost half of what could be seen for Batch 1 (Figure 4.21). Subsequently the mass decreased ca. 4 %, which again is similar to what was for seen for Batch 1 and continues to decrease throughout the 75 % RH stage. During the second drying stage gradual mass loss continues. Between the end of

the first drying stage and the end of 75 % RH stage a total of only ca. 4% weight is gained. This does not correspond to the two water molecules of trehalose dihydrate suggesting that the sample converts to some other physical form of trehalose. It could be a blend of hydrates and anhydrous forms. Similar gravimetric data was obtained for Batch 3, which also produced wet/fused particles (Figure 4.5b) due to an increase in the nozzle flow (Table 4.1).

The gravimetric data were further investigated by examining the NIR spectra of Batch 6 collected during the DVS experiment. Three stages of the sample spectra were compared; the end of the first drying stage, end of the 75 % RH stage and the end of the second drying stage. The spectra at the end of the 75 % RH stage and at the end of the second drying stage showed the characteristic double peak associated with the dihydrate form of trehalose (1954/1980 nm). The spectra for the end of the first drying stage were very similar to amorphous trehalose but showed the presence of the anhydrous forms (Figure 4.25). This double peak around 1860/1882 nm is present in all of the anhydrous forms of trehalose (α, β and Td). The same phenomena were seen for Batch 1.

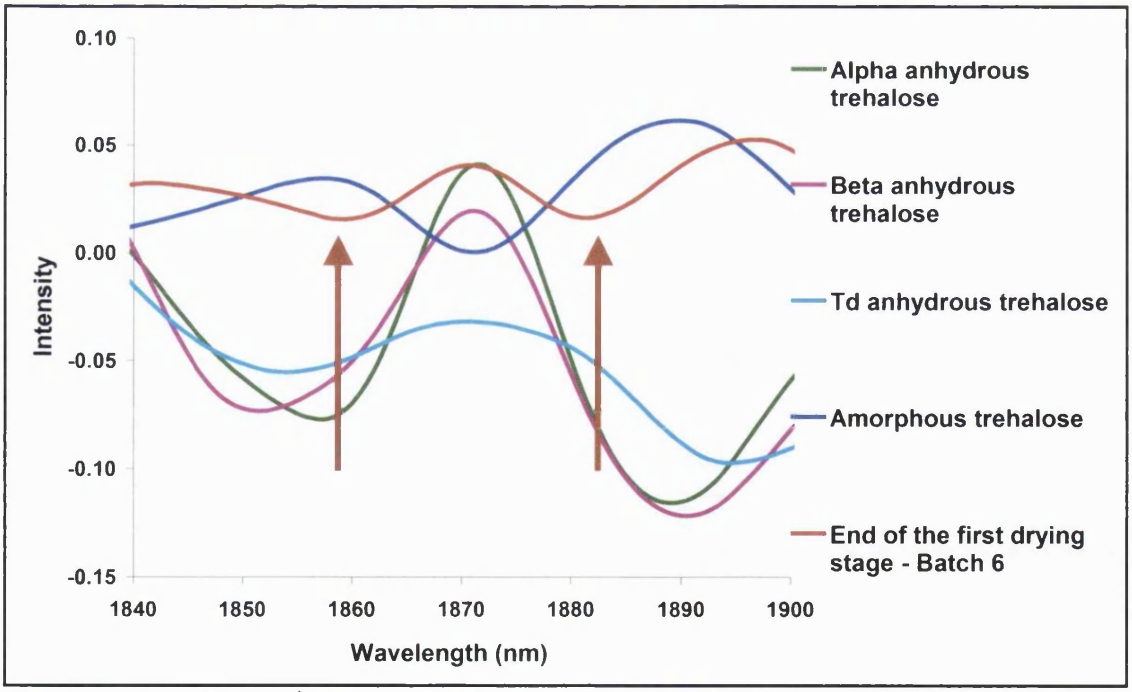

Figure 4.25. *SNV-2nd derivative NIR spectra (between 1840-1900 nm) of Batch 6, at the end of the first drying stage and the different forms of trehalose. The arrows indicate the double peak present in all of the anhydrous form as seen in Figure 4.20.*

The gravimetric data suggests that the entrapment of water is related to the initial water content of the sample, which also has an influence on particle morphology. Although the NIR data can show the conversion of the amorphous trehalose to the dihydrate, it does not give evidence of any specific stable hydrates/anhydrous forms

4.3.4.4 Gravimetric and NIR data for spray-dried trehalose - Batches 9, 10 and 11

Batches 9 and 10 were prepared using the same inlet and outlet temperatures and changing the nitrogen flows. The ratio between the nozzle and chamber nitrogen flow was maintained at 10 for Batch 1 but the two flows were increased for Batch 9 and decreased for Batch 10. The ratio was increased to 30 for Batch 11. The SEM pictures for Batches 9 and 10 did not show any great differences (Figures 4.9 a and b) but the particles for Batch 11 were generally bigger than what was observed for the other batches (Figure 4.9c). The DVS plots mimic the SEM pictures and the changes seen between the batches.

The first drying stage for Batches 9 and 10 show that these contain similar amounts of moisture, which correlates to the TGA data (Table 4.3). The subsequent moisture uptake caused by the increased humidity is similar for these two samples (ca. 12 %) (Figure 4.26). At the end of this re-hydration process the total mass increase for the samples is approximately 11 %. The weight gains for Batches 9 and 10 correspond to the 10.5 % increase required for the two water molecules of trehalose dihydrate. The only variable aspect of the water sorption behaviour of these two batches was the mass loss upon crystallisation. This is highlighted in Figure 4.27. Both samples demonstrated a crystallisation process indicated by mass loss at 75 % RH that was less than observed previously (Figures 4.21 and 4.24). However, Batch 9 crystallised at a faster rate than Batch 10, which showed a broader peak corresponding to water expulsion upon crystallisation, and a greater percentage mass loss at 75 % RH. Batch 10 displayed a gradual and constant mass loss suggesting that a slower crystallisation process was occurring. The gravimetric data were further investigated by examining the NIR spectra for these two samples. Once again the NIR spectra collected at the end of the 75 % RH stage and at the end of the second drying stage, showed the characteristic double band representative of the dihydrate form. However the NIR spectra collected at the end of the first drying stage did not show the characteristic double peak around 1850/1890 nm that is characteristic of the anhydrous forms (Figure 4.28).

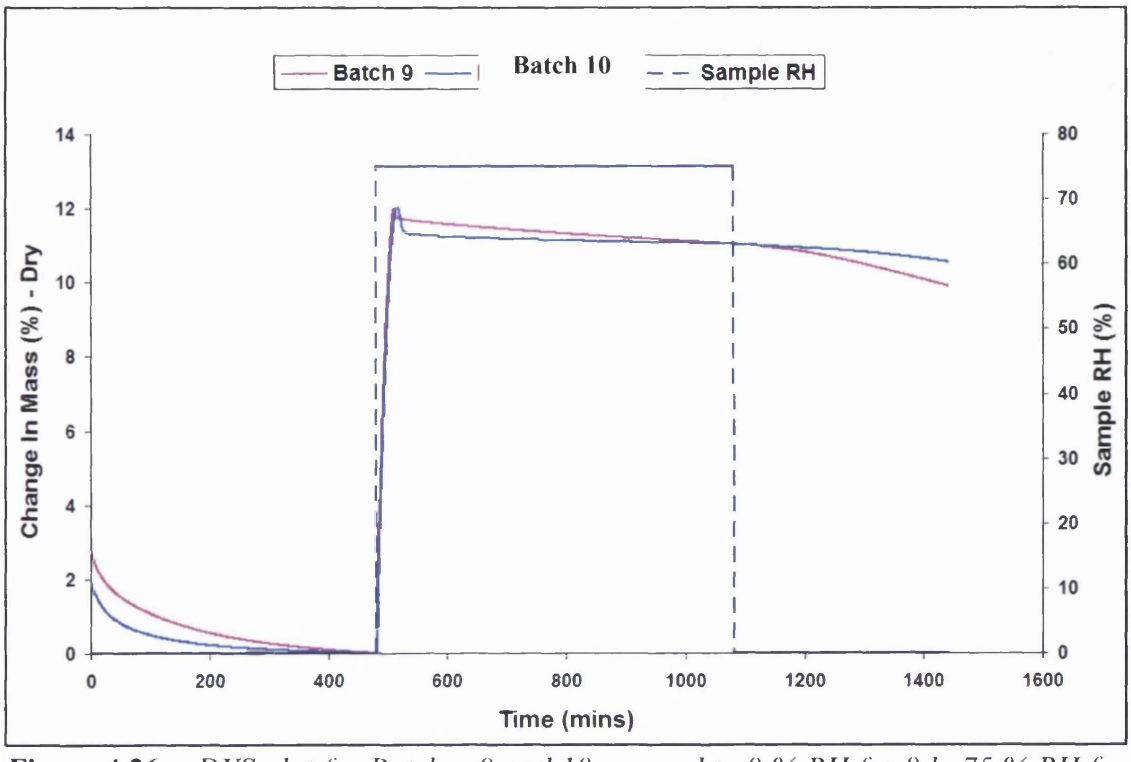

Figure 4.26. *DVS plot for Batches 9 and 10 exposed to 0 % RH for 8 h, 75 % RH for 10 h and then 0 % RH for a further 6 h (at 25 ℃).*

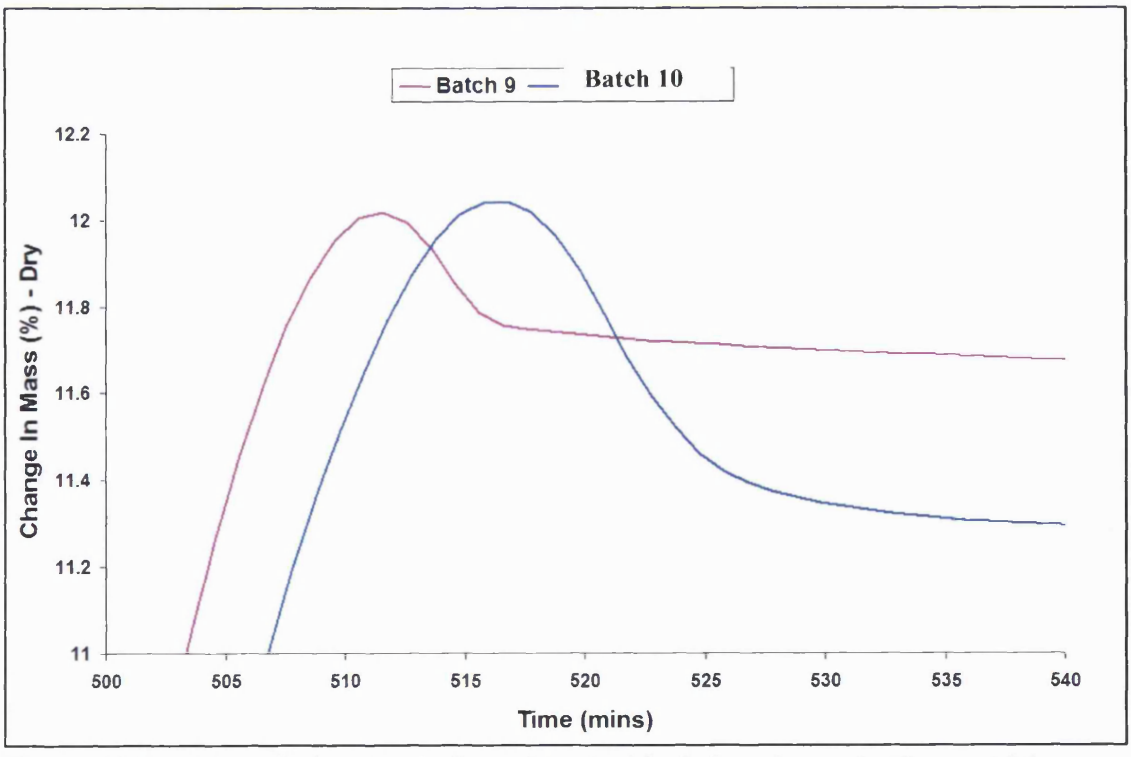

Figure 4.27. *Magnified region indicated by the black dotted area in Figure 4.26.*

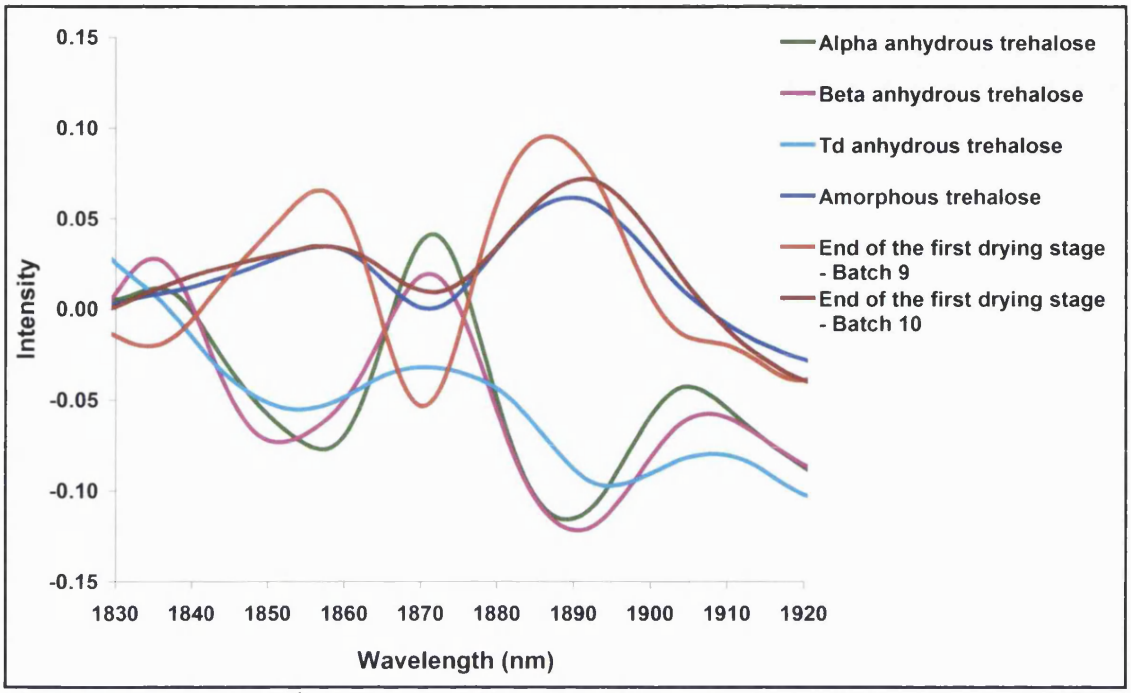

Figure 4.28. *SNV-2nd derivative NIR spectra (between 1830-1920 nm) of Batches 9 and 10, at the end of the first drying stage and the different forms of trehalose.*

In contrast, Batch 11 only increased by approximately 8 % when the re-hydration stage was commenced and at the end of this re-hydration process the total mass increase was approximately 4 % (Figure 4.29). This indicates that Batch 11 crystallises to some other physical form. The same phenomenon was seen for Batch 6. The common factor for both samples (Batches 6 and 11) is the elevated moisture content as described in Table 4.3. The NIR data collected for Batch 11 during the DVS experiment was investigated in order to elucidate the gravimetric data. The spectra for the end of the first drying stage show the double peak seen in all of the anhydrous forms (α, β and Td) (Figure 4.30). The data indicates that the residual moisture of the sample influences the water sorption behaviour. The samples with high residual moisture crystallise to presumably hydrates. In contrast, samples with relatively low moisture retention transform to the dihydrate form of trehalose.

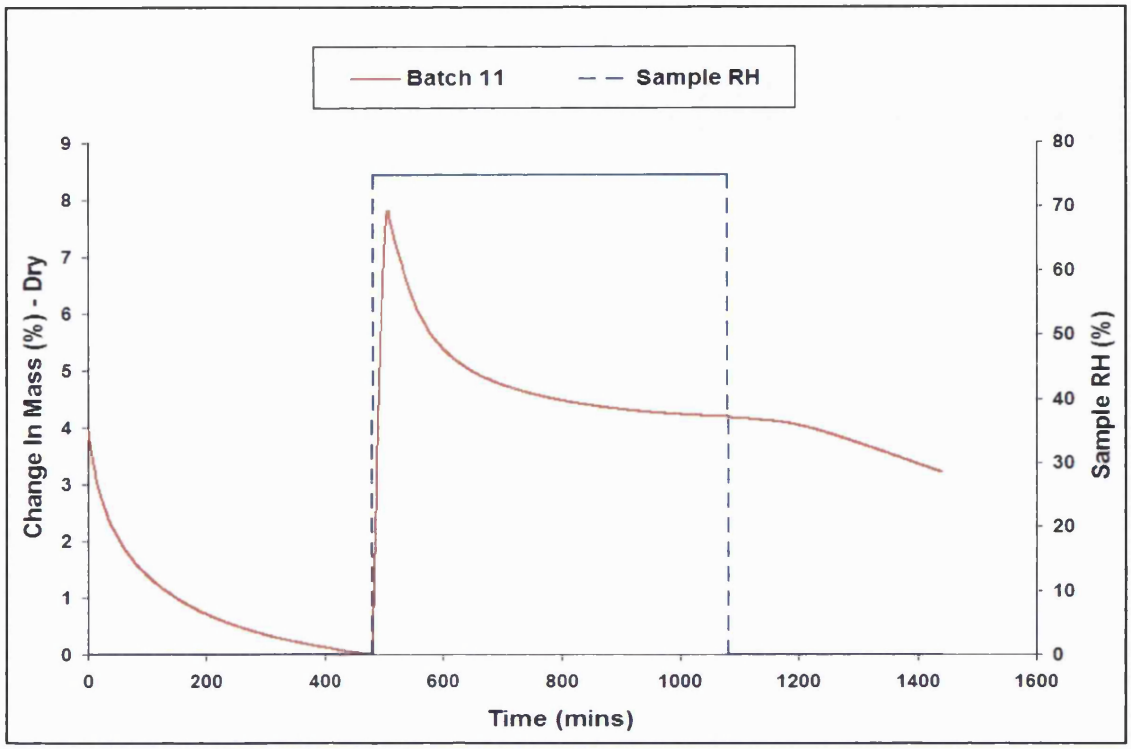

Figure 4.29. *DVS plot for Batch 11 exposed to 0 % RH for 8 h, 75 % RH for 10 h and then 0 % RH for a further 6 h (at 25 ℃).*

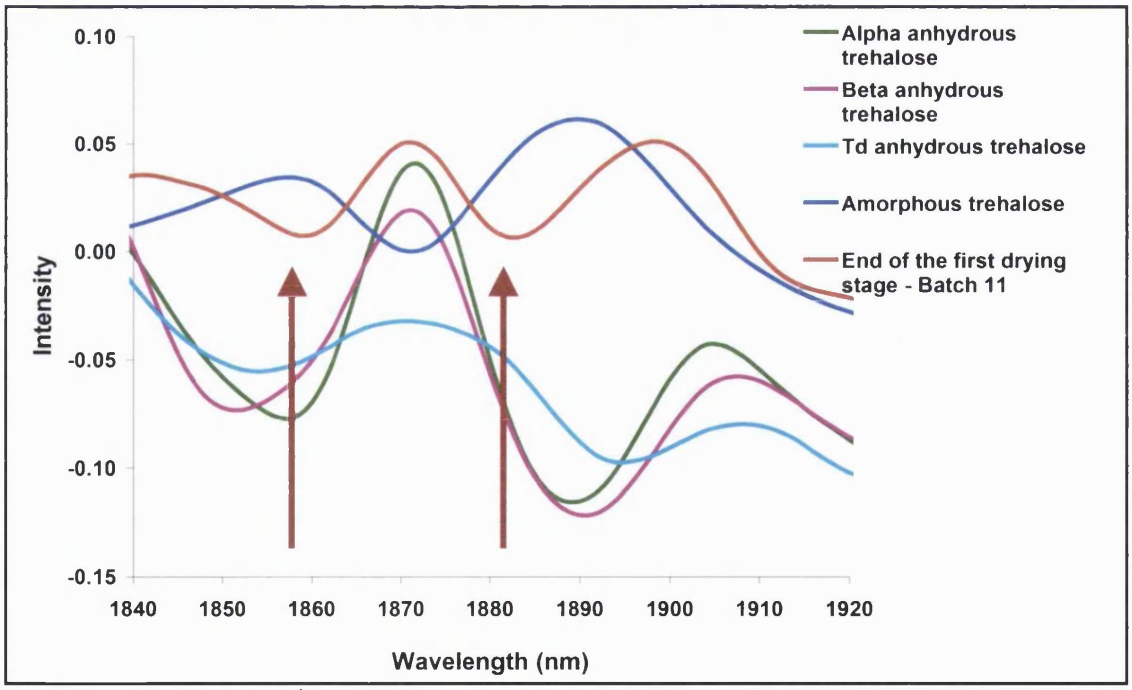

Figure 4.30. *SNV-2nd derivative NIR spectra (between 1840-1920 nm) of Batch 11, at the end of the first drying stage and the different forms of trehalose. The arrows indicate the double peak present in all of the anhydrous form as seen in Figure 4.20.*

4.3.4.5 Principal component analysis (PCA) of the NIR spectra

The NIR data collected during the DVS experiments for Batches 1-11 were analysed using principal component analysis (PCA) with the Unscrambler® software. Each run was first treated separately in the Unscrambler®, using full cross validation and looking at the first two PCs only, as this represented over 95 % of the difference. The scores were looked at to assess any patterns relating to the water intake or the change in form from amorphous to crystalline. The loading plots were compared to the difference between the amorphous form and each crystalline form, as the loadings represent the change between the spectral data.

Figure 4.15 highlighted the spectral differences between trehalose dihydrate, amorphous trehalose and the anhydrous forms. The major difference is between 1900-2000 nm were the dihydrate stands out with a double peak characteristic of the water region (Figure 4.19). This double peak at 1954 and 1980 nm associated with the dihydrate was also seen by Moran (2004) around same area. After establishing this as the distinguishing point between the trehalose dihydrate and the other anhydrous forms the NIR data collected during the gravimetric studies were also treated against all of these forms. After treating each of the runs separately in the Unscrambler® using full cross validation it was established that the first PC appeared to correspond to a change in form (amorphous to crystalline), which accounted to roughly 95 % of the spectral changes. PC2 in contrast followed the water in the system, through the increased and decreased RH stages and the expulsion of the water from the system. The loading plots for all forms of trehalose were very similar as were the PC2 loadings. By comparison of the PC1 loadings with the different spectral form changes, it can be seen that all spray-dried trehalose formulations changed to the α,α-trehalose dihydrate, which could be seen by the characteristic double peak (Figure 4.31).

The next step was to ascertain that by looking at spectra over a smaller number of data points when the trehalose form is changing whether different loading are seen and if trehalose is changing via an intermediate. Again the loadings for each spray-dried sample of trehalose were similar (both PC1 and PC2). The loading differences were greatest between the different spray-dried trehalose samples between 1820 nm and 1920

nm, but no pattern could be seen on closer inspection and the loadings did not correlate to any particular form of trehalose.

A typical plot for PC1 and PC2 showing the scores and the loadings is displayed in Figure 4.31. Similar plots were obtained for all of the spray-dried formulations. PC1 shows the transition of the amorphous trehalose to the crystalline dihydrate, which is evident by the appearance of the double peak. PC2 portrays the changes caused in the formulation due to the humidity changes. The expulsion of water is evident by the sharp tip seen in the score plot for PC2, which corresponds to the start of the re-hydration stage. At this stage the spray-dried trehalose takes up moisture seen by the weight gain in the DVS plots, which is subsequently decreased to allow crystallisation.

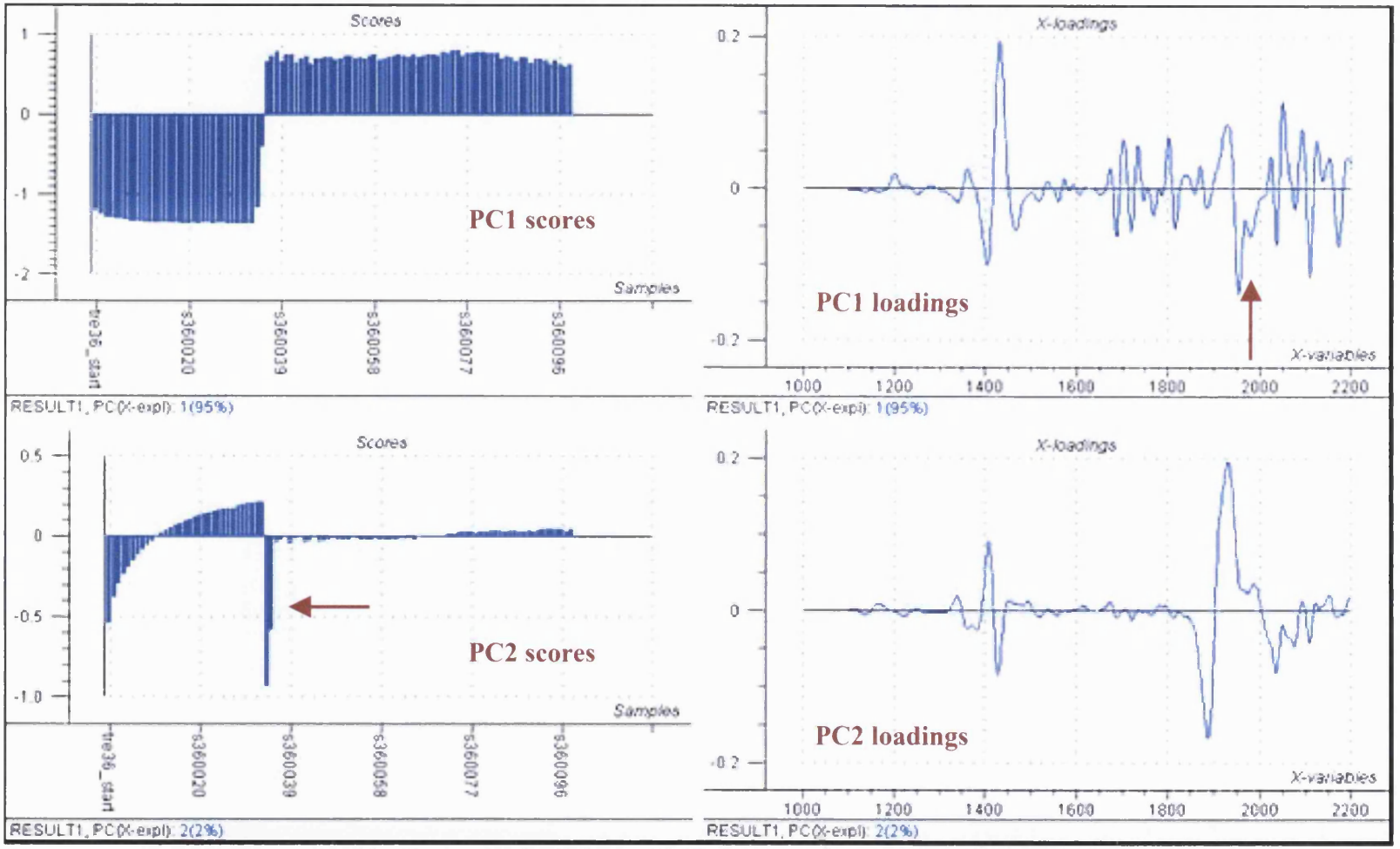

Figure 4.31. *A typical score and loadings plot for PC1 and PC2 for data obtained during gravimetric studies of spray-dried trehalose.*

4.4 CONCLUSIONS

The following conclusions can be made for the studies conducted in this chapter:

- The SDMicro^{TM} can be explored to control particle morphology and these characteristics depend on the processing. The most important and influential aspect in controlling the variability during spray drying is the feed solution rate, which can be manipulated indirectly by a range of parameters (inlet temperature, outlet temperature, nozzle flow and chamber flow).

- The spray-dried trehalose batches were amorphous regardless of the spray drying process and all of the formulations crystallised to the α,α-trehalose when subjected to high controlled humidity during the gravimetric studies. However the entrapment of water varied indicating formation of hydrates. This phenomena seemed to depend on the residual moisture in the sample.

- The NIR data highlighted the difference between the various polymorphic forms of trehalose and can be helpful for further investigation of these forms. The data also proved that the anhydrous forms do not influence the crystallisation process of the amorphous trehalose. Hence regardless of the initial differences in the various batches due to processing they all crystallised to the dihydrate form (though hydrates were presumably formed). This is encouraging from a pharmaceutical regulatory point of view as the ability of trehalose to convert into these various anhydrous forms would be alarming.

- Amorphous trehalose generally converted to the crystalline form via anhydrous forms. NIR data could not assign that the trehalose converted to the crystalline form via any specific anhydrous form. However a combination of all three forms (α, β and Td) could be seen. This confirms the findings of chapter 3 regarding the simultaneous occurrence of multiple pathways. However, even though the conditions provided here did not cause formation of specific intermediate anhydrous forms, these could perhaps still be generated if the conditions were different.

CHAPTER 5

Preparation and characterisation of spray-dried trehalose/alkaline phosphatase particles

5. PREPARATION AND CHARACTERISATION OF SPRAY-DRIED TREHALOSE/ALKALINE PHOSPHATASE PARTICLES

5.1 INTRODUCTION

The changes in the properties of dry powder forms of trehalose that were caused by the addition of alkaline phosphatase are described in this chapter. Two aspects of the protein were considered during these experiments. First, the impact of protein concentration on the spray-dried particles was examined. Then the influence of an organic solvent on the particulate properties was investigated. The solvent chosen for this study was acetone since it is miscible with water. Both the Food and Drug Administration and the European Agency for the Evaluation of Medicinal Products consider acetone to be safe (Class 3). This means that there is no absolute limit on the residual levels of this solvent as long as the levels in the finished product can be justified. The main purpose for using an organic solvent for these studies was to investigate the effect of a water miscible excipient on the protein, trehalose and the spray-dried particles.

The data obtained by measuring protein content and activity in the spray-dried powders is described in section 5.3.1. The physicochemical properties of the spray-dried particle are described in terms of morphology, moisture content, glass transition, surface area and surface energies (sections 5.3.2 and 5.3.3). Furthermore the water vapour sorption behaviour of the spray-dried samples was studied with regards to protein concentration and the impact of acetone (section 5.3.4). NIR data was collected during the gravimetric experiments to study the crystallisation process of trehalose in the presence of alkaline phosphatase. Stability studies on the spray-dried samples were conducted by exposing the samples to elevated humidity (75 %) and temperature (50 °C) (Section 5.3.5).

5.1.1 ALKALINE PHOSPHATASE (AP)

Alkaline phosphatase [orthophosphoric-monoester phosphohydrolase; EC 3.1.3.1] (AP) is a dimeric zinc containing glycoprotein with an alkaline pH optimum and was chosen as a therapeutic model protein in this study (Schoenau et al., 1986; Fournière et al., 1995). AP is one of the most frequently used biochemical markers for osteoblastic bone

formation (Rigg et al., 1965; Magnusson et al., 1995). Estimations of serum alkaline phosphatase activity are frequently made in the diagnosis of liver and bone diseases. AP is a membrane-bound enzyme present in many organs such as bone, liver, kidney and the intestine (Magnusson et al., 1995; Poelstra et al., 1997a). AP is found in both prokaryotes (Escherichia coli) and eukaryotes. The eukaryotic AP is a highly polymorphic enzyme. At least four human genes are known to encode for the AP isoenzymes; placental, small intestinal, germ cell and tissue non-specific (liver, bone, kidney) (Fournière et al., 1995; Magnusson et al., 1995). Although there are significant differences between the two types of AP (E. coli and human), sequence comparison shows 25-30% similarity. Both types of AP are metalloproteins that contain two to four ions of zinc and one to two ions of magnesium per mole of dimer (Fournière et al., 1995; Poelstra et al., 1997a). AP is known to catalyse the hydrolysis of phosphate monoesters in an alkaline environment to produce inorganic phosphate and alcohol (Poelstra et al., 1997b). The isoelctric point (pI) of alkaline phosphatase is around 4.5 (Eriksson et al., 2003b).

The placental AP is more heat stable than the other three isoforms, which lose their activity when treated at 56 °C for 30 min, while the placental form has been found to withstand a temperature of up to 70 °C for 30 min (Neale et al., 1965). AP from bovine intestinal mucosa has been found to preserve its secondary structure over a range of pH (5.4-10.4) and the conformation also shows stability over a range of temperature (25°C-70°C) but the activity is irreversibly lost under extreme conditions (Fournière et al., 1995). AP is currently under investigation for treatment of septic shock produced by gram-negative bacteria, Endotoxin. This lipopolysaccharide elicits an inflammatory reaction, which can allow the endotoxins to enter the blood stream across the intestinal wall. AP can detoxify these endotoxins by dephosphorylation (Poelstra et al., 1997a; Poelstra et al., 1997b).

The assay method for the activity of this enzyme is based on formation of the yellow colour of p-nitrophenol (p-NP) produced by hydrolysis of p-nitrophenylphosphate (p-NPP) in alkaline solution and measured spectrophotometrically at 405 nm at 37°C (Walter et al., 1974).

5.1.2 ALKALINE PHOSPHATASE STABILITY/ACTIVITY IN DRY POWDER FORM

Dry powder forms of alkaline phosphatase prepared by freeze-drying have been described (Ford et al., 1993a; Ford et al., 1993b; Hinrichs et al., 2001; Eriksson et al., 2002; Eriksson et al., 2003a). Ford and colleagues investigated AP from bovine intestinal mocusa. They freeze-dried AP solutions in the presence of carbohydrates at neutral pH (tris buffer, pH 7.3) (Ford et al., 1993b). The enzyme activity in the formulations prepared from tris buffer alone or with mannitol was considerably reduced by freeze-drying. Exposure of the samples to storage temperatures between 20 °C and 56 °C ("accelerated degradation" study) showed that formulations prepared with mannitol failed to maintain activity at a temperature of 37 °C over 21 days. The loss of activity was more gradual when freeze-dried in buffer alone and stored at high temperatures. Formulations containing lactose or trehalose maintained the AP activity after freeze drying even at elevated temperatures. When these samples were stored at 56 °C the AP activity did not show a significant drop until 14 days after with lactose formulations or until 21 days with trehalose containing formulations. After 84 days at 56 °C, 30 % of the activity still remained in the formulation containing trehalose, making this disaccharide the most effective cryoprotectant for stabilising AP in this study. The researchers further investigated the AP containing powders by comparing the impact of glycated proteins (deliberately glycated albumin and human serum albumin) and/or trehalose on the enzymatic activity (Ford et al., 1993a). These formulations were also subjected to "accelerated degradation" studies and showed that if albumin was used, the initial degree of glycation should be kept to a minimum and a combination of albumin and reducing sugar should be avoided.

Hinrichs and colleagues have also investigated the solid AP formulations comparing the impact of trehalose and inulin on the AP activity (Hinrichs et al., 2001; Eriksson et al., 2002; Eriksson et al., 2003a). Hinrichs et al. (2001) investigated the activity of bovine intestinal mocusa AP by comparing the impact of inulin against trehalose. Eriksson and colleagues further investigated AP activity by preparing tablets from the dry powders. By investigating the compaction behaviour of tablets and the effect of the compaction process, they concluded that inulin was by far superior to trehalose as stabiliser. They

blamed the poor stabilising capacities of trehalose after compaction to the crystallisation of trehalose induced by the compaction process and moisture in the material.

Freeze drying has by far been the most examined process to prepare dry alkaline phosphatase formulations. From the studies discussed above, it seems that the activity of AP is greatly affected by elevated temperatures and humidity regardless of the excipient being used. Thermally labile products are now being prepared by spray drying successfully and hence in light of these findings it seems logical to study AP by the process of spray drying (Cepeda et al., 1998; Seville et al., 2002).

5.1.3 NEAR INFRARED SPECTROSCOPY AND PROTEINS

Near infrared spectroscopy has been employed extensively to analyse agricultural products (Shenk, 1993). The use of the near infrared region to study pharmaceutical products has been less common due to the inherent variability of peaks caused by overtones and combinations. Due to advances in computer programmes, designed to analyse data through mathematic manipulation, near infrared spectroscopy is now being used more frequently by the pharmaceutical industry. It provides fast automatic acquisition of data, requiring little sample preparation and no sample destruction. This non-invasive technique has recently been used in pharmaceutical sciences to determine polymorphism, degree of crystallisation and changes in the physical forms (Aldridge et al., 1996; Buckton et al., 1999; Buckton et al., 2004). Proteins are complex molecules and hence band assignments for these have been more challenging. A brief overview of the relevant literature describing NIR analysis of proteins is provided below.

Sadler et al. (1984) examined the NIR spectra of proteins using photoacoustic spectroscopy (PAS). Using this method the proteins could be investigated in solution and in the solid state and concerns caused by light scattering and absorption flattening artifacts were limited (Sadler et al., 1984). They found that the NIR spectra of denatured protein and the native form were similar. This was observed for 20 model proteins and polypeptides. Conformationally altered proteins showed evidence of a small peak around 1.35 μm (1350 nm). Small changes in the regions 1.7-1.8 μm (1700-1800 nm) and 1.4-1.5 μm (1400-1500 nm) were also observed. However these small changes were specific to the individual proteins and the spectra were insensitive to the secondary

structures of the proteins. Sadler et al. (1984) concluded that identifying peaks for proteins was difficult to assign due to the complexity of bond vibrations in the proteins.

Photoacoustic near infrared spectroscopy of polypeptides was further investigated by Wang et al. (1994). The bands near 4850 cm^{-1} (~ 2062 nm) and 4600 cm^{-1} (~ 2174 nm) were combinations of amide A and II and amide B and II, respectively. Liu and colleagues applied these findings to identify a "marker band" for proteins and polypeptides (Liu, 1994). They focused on the band 4850 cm^{-1} (2062 nm), which had already been identified as amide A/II. Liu et al. (1994) compared the FT-IR and FT-NIR spectra of various proteins and polypeptides in order to find a "marker band" and concluded that all examined proteins except some types of collagen give the amide A/II band. No correlation between the frequency of the amide A/II band and the secondary structure was found. However the amide A/II bond showed sensitivity to the strength of the hydrogen bonding of the amide groups in polypeptides. This was concluded on the basis of a different extent of denatured pepsin, which showed a higher frequency shift (toward shorter wavelength) as more denaturation occurred. They suggested that this was caused by the destruction of the hydrogen bonds in the amide groups of pepsin. Similar observations were described for the structural changes of silk fibroin (Miyazawa et al., 1998).

The potential of near infrared spectroscopy to probe the secondary structure of a protein was investigated with twelve model proteins in a study by Robert et al. (1998). Bands were successfully assigned representing the α-helix structure (2172 nm and 2289 nm), the β-sheet (2205 nm, 2264 nm and 2313 nm) and the unordered structure of the protein (2265 nm). Miyazawa et al. (1998) measured the near infrared spectra of seven globular proteins, which varied widely in secondary structure. A common absorption band for the amide A/II at 4865 cm^{-1} (2055 nm) was found. Furthermore an absorption band at 4525 cm^{-1} (2210 nm) was assigned to sheet structures within the globular proteins.

The literature discussed above, highlights the complexity of assigning peaks in the NIR region for proteins with confidence. The similarities in the spectra of the denatured and native forms, makes the study of protein stability by NIR difficult. However changes in water and hydrogen bonds can be determined more readily and are described in the next section.

5.1.4 NEAR INFRARED SPECTROSCOPY FOR DETERMINING WATER AND HYDROGEN BONDS

NIR spectroscopy for studying protein hydration represents an approach where "bound water" can be distinguished from bulk water (Subramanian et al., 1972). Hydration changes may be associated with conformational changes of proteins and hence it is important to identify the bands related to bound and unbound water. A review by Workman in 1996 highlights that "free water", also known as "bulk water", is a result of three main molecular species with differences in the numbers of hydrogen bonds. These bonds vibrate differently and therefore can be seen as separate peaks in the NIR region. Shenk et al. (1993) describe the changes in hydrogen bonding as the largest observable change in the NIR region. These changes can be seen as peak shifts, broadening or narrowing of the bands. The formation of hydrogen bonds can be determined by bands shifting to higher wavelengths and by broadening or narrowing, and sometimes by changes in band shape and intensity. On the other hand the loss/cleavage of a hydrogen bond results in peak shifts to shorter wavelengths (Shenk, 1993).

By studying the hydrated spectra of coiled and uncoiled polypeptides, the following peaks have been assigned (Subramanian et al., 1972):

- 1405 nm – a combination band representative of water molecules hydrogen bonded to the $-NH_2$ groups of the polypeptides
- 1530 nm - free –NH groups
- 1540 nm – a shoulder representing hydrogen bonded to the NH groups

In another study the peak around 1900 nm in pure water was related to water molecules with free –OH groups (Bonner et al., 1974). Vandermeulen et al. (1980) studied the hydration of pepsin and bovine serum albumin (BSA) and found corresponding peaks near 1500 nm and 1950 nm. On the other hand, peaks for pure water were found near 1450 and 1928 nm (Vandermeulen et al., 1980b). In a different study, the effects of the interactions with sodium dodecyl sulphate (SDS) on the NIR spectra of three different proteins (BSA, ovalbumin and β-lactoglobulin) in aqueous solutions were examined

(Vandermeulen et al., 1980a). The alkyl chains in SDS provide hydrophobic environment that can lead to decreased hydration of the protein surface. This interaction resulted in the absorption band of water bound to proteins at 1490 nm to shift to 1430 nm.

Hogan et al. (2001) studied the water sorption behaviour of amorphous raffinose and identified the different hydrate forms of raffinose by concentrating on the peak at 1440 nm, which was assigned to –OH interactions. In a similar study concentrating on the different hydrate forms of a compound, the peak around 1904 nm was assigned to surface water (bulk water/free water) and the peak around 1936 nm to bound water (Zhou et al., 2003)

Although the absorption peaks in NIR samples are specific and given the complicated structure of proteins, the analysis of the NIR spectra can be complex. The difficulties are due to the many different types of bonds in these structures resulting in overlapping peaks. Nevertheless, NIR spectroscopy is increasingly being used routinely due to the fast and non-destructive manner in which the spectral data is collected.

5.1.5 WATER VAPOUR SORPTION AND PROTEINS

Water vapour sorption behaviour of proteins is very important to study protein stability, as the instability is usually caused by water. Protein formulations are often prepared by freeze drying or spray drying, resulting in a partially or fully amorphous product. These amorphous materials can sorb water vapours from the atmosphere into their bulk structure. In contrast, crystalline materials water vapour uptake is limited to the particle surface. This sorption of water can have a profound effect on protein properties (i.e. chemical stability, physical stability, biological activity). As already discussed, sugars are often used to stabilise proteins and the drying process would lead to an amorphous sugar. In order to protect the protein it is assumed that the sugar interacts in some manner with the protein (Crowe et al., 1998). If the amorphous sugar is affected by water vapour sorption, it could lead to crystallisation of the sugar, when the product is exposed to high humidity. In fact, in such a case, a very hydrophilic amorphous sugar would promote water vapour sorption and hence allow a greater degree of molecular mobility and decreased stability of the protein in the sample (Shamblin et al., 1998).

It has been suggested that proteins are surrounded by a loose "hydration shell". This is thought to be composed of several types of water. This is also known as the water monolayer (M_0) of a protein. Few water molecules (10-20 per protein) are tightly bound in specific binding locations such as in metal ions, active sites or in the protein interior (Kuntz et al., 1974). The M_0 of a protein is the water content required to exhaust all of the water-binding sites on the surface of the protein with additional clustering of water molecules. The M_0 is exceeded when further addition of the water displays "bulk" properties at which point the protein product would exhibit increased instability (Costantino et al., 1998). Drying the protein product to below the M_0 can also lead to instability of the protein and hence it is advisable to maintain the protein M_0 (Hsu et al., 1991). Costantino and colleagues investigated the water sorption behaviour of three model proteins freeze dried with mannitol, sucrose and trehalose. Their findings suggested interaction between the amorphous sugars and proteins in the solid-state, leading to a masking of the monolayer water binding sites of both components. Hence the M_0 for sugars and proteins are higher when they are not co-lyophilised (Costantino et al., 1998).

In a study investigating the hydration and interaction of proteins and sugars, trypsin, trehalose and sucrose were employed (Lopez-Diez et al., 2004). Samples containing trypsin/trehalose and trypsin/sucrose were freeze-dried and the hydration behaviour was studied using gravimetric water sorption experiments. They concluded that trehalose was a better biostabilising excipient than sucrose, as it exhibited increased interaction with trypsin. The interactions were determined by the hydration isotherms where reduced hydration indicated increased interactions.

When an amorphous sugar in a dried protein product is affected by the water vapour sorption its crystallisation and phase separation can destabilise the entire system. This can cause protein degradation. It has been suggested that the ratio between the sugar and protein can determine the extent of instability (Sarciaux et al., 1997; Forbes et al., 1998; Tzannis et al., 1999a). Various compositions of dried sugar/protein formulations were studied and it was concluded that by increasing the proportion of protein in these systems, the crystallisation of amorphous sugar could be decreased and the instability of the protein avoided. Tzannis and colleagues proposed a ratio of 1:1 of disaccharide:protein for a stable formulation. In contrast, Lopez-Diez et al. (2004),

observed that a higher sugar content compared to the protein content resulted in high protein activity. Hence the ideal proportion of sugar to protein remains unclear.

The protein formulations clinically used display a low protein concentration due to the potency of proteins. Thus regardless of the ideal ratio between proteins and disaccharides, the emphasis should remain on what is required of the protein/sugar systems for clinical use.

5.2 EXPERIMENTAL PROTOCOLS

5.2.1 PRODUCTION OF SPRAY-DRIED TREHALOSE/AP SAMPLES

Trehalose/AP solutions were spray-dried according to the formulation plan outlined in Table 5.1. All of the feed solutions consisted of 10 % (w/v) total solids. Trehalose was dissolved in water and then the AP was added into the solution, which was then made up to 100 ml in volumetric flasks. The feed solutions containing acetone were prepared by dissolving trehalose and AP in water as described above and then adding the measured amount of acetone. The acetone was added slowly and under constant gentle stirring to the aqueous solution in order to minimise the precipitation caused by acetone. The solutions containing high amounts of acetone showed clear signs of precipitation (Sample 5). All of the sample solutions were prepared just prior to spray drying, which was performed using the SDMicro™. The operating parameters were based upon those outlined in chapter 4 to spray dry standard solutions of 10 % (w/v) of trehalose and are shown below in Table 5.2.

Table 5.1. *Formulation plan for spray dried trehalose/AP samples.*

Sample	AP content		Trehalose content		Water content	Acetone content
	% (w/w)	g /100 ml	% (w/w)	g /100 ml		
1	5	0.5	95	9.5	100	0
2	1	0.1	99	9.9	100	0
3	0.5	0.05	99.5	9.95	100	0
4	5	0.5	95	9.5	80	20
5	5	0.5	95	9.5	50	50

Table 5.2. *Processing parameters for the preparation of spray-dried trehalose/AP particles using the SDMicro™.*

Operating Parameters	Settings
Inlet temperature (°C)	95
Outlet temperature (°C)	60
Nozzle pressure (Kg/h)	2.5
Nitrogen pressure (Kg/h)	25

5.2.2 SCANNING ELECTRON MICROSCOPY (SEM)

SEM images were carried out as described in section 2.6.

5.2.3 THERMOGRAVIMETRIC ANALYSIS (TGA)

TGA data was collected as described in sections 2.4 and 3.2.2.

5.2.4 DIFFERENTIAL SCANNING CALORIMETRY (DSC)

DSC data was collected using modulated DSC method described in section 2.3.2.

5.2.5 MEASUREMENT OF SURFACE AREA

The surface area of the co-spray-dried trehalose/AP samples was determined by BET theory using the method described in section 2.10. All the samples were out gassed at 30 ° C for 240 min. The measurements were performed in three replicates to ensure reproducibility.

5.2.6 INVERSE GAS CHROMOTOGRAPHY (IGC)

Surface energy of the spray-dried trehalose/AP samples was determined using techniques described in section 2.9. The measurements were performed three times on each sample to ensure reproducibility of the data.

5.2.7 DETERMINATION OF ALKALINE PHOSPHATASE (AP) CONTENT

Alkaline phosphatase concentration in the spray-dried trehalose/AP powders was determined by BCA assay (section 2.11). Measurements of protein content at 280 nm were used to confirm the results obtained by the BCA assay (section 2.12). Each experiment was performed in three replicates in order to confirm reproducibility.

BCA assay and absorbance readings at 280 nm were also performed on spray-dried powder prepared without AP. These samples were prepared by spray drying trehalose in water, in (4:1) water-acetone and in (1:1) water-acetone. The purpose of these additional experiments was to determine whether trehalose or the different amounts of acetone would give an absorbance reading at the wavelengths used to determine protein content. These various types of amorphous trehalose samples did not give absorbance reading at 562 nm (BCA assay) or at 280 nm. The precise protein content in each of the spray-dried samples was of paramount importance as it is used to determine the activity of alkaline phosphatase in each of the samples.

5.2.8 ACTIVITY ASSAY

The measurement of alkaline phosphatase activity is based upon the hydrolysis of para-nitrophenyl phosphate (PNPP) (section 2.13). Alkaline phosphatase activity assay was performed on solutions prepared for spray drying and on the spray-dried powders. This was necessary to predict the effect of the entire process (from solution to powder) on the protein activity. The spray-dried powders, stored at 0 % RH, were examined over time for their protein activity. The same assay was used for the stability study

As the assay is based on the active units per mg solid protein, the amount of protein in each of the spray-dried sample had to be determined (section 5.2.7) before the activity assay could be conducted. Hence if the protein content of the sample is not accurate, or the amount of the sample weighed is incorrect due to changes in the sample density, the activity results will not represent the "true" activity of alkaline phosphatase.

5.2.9 DYNAMIC VAPOUR SORPTION AND NEAR INFRARED SPECTROSCOPY (DVS-NIRS)

Gravimetric studies of spray-dried trehalose/AP samples were carried out using a humidity and temperature controlled microbalance, Dynamic Vapour Sorption (DVS) apparatus as described in section 2.8. Samples of approximately 40-60 mg were loaded onto flat-bottomed quartz glass pan of the DVS, dried at 0 % RH for 8 h and subsequently exposed to 75 % RH for 10 h to induce crystallisation of free amorphous trehalose in the samples, before a second drying stage for 6 h. The NIR spectrometer recorded a mean of 32 scans every 15 / 30 min of the DVS experiment as described in section 2.8.

5.2.10 STABILITY STUDY

The stability study was performed in order to investigate the effects of increased humidity (75 % RH, at room temperature) and of increased temperature (50 °C, at 0 % RH). The spray-dried samples were desiccated under these conditions (section 2.7). NIR spectroscopy was employed to study the changes occurring in the samples due to high humidity and heat. Activity assay was performed on the samples to follow protein activity in these samples.

5.3 RESULTS AND DISCUSSION

Five samples in total were prepared using the formulation plan listed in Table 5.1. Samples 1-3 were prepared to examine changes in alkaline phosphatase content from 5 % to 0.5 %. Samples 4 and 5 were prepared to examine the influence of acetone on the spray-dried particles.

5.3.1 QUANTIFICATION AND ACTIVITY OF ALKALINE PHOSPHATASE

Alkaline phosphatase content in the spray-dried samples was determined as described in section 5.2.7 and the obtained results are presented in Table 5.3.

Table 5.3. *Alkaline Phosphatase content of the spray-dried samples.*

Sample	Expected % (w/w) AP Content	Average % (w/w) AP Content measured by BCA assay (S.D.)	Average % (w/w) AP Content measured at 280 nm (S.D.)
1	5	5.43 (0.29)	5.12 (0.13)
2	1	1.10 (0.11)	0.95 (0.17)
3	0.5	0.57 (0.04)	0.48 (0.11)
4	5	5.17 (0.22)	4.98 (0.10)
5	5	2.75 (0.24)	2. 42 (0.11)

The above results indicate that AP is fully recovered in the spray-dried powders, except in Sample 5. Sample 5 was spray-dried from 50 % (v/v) acetone. The acetone caused precipitation in the spray drying solution and aggregation of AP was observed. While the solution was being spray-dried, it is possible that the aggregated protein separated from the rest of the solution. These aggregated "clusters" probably never reached the

collection vessel causing a drop in AP content in the spray-dried product. This was further investigated by performing the BCA assay on the solution prepared for spray drying. The results showed the expected AP content in the solution. Considering that the solution was under constant stir until it was pumped into the nozzle, it is likely that aggregation occurred/increased during the flow into the nozzle.

Protein content was also measured at 280 nm and confirmed the results obtained by the BCA assay (Table 5.3). Hence it was concluded that Samples 1-4 contained the same AP concentration pre and post spray drying but approximately half of the AP concentration was lost during spray drying of Sample 5. Hence the spray-dried Sample 5 only contains ca. 2.5 % w/w AP.

A summary of the activity data for the spray-dried trehalose/AP samples is given in Table 5.4. It was observed that the activity of the unprocessed alkaline phosphatase, which was kept at 0 % RH in the freezer was reduced over time. Hence activity of the original AP was measured every time just before spray drying the samples. This was done in order to use a reference value for 100 % (maximum) activity of AP for the particular sample. This way the relative decrease of AP activity in all of the samples could be compared to each other, as AP activity prior to addition in the sample solution was considered to be 100 %.

The activity assay on the spray-dried samples was performed within a week of spray drying. This activity was followed for 10 weeks, while the samples were kept at 0 % RH desiccation. Unprocessed AP was also desiccated at 0 % RH over 10 weeks and the activity was measured (Table 5.4). The AP activity in the spray-dried samples did not display any decrease over this period of time. However the unprocessed AP did lose activity (Table 5.4). All of the solutions prepared for spray dying were also tested for AP activity. The results show that the spray drying process did not affect alkaline phosphatase activity. In fact the activity observed in solution prior to undergoing spray drying was the activity recovered in the spray-dried product. In contrast AP activity was affected by the presence of acetone in the spray drying solutions. However no further loss of activity was observed during desiccation.

Table 5.4. *Summary of the activity for the spray-dried trehalose/AP samples and unprocessed AP, pre- and post-spray-drying.*

Sample	AP activity (%) pre-spray -drying (solution) (S.D.)	AP activity (%) post-spray-drying (week 1) (S.D.)	AP activity (%) post-spray-drying (week 10) (S.D.)
AP (unprocessed and was not subjected to spray drying)	100.00 (1.68) (activity of the dry form, as received)	90.10 (2.99) (desiccated at 0 % RH, as received)	65.34 (4.76) (desiccated at 0 % RH, as received)
1 (5 % w/w AP) (water)	95.59 (3.45)	98.47 (2.76)	99.55 (3.87)
2 (1 % w/w AP) (water)	96.78 (4.52)	99.91 (2.29)	97.63 (3.59)
3 (0.5 % w/w AP) (water)	98.12 (3.89)	106.88 (5.67)	99.15 (2.34)
4 (5 % w/w AP) (20 % v/v acetone)	74.12 (2.55)	75.65 (3.89)	72.69 (4.88)
5 (5 % w/w AP) (50 % v/v-acetone)	18.54 (2.67) (5 % w/w AP)	20.51 (3.03) (2.5 % w/w AP)	22.83 (4.05) (2.5 % w/w AP)

It can be concluded from the data that alkaline phosphatase is resistant to any degradation caused by the spray drying process. Previous studies on AP from bovine intestinal mucosa have shown that the secondary structure is preserved over a range of temperatures (25 °C-70 °C) (Fournière et al., 1995). Considering the inlet temperature was kept at 60 °C during drying for all of the samples, it is not surprising that no loss of activity was observed. Spray drying alkaline phosphatase and maintaining the activity does show that it is a good model protein, as dried protein powders can be produced, which can later be investigated under extreme conditions to follow the mechanism for protein degradation. This was performed in the stability study discussed in section 5.3.5.

5.3.2 PROTEIN CONCENTRATION DEPENDENT PROPERTIES

The morphology, water content, Tg value, surface area and surface energy of the spray-dried trehalose/AP particles were examined in this section. The spray-dried samples were prepared using the processing parameters in Table 5.2 and were stored in 0 % RH desiccators containing P_2O_5. Samples 1, 2 and 3 were prepared as described in Table 5.1 and contained 5 % w/w, 1 % w/w and 0.5 %w/w AP, respectively. The effects of protein concentration in the spray-dried samples are the focus of this section.

The SEM images in Figure 5.1 display the concentration dependent morphological changes caused by alkaline phosphatase in the spray-dried particles. Raisin-like particles were produced in Sample 1 (5 % AP), and as the amount of AP decreased the particles became more spherical. Sample 3 (0.5 % AP) produced smooth particles that were similar to the particles produced by spray drying trehalose alone. Some of these particles displayed a dimpled morphology. The particle size seems to be the same regardless of the protein concentration. Particle sizing was attempted using the mastersizer but without success as the spray-dried particles caused aggregation when dispersed. A range of organic solvents (sunflower oil, propanol and octanol) was used to disperse the spray-dried powder and all resulted in aggregation of the particles. Hence the SEM images were used to get an approximation of the particle size.

The spray drying conditions were kept constant for all of the above samples; hence the change in morphology seems to be formulation dependent. Raisin-like particles have been observed for spray-dried protein formulations. Maa and colleagues observed this phenomena when rhGH was spray-dried alone or with Zn^{2+} (Maa et al., 1997b). Similar morphology was seen for spray-dried BSA and rhuMAbE25/mannitol (3:2) (Maa et al., 1997a). The shape of the particle was dependent on the properties of the protein as well as the excipients. Factors such as spray drying parameters may also influence the particle morphology, as observed in chapter 4. In another study, maltodextrin particles were prepared by spray drying and varying the inlet and outlet temperatures (Alamilla-Beltran, 2005). The particle morphology was dependent on the spray drying temperatures with the lowest inlet and outlet temperatures leading to raisin like particles.

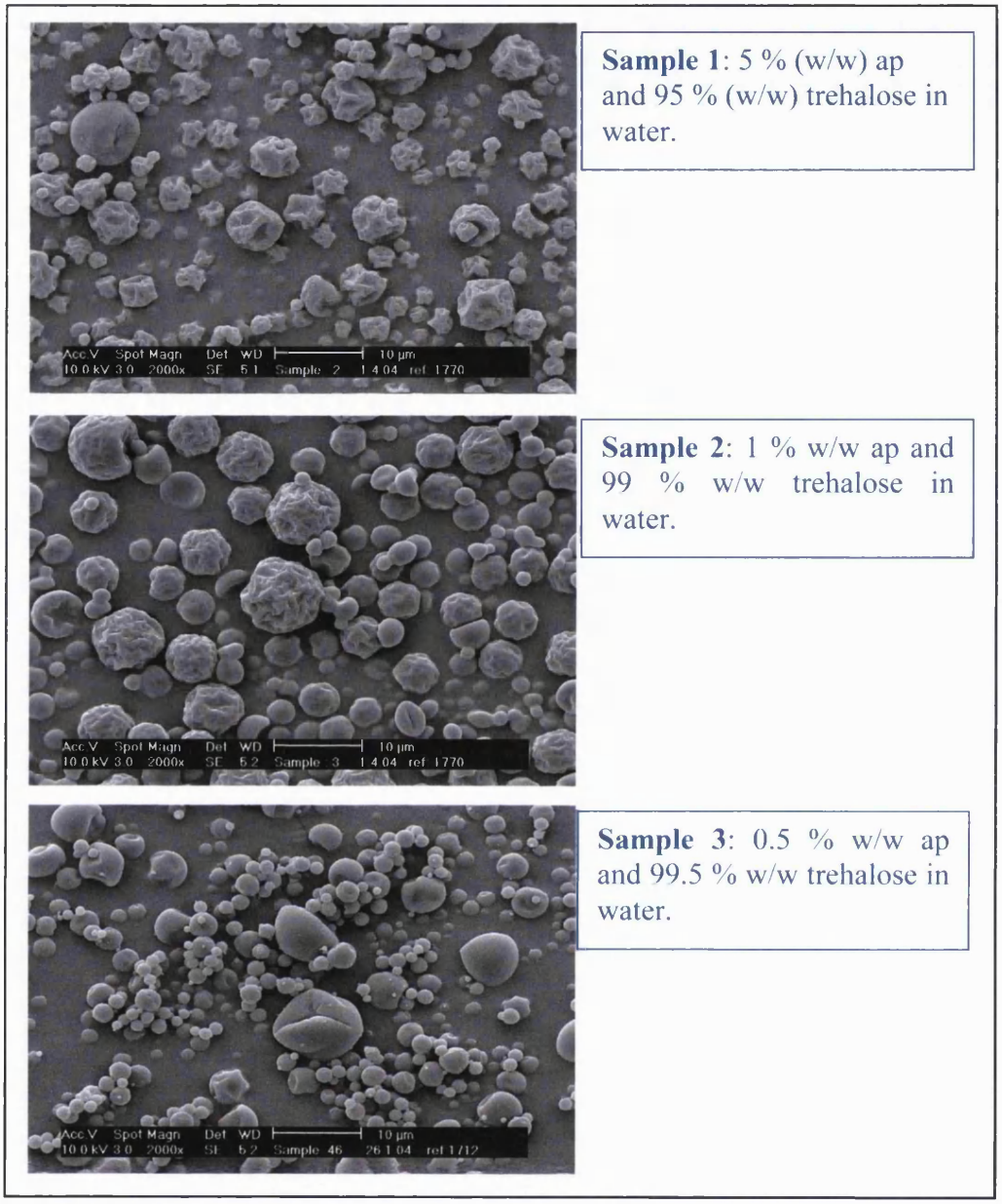

Figure 5.1. *SEM pictures of spray-dried trehalose/AP samples (1-3), containing 5 %, 1 % and 0.5 % w/w AP, respectively.*

It is suggested that the raisin like particles are produced by formation of a crust (skin), which allows the particle to inflate and the vapour pressure within the droplet causes it to break and thus the resultant particle collapses to a raisin like shape (Maa et al., 1997b; Walton et al., 1999; Alamilla-Beltran, 2005). Maa et al. (1997) investigated the morphology of spray-dried rhDNase/lactose particles. They produced dimpled particles from solutions containing higher concentrations of solids. They concluded that the observed dimpling was due to particles of increased density, which were more resistant

to collapse. The particles that were produced by spray drying with lower solution concentration showed deeper holes, indicating collapse of the particles (donut shape) (Maa et al., 1997a). These findings cannot be directly related to the SEM images shown above but it highlights the relevance of the density in regards to morphology. If the density of trehalose is higher than the density of AP, it is plausible that Sample 1 (5 % AP) would collapse producing raisin shape particles.

Fäldt and Bergenstål reported in 1994 that a small quantity of protein in a lactose solution caused a dramatic decrease in surface tension. This indicated a higher surface activity of protein compared to the carbohydrate on its own. Spray drying of the solution reflected the increased surface activity of the protein by the appearance of "dents" in the particles, indicating the presence of protein at the particle surface (Fäldt et al., 1994). Hence, accordingly Sample 1 (5 % AP), containing the highest amount of protein (the most surface active component), holds alkaline phosphatase on the surface of the spray-dried particles, which causes the raisin-like shape.

The effects of protein concentration in Samples 1-3 were not limited to particle morphology. The yield of the spray-dried powder was also influenced by protein concentration. As the relative amount of alkaline phosphatase decreased in the formulations, the yield also decreased (Figure 5.2).

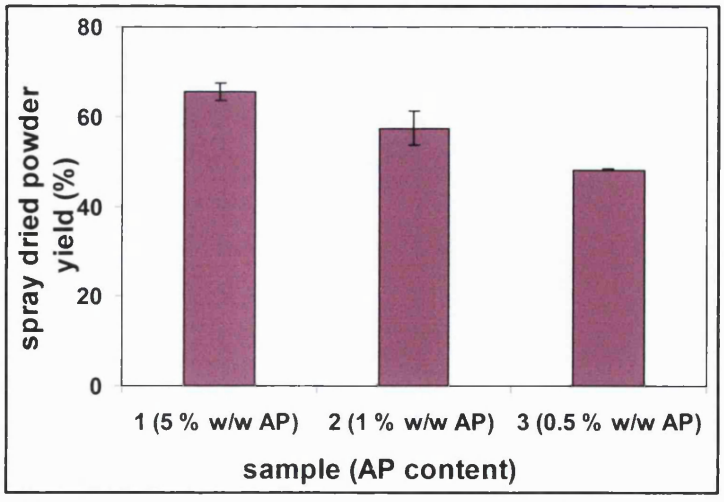

Figure 5.2. *The relationship between the yield of the spray-dried products and alkaline phosphatase concentration.*

The data from the thermogravimetric analysis presented in Table 5.5 displays that the presence of alkaline phosphatase in the samples causes an increase in the moisture content compared to amorphous trehalose (10 % w/v spray-dried trehalose). As the protein concentration is decreased through Samples 1 to 3, the water content is slightly reduced. Hence in the spray-dried trehalose/AP powders, alkaline phosphatase induces more moisture than amorphous trehalose. A typical trace for the thermogravimetric data is shown in Figure 5.3 and shows that these samples lose all the water just around 120 °C, which was also seen for amorphous trehalose samples in chapter 4 (Figure 4.4).

The impact of moisture on the protein in the solid-state can be severe causing crystallisation of the excipient, trehalose. The moisture levels can affect particle size and crystallisation of trehalose during long-term storage. Water acts as a plasticiser and lowers the Tg of the system. Though the water content for Samples 1 (5 % AP), 2 (1 % AP) and 3 (0.5 % AP) is comparatively not too different, it would be interesting to see whether it could be significant enough to cause differences in the powder characteristics. Considering that proteins consist of a large number of water molecules, it is not surprising that a relatively high amount of alkaline phosphatase, as in Sample 1 (5 % AP), would lead to a higher moisture content than seen for amorphous trehalose.

Table 5.5. *Thermogravimetric analysis data for samples 1-3 and amorphous trehalose.*

Sample	Water content (%)	S.D.
amorphous trehalose (Chapter 4)	2.40	0.42
Sample 1 (5 % w/w AP)	3.73	0.12
Sample 2 (1 % w/w AP)	3.67	0.08
Sample 3 (0.5 % w/w AP)	3.42	0.10

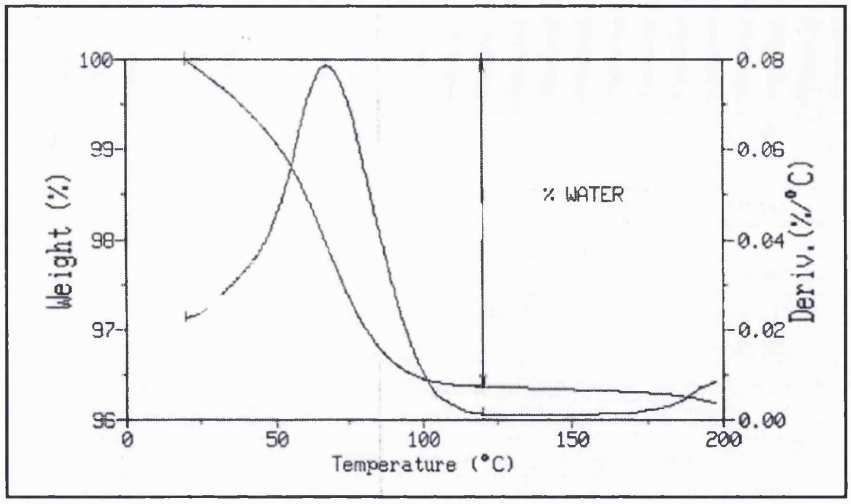

Figure 5.3. *A typical trace obtained by thermogravimetric analysis of samples 1, 2 and 3.*

The Tg values for Samples 1-3 are listed in Table 5.6. These data were obtained with modulated DSC. The samples were also subjected to heating rates of 10 °C/min to detect the presence of any thermal transitions associated with crystalline trehalose as described in chapter 3. These DSC data gave no indication of the presence of crystalline trehalose in Samples 1-3. The amorphous content was confirmed by XRPD. As alkaline phosphatase was not spray-dried alone due to the cost, the XRPD was obtained from unprocessed AP. The AP, as received had been freeze-dried and was amorphous (Figure 5.4).

Table 5.6. *Glass transition values for the samples (1-3) and amorphous trehalose.*

Sample	Glass transition (Tg) onset value (°C)	S.D.
amorphous trehalose	120.28	(1.50)
Sample 1 (5 % w/w AP)	115.23	(2.59)
Sample 2 (1 % w/w AP)	110.74	(1.63)
Sample 3 (0.5 % w/w AP)	109.96	(1.48)

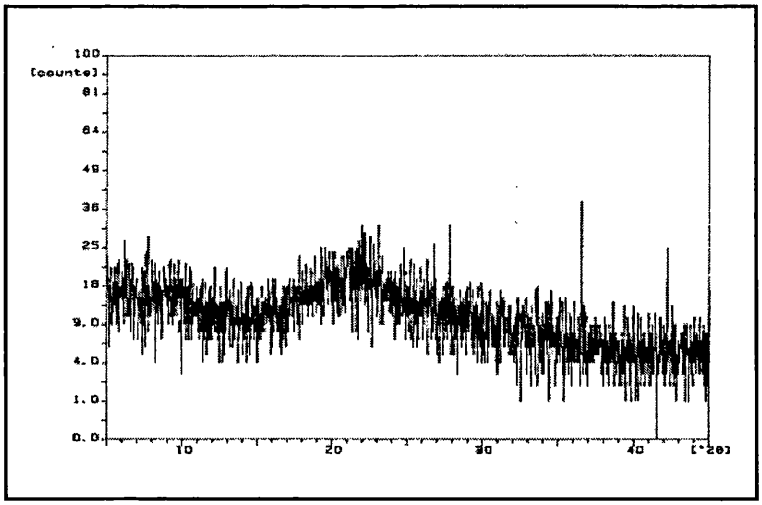

Figure 5.4. *Typical X-ray diffraction pattern for alkaline phosphatase.*

Efforts were made to find the Tg value of AP in the literature. No value could be found and all efforts to obtain the Tg by DSC failed because the protein degraded as it was heated. The spray-dried trehalose/AP samples displayed reduced Tg values compared to pure amorphous trehalose (Table 5.6). As the protein concentration is decreased so is the Tg value (Sample 1 compared to Samples 2 and 3). It was observed that spray-dried samples retained more residual water than amorphous trehalose (Table 5.5). This trend is reflected in the Tg values, as the Tg value is higher for amorphous trehalose as compared to the spray-dried trehalose/AP samples. The residual moisture (water) in the samples acts as a plasticiser and decreases the glass transition values.

The BET technique was initially used to investigate the potential porous properties of the spray-dried samples. However these could not be measured successfully but the surface area of the spray-dried particles was obtained in the process. The measured surface area (m^2/g) of the samples was compared to the surface area of amorphous and crystalline trehalose (Table 5.7). Crystalline trehalose exhibited the highest surface area. This is due to the crystal morphology compared to the amorphous particle morphology (Antila, 1991). Compared to amorphous trehalose obtained by spray drying, Sample 1 (5 % AP) had a higher surface area. The samples (Samples 2 and 3) with lower AP, displayed lower surface area than amorphous trehalose and Sample 1 (5 % AP). The surface area decreased as the particle morphology became less raisin-like. Hence the data suggest that the protein is concentrated/located on the particles surface in Sample 1 (5 % AP).

Table 5.7. *Surface area measurements for samples 1-3, amorphous trehalose and crystalline trehalose.*

Sample	Specific surface area (m^2/g)	S.D.
amorphous trehalose	1.11	0.01
α,α-trehalose dihydrate	2.13	0.12
Sample 1 (5 % w/w AP)	1.27	0.03
Sample 2 (1 % w/w AP)	0.96	0.04
Sample 3 (0.5 % w/w AP)	1.07	0.06

5.3.2.1 Influences of protein concentration on dispersive surface energy

Elution peaks were observed for Samples 1-3 with the five non-polar probes by inverse gas chromatography (IGC). These peaks were used to calculate the dispersive surface energy of the samples (Figure 5.5). The surface energies for amorphous trehalose, crystalline trehalose and unprocessed AP, are also shown in Figure 5.5. Variation (standard deviation) was much lower for the spray-dried samples as compared to the crystalline trehalose and the unprocessed AP. Sample 1 (5 % AP), exhibited the largest non-polar value (42.55 mJ/m^2). Since the particles do not contain crystalline trehalose, alkaline phosphatase seems to be the dispersive component at the surface of the particles in the spray-dried trehalose/AP particles. At 1 % or less AP (Samples 1 and 2), the surface energy is similar to that of amorphous trehalose. The surface energy of unprocessed protein is 41.4 mJ/m^2. This is similar to the value obtained for Sample 1 (5 % AP). This indicates and confirms the findings of the previous data that AP is located on the surface of the particles in Sample 1 (5 %).

The surface energies of the amorphous trehalose and the crystalline trehalose are similar, taking the standard deviations into account. It has been suggested by several researchers that the ratio between the sugar and protein can determine the extent of crystallisation of the amorphous sugar in the dried product (Sarciaux et al., 1997; Forbes et al., 1998; Tzannis et al., 1999a). Due to the similar dispersive energies of the

amorphous and crystalline trehalose, no conclusions can be made to what extent if any crystallisation is occurring in these spray-dried samples.

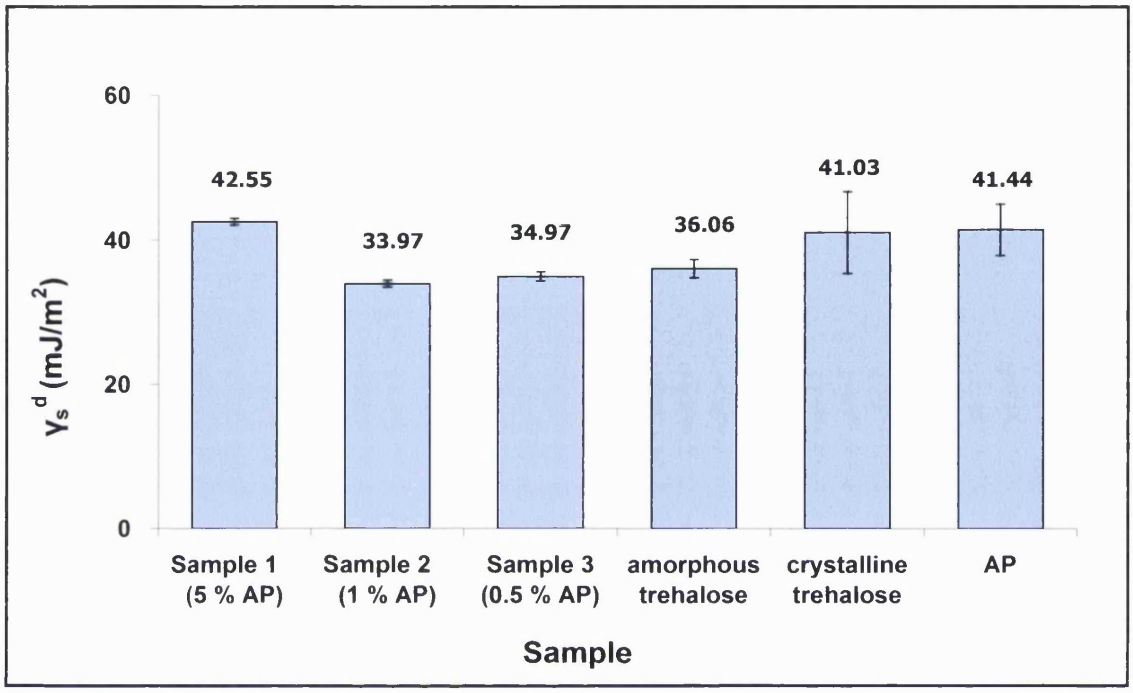

Figure 5.5. *Protein concentration dependent variations in dispersive components seen for samples (1-3) and compared to the surface energies of amorphous and crystalline trehalose and pure alkaline phosphatase.*

The acidic/basic character of the samples was used to further understand the surface properties of the spray-dried trehalose/AP powders. Of the four chosen polar probes, acetone did not elute within the maximum experimental time (40 min) for crystalline trehalose and unprocessed AP. This could possibly be due to a strong interaction between acetone and the powder surface of these two samples. Both of these samples were presumably subjected to unknown processing conditions prior to being supplied and hence cannot be compared directly to the spray-dried trehalose/AP samples. The data displayed in Figures 5.6 and 5.7 show that Sample 3 (0.5 % AP) with the lowest AP content has a greater K^A and K^D value than Samples 1 (5 % AP) and 2 (1 % AP), implying it will interact more with both acidic and basic materials. The negative values for K^D obtained for crystalline trehalose and unprocessed AP are difficult to explain due to their unknown processing history.

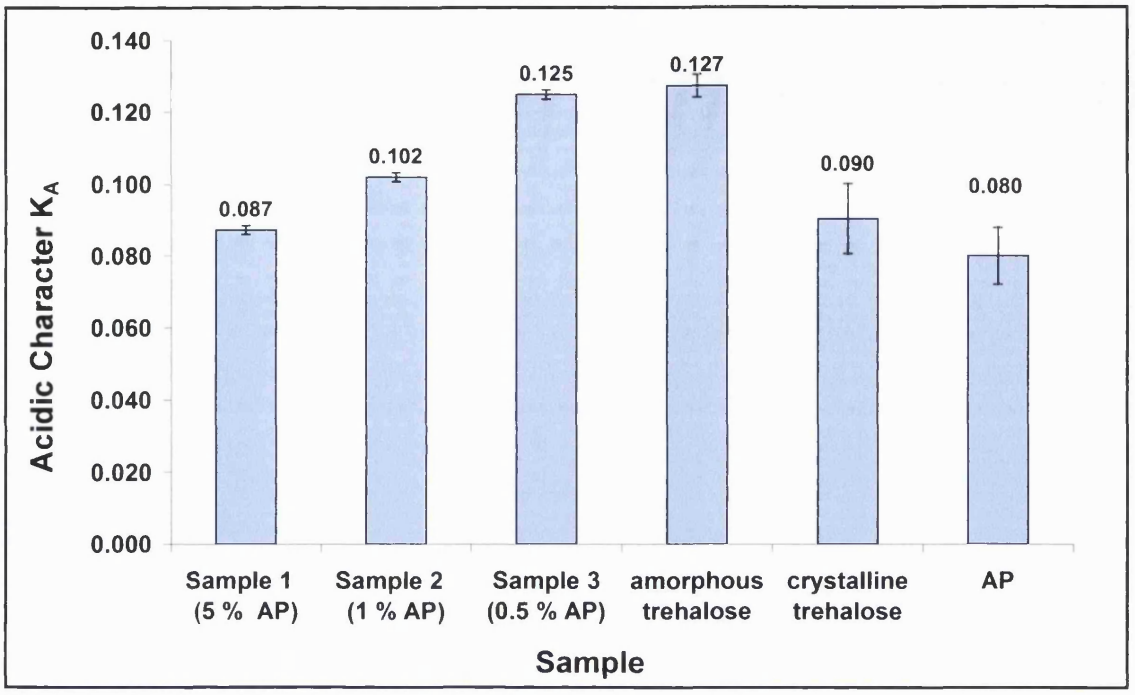

Figure 5.6. *Acidic character of samples 1-3, amorphous and crystalline trehalose and pure AP.*

The K^A value of the crystalline trehalose is much lower than what is seen for the amorphous trehalose and the spray-dried Sample 3 (0.5 % AP). This suggests that the powder surface displays a more acidic character after spray drying. Sample 3 contains the lowest amount of protein (0.5 % w/w) and Samples 1 (5% AP) and 2 (1 % AP) have lower K^A values and a higher protein concentration. The high protein concentration could be causing crystallisation of trehalose or the particle surface could be richer in AP. In a study by Lopez et al. (2004), high proportions of protein to sugar caused degradation of the protein, which could have been due to crystallisation of the sugar. However the spray-dried trehalose/AP samples did not display any crystalline properties seen by DSC measurements and therefore the presence of AP at the surface is the likely cause of the acidic character of the spray-dried particles. As the AP concentration is increased, the K^A value is decreased and the sample surfaces become more acidic in nature. The K^D value observed for amorphous trehalose is lower than that observed for the spray-dried trehalose/AP Sample 3 (0.5 % AP) (Figure 5.7). The basic nature of the spray-dried AP samples seems to increase with decreasing amounts of alkaline phosphatase. Sample 3 is more basic than amorphous trehalose. Thus the increase of AP content causes the spray-dried samples to be less basic in nature.

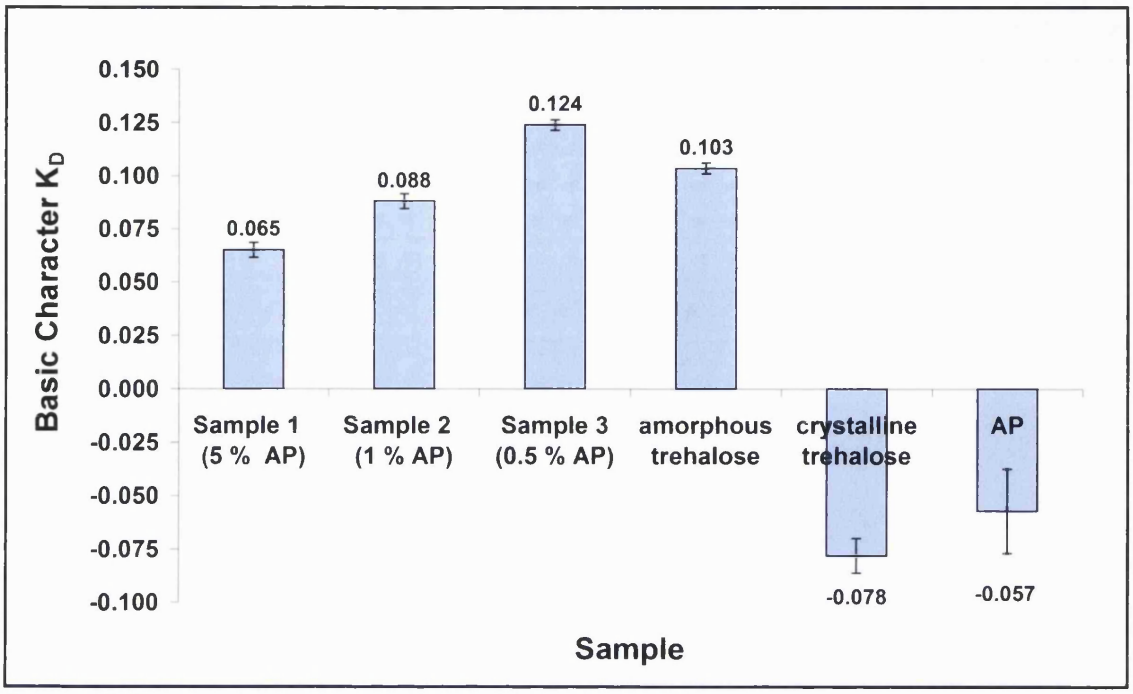

Figure 5.7. *Basic character of samples 1-3, amorphous and crystalline trehalose and pure AP.*

Considering the retention of the polar probes onto the sample surfaces provided an insight of the observed K^A and K^D values (Figure 5.8). Crystalline trehalose showed the highest amount of variation for all of the probes. The acidic probe, chloroform, interacted with the crystalline trehalose and pure AP sample the greatest. As an acidic probe, the strongest interaction with surfaces showed that these were more basic than any other of the batches (as acid interacts with base). After spray-drying trehalose with AP, the interaction of the probe is reduced, confirming a more predominantly acidic surface than before. This again correlates to higher K^A values observed for spray-dried samples (Samples 1-3 and amorphous trehalose) compared to crystalline trehalose and AP. The other acidic probe, ethanol, showed the greatest amount of interaction for Sample 1 (5 % AP), which constitutes the highest protein content and does not show the trends observed by chloroform probe or the K^A and K^D values. In a study by Ticehurst et al. (1996) ethanol displayed a strong affinity for the surface moisture of α-lactose monohydrate. Hence less emphasis was made on this probe. Ethyl acetate (basic probe) showed greatest interaction with the surface of amorphous trehalose and Sample 3 (0.5

% AP). The interaction decreased when the amount of AP was increased (Samples 1 and 2), making these surfaces less acidic in nature.

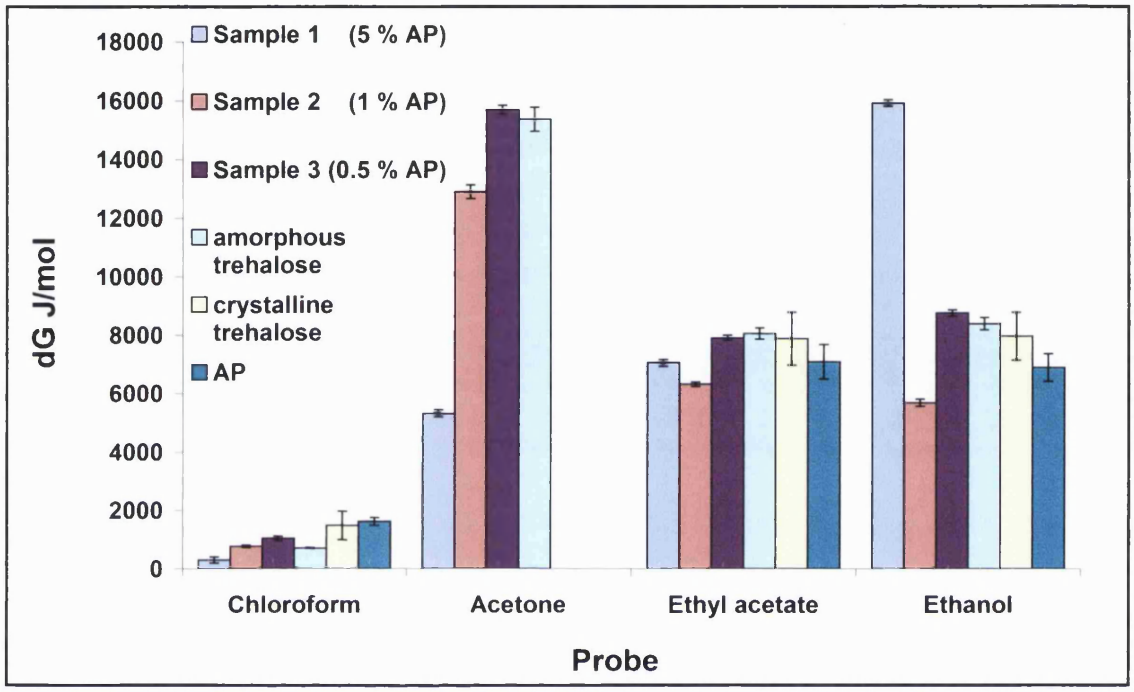

Figure 5.8. *The variation in interaction of the polar probes on the surfaces of spray-dried samples (1-3), amorphous and crystalline trehalose and pure AP.*

Finally acetone (basic probe) also showed greatest interaction for sample containing the least amount of protein (Sample 3) and the interaction decreased as the protein concentration was increased. The stronger interaction coincided with the increase in K^A values and thereafter the weaker interactions represented the drop in K^A values. The IGC results have been summarised in Table 5.8. The morphology of the particles, the surface area observed by BET theory and the data here indicate that in the spray dried trehalose/AP particles, alkaline phosphatase is located on the surface.

Table 5.8. *Summary of the non-polar surface energy and acid/base character of samples 1-3, amorphous and crystalline trehalose and pure AP.*

Sample	(Υ^d_s) (mJ/m^3) (S.D.)	K^A (S.D.)	K^D (S.D.)	K^D/ KA (S.D.)
amorphous trehalose	36.06 (1.26)	0.127 (0.003)	0.103 (0.002)	0.813 (0.003)
α,α-trehalose dihydrate	41.03 (5.63)	0.090 (0.010)	- 0.078 (0.008)	- 0.867 (0.086)
alkaline phosphatase	41.44 (3.53)	0.080 (0.008)	- 0.057 (0.020)	- 0.704 (0.190)
Sample 1 (5 % w/w AP)	42.55 (0.48)	0.087 (0.001)	0.065 (0.004)	0.747 (0.038)
Sample 2 (1 % w/w AP)	33.97 (0.52)	0.102 (0.001)	0.088 (0.004)	0.864 (0.025)
Sample 3 (0.5 % w/w AP)	34.97 (0.64)	0.125 (0.001)	0.124 (0.002)	0.992 (0.014)

5.3.2.2 Conclusions

The following conclusions can be made from the study of spray-dried trehalose/AP particles regarding the effects of AP concentration on the sample properties:

- High alkaline phosphatase content produces raisin like particles, which have a high surface area and indicate that the protein is located on the surface of the spray-dried particles.

- The presence of AP in the spray-dried particles increases the water content, which in turn decreased the glass transition temperature.

- The presence of alkaline phosphatase in the spray-dried samples increases the yield of the spray-dried product, which also highlights the surface active properties of AP.

- High alkaline phosphatase content in the spray-dried samples induces high surface energy, which also confirms that AP is located on the surface of the spray-dried particles.

- The acidic and the basic properties decrease as the AP content is increased in the spray-dried samples. This is again due the large amount of alkaline phosphatase present at the surface of the particles, which seems to buffer the acidic and basic properties of the particles. Crystallisation of trehalose could also be causing the change in the K^A and K^D values. Conclusive evidence could not be found from the IGC data, as the K^D values of the crystalline trehalose and AP were negative. The DSC data however did not provide any evidence for the presence of crystalline trehalose in the samples. Therefore the data indicate that by spray drying from large amounts of AP (Sample 1, 5 % AP) the produced particles have higher proportions of the protein at the surface.

5.3.3 ACETONE DEPENDENT PROPERTIES

The 5 % AP formulation, Sample 1, displayed a range of properties different from the 1 % and 0.5 % AP formulations (Samples 1 and 2). The data indicated that AP was localised at the surface of the particles in Sample 1 (5 % AP). To examine if it might be possible to modify morphology by varying compositions, Samples 4 and 5 were prepared. Both samples were formulated with 5 % AP, while varying the amounts of acetone used during spray drying. The effects of acetone during spray drying on the properties of the particles are the focus of this section. The results obtained from the quantification and activity studies conducted on the spray-dried samples (section 5.3.1) revealed that the AP concentration in Sample 5 decreases after spray drying and therefore it only contains ca. 2.5 % AP in the spray-dried powder.

The morphological variations caused by acetone are shown in the SEM images in Figure 5.9. The highest amount of acetone was (50 % v/v) in Sample 5 and produced smooth surfaced spherical particles. Compared to Sample 1 (5 % AP, spray-dried from only water), the raisin-like morphology was lost. The raisin shaped particles seem to be a combined result of alkaline phosphatase concentration and the spray drying solvent.

Maa et al. (1997) proposed that the density of the solution has an impact on the particle morphology. The high-density solutions in their study were more prone to produce "dimpled" particles, as these were resistant to collapse. The collapse of the particles produces the raisin and the donut shape particles. Samples 1, 4 (20 % v/v) and 5 (50 % v/v) differ in the solvent compositions used during spray drying. The density of acetone (0.78 g/cm^3) is lower than the density of water (1 g/cm^3) and hence the presence of acetone would lower the overall density of the solution, which is the case in Samples 4 and 5. Nevertheless these samples seem to be more resistant to the collapse associated with lower density particles. During the spray drying process, the samples containing acetone (Samples 4 and 5) would be expected to dry quickly in comparison to Sample 1, which is prepared from water. The same drying parameters were used for all of the samples. Thus the density would change during drying with solutions containing high amounts of acetone, potentially becoming relatively more dense than purely aqueous solutions. This may partially explain why Sample 5 (50 % v/v) produced particles that were resistant to collapse.

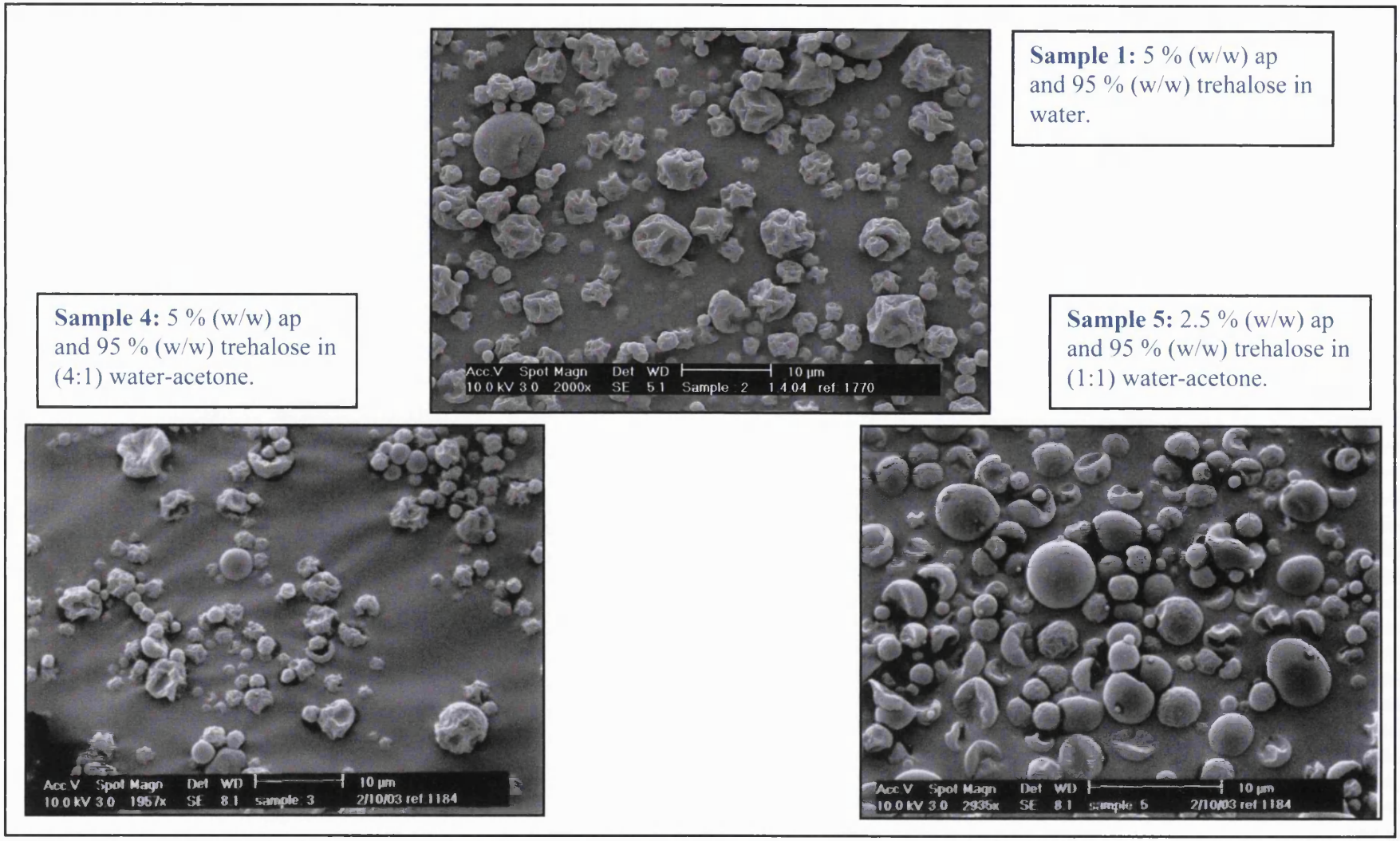

Figure 5.9. *SEM pictures of spray-dried trehalose/AP Samples 1, 4 and 5, containing water, (4:1) water-acetone and (1:1) water-acetone, respectively*

The effects of acetone are also evident on the spray-dried powder yields. As the amount of acetone was increased the yield decreased and a high standard deviation was observed (Figure 5.10). Acetone contributes to the static nature of trehalose and hence the yields decrease and are less consistent. This was observed in chapter 4 while spray-drying different compositions of trehalose, where the spray-dried powders were sticking to the internal surfaces of the spray dryer, SDMicro^{TM}.

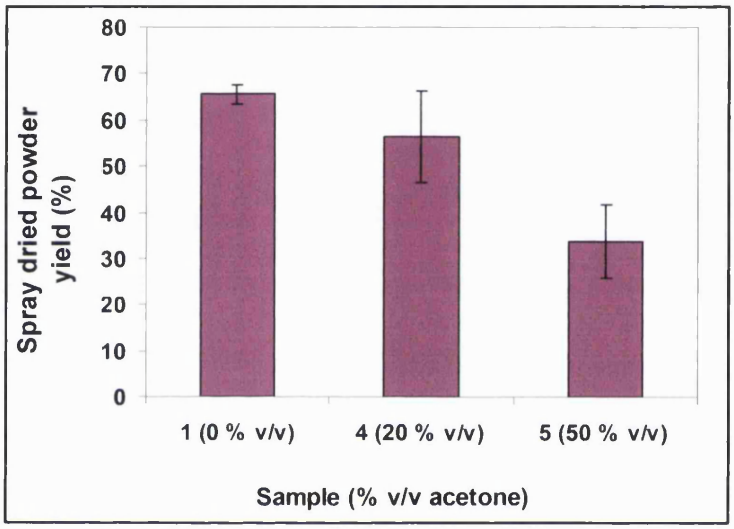

Figure 5.10. *The relationship between the yield of the spray-dried products and acetone concentration.*

Compared to the purely aqueous systems, the residual solvent content in the aqueous acetone Samples 4 and 5 was similar (Table 5.9). The thermogravimetric data indicate that Samples 4 (20 % v/v) and 5 (50 % v/v) lose all their initial moisture at a fast rate by around 120 °C and then slowly continue to lose more moisture during a second temperature range of 120-150 °C (Figure 5.11). Samples that are prepared by water alone lose their moisture by 120 °C as well (Figure 5.3). Acetone has a lower boiling temperature (~ 56 °C) than water and therefore logically cannot be the cause of the moisture retention seen at these high temperatures. The other reason for the two different rates of moisture removal can be the presence of bound and free water. If that were the case, the free water (bulk water) would be removed first followed by removal of the bound water.

Table 5.9. *Thermogravimetric analysis data for samples 4 and 5.*

Sample	Water content (%) (S.D.) Peak 1	Water content (%) (S.D.) Peak 2	Total water content (%) (S.D.)
Sample 1 (0 % v/v acetone)	3.73 (0.12)	Not present	3.73 (0.12)
Sample 4 (20 % v/v acetone)	3.39 (0.23)	0.28 (0.01)	3.67 (0.24)
Sample 5 (50 % v/v acetone)	3.55 (0.30)	0.45 (0.01)	3.99 (0.31)

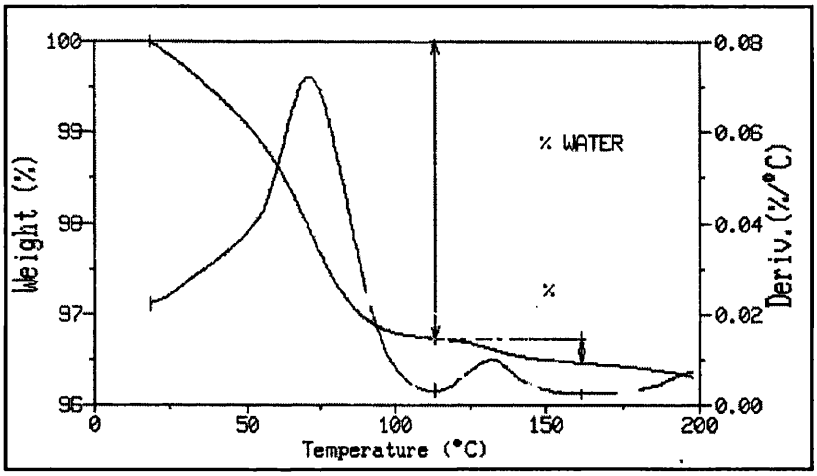

Figure 5.11. *A typical trace obtained by thermogravimetric analysis of Samples 4 (20 % v/v acetone) and 5 (50 % v/v acetone).*

The overall combined moisture content from the two peaks is higher than amorphous trehalose but similar to what was observed for Samples 1-3. This is surprising as the spray-dried Samples (4 and 5) prepared with aqueous acetone contain less water than when prepared by water alone (Samples1-3). It is possible that acetone causes some crystallisation of trehalose within the sample although the DSC data did not give any indication to crystalline trehalose. Thermogram traces collected for crystalline trehalose as seen in Figure 3.8 in Chapter 3, show that moisture removal continues up to 140 °C. This is due to the fact that the two water molecules of the crystalline trehalose are not equivalent (Taga et al., 1972; Brown, 1972). While preparing the aqueous acetone samples for spray drying, it was noted that the addition of acetone to the aqueous

solution containing protein and trehalose, could cause precipitation if the acetone was added too quickly and without stirring. It is also possible that the two moisture-retaining peaks observed for Samples 4 and 5 are due to a combination of trehalose crystallisation and bulk and bound water. It is likely that these partially crystallise as they are heated during the TGA experiments and the second peak is due to the phase separated crystalline trehalose. If any trehalose crystallisation had occurred within the samples, it was not significant enough to be detected by DSC or XRPD. DSC run at 10 °C/min were carried out on Samples 4 and 5 in order to detect transitions of crystalline trehalose as described in chapter 3, although none were found.

The spray-dried trehalose/AP samples from aqueous acetone (4 and 5) compared to the samples spray-dried from water (Samples 1-3) showed similar XRPD patterns. The glass transitions values for these two samples (4 and 5) were similar to the spray-dried Sample 1 and are listed in Table 5.10. Considering that the spray-dried powder of Sample 5 contained less AP (~ 2.5 %) it is surprising that the Tg value is still similar to the other samples with higher AP content (Samples 1 and 4).

Table 5.10. *Glass transition values for samples 1, 4 and 5.*

Sample	Glass transition (Tg) onset value	S.D.
Sample 1 (5 % w/w AP; 0 % v/v acetone)	115.23	2.59
Sample 4 (5 % w/w AP; 20 % v/v acetone)	115.46	2.15
Sample 5 (2.5 % w/w AP; 50 % v/v acetone)	116.62	2.28

Surface area measurements observed using the BET technique for the spray-dried samples for aqueous acetone are shown in Table 5.11. Samples 4 (20 % v/v) and 5 (50 % v/v) also have a high surface area similar to Sample 1, which is initially surprising, considering that Samples 4 and 5 produced particles, which were less raisin-like than the particles produced in Sample 1 (Figure 5.9). Sample 4 (20 % v/v) produced a mixture of raisin like and dimpled particles. Hence it is understandable that the surface

area of these particles is similar to what was observed for Sample 1 and higher than amorphous trehalose. When the amount of acetone was increased further in Sample 5 (50 % v/v), a blend of smooth swollen particles, collapsed particles and dimpled / rough surfaced particles were produced. The roughness of the particle surface could be indicative of porous particles, which would explain the large surface area (1.37 m^2/g) observed here.

Table 5.11. *Surface area measurements for samples 1, 4, 5 and amorphous trehalose.*

Sample	Specific surface area (m^2/g)	S.D.
amorphous trehalose	1.11	0.01
Sample 1 (5 % w/w AP)	1.27	0.03
Sample 4 (5 % w/w AP; 20 % v/v acetone)	1.32	0.09
Sample 5 (2.5 % w/w AP; 50 % v/v acetone)	1.37	0.03

5.3.3.1 Influence of acetone on dispersive surface energy

The non-polar surface energies of Samples 4 and 5 are shown in Figure 5.12. These are compared to Sample 1, which contains the same amount of protein and trehalose but is spray-dried from a purely aqueous solution (section 5.3.2). The non-polar surface energies of amorphous trehalose (spray-dried from water), crystalline trehalose, amorphous trehalose spray-dried aqueous acetone and AP are also shown in Figure 5.12. As control the amorphous trehalose prepared from aqueous acetone was spray-dried using the same parameters as described for all other samples (Table 5.2). This control was done to determine whether the presence of acetone in the spray drying solution would affect the surface energy of the produced particles. The sample presented here was spray dried from a ratio 4:1 (water:acetone) (chapter 4). No results regarding the surface energies could be obtained for amorphous trehalose spray-dried

from 1:1 (water:acetone) ratio. This was due to the spray-dried material being very sticky and the packaging of the column proving difficult.

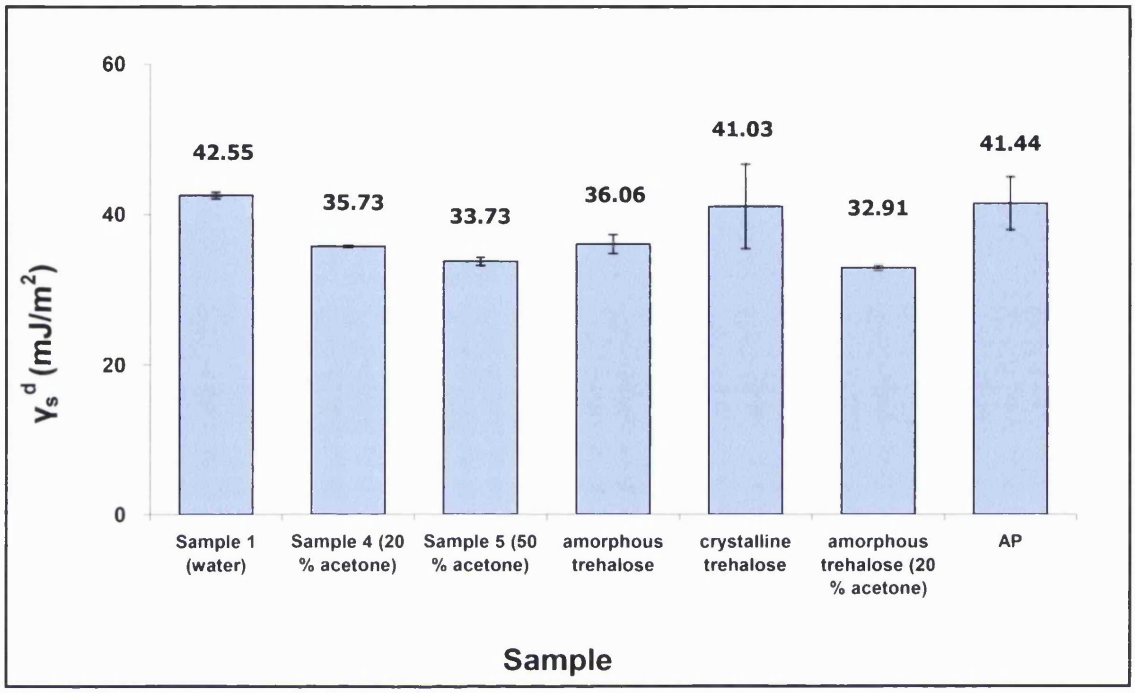

Figure 5.12. *Acetone dependent variations in dispersive components seen for samples (1, 4 and 5) and compared to the surface energies of amorphous trehalose prepared by two different compositions, crystalline trehalose and alkaline phosphatase.*

There were differences in the amorphous trehalose spray dried from aqueous acetone compared to when it was spray dried from water. As described previously, while preparing the samples containing acetone, precipitation of the solution (in particularly Sample 5) was observed. This is likely to cause protein degradation/denaturation to some extent (Banga, 1995; Brange, 2000). In the previous study comparing the protein concentration dependent changes of particle surface energies, it was concluded that alkaline phosphatase was present at the particle surface of Sample 1 (5 % AP). This was the reason the surface energy decreased as the amount of AP was decreased. The data suggests that the presence of acetone is somehow causing less of the protein to be at the surface of the particles. The denaturation/degradation of protein by acetone is a likely

cause for observed surface energies. On the other hand acetone could also be causing the protein to be encapsulated in the particles, giving rise to lower surface energies.

The acid/base character of the aqueous acetone samples was characterised and is shown in Figures 5.13 and 5.14. The K^A and K^D values indicate that the amorphous trehalose prepared from a purely aqueous solution interacts greatly with both acidic and basic materials, where as the addition of acetone in the preparation of amorphous trehalose diminishes these interactions resulting in lower K^A and K^D values. By comparing the K^A values of the two amorphous trehalose samples and crystalline trehalose, it is evident that trehalose becomes more acidic in nature after spray drying. The amorphous trehalose prepared by aqueous acetone displayed a lower K^A value than amorphous trehalose prepared by water. This may indicate that the acetone may be causing some amount of crystallisation in the sample.

The spray-dried trehalose/AP samples exhibit high K^A and K^D value for Sample 4 (20 %v/v acetone), followed by Sample 1 (0 % v/v acetone) and then Sample 5 (50 % v/v acetone). The highest amount of acetone (Sample 5) exhibits K^A and K^D, which are lower than what is observed for aqueous sample (Sample 1). This gives reason to believe that the differences in surface properties in the presence of acetone are different in the two samples (4 and 5).

The retention of the individual polar probes are shown in Figure 5.15 and provide an insight into the observed K^A and K^D values. The acidic probe, chloroform interacted greatest with the surface of Sample 4 (20 % v/v acetone) followed by sample 1 (0 % v/v acetone) and sample 5 (50 % v/v acetone). This corresponds to the observed K^D values for these samples. The other acidic probe, ethanol showed that Sample 1 had the greatest interaction followed by Sample 5 and Sample 4. This trend is different to that seen for the K^D values. Similarly, interpreting the results of the basic probe, acetone, followed the trend seen by the K^A values, where as this was not the case for the other basic probe, ethyl acetate.

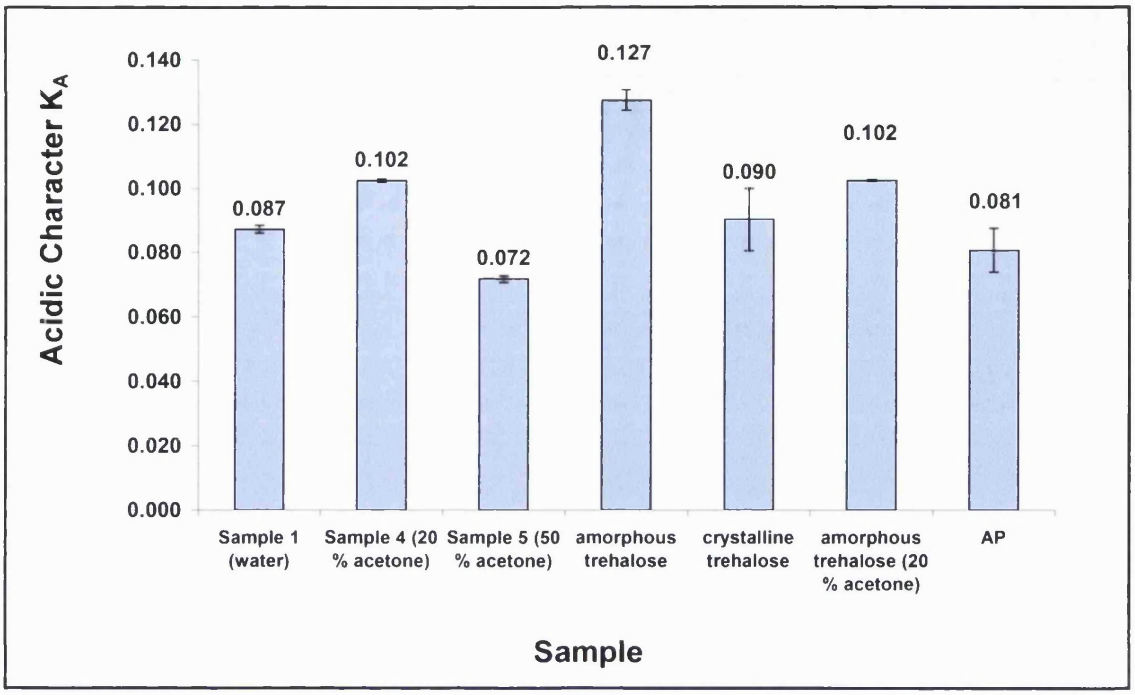

Figure 5.13. *Acidic character of samples 1, 4 and 5, two different types of amorphous trehalose prepared by different compositions, crystalline trehalose and AP.*

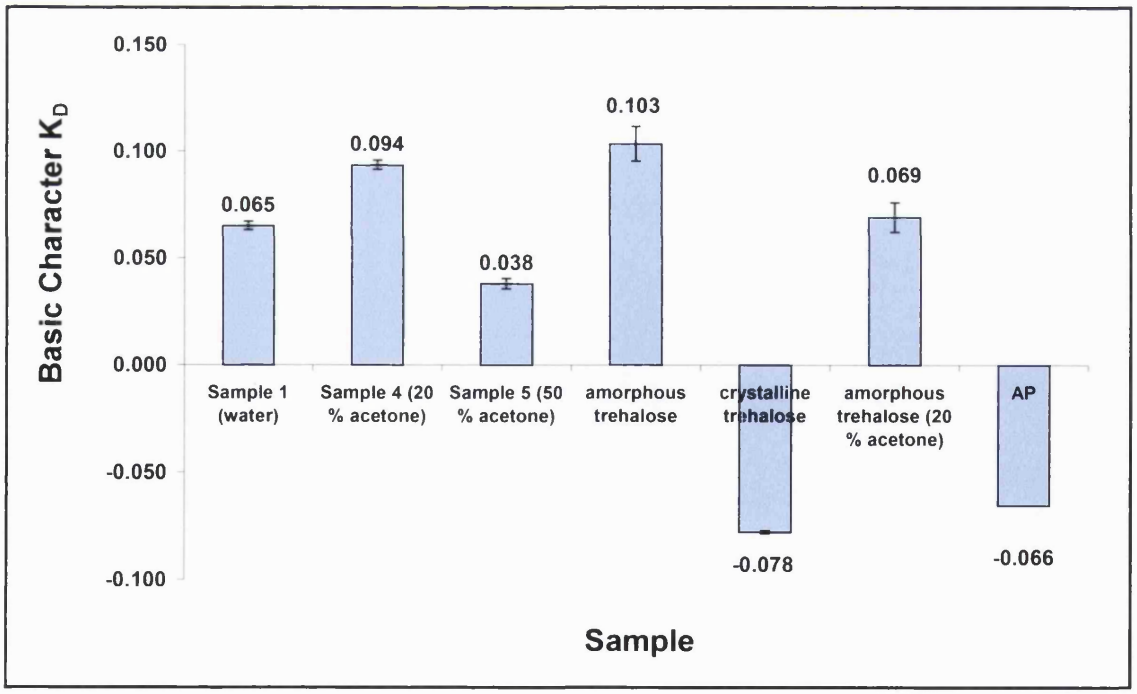

Figure 5.14. *Basic character of samples 1, 4 and 5, two different types of amorphous trehalose prepared by different compositions, crystalline trehalose and AP.*

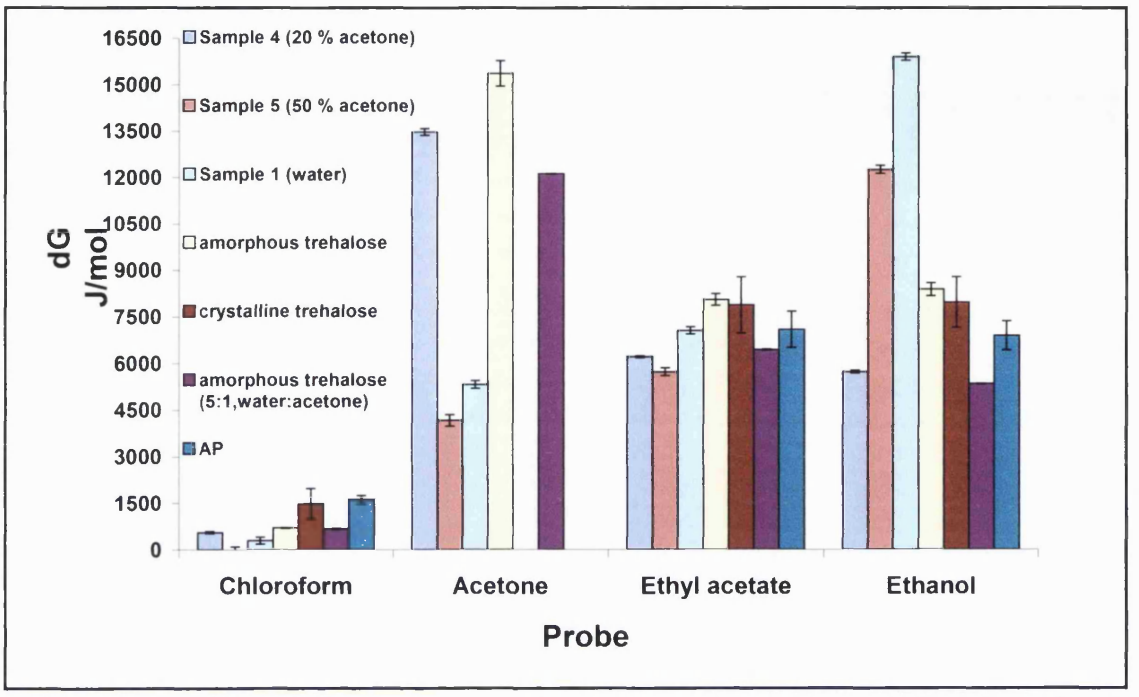

Figure 5.15. *The variations in interaction of the polar probes on the spray-dried samples (1, 4 and 5), two types of amorphous trehalose prepared by different compositions, crystalline trehalose and AP.*

Hence it is difficult to conclude what is causing the differences in the surface properties between Samples 4 (20 % v/v acetone) and 5 (50 % v/v acetone) but it is most likely due to lack of AP at the surface of the particles. It seems that in Sample 4 (20 % v/v), acetone is causing some trehalose crystallisation and therefore the acidic and basic surface properties in these particles are higher than in Sample 1 (100 % water). When the amount of acetone is increased further in Sample 5, a decrease in the K^A and K^D values indicate that the surface activity of the protein is diminishing due to protein degradation. The summary of the IGC results is given in Table 5.12.

Table 5.12. *Summary of the non-polar surface energy and acid/base character of samples 1,4,5, two types of amorphous trehalose, crystalline trehalose and pure AP.*

Sample	(Υ^d_s) (mJ/m^3) (S.D.)	K^A (S.D.)	K^D (S.D.)	K^D/KA (S.D.)
amorphous trehalose	36.06 (1.26)	0.127 (0.003)	0.103 (0.002)	0.813 (0.003)
amorphous trehalose (5:1 water-acetone)	32.91 (0.31)	0.102 (0.0003)	0.069 (0.001)	0.673 (0.010)
α,α-trehalose dihydrate	41.03 (5.63)	0.090 (0.010)	- 0.078 (0.008)	- 0.867 (0.086)
alkaline phosphatase	41.44 (3.53)	0.080 (0.008)	- 0.057 (0.020)	- 0.704 (0.190)
Sample 1 (5 % w/w AP)	42.55 (0.48)	0.087 (0.001)	0.065 (0.004)	0.747 (0.038)
Sample 4 (5% w/w AP; 20 % v/v acetone)	35.73 (0.22)	0.102 (0.0005)	0.094 (0.002)	0.915 (0.015)
Sample 5 (2.5% w/w AP; 20 % v/v acetone)	33.73 (0.56)	0.072 (0.001)	0.038 (0.002)	0.529 (0.036)

5.3.3.2 Conclusions

Overall the addition of acetone to the spray drying solution causes some changes in the 5 % w/w AP dry powders. These changes are summarised below:

- The amount of AP in the spray-dried powder is reduced as the amount of acetone in the spray drying solution is increased and the combined influence of variations in AP content and solvent properties is reflected by the data.

- As the amount of acetone is increased in the spray-dried samples, the raisin shaped particles become more spherical and possibly porous as suggested by the surface area measurements for Sample 5 (1:1 water-acetone).

- The presence of acetone in the spray-dried samples causes static interactions and hence the yield of the final product decreases.

- The thermogravimetric data suggest the presence of crystalline trehalose in the spray-dried trehalose/AP samples containing acetone. However this presumably occurs when the spray-dried sample is heated causing crystallisation.

- The surface energies of the spray-dried particles decreases with an increasing amount of acetone, suggesting trehalose crystallisation and/or protein degradation.

5.3.4 WATER VAPOUR SORPTION STUDIES USING DVS/NIR

The water vapour sorption behaviour of the spray-dried samples (Table 5.1) was studied by DVS/NIR as described in section 5.2.9. These experiments were performed to study the crystallisation of trehalose in the presence of alkaline phosphatase. Unprocessed alkaline phosphatase was also evaluated with the same DVS conditions. Activity data was collected for unprocessed alkaline phosphatase pre and post spray drying. Protein activity of the spray-dried samples was attempted post exposure of the samples in the DVS. The samples were exposed to a cycle of dehydration, rehydration and dehydration, which caused the crystallisation of the trehalose in the samples. This made it difficult to scrape the sample off the DVS pan without causing damage to the sample pan. Hence no activity data is presented for the damage caused to the spray-dried samples during DVS studies. Though the stability study performed in section 5.3.4 does highlight the effects of dehydration and humidity on the spray-dried samples and their activity.

5.3.4.1 Unprocessed alkaline phosphatase

The unprocessed AP was subjected to the same DVS condition as the spray-dried samples to elucidate the behaviour in the spray-dried trehalose/AP samples (Figure 5.16). The activity data performed on alkaline phosphatase after exposure in the DVS measured 85.58 % (±5.65) AP activity. It was expected that a change in protein activity would be reflected in the water sorption behaviour and NIR spectra. AP lost approximately 7 % mass during the initial drying stage, followed by a mass increase of 27 % upon exposure of AP to 75 % RH. The sample mass then reached a plateau at 75 % RH. During the final drying stage the sample mass returned to approximately the same as displayed at the end of the first drying stage (Figure 5.16). The NIR data collected for AP during the critical stages of the DVS experiment are presented in Figures 5.17, 5.18 and 5.19.

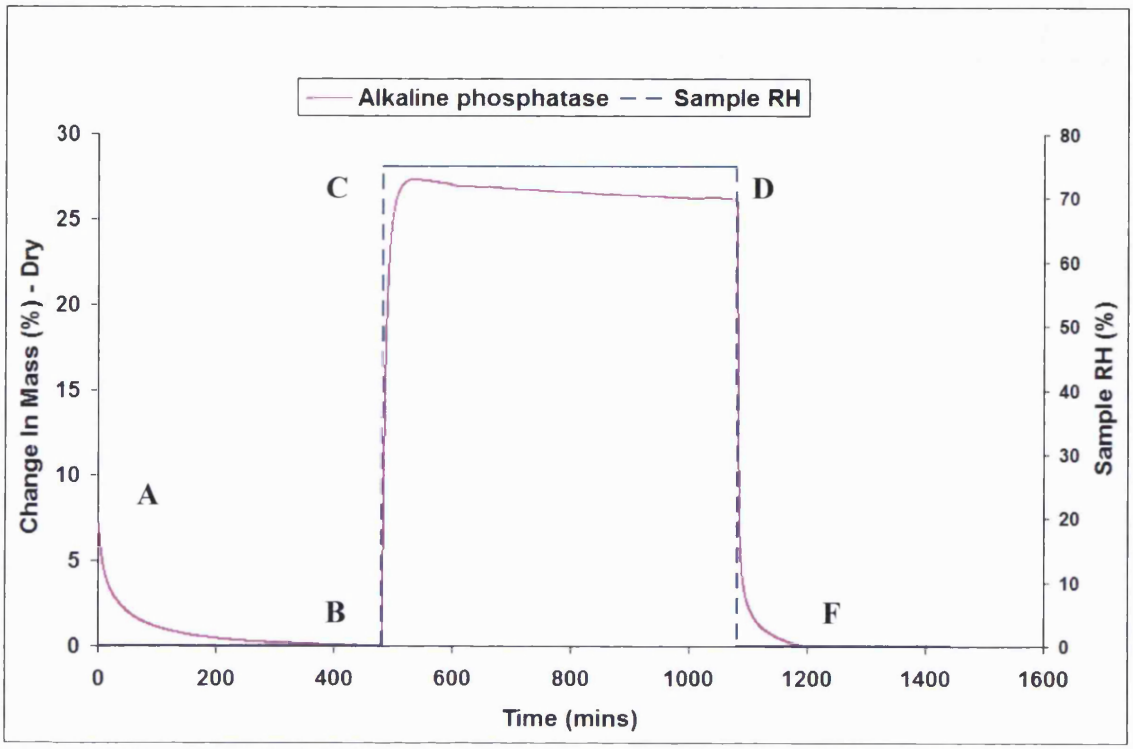

Figure 5.16. *DVS plot for alkaline phosphatase exposed to 0 % RH for 8 h (A-B), 75 % RH for 10 h (C-D) and then 0 % RH for a further 6 h (E-F) (at 25 °C).*

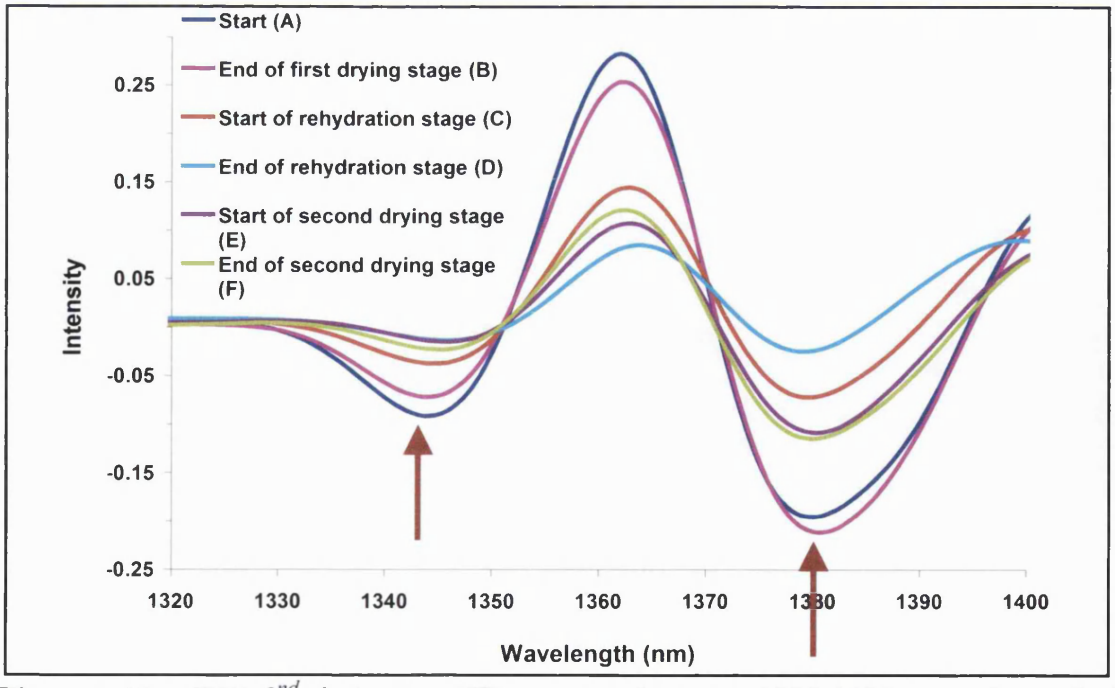

Figure 5.17. *SNV 2nd-derivative NIR spectra between 1320-1400 nm of supplied alkaline phosphatase during critical stages of the DVS experiment.*

NIR data between 1320-1400 nm is displayed in Figure 5.17. Peaks in this region are generally indicative of the first overtone of C-H combination bands (-CH_3 group C-H stretch and bend, 1355-1365 nm) (Ciurczak, 2001). Alternatively, peaks in this region may be representative of water combination variations (1375-1385 nm, OH symmetrical and anti-symmetrical stretch). The two negative peaks seen in Figure 5.17 represent the C-H combination band around 1345 nm and H_2O combination band around 1380 nm. These peaks do not show any major shift during the experiment.

Differences between 1840-1900 nm in the spectra of alkaline phosphatase are shown in Figure 5.18. According to Siesler et al. (2002), phosphorus group moieties are found in this region (P-H, 1890-1900 nm). Free –OH groups in water molecules have also been reported in this region (1890 nm) (Vandermeulen et al., 1980b). Shifts are seen in the two negative peaks around 1860 nm and 1885 nm. The changes occur when the rehydration is initiated in the DVS and are most obvious towards the end of the rehydration stage. By the end of the second drying stage the shifts resume their initial appearance implying the changes occurring in this region are reversible with drying.

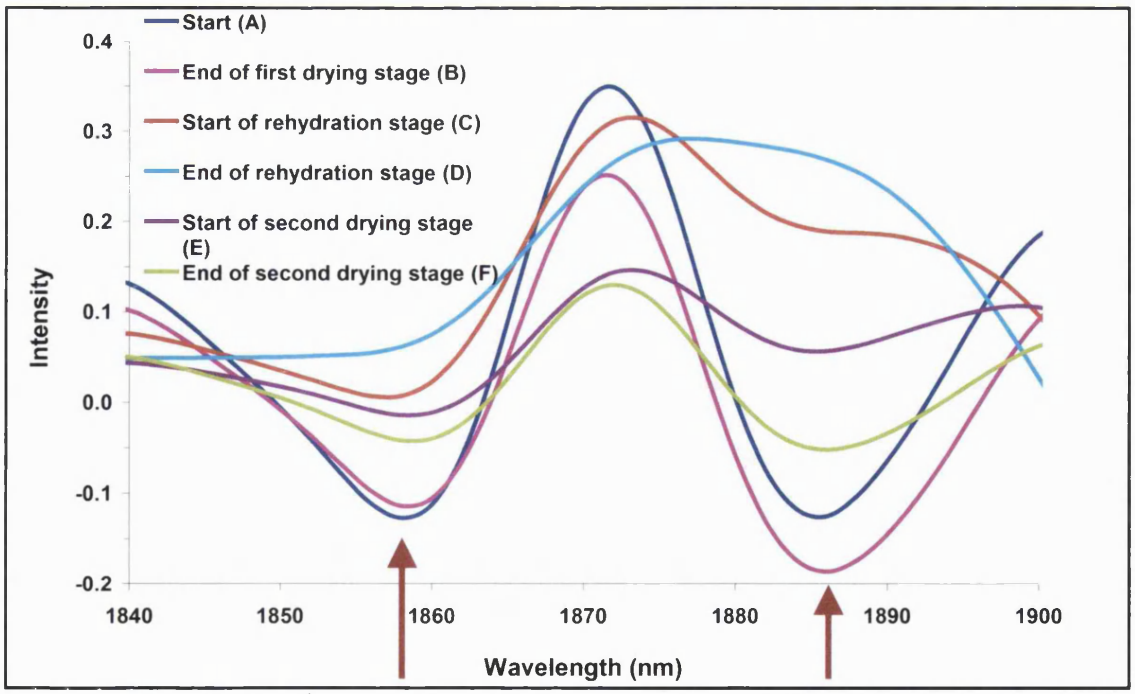

Figure 5.18. *SNV 2nd-derivative NIR spectra between 1840-1900 nm of supplied alkaline phosphatase during critical stages of the DVS experiment*

The region between 1900-2080 nm is presented in Figure 5.19 and shows three negative peaks, around 1930 nm, 1980 nm and 2060 nm, respectively. Several absorptions bands have been reported in this region in the literature. Pure water has been reported near 1950 nm (Vandermeulen et al., 1980b). In another study a peak approximately 1904 nm was assigned to surface water (bulk/free water) and another peak at 1936 nm for bound water (Zhou et al., 2003). The initial spectra of AP showing a broad peak around 1930 nm, in fact consists of three peaks around 1915 nm, 1930 nm and 1945 nm. These seem to be consistent with water activity. These peaks also change when rehydration occurs, but by the end of the second drying stage they revert to their initial spectra. The same trend is seen in the peaks at 1980 nm and 2055 nm.

In a study by Sadler et al. (1984) a peak near 1350 nm was assigned in the denatured proteins. This was not evident in our study, concurring with the activity assay result, which did not show a major drop in AP activity pre and post DVS. At the end of the DVS experiment, some aggregation of alkaline phosphatase sample was observed, which would change the sample density.

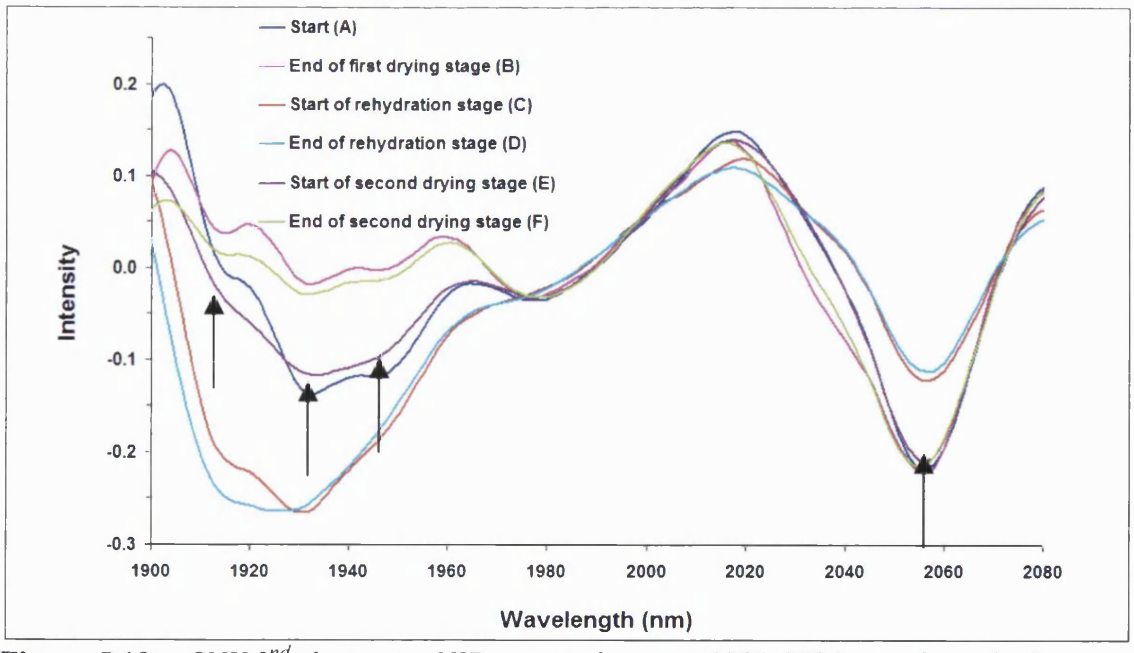

Figure 5.19 *SNV 2nd-derivative NIR spectra between 1900-2080 nm of supplied alkaline phosphatase during critical stages of the DVS experiment.*

Examining the raw reflectance spectra for alkaline phosphatase taken during the DVS experiment indicates that there is a tendency for aggregation (Figure 5.20) (O'Neil et al., 1999). In Figure 5.20, the absorbance around 1950 nm increases when the humidity is increased from 0 % to 75 % RH. These variations in the raw absorbance spectra are retained in the corresponding second derivative spectra. From these representative spectra, a quantitative relationship between the intensity of absorbance and the moisture level is indicated. The maximum absorbance is seen at the end of the rehydration stage (D). The absorbance intensity decreases during the second drying stage (E-F) but is still higher than what was obtained at the start of the experiment (A).

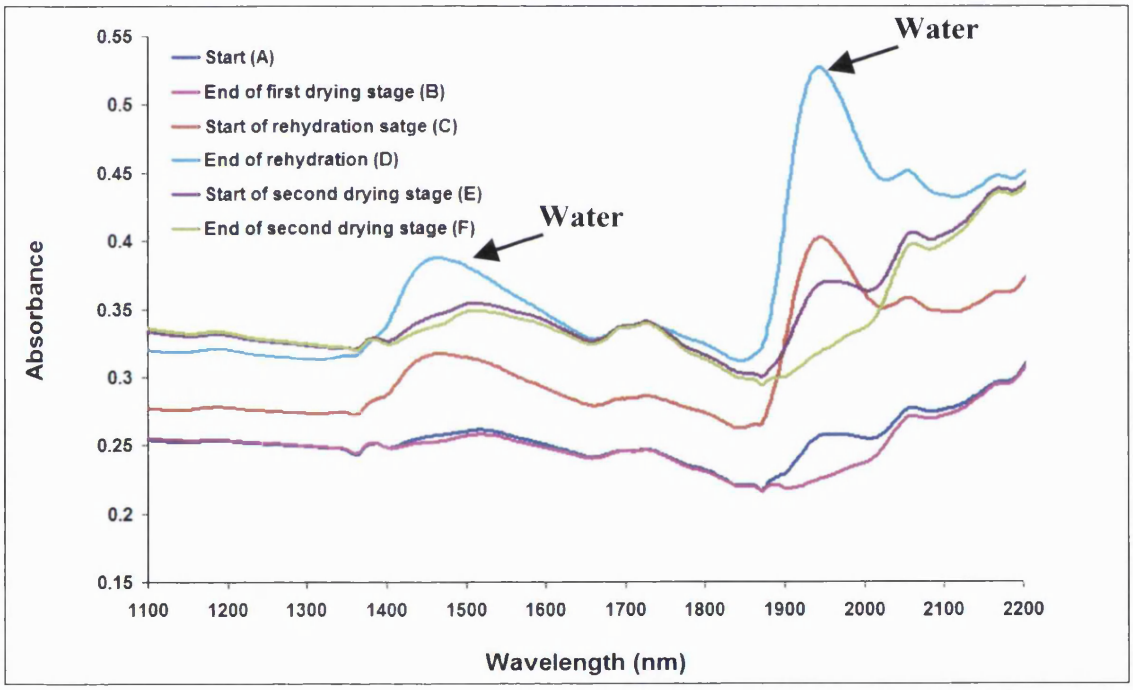

Figure 5.20 *Absorbance spectra of alkaline phosphatase at stages (A-F) depicting changes in particle size.*

In Figure 5.20, the changes due to moisture are concentrated around 1500 nm and 1950 nm and both regions change intensities after the sample (AP) has been rehydrated. Vandermeulen et al. (1980) found that the water of hydration for the proteins studied (pepsin and BSA) gave peaks near 1500 nm and 1950 nm, whereas the peaks for pure water were found at 1450 nm and 1928 nm. The region around 1500 nm represents

water that is associated near the surface of the protein and the region around 1900 nm represents bound water (Zhou et al., 2003).

The amount of AP used in the spray-dried samples compared to trehalose was less and it was anticipated that the changes occurring in the spray-dried trehalose/AP powders would therefore mainly reflect the properties of trehalose. The unprocessed alkaline phosphatase was studied by DVS/NIR in order to understand the changes that may be due to the protein in the trehalose/AP powders. The difficulties in examining the spray-dried trehalose/AP powders by NIR are due to the overlapping of the AP spectra with the NIR spectra of amorphous and crystalline trehalose (Figure 5.21).

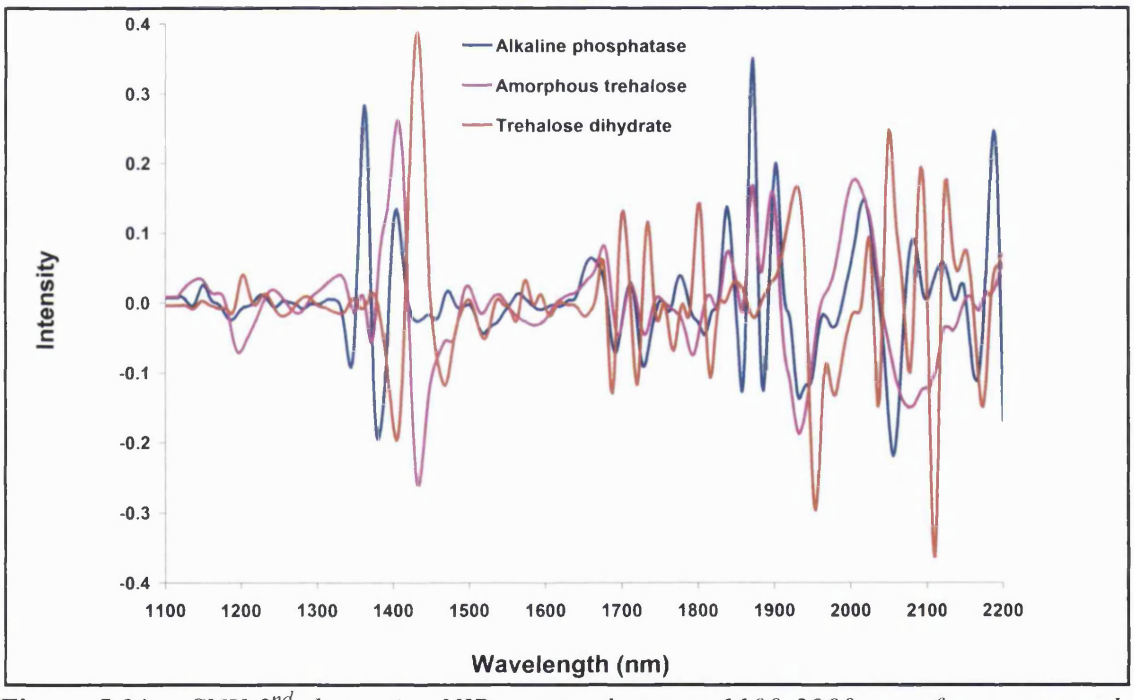

Figure 5.21 *SNV 2nd-derivative NIR spectra between 1100-2200 nm of un-processed alkaline phosphatase, amorphous trehalose and crystalline trehalose.*

5.3.4.2 Protein concentration dependent changes

The DVS profiles for the samples prepared from water are displayed in Figure 5.22. After the initial dehydration stage, all three samples increase in weight due to 75 % RH exposure. The amounts of this weight increase varies, with approximately 13 %-16.5 %. It was anticipated that a high AP content would lead to an increase in the moisture

content when exposed to 75 % RH. No correlation between protein content and weight increase was evident in these samples due to a relatively low AP content in all of the samples. The weight increase seen here is similar to what is seen for amorphous trehalose as presented in chapter 4. The moisture increase in all three samples is sufficient to lower the Tg value below the experimental temperature (25 °C) and gives the material mobility to allow crystallisation (Saleki-Gerhardt et al., 1995). At this point, collapse of the sample with related mass loss is seen. The mass loss is indicative of excess water from the system, which is followed by the rearrangement of molecules to the crystal form.

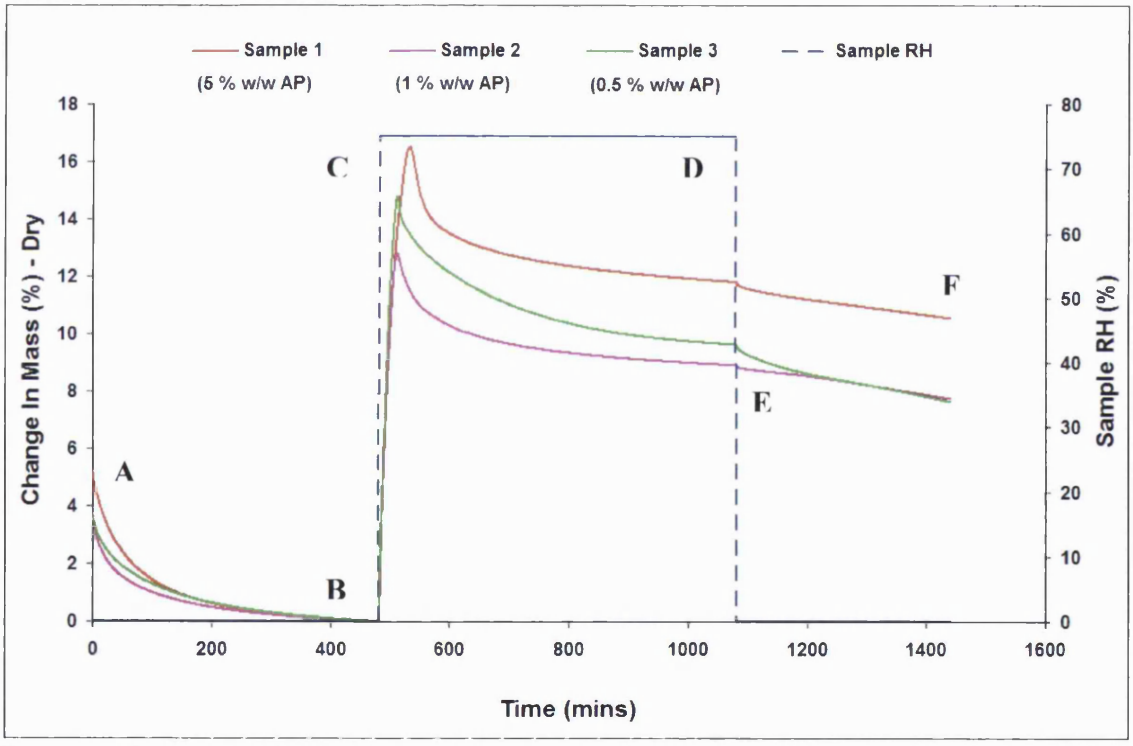

Figure 5.22. *DVS plot for the three spray-dried trehalose/AP samples exposed to 0 % RH for 8 h (A-B), 75 % RH for 10 h (C-D) and then 0 % RH for a further 6 h (E-F) (at 25 °C). Spray dried samples were dried from 5 %, 1 % and 0.5 % (w/w) AP in the solutions.*

Tzannis et al. (1999) observed that an increase in the concentration of sugar (sucrose) in the spray-dried carbohydrate/protein formulations led to a reduction in the critical percentage RH required to facilitate crystallisation of the amorphous carbohydrate in the formulations. They suggested that at high sucrose content, preferential sugar-sugar

interactions prevailed, resulting in phase separation within the formulation, inhibiting the crystallisation of amorphous sugar. The preferential absorption of the sucrose molecules in the sugar-rich phase reduced the amount of sucrose available to interact with the protein (trypsinogen) and consequently could not effectively protect the protein during spray drying (Tzannis et al., 1999b). The results obtained by the activity assay do not concur with the findings of these researchers, as the high trehalose content (samples 1-3) protected alkaline phosphatase in solution and during spray drying.

By the end of 75 % RH stage Sample 1 (5 % w/w AP) shows a higher moisture retention than Samples 2 and 3, which both contain between 9-9.5 % water. In contrast Sample 1 displays a moisture increase of ca. 11.5%. These differences were also seen in the water sorption studies conducted on the different batches of amorphous trehalose (chapter 4). The NIR data collected during these DVS experiments did not elucidate on the changes occurring due to the AP. However the characteristic double peak associated with trehalose dihydrate was observed. The NIR data was examined by principal component analysis and will be discussed later in this chapter.

5.3.4.3 Acetone dependent changes

The DVS data for the two samples prepared from aqueous acetone are displayed in Figure 2.23. The trace for 5 % AP prepared from water is also included for comparison. After the first drying stage (A-B) all samples are dry and are exposed to 75 % RH (C). This results in a moisture uptake, seen as weight increase of approximately 16 % for Sample 1 (0 % v/v acetone) and Sample 4 (20 % v/v acetone) and an increase of around 11.5 % for sample 5 (50 % v/v acetone).

The rate of crystallisation broadly followed the trend Sample 1 > Sample 4 > Sample 5. Thus Sample 1 crystallised the fastest. The amount of acetone in these spray-drying solutions seemed to correlate with the ability of trehalose crystallisation in the spray-dried samples. By the end of the rehydration stage (D) the total weight is around 11.5 %, 10.5 % and 9 % for 0 % (v/v), 20 % (v/v) and 50 % (v/v) acetone, respectively. The decrease in weight is gradually continued through the final dehydration stage (E-F) and results in Sample 1 having retaining the highest mass (10.5 %). As the amount of acetone in the spray-drying solutions is increased the mass seen at the end of the second dehydration stage is decreased.

The NIR spectra for the three samples showed the double peak at 1954/1978 nm representative of the dihydrate form of trehalose at the end of the final drying stage and the spectra was examined by PCA, which is discussed later in the chapter.

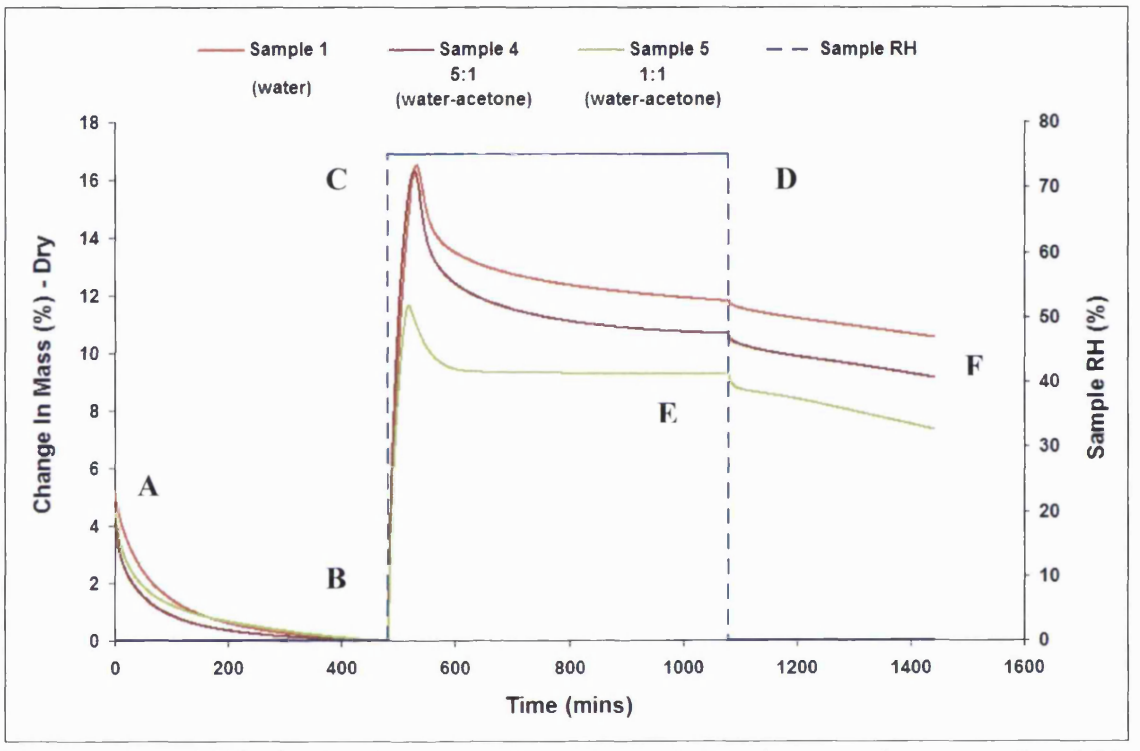

Figure 5.23. *DVS plot for the three spray-dried trehalose/AP samples exposed to 0 % RH for 8 h (A-B), 75 % RH for 10 h (C-D) and then 0 % RH for a further 6 h (E-F) (at 25 °C). Spray dried samples were dried from 0 %, 20 % and 50 % (v/v) acetone in the solution.*

5.3.4.4 Principal component analysis (PCA)

The NIR data from all of the DVS experiments were analysed to determine if any correlations could be observed. All of the dried samples, regardless of alkaline phosphatase concentration or amount of acetone in the solution showed the same trends. These were similar to what was observed in chapter 4 for amorphous trehalose and are presented in Figures 5.24 and 5.25. After treating each of the runs separately in the Unscrambler® using full cross validation it was established that the first PC appeared to correspond to a change in form (amorphous to crystalline), which accounted fot roughly

94 % of the spectral changes. This was clearly seen in the loadings, where the double peak (1950/1978 nm) corresponding to the dihydrate form is observed. PC2 on the other hand clearly followed the water in the system, through the increased and decreased RH stages and the "kicking out" of the water from the system. The loading plot also shows that the changes occur in the water region of the spectra.

The next step was to ascertain that by looking at spectra over a smaller number of data points, where the trehalose form is changing, whether different loading are seen. Again the loadings for each of the spray-dried samples were similar (both PC1 and PC2). The loading differences were greatest, around 90 %, between 1800 –2000 nm (water region). Since protein content was low relative to trehalose it was anticipated that no definitive NIR peaks would be observed for alkaline phosphatase. This was found to be the case. It was hoped that small changes in trehalose might be observed, however this was not the case either. The results obtained here are similar to the results observed in Chapter 4 for amorphous trehalose. The amount of protein in the spray-dried samples is too small to be detected in the presence of trehalose. This does not mean that changes in alkaline phosphatase are not occurring, they just cannot be detected.

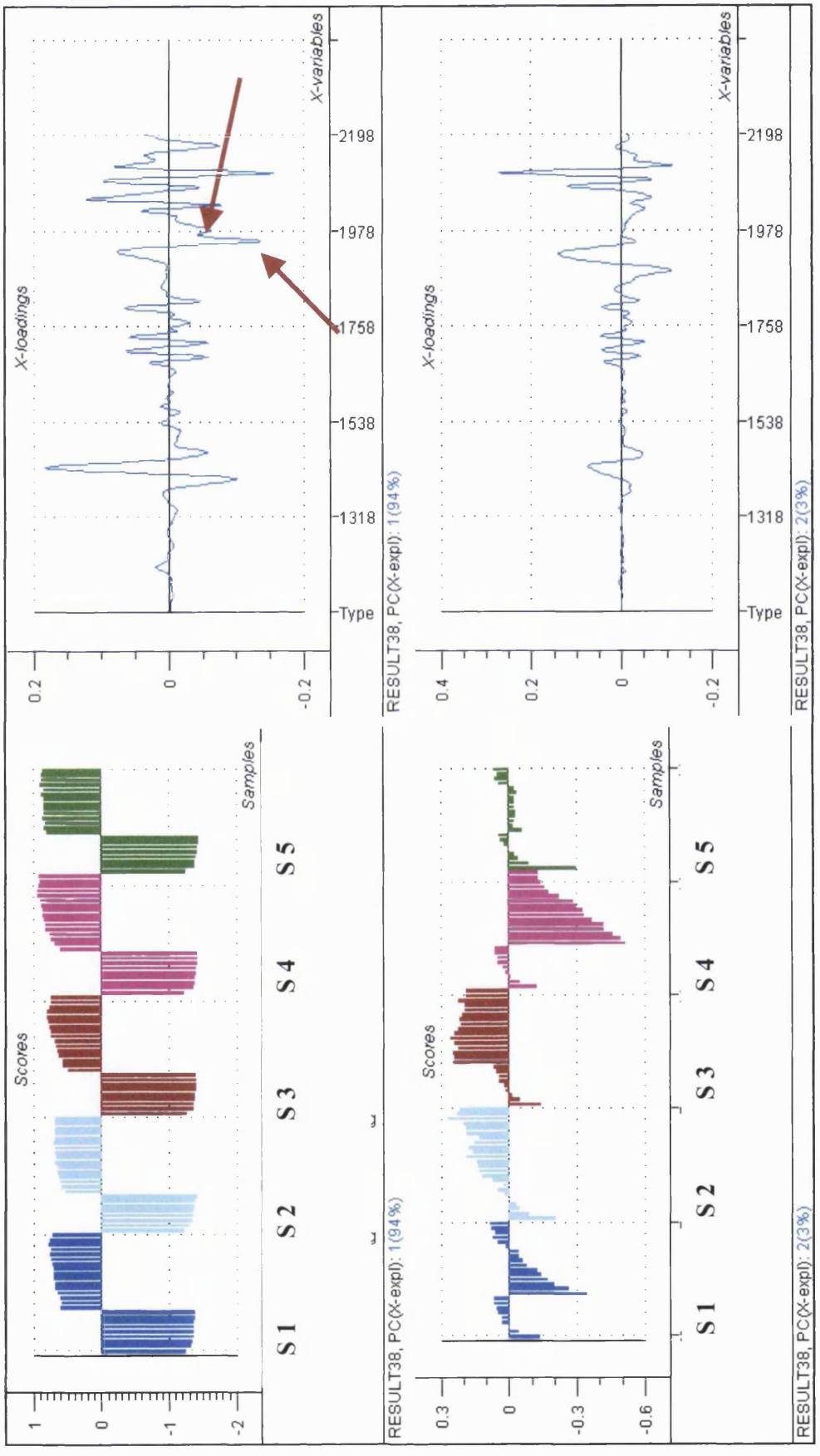

Figure 5.24. *Score and loadings plot for PC1 (top) and PC2 (bottom) for data obtained during gravimetric studies of co-spray dried trehalose/AP samples between 1100-2200 nm.*

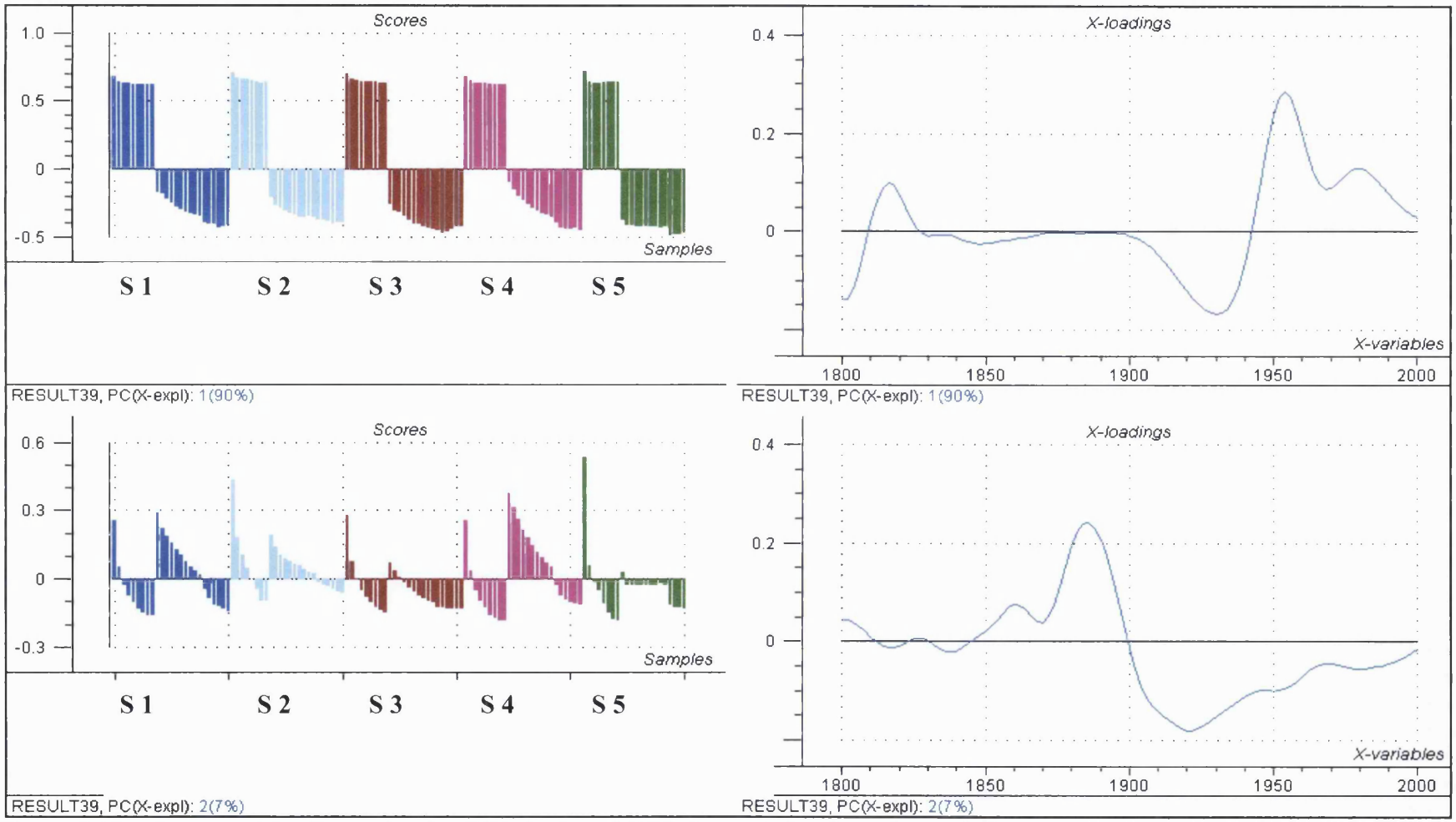

Figure 5.25. *Score and loadings plot for PC1 (top) and PC2 (bottom) for data obtained during gravimetric studies of co-spray dried trehalose/AP samples between 1800-2000 nm.*

5.3.5 STABILITY STUDY

All of the spray-dried trehalose/AP samples were subjected to stability study, where they were examined under high temperature (50 °C) and high relative humidity (75 % RH). The samples incubated under these conditions were examined after one week and then again after 5 weeks. The NIR data was also collected prior to incubation and at the five time points (start, week 1-3 and week 5). Activity assays were performed at these time points on all of the samples to investigate the effects of temperature and humidity on the spray-dried-samples. Principal component analysis (PCA) was performed on all of the collected NIR data and is discussed in section 5.3.4.4.

5.3.5.1 Desiccation at 50 °C

Incubating the spray-dried samples at 50 °C at 0 % RH did not affect the protein activity over five weeks. The samples retained their activity through out the five weeks. Fluctuations were seen, as alkaline phosphatase activity seemed to be higher after incubation. This "false" result was due to the dehydration of the samples at 50 °C, which caused the sample density to change. Hence, as the samples were weighed to perform protein activity measurements, the AP content was actually higher than the theoretical amount needed, resulting in an increase of protein activity.

The NIR data showed that the dehydration had already occurred after one week of incubation and no major differences could be seen between week 1 and week 5. The changes in the NIR data were concentrated in the region between 1850-1960 nm and were limited to the intensity of the peaks. This represents the dehydration of the samples due to elevated temperature.

By examining the raw spectra of the NIR data collected, change in particle size due to aggregation is seen (Figure 5.26). This change is not present in sample 1,which has the highest protein content (5% w/w). As the protein content is decreased in samples 2 (1 % w/w) and 3 (0.5 % w/w) the particle size change becomes more evident. This particle aggregation is also is seen in the sample prepared with high acetone concentration (sample 5).

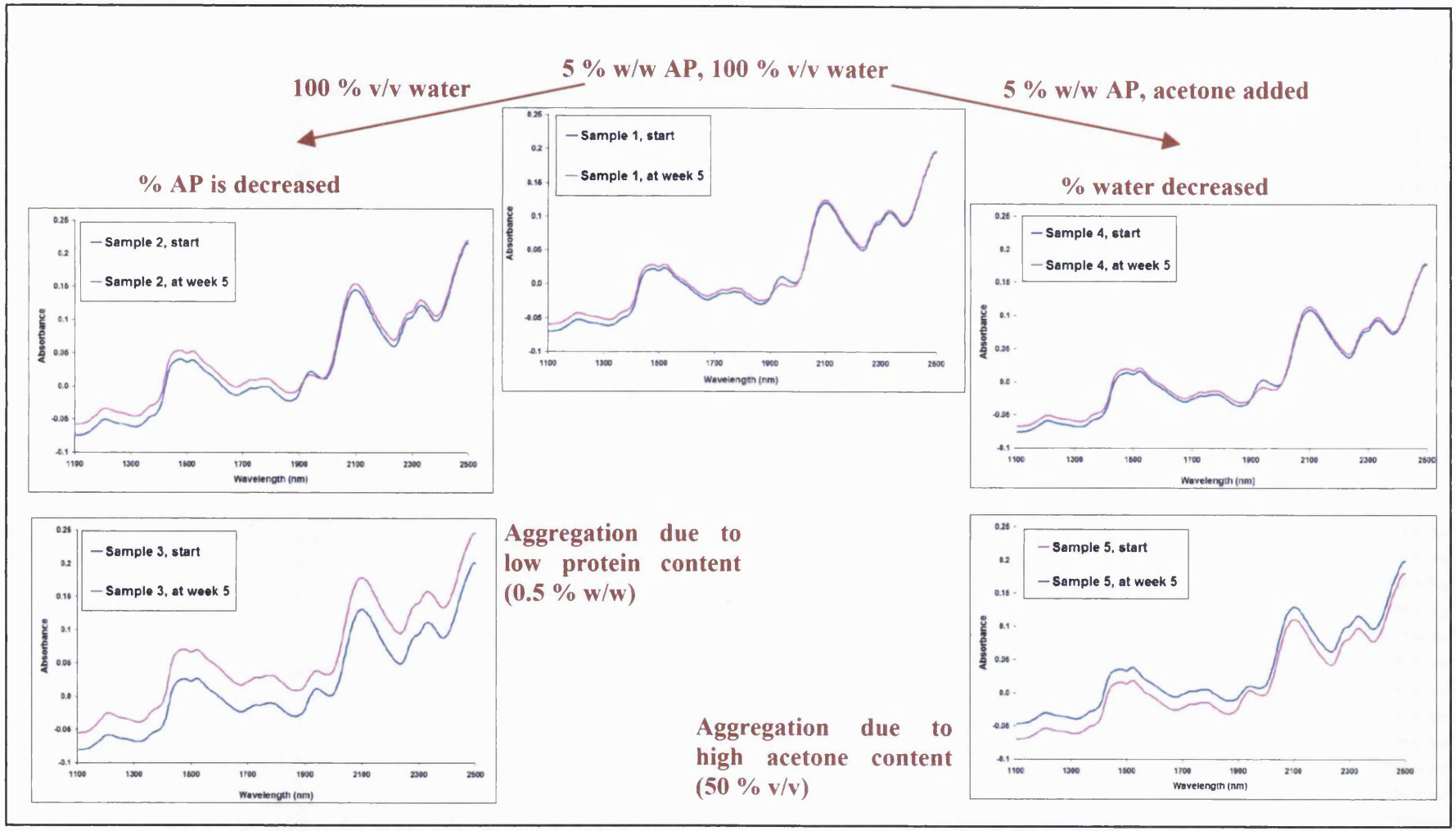

Figure 5.26. *Raw spectra for the spray-dried samples (1-5) at the start and the end of the 5 week incubation period at 50 °C.*

The higher absorbance readings for samples at all wavelengths represent a change in the particle size. This method has been used to measure the cumulative particle size distribution of microcrystalline cellulose (O'Neil et al., 1999). It can be concluded from the above studies that temperatures up to 50 °C do not affect the spray-dried samples. The protein activity is maintained for all of the samples for up to five weeks under these conditions. The aggregation in the samples increased as the amount of protein is decreased and is evident in sample 3 (Figure 5.26). Hence alkaline phosphatase in the spray-dried samples protects the samples from aggregation. The presence of acetone in solution of sample 5 also results in aggregated particles during incubation at 50 °C (Figure 5.31). The protein concentration and activity results for sample 5, showed that the spray dried sample retained only half of the initial protein content and the activity was greatly reduced in solution prior to spray drying. Hence it is not surprising that the sample exhibits aggregation in this study.

5.3.4.2 Incubation at 75 % RH

Incubating the spray-dried samples at 75 % RH showed by NIR, that trehalose crystallisation occurred after week 1. No spectral changes were seen after week 1. If changes were occurring with the alkaline phosphatase within the samples, it could not be detected by NIR, as the amount of trehalose is much higher than the protein content, hence the NIR spectra for trehalose prevailed.

The protein activity data also showed that the drop in protein content, seen after the first week of incubation, was not further decreased after the fifth week and is presented in Table 5.13. The sample were completely crystallised after the first week and therefore they were some issue with solubilisation. Due to the increase of the sample density the measurement of protein activity presented a problem due to the fact that the "actual" amount of alkaline phosphatase was not used. Rather the amount of AP assumed to be in the sample was used. The AP sample stored at 75 % RH exhibited solubility issues, especially after 5 weeks of incubation. The activity assay could not be performed successfully as the sample would not dissolve in the buffer/water used for the assay.

Table 5.13. *Summary of alkaline phosphatase activity in the spray-dried samples exposed to high humidity (75 % RH).*

Sample	AP activity (%)	AP activity (%) week 1 (S.D.)	AP activity (%) week 5 (S.D.)
AP	99.43 (1.02)	60.15 (3.76)	Not possible
Sample 1 (5 % w/w AP, water)	98.47 (2.76)	80.67 (5.88)	78.59 (4.33)
Sample 2 (1 % w/w AP, water)	99.91 (2.29)	83.53 (6.01)	83.67 (4.16)
Sample 3 (0.5 % w/w AP, water)	106.88 (5.67)	88.26 (3.02)	86.19 (3.99)
Sample 4 (5 % w/w AP, 5:1 water-acetone)	75.65 (3.89)	63.34 (2.98)	64.13 (3.19)
Sample 5 (5 % w/w AP, 1:1 water-acetone)	20.51 (3.03)	10.45 (4.15)	9.88 (2.09)

The SEM images of co-spray-dried samples after incubation at 75 % RH for 5 weeks showed that crystallised particles. The NIR data collected after week 1 and up to week showed the double peak representative of the dihydrate form in all of the spray-dried samples. This confirmed the results of the DVS/NIR data, which also showed the distinctive double peak at the end of the experiment. Aggregation was observed in all of the samples after the first week at 75 % RH, much higher than seen previously at 50 °C. This is not surprising, considering the particles are changing form (amorphous to crystalline).

Pure (as supplied) alkaline phosphatase was also subjected to the same conditions and as highlighted in Table 5.13, the impact of moisture uptake was grave. The protein almost looked as it was dissolving. The activity assay after the fifth week was not successful, but the NIR data collected showed interesting results (Figure 5.27). It was very different to the observations made for pure alkaline phosphatase during the DVS experiments. The protein seemed to degrade when exposed to high humidity in this study.

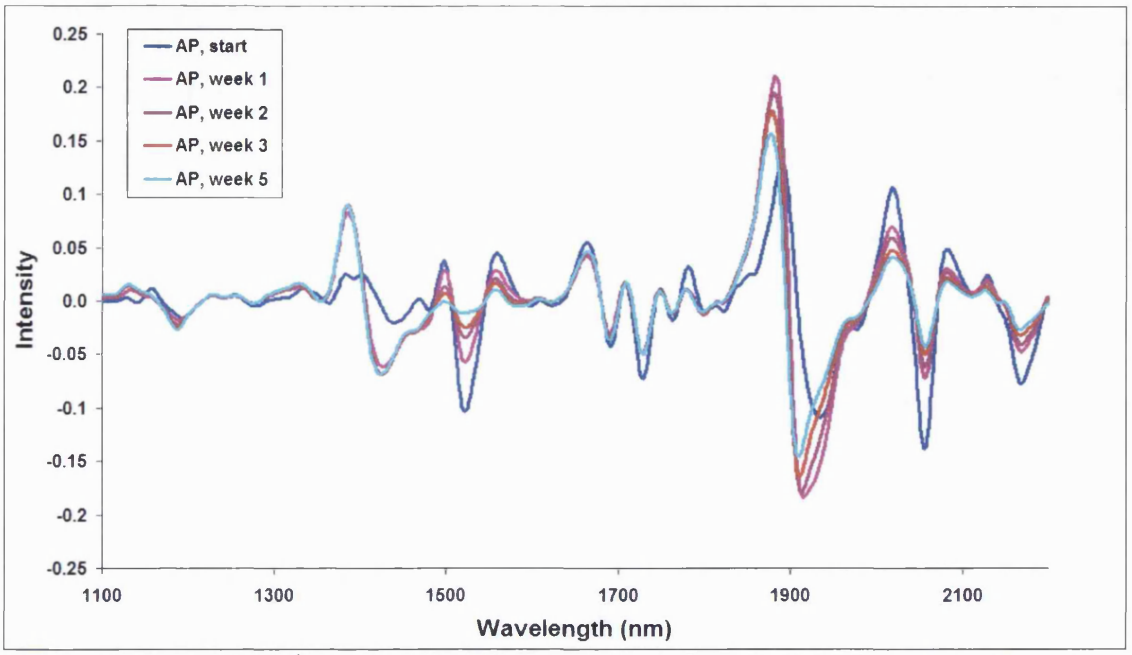

Figure 5.27. *SNV 2nd-derivative NIR spectra between 1100-2200 nm of supplied alkaline phosphatase during stability study conducted at 75 % RH.*

Figure 5.27 shows that the major changes in the spectra of alkaline phosphatase occur after the first week of incubation at 75 % RH, but the shift in the peaks continues during the incubation period. The most evident changes occur in the water region and are depicted in Figure 5.28. After the first week of incubation, the peak around 1935 nm is shifted to around 1915 nm and is at 1910 nm at week 5. This shift indicates that movement of water, which changes from being bound water to being surface water (Zhou et al., 2003).

This shift could not be observed in the spray-dried samples as the characteristic double peak for trehalose dihydrate resides around the same region 1950/1978 nm. This means that the changes in the spray-dried samples due to AP cannot be detected. The spectra of the spray-dried samples merely follow the changes occurring in trehalose. All of the spray-dried samples show the change from the amorphous to the crystalline form after week 1. The raw spectra of these co-spray-dried samples also showed aggregation for all of the samples (Figure 5.29). The sample containing the lowest amount of AP (sample 3) showed the highest magnitude for aggregation. This confirms the results obtained through the DVS-NIR data.

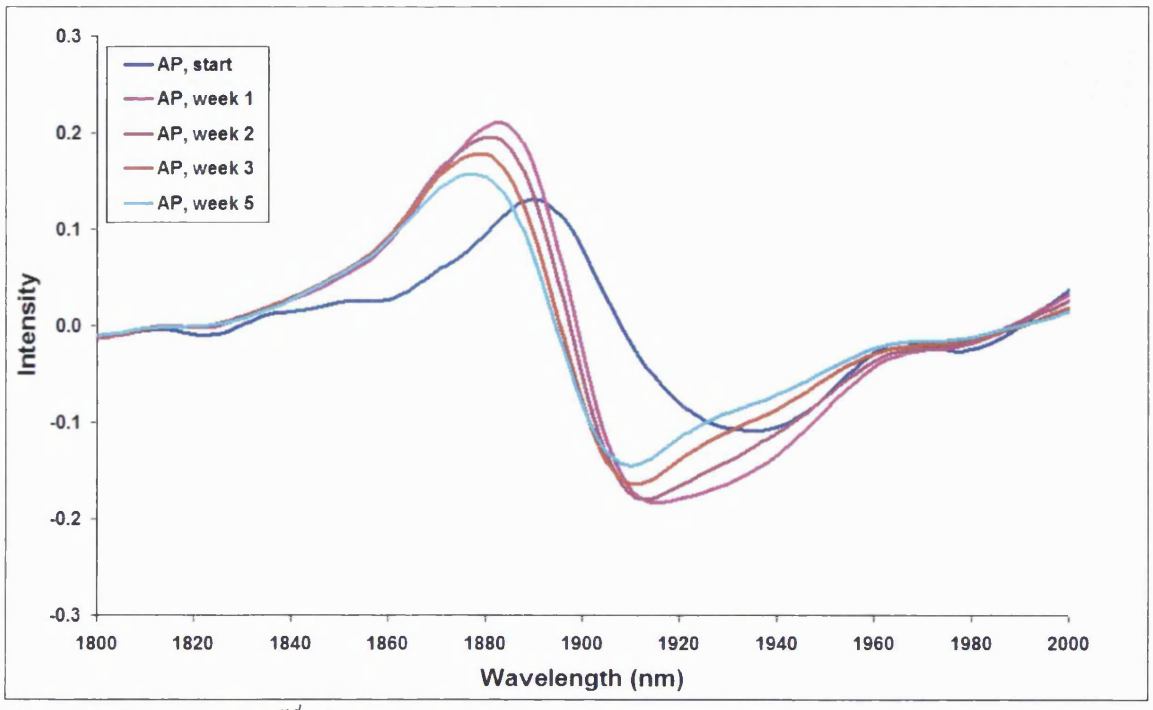

Figure 5.28. *SNV 2nd-derivative NIR spectra between 1800-2000 nm of alkaline phosphatase during incubation at 75 % RH.*

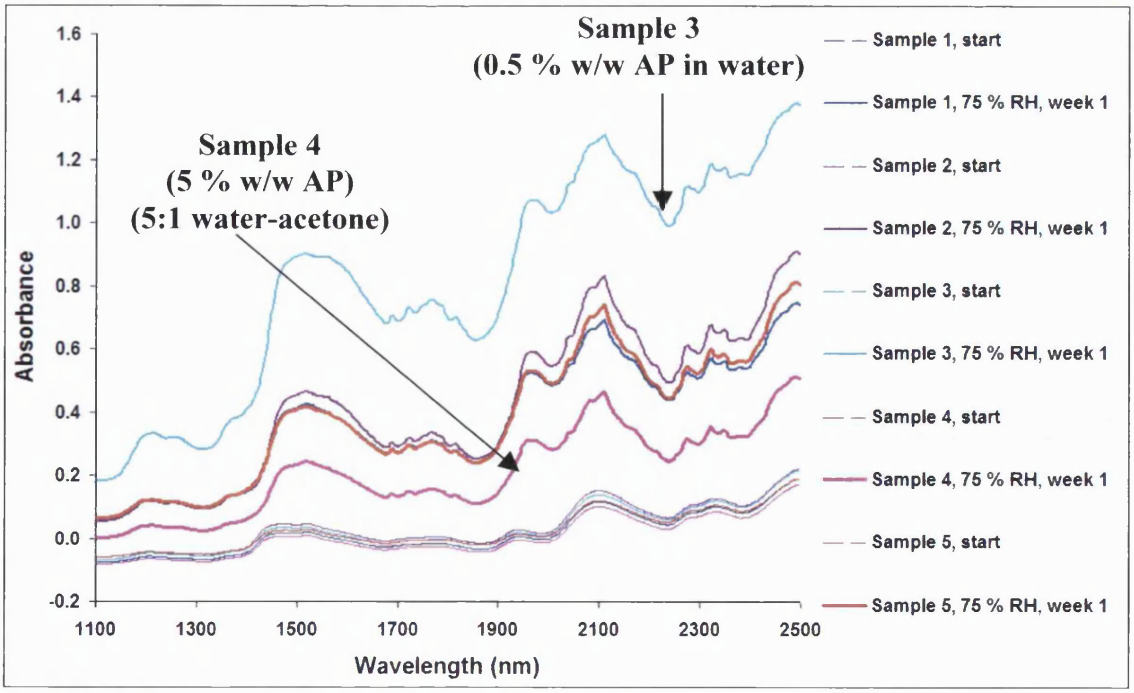

Figure 5.29. *Raw spectra for the spray-dried samples before and after incubation at 75 % RH for 1 week.*

Figure 5.29 shows that sample 4, prepared with a ratio of 4:1 (water:acetone) exhibits the least amount of aggregation. The results depicted in Figure 5.29 show the changes that occur after 1 week of incubation at 75 % RH. These trends continue for the remaining incubation time (5 weeks).

The spectra for completely degraded protein were also recorded. The protein was degraded by heating the sample slowly up to 100 °C, which was then left at room temperature without any desiccation for 1 week. The activity assay performed showed no AP activity. The spectra was recorded and is compared to the spectra of raw AP and AP desiccated at 75 % RH for 1 week and is shown in Figure 5.30. By comparing the spectra of AP subjected to 75 % RH for 1 week and the completely degraded protein, it is evident that the protein is not completely degraded after incubation at 75 % RH. Sadler et al. (1984) found that the difference between the native protein and the denatured protein was in a small peak around 1350 nm in the denatured protein. This peak also appears in the denatured alkaline phosphatase

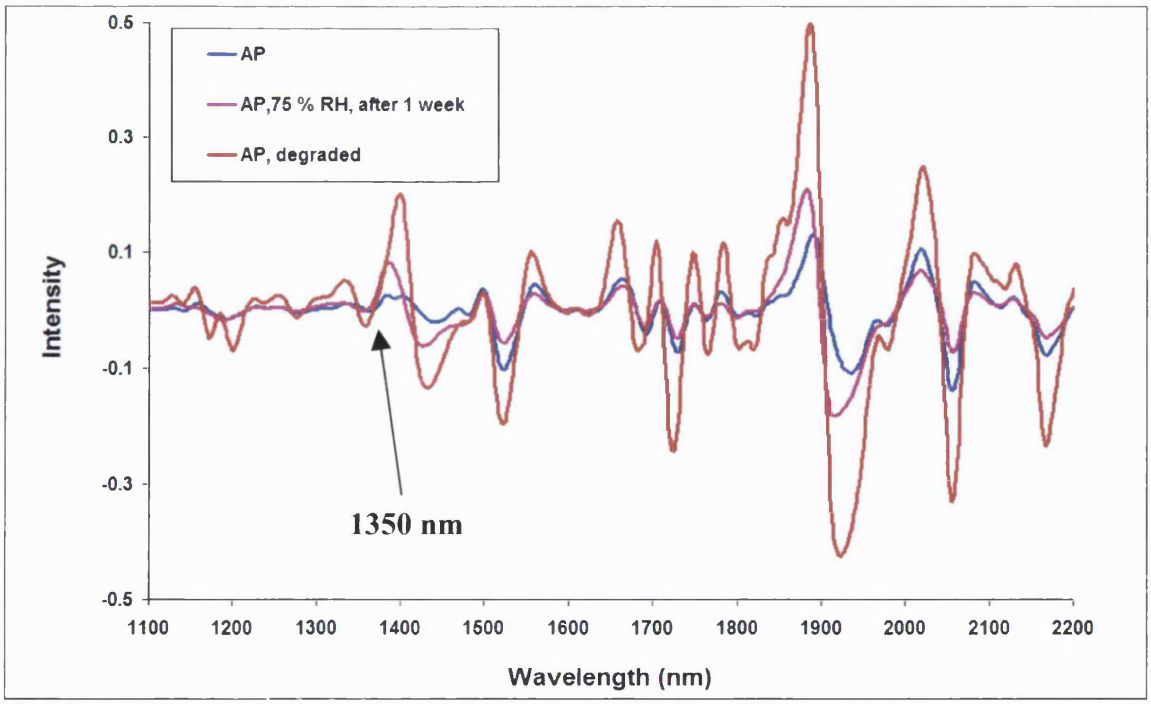

Figure 5.30. *SNV 2nd-derivative NIR spectra between 1100-2200 nm of supplied alkaline phosphatase, alkaline phosphatase after 1 week of incubation at 75 % RH and denatured alkaline phosphatase.*

The peak around 1350 nm indicating the degradation of AP could not be found in the spray-dried samples. This is not surprising as the samples did not fully degrade even after 5 week of incubation at 75 % RH. Secondly the spectra for trehalose prevail in the spray-dried samples due to the low amount of AP.

The spectra obtained from all of the spray-dried samples and AP were compared to each other using PCA and showed the change of the trehalose from amorphous to the crystalline form.

5.4 CONCLUSIONS

Conclusion and possible hypotheses drawn for this chapter are:

- The peak assigned for the denaturation of alkaline phosphatase could not be observed in the spray-dried samples. This was partially due to the low amounts of protein in the samples compared to trehalose.

- All of the spray-dried samples crystallised after subjected to 75 % RH. Though the sample prepared with 20 % (v/v) acetone showed the least amount of aggregation as compared to the rest of the co-psray-dried samples.

- The activity of alkaline phosphatase is not affected by the spray-drying process but by the stresses induced in solution. The high amounts of acetone cause noticeable degradation of the protein in solution.

- During storage at 0 % RH of the spray-dried samples the activity was retained for all of the samples. Temperatures up to 50 °C did not have any impact on protein activity. When the samples were exposed to high humidity (75 % RH) the trehalose was crystallised and protein activity decreased. The rate of degradation for all of the spray-dried samples seems to be the same regardless of the activity prior to spray drying.

- Though the activity of sample 5 (50 % v/v acetone) was much lower than the other spray-dried samples, it followed the same trends as seen for other samples when exposed to humidity.

- All of the samples crystallised to the dihydrate form.

CHAPTER 6

Surfactants in spray-dried trehalose/alkaline phosphatase particles

6. SURFACTANT IN SPRAY-DRIED TREHALOSE/ALKALINE PHOSPHATASE PARTICLES

6.1 INTRODUCTIONS

The changes in the properties of spray-dried trehalose/alkaline phosphatase particles that were caused by the addition of surfactants are described in this chapter. The main purpose for using surfactants was to manipulate the localisation of alkaline phosphatase in the spray-dried particulates. The surfactants that were used in this study are, Tween 20, sodium taurocholate and benzalkonium chloride and are described later in this chapter.

The physicochemical properties of the surfactant containing spray-dried particles prepared from aqueous and aqueous acetone solutions are described in terms of morphology, moisture content and glass transition. The surface energy was also investigated and compared to the findings of the previous chapter. The spray-dried samples were also studied with regards to the surfactant properties and the impact of spray drying solvents with the aid of NIR spectroscopy. This was done by exposing the spray-dried samples to elevated humidity (75 % RH) and determining the effect of surfactant on trehalose crystallisation. Protein concentration and protein activity of the samples was also determined as described in the previous chapter.

6.1.1 SURFACTANTS IN THE PRESENCE OF PROTEINS

The term surfactant is derived from the phrase 'surface-active agent' and is named due to its behaviour at surface and interfaces. Low molecular weight surfactants reduce the surface tension of water by adsorbing at the air-water interface. This is why they are common in pharmaceutical formulations, where their purpose is to stabilise suspensions, emulsions and provide the suitable rheology (Bos, 2001). Surface tension is the driving force behind formation of spherical droplets (Masters, 2002). During spray drying the adsorption of the individual surface-active components at the air-water interface during atomisation can be decisive for the particle morphology. If a formulation containing surfactant and another surface-active compound, e.g. protein is spray dried, competition for the air-water interface between the different surface-active

components may influence the localisation of the protein in the spray-dried powder (Adler et al., 2000). This can result in conformational changes in the protein molecules. It has been claimed that protein stability is better preserved when its presence at the surface is reduced (Maa et al., 1997).

Low molecular weight surfactants are divided into two groups according to the charge of the polar head group, non-ionic uncharged surfactants and ionic surfactant that are either anionic (negatively charged) or cationic (positively charged) (Bos, 2001). The displacement of protein from solid and liquid surfaces is described by two extreme mechanisms below (Bos et al., 1997):

- Solubilisation: The water-soluble surfactant binds to the protein and forms a soluble protein-surfactant complex. By this mechanism, the surfactants do not need to be adsorbed at the interface but they must interact with the proteins.

- Replacement: The surfactant adsorbs at the interface and displaces the protein as the interfacial tension for the surfactant is lower than the protein (or any protein-surfactant complex). By this mechanism, the surfactants do not need to interact with the proteins but they have to bind at the surface.

The actual mechanism is a combination of both extremes where ionic surfactants mainly proceed by the solubilisation and non-ionic surfactants proceed via replacement. Non-ionic surfactants are generally preferred in protein stabilisation. Low concentrations of non-ionic surfactants are often sufficient to prevent or reduce the driving force of protein adsorption and/or aggregation at these interfaces (Bam et al., 1995; Chang et al., 1996). Ionic surfactants are usually not used in protein stabilisation because they can bind to both the polar and non-polar groups in proteins causing denaturation. However these surfactants have been reported to stabilise proteins successfully (Giancola et al., 1997; Giancola et al., 2006).

Protein unfolding at the air-water interface can induce aggregation (Maa et al., 1997). Low molecular weight surfactants can adsorb faster to the surface compared to proteins such as BSA leading to a partial blocking of the surface (Maa et al., 1997; Adler et al., 2000). Consequently by reducing the surface load of protein at the interface during

atomisation by the addition of a surfactant can prevent or delay the surface induced denaturation of the protein. The surfactants used in the study are described below. They were used in the spray-dried trehalose/AP formulations to see their impact on protein localisation in the spray–dried particles and on trehalose crystallisation. All of the chosen surfactants were water soluble and were selected on the basis of their varied physicochemical properties.

6.1.2 TWEEN 20

Tween 20, also known as polyethylene glycol sorbitan monolaurate/ polyoxyethylenesorbitan monolaurate is a non-ionic surfactant with a molecular weight of approximately 1128 Da. This surfactant contains 20 units of oxyethylene, which makes it highly water soluble (Figure 6.1). Tweens have been used successfully to stabilise proteins during freeze-drying and thawing (Chang et al., 1996; Wang, 1999).

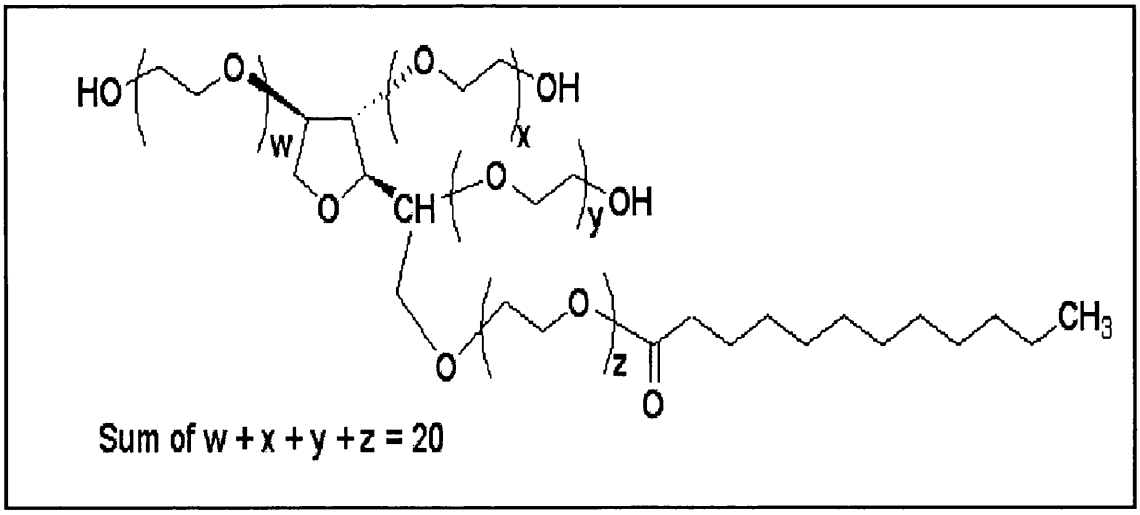

Figure 6.1. *Structure of Tween 20.*

6.1.3 SODIUM TAUROCHOLATE

Sodium taurocholate is an anionic surfactant with a molecular weight of approximately 538 Da and is freely soluble in water (Figure 6.2). Sodium taurocholate has been studied for the purpose of pulmonary delivery of proteins and peptides as an enzyme inhibitor (Johansson, 2002; Hussain et al., 2004). This surfactant has relatively low toxicity and has already been tested *in vivo* (Hussain et al., 2004).

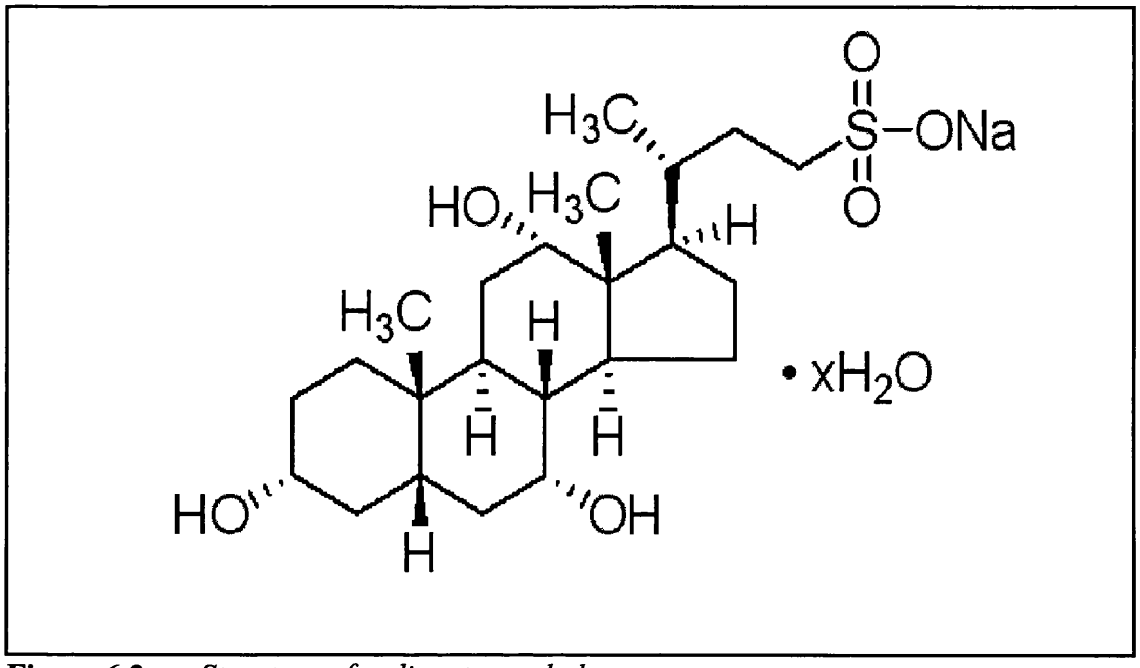

Figure 6.2. *Structure of sodium taurocholate.*

6.1.4 BENZALKONIUM CHLORIDE

Benzalkonium chloride is a cationic surfactant with a molecular weight of 424 Da and is freely soluble in water (Figure 6.3). Cationic surfactants are often used as surfactants for their antimicrobial properties. Benzalkonium chloride is commonly used in hand and face washes and is also used as a preservative in eye treatment solutions.

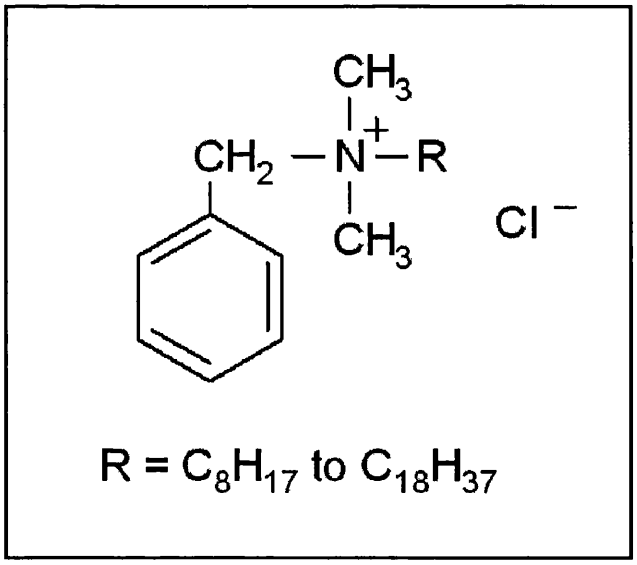

Figure 6.3. *Structure of benzalkonium chloride.*

6.2 EXPERIMENTAL PROTOCOLS

6.2.1 PRODUCTION OF SPRAY/DRIED TREHALOSE/AP/SURFACTANT PARTICLES

Surfactants in trehalose/AP solutions were spray dried using exactly the same parameters used to spray dry trehalose with AP (Table 5.2). All of the feed solutions consisted of 10 % (w/v) total solids and were prepared as described earlier in section 5.2.1. Surfactants were added to the trehalose in solution prior to the addition of AP. Sodium taurocholate and benzalkonium chloride formulations were prepared from 5 % w/w AP, 1 % w/w surfactant and 94 % w/w trehalose in water or aqueous acetone (20 % v/v). The composition for Tween 20 was different as outlined in the formulation plan, Table 6.1.

Table 6.1. *Formulation plan for spray dried trehalose/surfactant/AP samples.*

Sample	AP content (% w/w)	Surfactant content (% w/w)	Surfactant	Trehalose content (% w/w)	Water content (% v/v)	Acetone content (% v/v)
TW	1	5	Tween 20	94	100	0
TWac	1	5	Tween 20	94	80	20
ST	5	1	Sodium taurocholate	94	100	0
STac	5	1	Sodium taurocholate	94	80	20
BC	5	1	Benzalkonium chloride	94	100	0
BCac	5	1	Benzalkonium chloride	94	80	20

Tween was the first surfactant to be used in the study and hence a few different compositions were prepared to optimise the surfactant/trehalose/AP particulates. Tween was initially spray-dried using the following composition; 0.5 % w/w AP, 0.5 % w/w Tween 20 and 9.0 % w/w trehalose in water. The SEM images showed particles that

were fused together and hence the composition was discarded. When a composition containing 5 % w/w AP, 1 % w/w Tween and 94 % w/w trehalose was spray-dried the particles produced were raisin-like. As Tween 20 is a highly viscous material a 1 % w/w amount in a 100 ml solution was equivalent of one drop. It was suspected that Tween adsorbed to the glass surfaces and therefore the particle morphology was not affected by the presence/absence of Tween in the formulation. Hence the amount of Tween was increased (5 % w/w) while decreasing the amount of AP (1 %) in the formulations as outlined in Table 6.1.

6.2.2 SCANNING ELECTRON MICROSCOPY (SEM)

SEM images were carried out as described in section 2.6.

6.2.3 THERMOGRAVIMETRIC ANALYSIS (TGA)

TGA data was collected as described in section 3.3.2

6.2.4 DIFFERENTIAL SCANNING CALORIMETRY (DSC)

DSC data was collected using modulated DSC method described in section 2.3.2.

6.2.5 INVERSE GAS CHROMOTOGRAPHY (IGC)

Surface energy of the spray-dried surfactant/trehalose/AP/ samples was determined using techniques described in sections 2.9 and 5.2.6.

6.2.6 DETERMINATION OF ALKALINE PHOSPHATASE CONTENT

Alkaline phosphatase concentration in the spray-dried surfactant/trehalose/AP powders was determined by BCA assay (sections 2.11 and 5.2.7). Absorbance measurements of AP at 280 nm were used to confirm the results obtained by the BCA assay (sections 2.12 and 5.2.7).

BCA assay and the molar coefficient measurements at 280 nm were also performed on spray-dried samples of surfactant/trehalose/ spray-dried from water and aqueous acetone (20 % v/v). The purpose of these additional experiments was to determine whether the surfactants would give an absorbance reading at the wavelengths used to determine protein content. These readings were recorded and then subtracted from their

AP containing counter part in order to determine the precise amount of AP in each of the spray-dried samples.

6.2.7 ACTIVITY ASSAY

The measurement of alkaline phosphatase activity is based upon the hydrolysis of para-nitrophenyl phosphate (PNPP) and was conducted as described in sections 2.13 and 5.2.8.

6.2.8 STABILITY STUDY

The stability study was performed to investigate the effects of increased humidity (75 % RH, at room temperature) on the spray-dried surfactant/trehalose/AP samples. The co-spray-dried samples were desiccated as described in sections 2.7 and 5.10. NIR spectroscopy was employed to study the changes occurring in the samples due to high humidity. An activity assay was performed on the samples.

6.3 RESULTS AND DISCUSSION

Samples were prepared using the formulation plan listed in Table 6.1. The influence of surfactant properties and acetone on the spray-dried particles, are the focus of this chapter.

6.3.1 INFLUENCE OF SURFACTANT ON THE PROPERTIES OF SPRAY-DRIED TREHALOSE/AP PARTICLES

The main purpose of introducing Tween 20 to the trehalose/AP formulations was to study the impact of competing surface-active compounds during spray drying. In the previous chapter it was observed that by spray-drying 1 % w/w AP with 99 % trehalose in water, a combination of raisin-like and spherical particles were produced (Figure 5.1, Sample 2). The addition of Tween 20 (Sample TW) resulted in very smooth spherical particles (Figure 6.4a). Hence this composition was considered most favourable for examining the changes in the surface properties of the spray-dried AP particles. Tween 20 was also spray-dried with trehalose/AP from aqueous acetone (sample TWac) (Figure 6.4b).

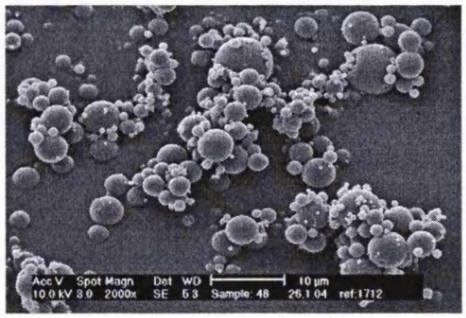

a) Sample TW: 5 % Tween 20, 94 % trehalose and 1 % AP in water.

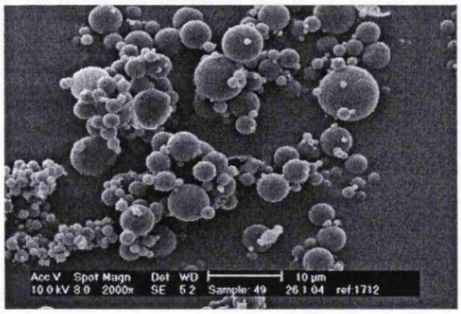

b) Sample TWac: 5 % Tween 20, 94 % trehalose and 1 % AP in aqueous acetone (20 %).

Figure 6.4. *SEM pictures of spray-dried Tween 20/trehalose/AP particles from water and aqueous acetone solutions.*

Sodium taurocholate and benzalkonium chloride were also introduced to the trehalose/AP formulations, respectively. It was observed in the previous chapter that spray drying high amounts of AP with trehalose from water produced raisin-like particles (Figure 5.1, Sample 1). When the same composition was spray-dried from aqueous acetone (20 % v/v), combinations of spherical and raisin-like particles were produced (Figure 5.9, Sample 4). The presence of sodium taurocholate and benzalkonium chloride in the compositions resulted in slightly dimpled spherical particles (Figure 6.5). Higher amounts of these two surfactants (5 % w/w) in the compositions resulted in particles that were fused together and therefore the above produced formulations were considered favourable for studying the changes in surface properties of the spray-dried AP particles. Although both surfactants (benzalkonium chloride and sodium taurocholate) produced the dimple particles, the SEM picture indicate that this phenomena was more pronounced in the presence of benzalkonium chloride.

The changes in the morpholgy induced by the presence of the surfactants indicate an alteration/modification at the surface of the spray-dried particles. All of the samples produced were amorphous according to the X-ray diffraction patterns. The residual moisture content and the glass transition values were measured to see whether these

reflected the changes of particle morphology. The data obtained were compared to the findings described in Chapter 5 and are presented in Tables 6.2 and 6.3.

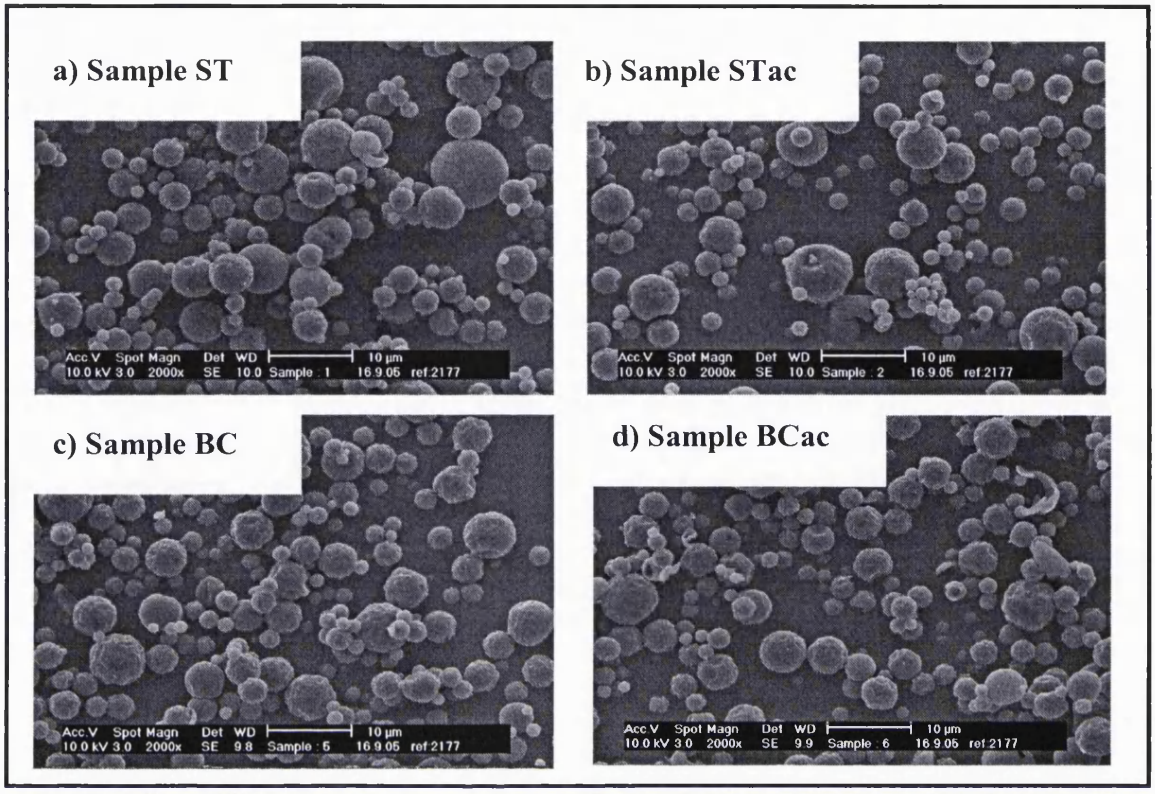

Figure 6.5. *SEM pictures of surfactant/trehalose/AP particles spray dried from; a) sodium taurocholate in water, b) sodium taurocholate in water-acetone, c) benzalkonium chlorid in water and d) benzalkonium chloride in water-acetone.*

Thermogravimetric data obtained show that generally the spray-dried formulations have more residual moisture than amorphous trehalose (Table 6.2). The moisture retention increases when AP is introduced to the aqueous trehalose solutions. The moisture increases further upon addition of the ionic surfactants sodium taurocholate and benzalkonium chloride. However the moisture content is decreased in the presence of Tween 20, the non-ionic surfactant. The addition of acetone to the formulation also induced increased moisture retention compared to the formulations spray-dried without surfactants. The two samples containing Tween 20, TW and TWac, displayed two peaks during the TGA experiments. As discussed in the previous chapter this could be due to the crystallisation of the hydrated form of trehalose, which occurs during the heating of

the sample in the TGA experiments. The results for TW and TWac listed in Table 6.2 are the total moisture lost seen by both peaks.

Table 6.2. *Thermogravimetric analysis data for spray-dried surfactant/trehalose/AP samples. The shaded cells present data obtained in the previous Chapter for the purpose of comparison.*

Sample	Water content (%)	S.D.
amorphous trehalose (Chapter 4)	2.40	0.42
5 % AP compositions with trehalose and surfactants in water		
Sample 1 (Chapter 5, without surfactant)	3.73	0.12
Sample ST (1 % sodium taurocholate)	4.26	0.21
Sample BC (1 % benzalkonium chloride)	4.51	0.19
5 % AP compositions with trehalose and surfactant in aqueous acetone (20 % v/v)		
Sample 4 (Chapter 5, without surfactant) (Total moisture content of two peaks)	3.67	0.24
Sample STac (1 % sodium taurocholate)	4.02	0.15
Sample BCac (1 % benzalkonium chloride)	5.44	0.35
1 % AP compositions with trehalose and surfactant in water and aqueous acetone (20 % v/v)		
Sample 2 (Chapter 5, without surfactant)	3.67	0.08
Sample TW (5 % Tween 20 in water) (Total moisture content of two peak)	2.32	0.29
Sample TWac (5 % Tween 20 in water-acetone) (Total moisture content of two peak)	3.23	0.21

The water content for the samples containing benzalkonium chloride is highest followed by sodium taurocholate and Tween 20 samples. In the previous chapter the data showed that the moisture content was affected by the amount of AP. Samples with high amounts of AP retained more water (5 % AP) than samples with low amounts of AP (0.5 % AP). This subsequently coincided with the change of particle morphology. Where high amounts of AP produced raisin-like particles and the low amounts of AP in the samples produced spherical particles. The same trends are seen in the presence of surfactants. The dimpled particles produced with benzalkonium chloride retained more moisture than the smooth spherical particles produced by Tween 20.

The surface properties were further investigated by the glass transition values (Table 6.3). All of the AP samples display a decrease in their glass transition temperature compared to amorphous trehalose. The amount of AP also had an influence on the Tg values, which were decreased as the amount of AP in the samples was decreased (Table 5.4). The lowest Tg values are obtained for samples containing benzalkonium chloride. This corresponds to the moisture retention data, where these samples retained more moisture than the other surfactants. The moisture may have acted as a plasticiser and decreased the Tg values. The presence of acetone did not affect the Tg values greatly compared to the values obtained by the samples prepared from water. This corresponds to the finding of the previous chapter, where the Tg values were not influenced by the presence of acetone (Table 5.8). The glass transition values were depressed the most by benzalkonium chloride followed by sodium taurocholate and Tween 20. This was also the order of the moisture content, where Tween 20 displayed the lowest amount of moisture retention. The data presents the effects of surface morphologies and the properties of the spray-dried particulates. This relationship was further investigated by measuring the surface energies of the surfactant/trehalose/AP samples.

Table 6.3. *Glass transition values for spray-dried surfactant/trehalose/AP samples. The shaded cells present data obtained in the previous Chapter for the purpose of comparison.*

Sample	Glass transition (Tg) onset value (°C)	S.D.
Amorphous trehalose	120.28	1.50
Sample 1 (aqueous 5 % AP, Chapter 5)	115.23	2.59
Sample 2 (aqueous 1 % AP, Chapter 5)	110.74	1.63
Sample 4 (5 % AP; 20 % acetone, Chapter 5)	115.46	2.15
Sample ST (aqueous 5 % AP, 1 % sodium taurocholate)	112.35	1.57
Sample STac (aqueous 5 % AP, 1 % sodium taurocholate, 20 % acetone)	110.90	1.44
Sample BC (aqueous 5 % AP, 1 % benzalkonium chloride)	108.13	2.07
Sample BC (aqueous 5 % AP, 1 % benzalkonium chloride, 20 % acetone)	105.22	1.89
Sample TW (aqueous 1 % AP, 5 % Tween 20)	113.62	2.15
Sample TWac (aqueous 1 % AP, 5 % Tween 20, 20 % acetone)	111.83	1.35

6.3.2 INFLUENCE OF SURFACTANT ON DISPERSIVE SURFACE ENERGY

Elution peaks were observed for the surfactant/trehalose/AP samples with the five non-polar probes by inverse gas chromatography (IGC). These peaks were used to calculate the dispersive surface energy of the samples, (Table 6.4). The formulations prepared with 5 % AP in aqueous solution, showed a decrease in the surface energy caused by the presence of surfactant (Samples ST and BC). The dispersive surface energy decreased from 42.55 mJ/m^3 to 33.62 mJ/m^3 when 1 % sodium taurocholate was added in the trehalose/AP solution (Sample ST). The dispersive surface energy decreased even more due to the addition of benzalkonium chloride (Sample BC). This coincided with the change in the particle morphology. As discussed in Chapter 5, the raisin-like particles

(Sample 1) indicate the presence of AP on the surface of the particle. This was confirmed by the surface energy data. Samples ST and BC did not produce raisin-like particles. Hence the decrease of the surface energy indicates that the presence of AP at the surface is reduced/diminished. Sodium taurocholate and benzalkonium chloride are ionic surfactants and therefore interact with AP but do not necessarily adsorb at the interface (Bos, 2001). Aqueous acetone formulations of these two surfactants (STac and Bcac) displayed surface energies similar to when prepared from water alone. The addition of acetone (20 % v/v) had a greater impact on trehalose/AP samples than in the presence of sodium taurocholate and benzalkonium chloride.

Table 6.4. *Summary of the non-polar surface energy and acid/base character as a result of surfactants in trehalose/AP particulates. The shaded cells present data obtained in the previous Chapter for the purpose of comparison.*

Sample	(Υ^d_s) (mJ/m^3) (S.D.)	K^A (S.D.)	K^D (S.D.)	K^D/KA (S.D.)
Sample 1 (5 % AP, aqueous)	42.55 (0.48)	0.087 (0.001)	0.065 (0.004)	0.747 (0.038)
Sample ST (5 % AP, 1 % sodium taurocholate, aqueous)	33.62 (0.89)	0.078 (0.001)	-0.024 (0.001)	-3.030 (0.004)
Sample BC (5 % AP, 1 % benzalkonium chloride) (aqueous)	31.37 (0.35)	0.076 (0.001)	0.013 (0.003)	0.169 (0.035)
Sample 4 (5% AP, aqueous acetone)	35.73 (0.22)	0.102 (0.0005)	0.094 (0.002)	0.915 (0.015)
Sample STac (5 % AP, 1 % sodium taurocholate) (aqueous acetone)	33.30 (1.86)	0.080 (0.002)	-0.018 (0.001)	-0.228 (0.004)
Sample BCac (5 % AP, 1 % benzalkonium chloride) (aqueous acetone)	29.95 (0.79)	0.072 (0.001)	-0.006 (0.003)	-0.082 (0.048)
Sample 2 (1 % AP, aqueous)	33.97 (0.52)	0.102 (0.001)	0.088 (0.004)	0.864 (0.025)
Sample TW (1 % AP, 5 % Tween 20, aqueous)	33.08 (0.10)	0.107 (0.001)	0.162 (0.002)	1.507 (0.026)
Sample TWac (1 % AP, 5 % Tween 20) (aqueous acetone)	30.74 (0.14)	0.093 (0.002)	0.171 (0.001)	1.848 (0.022)

The samples prepared with Tween 20 (Tw and TWac) did not show major changes in their surface energies compared to the sample prepared with just trehalose and AP (Sample 2). These samples were prepared from a lower amount of AP (1 %). The results of the previous Chapter indicate that the amount of AP at the surface is dependent on the amount of AP in the spray-drying solutions. Therefore 5 % AP (Sample 1) produced more raisin-like particles than compared to 1 % AP (Sample 2).

The acidic/basic character of the samples was evaluated to further understand the surface properties of the spray-dried surfactant/trehalose/AP powders and the data are summarised in Table 6.4. The acidic character of surfactant/trehalose/AP samples is displayed in Figure 6.6. The K^A value is greatest for samples prepared with Tween 20, followed by the ionic surfactants, sodium taurocholate and benzalkonium chloride. This corresponds to the findings of the previous Chapter that the acidic character increases as the amount of AP decreases. This is a direct consequence of the absence/reduction of AP at the surface of the particles, as high levels of AP at the surface decreased the acidic character.

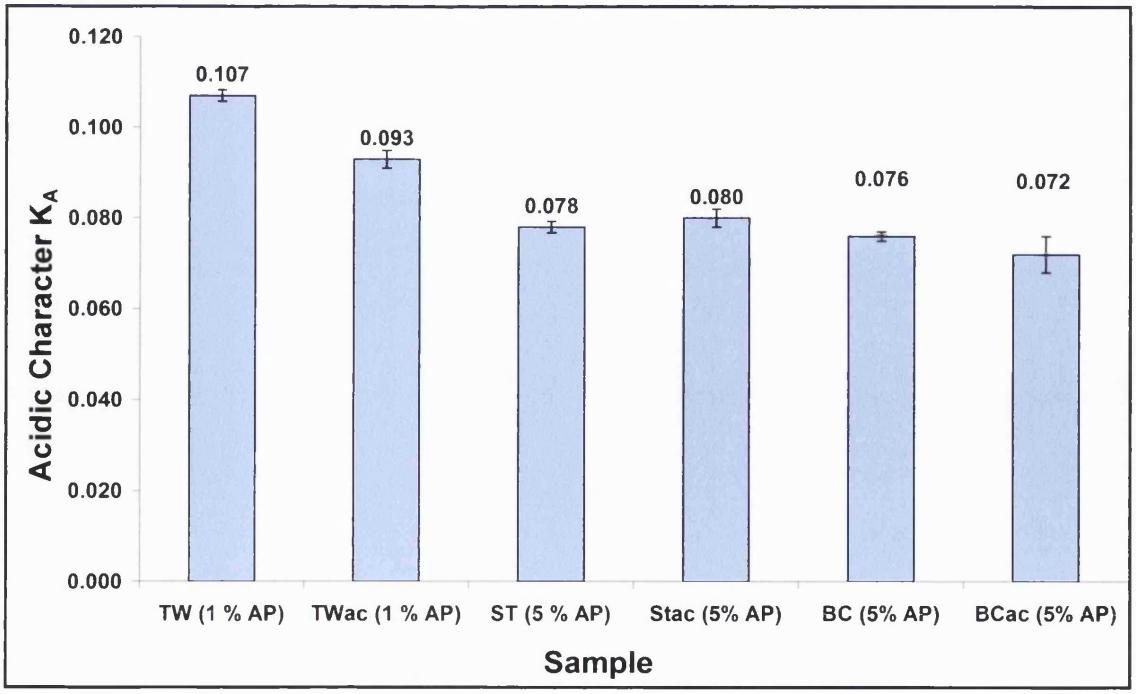

Figure 6.6. *Acidic character of the surfactant/trehalose/AP samples.*

The basic character of the surfactant/trehalose/AP samples summarised in Table 6.4, show that the ionic surfactant gave negative values. These values cannot be used to make conclusions about the basic character of the samples. The retention of the individual polar probes onto the sample surface was investigated to provide an insight of the observed K^A and K^D values (Figure 6.7). The Tween 20 samples (TW and TWac) overall, show strong interaction with the acidic (chloroform and ethanol) and the basic (acetone and ethylacetate) probes. The surface properties of the particles seem to be influenced greatly by the physicochemical properties of the surfactants. The non-ionic surfactant, Tween 20, did not affect the surface energy of the trehalose/AP particles but the increase in the K^D values compared to Sample 2 (1 % AP without surfactant) show that it made the particle surfaces more basic (Table 6.4). The anionic surfactants, sodium taurocholate and benzalkonium chloride, displayed changes in the surface energies and changes in the acid/basic character. However due to the negative values obtained, it is difficult to characterise those changes, though the decrease in K^A values indicate that the samples surfaces are less acidic.

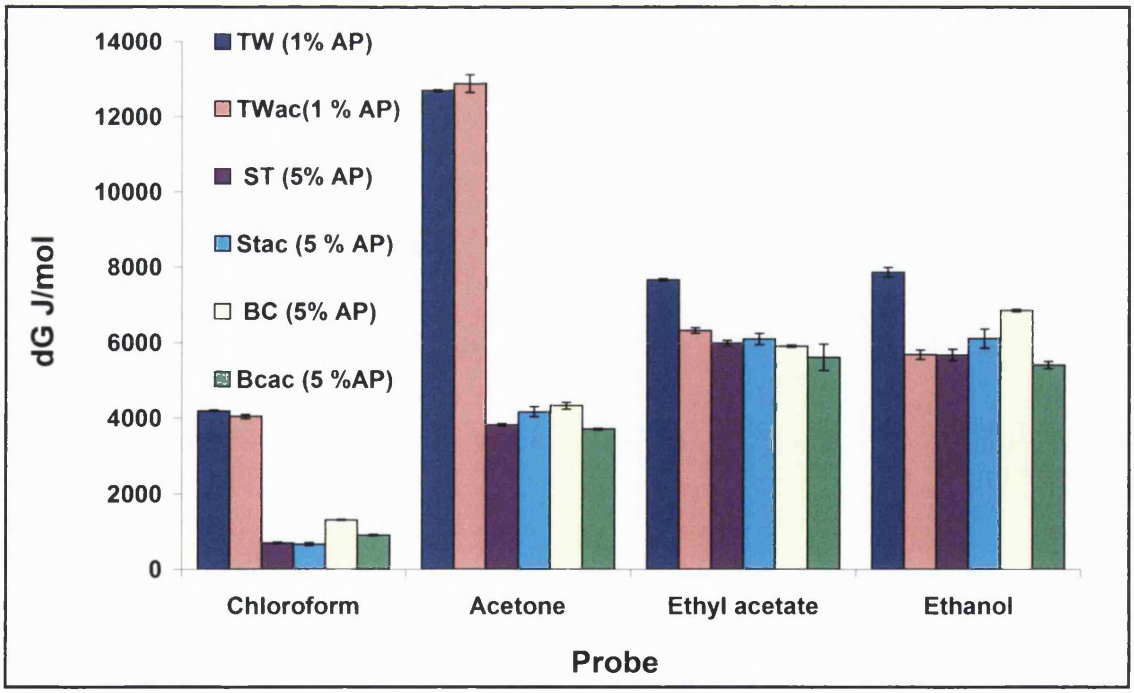

Figure 6.7 *The variation in interaction of the polar probes due to surfactants on the surfaces of spray–dried trehalose/AP particles.*

To summarise, the surface properties of the trehalose/AP particles change due to the presence of surfactants. The ionic surfactants change/modify the surface properties differently compared to the non-ionic surfactant. It was hoped that by studying these samples by NIR the differences of the three surfactants could be elucidated. This study is described in the next section.

6.3.3 STABILITY STUDY

The surfactant/trehalose/AP samples were measured for their protein content. The AP activity of the spray-dried samples was recorded over 10 weeks. The samples were desiccated at 75 % RH to induce trehalose crystallisation in the samples. The changes were followed by NIR daily for a week.

6.3.3.1 Determining protein content and activity

Protein content measured by BCA assay and at 280 nm, showed that the loading of the protein in the spray-dried samples was almost 100 % (Table 6.5). This confirms the findings of the previous chapter, where similar results were obtained. The activity of AP showed that it was only affected in solution prior to the spray drying process. During a dissociation period of 10 weeks at 0 % RH, the samples did not show any signs of protein degradation (Table 6.6). The samples prepared from water alone showed the greatest protein stability. In contrast, the samples prepared from aqueous acetone showed reduced AP activity for the samples made with ionic surfactants, sodium taurocholate and benzalkonium chloride. Aqueous acetone solutions prepared with Tween 20, did not affect AP activity. Unprocessed AP was also desiccated at 0 % RH over 10 weeks and showed a drop in activity greater than in the spray-dried surfactant/trehalose/AP samples.

Table 6.5. *Alkaline Phosphatase content of the spray-dried surfactant/trehalose/AP samples.*

Sample	Expected % (w/w) AP Content	Average % (w/w) AP Content measured by BCA (S.D.)	Average % (w/w) AP Content measured by absorption at 280 nm (S.D.)
ST	5	5.39 (0.65)	4.78 (0.54)
STac	5	5.18 (0.51)	4.96 (0.37)
BC	5	4.89 (0.47)	4.93 (0.29)
BCac	5	5.19 (0.32)	4.88 (0.24)
TW	1	1.12 (0.24)	0.91 (0.20)
TWac	1	1.07 (0.13)	0.96 (0.22)

Table 6.6. *Summary of the activity for the spray-dried surfactant/trehalose/AP samples pre- and post-spray-drying.*

Sample	AP activity (%) pre-spray -drying (solution) (S.D.)	AP activity (%) post-spray-drying (week 1) (S.D.)	AP activity (%) post-spray-drying (week 10) (S.D.)
AP (unprocessed and was not subjected to spray drying)	100.00 (1.68) (activity of the dry form, as received)	90.10 (2.99) (desiccated at 0 % RH, as received)	65.34 (4.76) (desiccated at 0 % RH, as received)
ST	95.59 (3.45)	98.47 (2.76)	99.55 (3.87)
Stac	83.49 (3.77)	85.65 (2.44)	85.71 (3.91)
BC	98.12 (3.89)	106.88 (5.67)	99.15 (2.34)
BCac	74.12 (2.55)	75.65 (3.89)	72.69 (4.88)
TW	98.69 (3.43)	101.00 (4.35)	97.63 (5.35)
TWac	96.78 (3.45)	99.91 (2.29)	97.63 (3.59)

6.3.3.2 Determining crystallisation of trehalose by NIR

As discussed in the previous chapter, alkaline phosphatase has shown to be a stable protein. Hence it was subjected to high humidity to induce trehalose crystallisation. It was hoped that these conditions would cause protein degradation, which could be monitored by NIR. As shown in previous chapters, AP could not be detected by NIR due to low proportion of AP to trehalose in the samples. Hence the crystallisation of trehalose was monitored by NIR to detect whether the presence of surfactants in the samples caused any changes to the crystallisation process. The crystallisation of trehalose in the spray-dried samples was delayed as compared to amorphous trehalose (Table 6.7). Samples prepared with Tween 20 were most resistant to crystallisation and only crystallised after 7 days. The double peak at 1954/1980 nm was used as a diagnostic to identify the crystallisation of trehalose. The samples containing the cationic surfactant, benzalkonium chloride, were most susceptible to trehalose crystallisation, followed by sodium taurocholate and Tween 20. The presence of acetone in the spray drying solutions did not have any impact on trehalose crystallisation.

Table 6.7. *Trehalose crystallisation of the spray-dried samples induced by incubation at 75 % RH.*

Sample	Trehalose crystallisation, identified by the dihydrate peak (1954/1980 nm)
Amorphous trehalose	Day 3
BC	Day 4
BCac	Day 4
ST	Day 5
STac	Day 5
TW	Day 7
TWac	Day 7

The changes in the NIR spectra as a result of 75 % RH exposure to the spray-dried samples were similar. The only difference was when the double peak appeared in the different samples. The water regions in the spectra also changed during incubation at 75 % RH. The spectra shown below are for the aqueous benzalkonium chloride sample, but similar NIR spectra was observed for all of the other surfactant/trehalose/AP samples (Figures 6.8 and 6.9). The peak at 1435 nm shifts to 1466 nm when trehalose crystallisation occurs (Figure 6.8). This region represents surface water (Shenk, 1993; Zhou et al., 2003). The peak shifted as the moisture was absorbed presumably within the trehalose molecular structure. The water within the sample changed from being surface water to becoming bound water. This would be consistent with trehalose crystallisation. In Figure 6.9, NIR spectra between 1900-2000 nm are presented for the same time points as shown in Figure 6.8. The peak at 1932 nm is consistent with bound water in the sample (Zhou et al., 2003). The intensity of the peak increased as more moisture was adsorbed by trehalose. The double peak at day 4 is the peak associated with α,α-dihydrate. The activity data obtained after 1 week of incubation at 75 % RH also follow the trend observed for the crystallisation behaviour of the samples (Table 6.10). The samples containing Tween 20 were the most stable followed by sodium taurocholate and benzalkonium chloride.

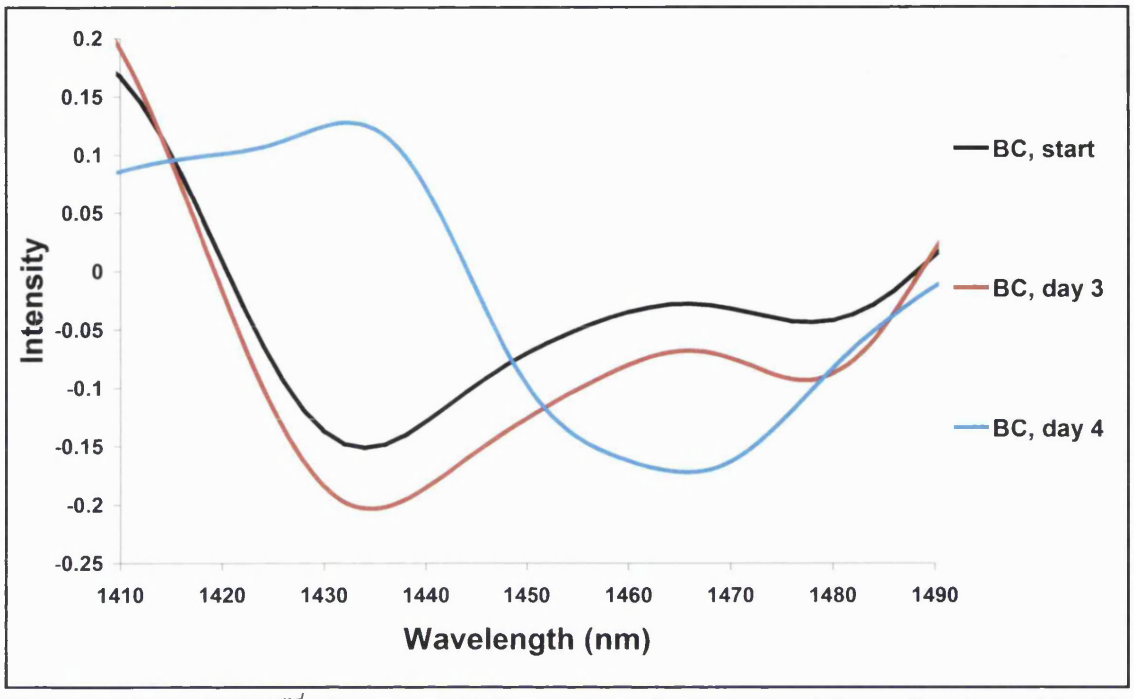

Figure 6.8. *SNV-2nd derivative NIR spectra of spray-dried benzalkonium chloride Sample BC between 1410-1490 nm at different days through incubation at 75 % RH.*

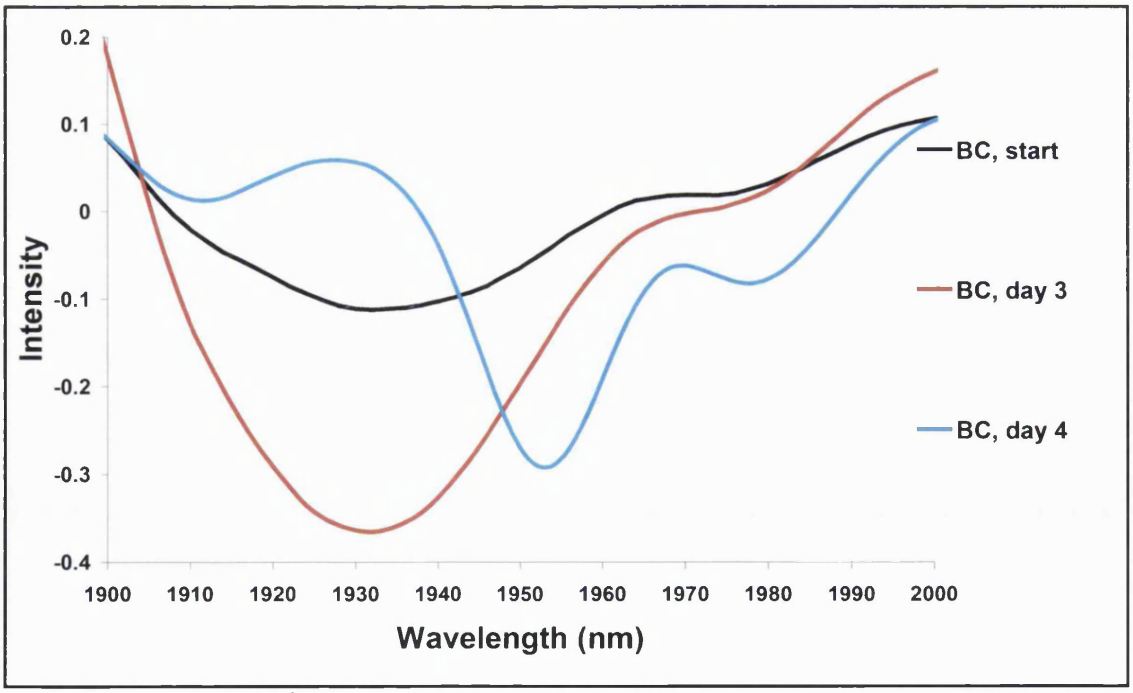

Figure 6.9. *SNV-2nd derivative NIR spectra of spray-dried benzalkonium chloride Sample BC between 1900-2000 nm at different days through incubation at 75 % RH.*

Table 6.8 *Summary of alkaline phosphatase activity in the surfactant/trehalose/AP spray-dried samples exposed to high humidity (75 % RH).*

Sample	AP activity (%) start (S.D.)	AP activity (%) week 1 (S.D.)
unprocessed AP	101.34 (2.17)	65.22 (3.76)
ST	95.34 (1.98)	78.67 (5.88)
STac	86.64 (2.98)	71.32 (5.16)
BC	99.17 (5.67)	66.26 (3.02)
BCac	75.35 (2.57)	58.41 (3.02)
TW	100.55 (3.57)	86.12 (2.54)
TWac	101.11 (4.19)	83.50 (3.88)

After the surfactant/trehalose/AP samples were incubated for a week at 75 % RH, the samples in the glass vials were completely "rock" solid except for Tween 20 samples. Although trehalose in the Tween 20 samples (TW and TWac) had crystallised, which was seen by NIR, the powder was still free flowing. The SEM images taken after 5 weeks of incubation also showed a difference in morphology (Figure 6.10).

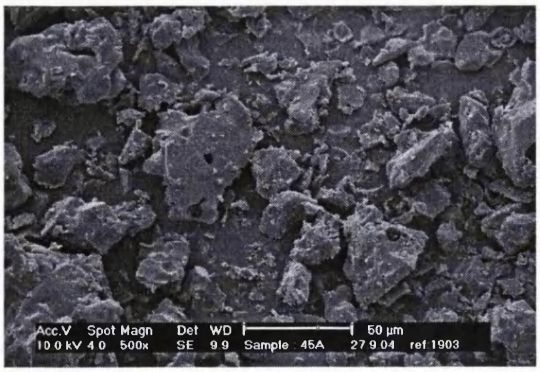

a) Sample BC after 5 weeks of incubation at 75 % RH.

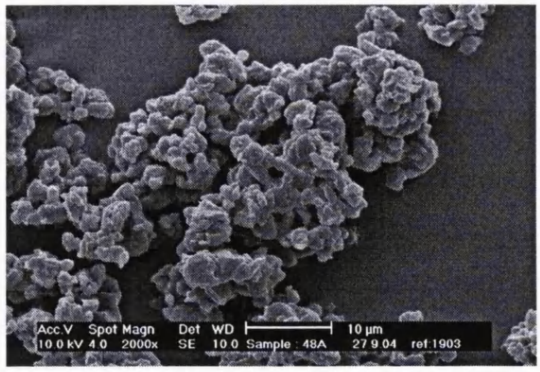

b) Sample TW after 5 weeks of incubation at 75 % RH.

Figure 6.10. *SEM images of Samples BC and TW after 5 weeks of incubation at 75 % RH.*

6.4 CONCLUSIONS

The following conclusions can be made from the data that are in this chapter:

- The addition of surfactants in the trehalose/AP formulations changes the surface properties of the spray-dried particles.

- The anionic surfactant, Tween 20, and the ionic surfactants, sodium taurocholate and benzalkonium chloride, alter the particle surfaces differently.

- Trehalose crystallisation occurs in all of the spray-dried surfactant/trehalose/AP samples but at different rates. Samples containing Tween 20 are most resistant to trehalose crystallisation, followed by sodium taurocholate and benzalkonium chloride. The order of efficacy is seen in glass transitions temperatures as well with benzalkonium chloride samples depressing the Tg value the most, followed by sodium taurocholate and Tween 20.

- Although AP proved to be very stable, the activity data does indicate that the degradation of the protein coincides with the ability of the sample to resist trehalose crystallisation.

CHAPTER 7

Conclusions and further work

7. CONCLUSIONS AND FURTHER WORK

STUDIES ON THE POLYMORPHIC PROPERTIES OF TREHALOSE. These studies were conducted to develop an understanding of the polymorphic forms of α,α-trehalose. These properties are considered important with regards to the biostabilising qualities of trehalose. The α,α-trehalose was subjected to dehydration by differential scanning calorimetry (DSC) at two different heating rates (10 °C/min and 100 °C/min) and sample sizes (1 mg and 5 mg). Three different pathways were assigned to the transformation of α,α-trehalose to β-form (A-C). These routes were dependent on the heating rate and the sample size.

At 10 °C/min the 1 mg samples primarily followed route "B" that transformed the α,α-trehalose to the β-form through the amorphous form. In contrast the 5 mg samples followed route "A", which transformed the α,α-trehalose via the α-anhydrous form. Dehydration at 100 °C/min of 1 mg samples transformed the α,α-trehalose directly to the β-form. This route was termed "C". However the 5 mg samples followed route "A". The data reported here differed from the previous findings as it demonstrated the occurrence of competing pathways. These pathways emerged simultaneously but at varying degrees depending on the heating rate and sample size.

Future work, to build on chapter 3, could be based on studying each of the observed pathways with the aid of near- infrared (NIR) spectroscopy and then comparing the results to other reported forms of trehalose (γ-form, Form II, kappa form, Td etc.). This will determine whether these are "new" forms of trehalose or just an artifact of two combined forms.

PREPARATION AND CHARACTERISATION OF AMORPHOUS TREHALOSE AS A FUNCTION OF PROCESSING. The new SDMicro^{TM} spray dryer was commissioned and evaluated to establish the general procedure and parameters for spray drying trehalose. The different batches of trehalose were prepared and the impact of processing parameters on particle morphology was studied. By

systematically varying the processing parameters it was determined that the solution feed rate was a dominant parameter that influenced all other parameters. This is directly or indirectly affected by all of the processing parameters (inlet and outlet temperature and nozzle and chamber flow). Amorphous trehalose was also prepared successfully using aqueous acetone as processing solutions. Acetone was used as it is miscible in water and is a Class 3 solvent. It was anticipated that by spray drying small batches of solution the yield would be relatively low. However, this was important as small batches of protein formulations had to be prepared due to cost (chapters 5 and 6). Trehalose proved to be very static and as expected large portions of the powder was lost in the spray dryer. It was also anticipated that yields would increase by the addition of a surface-active agent (e.g. protein).

The amorphous trehalose batches prepared form water were subjected to a cycle of dehydration-hydration-dehydration in the dynamic vapour sorption (DVS). NIR spectra were collected during the experiments. The data were compared to the spectra of the different physical forms of trehalose (amorphous, crystalline, α, β and Td). The spectra of forms α, β and Td were provided by Moran (2004). The different physical forms of trehalose were studied with regards to the findings of chapter 3. The gravimetric studies revealed that the moisture retention of the sample had some impact on the water sorption behaviour of the samples. Amorphous trehalose batches with relatively low moisture retention (approximately 2-2.5 %) displayed a weight increase of approximately 10.5 %. This corresponds to the gain of two water molecules of the dihydrate form. In contrast, the amorphous trehalose batches that retained more than approximately 4 % moisture, displayed a smaller weight increase by the end of the hydration stage (75 % RH). This indicated that these samples could be transforming into hydrates. It appeared from the NIR spectra that all batches crystallised to the dihydrate form. This could be established by identifying the diagnostic double peak for trehalose dihydrate at 1954/1980 nm. This confirmed that some of the amorphous trehalose batches transformed into hydrates upon hydration at 75 % RH. These are known as the isomorphic desolvates and are defined as desolvates that retain the structure of there parent solvate form. It could be concluded from the data that the processing parameters have a significant impact on the spray-dried powder characteristics.

Diagnostic peaks for the different physical forms of trehalose were assigned. These were intended to examine the properties of trehalose in the spray-dried alkaline phosphatase formulations. The NIR data of the different amorphous trehalose batches collected during the DVS experiments revealed that the transformation of amorphous trehalose to the crystalline form might occur via a combination of different anhydrous forms (α, β and Td). This confirms the findings of chapter 3 where multiple transformation pathways were shown to occur simultaneously in varying degrees. Future work could be based on trehalose/protein batches spray-dried from different processing parameters and to study their impact on trehalose crystallisation and protein activity.

PREPARATION AND CHARACTERISATION OF TREHALOSE/ALKALINE PHOSPHATASE PARTICLES. The properties of trehalose were further investigated in the presence of alkaline phosphatase (AP). The focus of chapter 5 was on compositions. Different amounts of AP were spray-dried with trehalose from aqueous and aqueous acetone solutions. The dried powders were studied with regards to particle morphology, residual moisture retention, glass transition values and surface properties.

The samples prepared with varying concentrations of AP, indicated the presence of the protein at the surface of the particles was related to the amount of protein in the composition. When spray-dried with large amounts of AP (5 % w/w), raisin-like particles were produced. In contrast the particles prepared from a lower AP content (0.5 % w/w) produced spherical smooth particles. The trehalose/AP samples retained more residual water than amorphous trehalose prepared with the same processing parameters. This subsequently resulted in the decrease of the glass transition temperatures. Surface area measurements revealed a higher surface area for the raisin-like particles compared to the spherical particles. The inverse gas chromatography (IGC) data displayed a high surface energy for samples prepared with a large amount of AP. The surface energy decreased as the amount of AP in the composition was decreased. This coincided with the high surface energy value obtained for unprocessed AP compared to the lower surface value of amorphous trehalose. Hence the data indicated that the raisin-like particles, prepared form 5 % w/w AP, displayed a high surface energy due to the presence of the protein at the surface of the particles.

The trehalose/AP compositions prepared with aqueous acetone displayed changes in the particle morphology. The particles became more spherical and smooth as the amount of acetone in the compositions was increased. This was compared to the trehalose/AP solution prepared from water alone. All of the compositions in this study were prepared with 5 % AP. The protein quantification data revealed that a high amount of acetone (50 % v/v) resulted in a decrease of the AP content in the spray-dried powders. The residual moisture content was similar to the samples spray dried from water alone and this was also true for the glass transitions temperatures. However the moisture removal during TGA occurred at two rates in the samples prepared from aqueous acetone. This indicated that these samples may be crystallising during the thermogravimetric analysis (TGA) experiments. The surface area measurements indicated that the samples prepared from aqueous acetone might be porous as the surface area for these spherical particles was higher than for the raisin-like particles. The IGC data also displayed a decrease in the surface energy due to the presence of acetone in the composition. This indicated that the aqueous acetone particles had less AP at the surface compared to the particles prepared from water alone.

It can be concluded from the data that the trehalose/AP particles can be modified with regards to the localisation of protein in the particles. This could be useful in preparing protein formulations as it has been proposed that the presence of protein at the surface may promote protein degradation. It was anticipated that the AP activity data obtained for the samples could correlate the different surface properties to the stability of the samples. However alkaline phosphatase proved to be a very stable protein and was neither affected by the spray drying process nor by the desiccation at 0 % RH for 10 weeks. AP did degrade in the solutions prepared for spray drying. The degradation was observed in the aqueous acetone solutions, especially when prepared with large amounts of acetone (50 % v/v).

Gravimetric and stability studies conducted on the samples revealed that AP was not affected when desiccated at 50 °C (0 % RH) but the trehalose in the samples crystallised when exposed to high humidity 75 % RH. Even though trehalose was fully crystallised in the samples the AP displayed activity. NIR spectra was recorded and showed the changes in the water regions during dehydration and hydration of the samples. No peak could be assigned for the AP as the spectra were similar to trehalose spectra. The data

were analysed using principal component analysis (PCA) and confirmed that the differences in NIR spectra were concentrated in the water regions and presumably related to trehalose.

For further development of this work it may be useful to spray-dry higher amounts of AP or another protein to study its effect on the crystallisation behaviour of trehalose. AP was chosen as model protein because it is being investigated as a therapeutic protein. The studies so far conducted on the dry solid form of AP have been by freeze drying (Hinrichs et al., 2001). In these studies the dry solids of AP freeze-dried in trehalose showed reduced activity during stability studies. The results obtained by spray drying seems to be very different. However, when choosing another protein to be tested in these compositions it may be interesting to examine a less stable protein. Further work could also include the study the NIR spectra of different proteins. If a protein with a different NIR spectra compared to trehalose is selected the changes in the protein due to trehalose crystallisation can be examined.

THE EFFECTS OF SURFACTANTS IN THE TREHALOSE/ALKALINE PHOSPHATASE PARTICLES. Three different types of surfactants were introduced to the compositions prepared in the previous chapter. relatively high amounts of protein were generally preferred as it was observed in the previous chapter that this composition would result in particles with high protein coverage at the surface. Low concentration of acetone was used as high levels (50 %v/v) induced degradation and precipitation in solution. The surfactants used were the non-ionic surfactant, Tween 20, the anionic surfactant, sodium taurocholate and the cationic surfactant, benzalkonium chloride. The compositions were prepared by dissolving trehalose and surfactant and then adding the protein. The surfactant/trehalsose/AP particles were prepared from water and aqueous acetone.

The SEM images displayed spherical smooth particles for Tween 20 and dimpled particles for the ionic surfactants. The residual moisture content was highest for samples prepared with benzalkonium chloride, followed by sodium taurocholate and then Tween 20. This was reflected in the glass transition temperatures, with benzalkonium chloride displaying the lower glass transition temperature compared to amorphous trehalose. The IGC data also confirmed changes in the surface properties of these particles. The surface

energy was decreased for the particles prepared with ionic surfactants compared to the particles prepared without these surfactants. The data indicate that the coverage of the particle surfaces by the AP is reduced due to the addition of surfactants.

The stability data that was collected by exposing the samples to 75 % RH displayed differences in AP activity. This corresponded to the crystallisation rate of the trehalose in the samples. The samples prepared with the cationic surfactant, benzalkonium chloride, displayed the fastest trehalose crystallisation (4 days). This was identified by the double peak associated with the dihydrate form (1954/1980 nm) in the NIR spectra. The AP activity in the benzalkonium chloride samples also displayed lower AP activity after 1 week of incubation at 75 % RH compared to the other samples. The samples prepared with the anionic surfactant, sodium taurocholate, displayed crystallisation at day 5 and retained more AP activity compared to the benzalkonium chloride samples. The samples prepared with Tween 20, the non-ionic surfactant, were most resistant to trehalose crystallisation and retained the highest levels of AP activity compared to the other surfactant containing samples.

It can be concluded from the data that the surface properties of the AP containing particles can be altered/modified by the addition of surfactants. The physicochemical properties of the surfactant can not only have an impact on the protein stability but also on the crystallisation behaviour of trehalose. The surface properties of the particles also indicate that the protein stability is retained when the protein coverage at the particle surface is minimised. Future work should be performed on a different model protein to investigate the relationship between particle surface properties and protein stability.

GENERAL CONCLUSIONS. The work described in this thesis has shown that both processing parameters and composition influence the properties of the spray-dried particles. AP as a model protein displayed its limitations as it retained activity even when the samples were subjected to extreme conditions. However, the results were encouraging as they indicated a relationship between surface properties and particle characteristics. The surfactant containing samples also pointed towards a correlation between the surface properties and protein activity.

REFERENCES

Adler,M., Unger,M., Lee,G., 2000. Surface Composition of Spray-Dried Particles of Bovine Serum Albumin/Trehalose/Surfactant. Pharmaceutical Research, 17, 863-870.

Akao,K.-I., Okubo,Y., Asakawa,N., Inoue,Y., Sakurai,M., 2001. Infrared spectroscopic study on the properties of the anydrous form II of trehalose. Implications for the functional mechanism of trehalose as a biostabilizer. Carbohydrate Research, 334, 233-241.

Akers,M.J., DeFelippis,M.R., 2000. Peptides and proteins as Parenteral solutions. In: Frokjaer,S., Hovgaard,L. (Eds.), Taylor & Francis, 145-177.

Al Hadithi,D., Buckton,G., Brocchini,S., 2004. Quantification of amorphous content in mixed systems: amorphous trehalose with lactose. Thermochimica Acta, 417, 193-199.

Alamilla-Beltran,L., 2005. Description of morphological changes of particles along spray drying. Journal of Food Engineering, 67, 179-184.

Aldous,B.J., Auffret,A.D., Franks,F., 1995. The crystallisation of hydrates from amorphous carbohydrates. Cryo-letters, 16, 181-186.

Aldridge,P.K., Evans,C.L., Ward,H.W., Colgan,S.T., Boyer,N., Gemperline,P.J., 1996. Near-IR detection of polymorphism and process-related substances. Analytical Chemistry, 68, 997-1002.

Allison,S.D., Randolph,T.W., Manning,M.C., Middleton,K., Davis,A., Capenter,J.F., 1998. Effects of Drying Methods and Additives on Structure and Function of Actin: Mechanisms of Dehydration-Induced Dammage and Its Inhibition. Archives of Biochemistry and Biophysics, 358, 171-181.

Anchordoquy,T.J., Capenter,J.F., 1996. Polymer Protect Lactate Dehydrogenase during Freeze-Drying by Inhibition Dissociation in the Frozen State. Archives of Biochemistry and Biophysics, 332, 231-238.

Angell,C.A., 1995. Formation of Galsses from Liquids and Biopolymers. Science, 267, 1935.

Angell,C.A., 1996. The galss transition. Current Opinion in Solid State & Material Science, 1, 578-585.

Antila,R., 1991. Meausurements of specific surface area of pharmaceutical powders by BET method: effect of drying time and drying temperature. Acta Pharma. Nord., 3, 15-18.

Arakawa,T., Prestrelski,S.J., Kenney,W.C., Capenter,J.F., 2001. Factors affecting short-term and long-term stabilities of proteins. Advanced Drug Delivery Reviews, 46, 307-326.

Bam,N.B., Randolph,T.W., Cleland,J.L., 1995. Stability of protein formulations: investigation of surfactant effects by a novel EPR spectroscopic technique. Pharmaceutical Research, 12, 2-11.

Banga,A.K., 1995a. Pharmaceutical Processing and Handling of Therapeutic Peptides and Proteins. In: Banga,A.K. (Ed.), Technomic publishing company, 131-163.

Banga,A.K., 1995b. Stability of Therapeutic Peptides and Proteins. In: Banga,A.K. (Ed.), Technomic Publishing Company, 61-80.

Banga,A.K., 1995c. Structure and Analysis of therapeutic Peptides and Proteins. In: Banga,A.K. (Ed.), Technomic publishing company, 29-59.

Belton,P.S., Gil,A.M., 1994. IR and raman spectroscopic studies of the interaction of trehalose with hen egg white lysozyme. Biopolymers, 34, 957-961.

Bonner,O.D., Choi,Y.S., 1974. Hydrogen bonding of water in organic solvents. I. The Journal of Physical Chemistry, 78, 1723-1727.

Bos,M.A., 2001. Interfacial rheological properties of adsorbed protein layers and surfactants: a review. Advances in Colloid and Interface Science, 91, 437-471.

Bos,M.A., Nylander,T., Arnebrant,T., Clark,D.D., 1997. Food emulsifiers and their applications. In: Hasenhuettle,G.L., Hartel,R.W. (Eds.), Chapmann and Hall, New York.

Bosquillon,C., Lombry,C., Preat,V., Vabever,R., 2001. Influence of formulation excipients and physical characteristics of inhalation dry powders on their aerosolization performance. Journal of Controlled Release, 70, 329-339.

Brange,J., 2000. Physical Stability of Proteins. In: Frokjaer,S., Hovgaard,L. (Eds.), Taylor & Francis Limited, 89-112.

Brittain,H.G., 1999. Methods for the Characterization of Polymorphs and Solvates. In: Brittain,G.H. (Ed.), Vol. Drugs And The Pharmaceutical Science, Marcel Dekker, Inc., New York-Basel, -278.

Broadhead,J., Rounan,S.K.E., Rhodes,C.T., 1992. The spray drying of pharmaceuticals. Drug Development and Industrial Pharmacy, 18, 1169-1206.

Brown,G.M., 1972. The crystal structure of α,α-trehalose dihydrate from three independent x-ray determination. Acta Crystallography Section B, 28, 3145-3158.

Brunauer,S., Emmet,P.H., Teller,E., 1938. Adsorptopn of gases in multimolecular layers. Journal of American Chemical Society, 60, 309-319.

Buckton,G., Darcy,P., 1995. The use of gravimetric studies to assess the degree of crystallinity of predominantly crystalline powders. International Journal of Pharmaceutics, 123, 265-271.

Buckton,G., Yonemochi,E., Hammond,J., Moffat,A., 1998. The use of near infra-red spectroscopy to detect changes in the form of amorphous and crystalline lactose. International Journal of Pharmaceutics, 168, 231-241.

Buckton,G., Yonemochi,E., Yoon,W.L., Moffat,A.C., 1999. Water sorption and near IR spectroscopy to study the differences between microcrystalline cellulose and silicified microcrystalline cellulose before and after wet granulation. International Journal of Pharmaceutics, 181, 41-47.

Bugay,D.E., 2001. Characterization of the solid-state: Spectroscopic techniques. Advanced Drug Delivery Reviews, 48, 43-65.

Carpenter,J.F., Crowe,J.H., 1989. An infrared spectroscopic study of the interactions of carbohydrates with dried proteins. Biochemistry, 28, 3916-3922.

Carpenter,J.F., Pikal,M.J., Chang,B.S., Randolph,T.W., 1997. Rational Design of Stable Lyophilized Protein Formulations: Some Practical Advice. Pharmaceutical Research, 14, 969-975.

Carpenter,J.F., Prestrelski,S.J., Arakawa,T., 1993. Separation of Freezing- and Drying-Induced Denaturation of Lyophilized Proteins Using Stress-Specific Stabilization
I. Enzyme Activity and Calorimetric Studies. Archives of Biochemistry and Biophysics, 303, 456-464.

Cepeda,E., Villaran,M.C., Aranguiz,N., 1998b. Functional properties of faba bean (Vicia faba) protein flour dried by spray drying and freeze drying
6. Journal of Food Engineering, 36, 303-310.

Cepeda,E., Villaran,M.C., Aranguiz,N., 1998a. Functional properties of faba bean (Vicia faba) protein flour dried by spray drying and freeze drying
6. Journal of Food Engineering, 36, 303-310.

Chang,B.S., Beauvais,R.M., Dong,A., Carpenter,J.F., 1996a. Physical Factors Affecting the Storage Stability of Freeze-Dried Interleukin-1 Receptro Antagonist: Glass Transition and Protein Conformation. Archives of Biochemistry and Biophysics, 331, 249-258.

Chang,B.S., Kendric,B.B., Carpenter,J.F., 1996b. Surface induced denaturation of protein during freezing and its inhibition by surfactants. Journal of Pharmaceutical Sciences, 85, 1325-1330.

Chatterjee,K., Shalaev,E.Y., Suryanarayanan,R., 2005a. Partially crystalline systems in lyophilization: II Withstanding collapse at high primary drying temperatures and impact on protein activity recovery. Journal of Pharmaceutical Sciences, 94, 809-820.

Chatterjee,K., Shalaev,E.Y., Suryanarayanan,R., 2005b. Raffinose crystallisation during freeze-drying and its impact on recovery of protein activity. Pharmaceutical Research, 22, 303-309.

Ciurczak,E.W., 2001. Principles of near infrared spectroscopy. In: Burns,D.A., Ciurczak,E.W. (Eds.), Marcel Dekker, New York, 7-18.

Colaco,C.A.L.S., Smith,C.J.S., Sen,S., Roser,D.H., Newman,Y., Ring,S., Roser,B.J., 1994. Chemistry of Protein Stabilization by Trehalose. Washington DC, 222-240.

Corrigan,O.I., 1995. Thermal analysis of spray dried products. Thermochimica Acta, 248, 245-258.

Costantino,H.R., Curley,J.G., Wu,S., Hsu,C.C., 1998. Water sorption behavior of lyophilized protein-sugar systems and implications for solid-state interactions. International Journal of Pharmaceutics, 166, 211-221.

Coutinho,C., Bernardes,E., Felix,D., Panek,A.D., 1998. Trehalose as cryoprotectant for preservation of yeast strains. Journal of Biotechnology, 7, 23-32.

Craig,D.Q.M., Royall,P.G., Kett,V.L., Hopton,M.L., 1999. The relevance of the amorphous state to pharmaceutical dosage forms: glassy drugs and freeze dried systems. International Journal of Pharmaceutics, 179, 179-207.

Crowe,J.H., 1971. Anhydrobiosis: An Unsolved Problem. The American Naturalist, 105, 563-573.

Crowe,J.H., Carpenter,J.F., Crowe,L.M., 1998. The Role of Vitrification in Anhydrobiosis. Annual Review of Physiology, 60, 73-103.

Crowe,J.H., Carpenter,J.F., Crowe,L.M., Anchordoquy,T.J., 1990. Are freezing and dehydration similar stress vectors? A comparison of modes of interaction of stabilizing solutes with biomolecules. Cryobiology, 27, 219-231.

Crowe,J.H., Crowe,L.M., Carpenter,J.F., 1993a. Preserving Dry Biomaterials: The Water Replacement Hypothesis, Part 1. BioPharm, 28-37.

Crowe,J.H., Crowe,L.M., Carpenter,J.F., 1993b. Preserving Dry Biomaterials: The Water Replacement Hypothesis, Part 2. BioPharm, 40-43.

Crowe,J.H., Hoekstra,F.A., Crowe,L.M., 1992. Anhydrobiosis. Annual Review of Physiology, 54, 579-599.

Crowe,L.M., 2002. Lessons from nature: the role of sugar in anhydrobiosis. Comparative Biochemistry and Physiology, 131A, 505-513.

Crowe,L.M., Mouradian,R., Crowe,J.H., Jackson,S.A., Womersley,C., 1984. Effects of carbohydrates on membrane stability at low water activities. Biochimica et Biophysica Acta, 769, 141-150.

Crowe,L.M., Reid,D.S., Crowe,J.H., 1996. Is trehalose special for preserving dry biomaterials? Biophysical Journal, 71, 2087-2093.

Darcy,P., Buckton,G., 1997. The influence of heating/drying on the crystallisation of amorphous lactose after structural collapse. International Journal of Pharmaceutics, 158, 157-164.

De Boer,J.J., 1953. The dynamic character of adsoprtion. Clarendon Press, Oxford.

DePaz,R.A., Dale,D.A., Barnett,C.C., Carpenter,J.F., Gaertner,A.L., Randolph,T.W., 2002. Effects of drying methods and additives on the structure, function, and storage stability of subtilisin: role of protein conformation and molecular mobility. Enzymes and Microbial Technology, 31, 765-774.

Ding,S.P., Green,F.J.L., Lu,E., Sanchez,E., Angell,C.A., 1996. Vitrification Of Trehalose By Water Loss From Its Crystalline Dihydrate. Journal of Thermal Analysis, 47, 1391-1405.

Dobson,C.M., Hore,P.J., 1998. Kinetic studies of protein folding using NMR spectroscopy. Nature structural biology, 5, 504-507.

Duddu,S.P., Zhang,G., Dal M.,P.R., 1997. The Relationship Between Protein Aggregation and Molecular Mobility Below the Glass Transition Temperature of Lyophilized Formulations Containing a Monoclonal Antibody. Pharmaceutical Research, 14, 596-600.

Elamin,A.A., Sebhatu,T., Ahlneck,C., 1995. The use of amorphous model substances to study mechanically activated materials in the solid state. International Journal of Pharmaceutics, 119, 25-36.

Eriksson,H.J.C., Hinrichs,W.L.J., Veen,B.V., Somsen,G.W., Jong,G.J.d., Frijlink,H.W., 2002. Investigations into the stabilisation of drugs by sugar glasses: I. Tablets prepared from stabilised alkaline phosphatase. International Journal of Pharmaceutics, 249, 59-70.

Eriksson,H.J.C., Verweij,W.R., Poelstra,K., Hinrichs,W.L.J., Jong,G.J.d., Somsen,G.W., Frijlink,H.W., 2003a. Investigation into stabilisation of drugs by sugar glasses: II Delivery of an inulin-stabilised alkaline phosphatase in the intestinal lumen via the oral route. International Journal of Pharmaceutics, 257, 273-281.

Eriksson,H.J.C., Wijngaard,M., Hinrichs,W.L.J., Frijlink,H.W., Somsen,G.W., Jong,G.J.d., 2003b. Potential of capillary electropheresis for the monitoring of the stability of placental alkaline phosphatase. Journal of Pharmaceutical and Biomedical Analysis, 31, 351-357.

Fäldt,P., Bergenstahl,B., 1994. The surface composition of spray-dried protein--lactose powders. Colloids and Surfaces A: Physicochemical and Engineering Aspects, 90, 183-190.

Farid,M., 2003. A new approach to modelling of single droplet drying. Chemical Engineering Science, 58, 2985-2993.

Fitzpatrick,S., 2003. Understanding the physical stability of freeze dried dosage forms the glass transition temperature of the amorphous components. Journal of Pharmaceutical Sciences, 92, 2504-2510.

Forbes,R.T., Davis,K.G., Hindle,M., Clarke,J.G., Maas,J., 1998. Water vapor sorption studies on the physical stability of a series of spray-dried protein/sugar powders for inhalation. Journal of Pharmaceutical Sciences, 87, 1316-1321.

Ford,A.W., Allahiary,Z., 1993a. The Adverse Effect of Glycation of Human Serum Albumin on its Preservative Activity in the Freeze-Drying and Accelerated Degradation of Alkaline Phosphatase. Journal of Pharm. Pharmacol., 45, 900-906.

Ford,A.W., Dawson,P.J., 1993b. The effect of Carbohydrate Additives in the Freeze-Drying of Alkaline Phosphatase. Journal of Pharm. Pharmacol., 45, 86-93.

Fournière,L.d.La., Nosjean,O., Buchet,R., Roux,B., 1995. Thermal and pH stabilities of alkaline phosphatase from bovine intestinal mucosa: a FTIR study. Biochimica et Biophysica Acta, 1248, 186-192.

Fowkes,F.M., 1964. Attractive forces at interfaces. Industrial and Engineering Chemistry, 56, 40-52.

Fowkes,F.M., 1978. Acid-base interactions in polymer adsoprtion. Industrial and Engineering Chemistry, 17, 3-7.

Franks,F., Hatley,R.H.M., 1993. Stable enzymes by water removal. In: W.J.J van den Tweel, A.Harder and R.M.Buitelaar (Eds.), Elsevier Scienc3, The Netherlands, 22-25.

Franks,F., Hatley,R.H.M., Mathias,S.F., 1991. Material Science and the Production of Shelf-Stable Biologicals. Pharmaceutical Technology International, 24-28.

Furuki,T., Kishi,A., Sakurai,M., 2005. De- and rehydration behavior of α,α-trehalose dihydrate under humidity-controlled atmosphere. Carbohydrate Research, 304, 429-438.

Gadd,G.M., Chalmers,K., Reed,R.H., 1987. The role of trehalose in dehydration resistance of *Saccharomyces cerevisiae*. FEMS Microbiology Letters, 48, 249-254.

Giancola,C., De Sena,C., Fessas,D., Graziano,G., Barone,G., 1997. DSC studies on bovine serum albumin denaturation: effects of ionic strength and SDS concentration. Journal of Biological macromolecules, 20, 193-204.

Gil,A.M., Belton,P.S., Felix,V., 1996. Spectroscopic studies of solids α–α trehalose. Spectrochimica Acta Part A, 52, 1649-1659.

Grant,J.W.D., 1999. Theory and Origin of Polymorphism. In: Brittain,G.H. (Ed.), Vol. 95, Marcel Dekker, Inc., New York - Basel, 1-33.

Green,J.L., Angell,A., 1989. Phase relations and vitrification in saccharide-water solutions and the trehalose anomaly. Journal of Physical Chemistry, 93, 2880-2882.

Gutmann,V., 1978. The donor-acceptor approach to molecular interactions. Plenum Press, New York.

Hancock, Shamblin,S.L., 1998. Water vapour sorption by pharmaceutical sugar. Pharmaceutical Science & Technology Today, 1, 345-351.

Hancock, Shamblin,S.L., 2001. Molecular mobility of amorphous pharmaceuticals determined using differential scanning calorimetry. Thermochimica Acta, 380, 95-107.

Hancock,B.C., Parks,M., 2000. What is the true solubility advantage for amorphous pharmaceuticals? Pharmaceutical Research, 17, 397-404.

Hancock,B.C., Shamblin,S.L., Zografi,G., 1995. Molecular Mobility of Amorphous Pharmaceutical Solids Below Their Glass-Transition Temperatures. Pharmaceutical Research, 12, 799-806.

Hancock,B.C., Zografi,G., 1997. Characteristics and Significance of the Amorphous State in Pharmaceutical Systems. Journal of Pharmaceutical Sciences, 86, 1-12.

Hatley,R.H.M., Blair,J.A., 1999. Stabilisation and delivery of labile materials by amorphous carbohydrates and their derivatives. Journal of Molecular Catalysis B: Enzymatic, 7, 11-19.

Hillgren,A., Lindgren,J., Alden,M., 2002. Protection mechanism of Tween 80 during freeze-thawing of a model protein, LDH. International Journal of Pharmaceutics, 237, 57-69.

Hinrichs,W.L.J., Prinsen,M.G., Frijlink,H.W., 2001. Inulin glasse for the stabilization of therapeutic proteins. International Journal of Pharmaceutics, 215, 163-174.

Hogan,S.E., Buckton,G., 2000. The quantification of small degrees of disorder in lactose using solution calorimetry. International Journal of Pharmaceutics, 207, 57-64.

Hogan,S.E., Buckton,G., 2001. Water sorption/desorption-near IR and calorimetric study of crystalline and amorphous raffinose. International Journal of Pharmaceutics, 57-69.

Hohne,G.W.H., Hemminger,W.F., Flammersheim,H.J., 1997. Differential Scannig Calorimetry. Second Ed., In Springer-Verlag, Berlin/Heidelberg/New York.

Holmer,A.F., 2004. Survey: Medicines in development. Pharmaceutical research and manufacturers association.

Hovgaard,L., Skriver,L., Frokjaer,S., 2000. Protein Purification. In: Frokjaer,S., Hovgaard,L. (Eds.), Taylor & Francis Limited, 29-40.

Hsu,C.C., Ward,C.A., Pearlman,R., Nguyen,H.M., Yeung,D.A., Curley,J.G., 1991. Determining the optimum residual moisture in lyophilized protein pharmaceuticals. Development in Biological Standardization, 74, 255-271.

Hussain,A., Arnold,J.J., Khan,M.A., Ahsan,F., 2004. Absorption enhancers in pulmonary protein delivery. Journal of Controlled Release, 94, 15-24.

Izutsu,K.-I., Yoshioka,S., Terao,T., 1994. Effect of Mannitol Crystallinity on the Stabilization of Enzymes during Freeze-Drying. Chemical Pharmaceutical Bulletin, 42, 5-8.

Izutsu,K., Yoshioka,S., Kojima,S., 1995. Increased Stabilizing Effects of Amphiphilic Excipients on Freeze-Drying of Lactate-Dehydrogenase (Ldh) by Dispersion Into Sugar Matrices. Pharmaceutical Research, 12, 838-843.

Jee,R.D., 2004. Near-infrared spectroscopy. In: Moffat,A.C., Osselton,M.D., Widdop,B. (Eds.), Pharmaceutical Press, 346-357.

Johansson,F., 2002. Mechanisms for absorptiopn enhancement of inhaled insultin by sodium taurocholate. European Journal of Pharmaceutical Sciences, 17, 63-71.

Kohn,W.D., Kay,C.M., Hodges,R.S., 1997. Salt effects on protein stability: two-stranded[alpha]-helical coiled-coils containing inter- or intrahelical ion pairs. Journal of Molecular Biology, 267, 1039-1052.

Kuntz,I.D., Kauzmann,W., 1974. Hydration of proteins and polypeptides. Advances in Protein Chemistry, 28, 238-347.

Lane,R.A., Buckton,G., 2000. The novel combination of dynamic vapour sorption gravimetric and near infra-red spectroscopy as a hyphenated technique. International Journal of Pharmaceutics, 207, 49-56.

Langumir,I., 1916. Constitution and fundamental properties of solids and liquids - Part I Solids. Journal of American Chemical Society, 38, 2221-2295.

Langumir,I., 1918. The adsorption of gases on plane surfaces of glass, mica and platinum. Journal of American Chemical Society, 40, 1361-1404.

Levine,H., Slade,L., 1992. Another view of trehalose for drying and stabilizing biological materials. BioPharm, 5, 36-40.

Liao,Y.H., Brown,M.B., Martin,G.P., 2004. Investigation of the stabilisation of freeze-dried lysozyme and the physical properties of the formulations
3. European Journal of Pharmaceutics and Biopharmaceutics, 58, 15-24.

Liapis,A.I., Bruttini,R., 1995. Freeze drying. In: Mujumdar,A.S. (Ed.), Marcel Dekker, Inc., New York, 309-343.

Liu,Y., 1994. Studies on spectra/Structure Correlations in Near-Infrared Spectra of Proteins and Polypeptides. Part 1: A Marker Band for Hydrogen Bonds. Applied Spectroscopy, 48, 1249-1254.

Lopez-Diez,E.C., Bone,S., 2004. The interaction of trypsin with trehalose: an investigation of protein preservation mechanisms. Biochemica et Biophysica acta, 1673, 139-148.

Maa,Y.-F., Costantino,H.R., Nguyen,P.-A., Hsu,C.C., 1997a. The Effect of Operating and Formulation Variables on the Morphology of Spray-Dried Protein Particles. Pharmaceutical Development and Technology, 2, 213-223.

Maa,Y.-F., Nguyen,P.-A., Andya,J.D., Dasovich,N., Hsu,C.C., 1998a. Effect of Spray Drying and Subsequent Processing Conditions on Residual Moisture Content and Physical/Biochemical Stability of Protein Inhalation Powders. Pharmaceutical Research, 15, 768-775.

Maa,Y.-F., Nguyen,P.-A., Sit,K., Hsu,C.C., 1998b. Spray-Drying Performance of a Bench-Top Spray Dryer for Protein Aerosol Powder Preparation. Biotechnology and Bioengineering, 60, 301-309.

Maa,Y.-F., Nguyen,P.-A.T., Hsu,S.W., 1997b. Spray-Drying of Air-Liquid Intrface Sensitive Recombinant Human Growth Hormone. International Journal of Pharmaceutical Science, 87, 152-159.

Maa,Y.-F., Prestrelski,S.J., 2000. Biopharmaceutical Powders: Particle Formation and Formulation Consideration. Current Pharmaceutical Biotechnology, 1, 283-302.

Magnusson,P., Häger,A., Larsson,L., 1995. Serum osteocalcin and bone and liver alkaline phosphatase isoforms in healthy children and adolescents. International pediatric research foundation, 38, 955-961.

Masters,K., 1991. Spray Drying Handbook. Longman, Harlow.

Masters,K., 2002a. Atomization. In: Masters,K. (Ed.), SprayDryConsult International ApS, Copenhagen, 129-179.

Masters,K., 2002b. Atomization, spray-air contact and particle formation. In: Masters,K. (Ed.), SprayDryConsult International ApS, Chalottelund, 129-179.

Masters,K., 2002c. Process Stages and Spray Dryer Systems. In: Masters,K. (Ed.), SprayDryConsult International ApS, Copenhagen, 39-96.

Masters,K., 2002d. Introduction and Historical Background. In: Masters,K. (Ed.), SprayDryConsult International ApS, Copenhagen, 1-16.

Masters,K., 2002e. Spray - air contact, particle formation and drying. In: Masters,K. (Ed.), SprayDryConsult International ApS, Copenhagen, 180-216.

Mazzobre,M.F., Longinotti,M.P., Corti,H.R., Buera,M.P., 2001. Effect of Salts on the Properties of Aqueous Sugar Systems, in Relation to Biomaterial Stabilization. 1. Water Sorption Behavior and Ice Crystallization/Melting. Cryobiology, 43, 199-210.

Miao,S., Roos,Y.H., 2004. Comparison of nonenzymatic browning kinetics in spray-dried and freeze-dried carbohydrate-based food model systems. Journal of Food Science, 69, E322-E331.

Miller,D.P., Anderson,R.E., de Pablo,J.J., 1998. Stabilization of Lactate Dehydrogenase Following Freeze-Thawing and Vacuum-Drying in the Presence of Trehalose and Borate. Pharmaceutical Research, 15, 1215-1221.

Miyazawa,M., Sonoyama,M., 1998. Second derivative near infrared studies on the structural characterisation of proteins. Near Infrared Spectroscopy, 6, A253-A257.

Mohammed,H.A.H., Fell,J.T., 1982. Contact angles of powder mixtures consisting of spherical particles. International Journal of Pharmaceutics, 11, 149-154.

Moran, A. E. Characterisation of spray-dried protein/carbohydarte formulations using gravimetric vapour sorption/near infrared spectroscopy. 2004.
Ref Type: Thesis/Dissertation

Mouradian,R., Womersley,C., Crowe,L.M., Crowe,J.H., 1984. Preservation of functional integrity during long term storage of a biological membrane. Biochimica et Biophysica Acta (BBA) - Biomembranes, 778, 615-617.

Nagase,H., Endo,T., Ueda,H., Nakagaki,M., 2002. An Anhydrous polymorphic form of trehalose. Carbohydrate Research, 337, 167-173.

Nardin,M., Papirer,E., 1990. Relationship between vapour pressure and surface energy of liquids: Application to inverse gas chromatography. Jounal of Colloid and Interface Science, 137, 534-545.

Neale,F.C., Clubb,J.S., Hotchkis,D., Posen,S., 1965. Heat stability of human placental alkaline phosphatase. Journal of clinical pathology, 18, 359-363.

Nyqvist,H., 1983. Saturated salt solutions for maintaining specified relative humidities. International Journal of Pharmaceutical Technology and Products, 4, 47-48.

O'Neil,A.J., Jee,R.D., Moffat,A.C., 1999. Measurement of the cumulative particle size distribution of microcrystalline cellulose using near infrared reflectance spectroscopy. Analyst, 124, 33-36.

Pace,C.N., Vajdos,F., Fee,L., Grimslet,G., Gray,T., 1995. How to measure and predict the molar absorption coefficient of a protein. The Protein Society, 4, 2411-2423.

Pakowski,Z., Mujumdar,A.S., 1995. Drying of pharmaceutical products. In: Mujumdar,A.S. (Ed.), Marcel Dekker, Inc., New York, 743-773.

Papirer,E., Balard,H., Vidal,A., 1988. Inverse gas chromatography: a valuable method for the surface characterisation of fillers for polymers (glass fibers and silicas). European Polymer Journal, 24, 783-790.

Pijpers,T.F.J., Mathot,V.B.F., Goderis,B., Scherrenberg,R.L., Vegte,E.W.V.D., 2002. High-Speed Calorimetry for the Study of the Kintetics of (De)vitrification, Crystallisation, And Melting of Macromolecules. Macromolecules, 35, 3601-3613.

Poelstra,K., Bakker,W.W., Klok,P.A., Hardonk,M.J., Meijer,D.K.F., 1997a. A Physiologic Function for Alkaline Phosphatase: Endotoxin Detoxification. Laboratory Investigation, 76, 319-327.

Poelstra,K., Bakker,W.W., Klok,P.A., Kamps,J.A.A.M., Hardonk,M.J., Meijer,D.K.F., 1997b. Dephosphorylation of Endotoxin by Alkaline Phosphatase in Vivo. American Journal of Pathology, 151, 1163-1169.

Prestrelski,S.J., Arakawa,T., Capenter,J.F., 1993a. Separation of Freezing- and Drying-Induced Denaturation of Lyophilized Proteins Using Stress-Specific Stabilization
II. Structural Studies Using Infrared Spectroscopy. Archives of Biochemistry and Biophysics, 303, 465-473.

Prestrelski,S.J., Pikal,K.A., Arakawa,T., 1995. Optimization of Lyophilization Conditions of Recombinant Human Interleukin-2 by Dried-State Conformational

Analysis Using Fourier-Transform Infrared Spectroscopy. Pharmaceutical Research, 12, 1250-1259.

Prestrelski,S.J., Tedeschi,N., Arakawa,T., Capenter,J.F., 1993b. Dehydration-induced Conformational Tranistions in Proteins and their Inhibition by Stabilizers. Biophysical Journal, 65, 661-671.

Reisener,H.J., Goldschmid,H.R., Ledingham,G.A., Perlin,S.A., 1962. Formation Of Trehalose And Polyols By Wheat Stem Rust (Puccinia Graminis Tritici) Uredospores. Canadian Journal Of Biochemsitry And Physiology, 40, 1248-1251.

Rigg,B.M., Baird,C.W., 1965. Association of intravenous albumin with alkaline phosphatase activity. Journal of clinical pathology, 18, 441-442.

Robert,P., Devaux,M.F., Mouhous,N., Dufour,E., 1999. Monitoring the secondary structure of proteins by near-infrared spectroscopy. Applied Spectroscopy, 53, 226-232.

Roos,Y., 1993. Melting and glass transition of low molecular weight carbohydrates. Carbohydrate Research, 238, 39-48.

Roos,Y.H., 2002. Importance of glass transition and water activity to spray drying and stability of dairy powders. Lait, 82, 475-484.

Roser,B., 1991. Trehalose, a new approach to premium dried foods. Trends in Food Science & Technology, 2, 166-169.

Sadler,A.J., Horsch,J.G., Lawson,E.Q., Harmatz,D., Brandau,D.T., Middaugh,C.R., 1984. Near-infrared photoacoustic spectroscopy of proteins. Analytical Biochemistry, 138, 44-51.

Saleki-Gerhardt,A., Ahlneck,C., Zografi,G., 1994a. Assessment of disorder in crystalline solids. International Journal of Pharmaceutics, 101, 237-247.

Saleki-Gerhardt,A., Stowell,J.G., Byrn,S.R., Zografi,G., 1995. Hydration and dehydration of crystalline and amorphous froms of raffinose. Journal of Pharmaceutical Sciences, 84, 318-323.

Saleki-Gerhardt,A., Zografi,G., 1994b. Non-Isothermal and Isothermal Crystallization of Sucrose from the Amorphous State. Pharmaceutical Research, 11, 1166-1173.

Sarciaux,J.-M.E., Hageman,M., 1997. Effects of bovine somatotropin (rbSt) concentration at different moisture levels on the physical stability of sucrose in freeze-dried rbSt/sucrose mixtures. Journal of Pharmaceutical Sciences, 86, 365-371.

Saunders,M., Podluii,K., Shergill,S., Buckton,G., Royall,P., 2004. The potential of high speed DSC (Hyper-DSC) for the detection and quantification of small amounts of

amorphous content in predominantly crystalline samples. International Journal of Pharmaceutics, 274, 35-40.

Schoenau,E., Herzog,K.H., Boehles,H.-J., 1986. Liquid-chromatographic determination of isoenzymes of alkaline phosphatase in serum and tissue homogenates. Clinical chemistry, 32, 816-818.

Schultz,J., Lavielle,L., Martin,C., 1987. The role of the interface in carbon fibre-epoxy composites. Journal of Adhesion, 23, 45-60.

Seville,P.C., Kellaway,I.W., Birchall,J.C., 2002. Preparation of dry powder dispersions for non-viral gene delivery by freeze-drying and spray-drying. The Journal of Gene Medicine, 4, 428-437.

Shafizadeh,F., Susott,R.A., 1973. Crystalline Transitions of Carbohydrates. Journal of Organic Chemistry, 38, 3710-3715.

Shamblin,S.L., Hancock,B.C., Zografi,G., 1998. Water vapor sorption by peptides, proteins and their formulations. European Journal of Pharmaceutics and Biopharmaceutics, 45, 239-247.

Shenk,J.S., 1993. Application of NIR spectroscopy to agriculture products. 383-431.

Sing,K., Everett,D., Haul,R., Moscou,L., Pierotti,R., Rouquerol,J., Siemieniewska,T., 1985. Reporting physiosorption data gas/solid systems with special reference to the determination of surface area and porosity. Pure Applied Chemistry, 57, 603-609.

Smith,P.K., Krohn,R.I., Hermanson,G.T., Mallia,A.K., Gartner,F.H., Provenzano,M.D., Fujimoto,E.K., Goeke,N.M., Olson,B.J., Klenk,D.C., 1985. Measurement of protein using bicinchoninic acid. Analytical Biochemistry, 150, 76-85.

Souillac,P.O., Constantino,H.R., Middaugh,C.R., Rytting,J.H., 2002. Investigation of Protein/Carbohydrate Interactions in the Dried State. 1. Calorimetric Studies. Journal of Pharmaceutical Sciences, 91, 206-216.

Stephenson,G.A., Groleau,E.G., Kleeman,R.L., Xu,W., Rigsbee,D.R., 1998. Formation of isomrphic desolvates: Creating a molecular vacuum. Journal of Pharmaceutical Sciences, 87, 536-542.

Streefland,L., Auffret,A.D., Franks,F., 1998. Bond Cleavage Reactions in Solid Aqueous Carbohydrate Solutions. Pharmaceutical Research, 15, 843-849.

Subramanian,S., Fisher,H.F., 1972. Detection of polar side-chain hydration in polypeptides by near-infrared spectroscopy. Biopolymers, **11**, 1305-1310.

Sun,W.Q., Davidson,P., 1998. Protein inactivation in amorphous sucrose and trehalose matrices: effects of phase separation and crystallization. Biochimica et Biophysica Acta, 1425, 235-244.

Sussich,F., Bortoluzzi,S., Cesaro,A., 2002. Trehalose dehydration under confined conditions. Thermochimica Acta, 391, 137-150.

Sussich,F., Cesaro,A., 2000. Transitions and Phenomenology of α,α - Trehalose Polymorphs Inter-Conversion. Journal of Thermal Analysis and Calorimetry, 62, 757-768.

Sussich,F., Princivalle,F., Cesaro,A., 1999. The interplay of the rate of water removal in the dehydration of α,α–trehalose. Carbohydrate Research, 322, 113-119.

Sussich,F., Skopec,C., Brady,J., Cesaro,A., 2001. Reversibel dehydration of trehalose and anhydrobiosis: from solution state to an exotic crystal? Carbohydrate Research, 334, 165-176.

Sussich,F., Urbani,R., Cesaro,A., 1997. New crystalline and amorphous froms of trehalose. Carbohydrate Letters, 2, 403-408.

Sussich,F., Urbani,R., Princivalle,F., Cesaro,A., 1998. Polymorphic Amorphous and Crystalline Forms of Trehalose. Journal of The American Chemical Society, 120, 7893-7899.

Taga,T., Senma,M., Osaki,K., 1972. The crystal and molecular structure of trehalose dihydrate. Acta Crystallography Section B, 28, 3258-3263.

Tanaka,K., Takeda,T., Miyajima,K., 1991. Cryoprotective Effect of Saccharides on Denaturation of Catalase by Freeze-Drying. Chemical & Pharmaceutical bulleitin, 39, 1091-1094.

Taylor,L.S., Williams,A.C., York,P., 1998a. Particle Size Dependent Molecular Rearrangement During the Dehydration of Trehalose Dihydrate- In Situ FT-Raman Spectroscopy. Pharmaceutical Research, 15, 1207-1214.

Taylor,L.S., York,P., 1998b. Characterization of the Phase Transitions of Trehalose Dihydrate on Heating and Subsequent Dehydration. Journal of Pharmaceutical Sciences, 87, 347-355.

Taylor,L.S., York,P., 1998c. Effect of particle size and temperature on the dehydration kinetics of trehalose dihydrate. International Journal of Pharmaceutics, 167, 215-221.

Ticehurst,M.D., York,P., Rowe,R.C., Dwivedi,S.K., 1996. Characterisation of the surface properties of [alpha]-lactose monohydrate with inverse gas chromatography, used to detect batch variation. International Journal of Pharmaceutics, 141, 93-99.

Timasheff,S.N., 1992. Water as Ligand: Preferential Binding and Exclusion of Denaturants in Protein Unfolding. Biochemistry, 31, 9857-9864.

Troung,V., 2005. Optimization of co-current spray drying process of sugar-rich foods. Part I - Moisture and glass transition temperature profile during drying. Journal of Food Engineering, 71, 66-72.

Tzannis,S.T., Prestrelski,S.J., 1999a. Activity-stability considerations of trypsinogen during spray drying: Effects of sucrose. Journal of Pharmaceutical Sciences, 88, 351-359.

Tzannis,S.T., Prestrelski,S.J., 1999b. Moisture effects on protein-excipient interaction in spray-dried powders. Nature of destabilizing effects of sucrose. Journal of Pharmaceutical Sciences, 88, 360-370.

Vandermeulen,D.L., Ressler,N., 1980a. A near-infrared method for studying hydrtaion changes in aqueous solution: Illustration with protease reactions and protein deanturation. Archives of Biochemistry and Biophysics, 205, 180-190.

Vandermeulen,D.L., Ressler,N., 1980b. Near-Infrared Analysis of Water-Macromolecule Interactions: Hydration and the Spectra of Aqueous Solutions of Intact Proteins. Archives of Biochemistry and Biophysics, 199, 197-205.

Vippagunta,S.R., Brittain,H.G., Grant,D.J.W., 2001. Crystalline solids. Advanced Drug Delivery Reviews, 48, 3-26.

Vogel,R., 2004. Influence of salts on rhodopsin photoproduct equilibria and protein stability. Current Opinion in Colloid & Interface Science, 9, 133-138.

Vora,K.L., Buckton,G., Clapham,D., 2004. The use of dynamic vapour sorption and near infra-red spectroscopy (DVS-NIR) to study the crystal transitions of theophylline and the report of a new solid-state transition. European Journal of Pharmaceutical Sciences, 22, 97-105.

Walter,K., Schutt,C., 1974. Methods of enzymatic analysis. In: Bergmeyer,H.U. (Ed.), Academic Press, New York, 860-864.

Walton,D.E., Mumford,C.J., 1999. The Morphology of Spray-Dried Particles, The Effect of Process Variables upon the Morphology of Spray-dried Particles. Trans IChemE, 77, 442-460.

Wang,J., Sowa,M.G., Ahmed,M.K., Mantsch,H.H., 1994. Photoacoustic near-infrared of homo-polypeptides. Journal of Physical Chemistry, 98, 4748-4755.

Wang,W., 1999. Instability, stabilization, and formulation of liquid protein pharmaceuticals. International Journal of Pharmaceutics, 185, 129-188.

Wang,W., 2000. Lyophilization and development of solid protein pharmaceuticals. International Journal of Pharmaceutics, 203, 1-60.

Williams,D.R., Levoguer,C.L., 1991. Inverse gas chromatography of solid surfaces. Chromatography and Analysis, Feb, 9-11.

Yoshioka,M., Hancock,B.C., Zografi,G., 1994. Crystallization of Indomethacin from the Amorphous State Below and Above Its Glass-Transition Temperature. Journal of Pharmaceutical Sciences, 83, 1700-1705.

Yoshioka,M., Hancock,B.C., Zografi,G., 1995. Inhibition of Indomethacin Crystallization in Poly(Vinylpyrrolidone) Coprecipitates. Journal of Pharmaceutical Sciences, 84, 983-986.

Yu,L., 2001. Amorphous pharmaceutical solids: preparation, characterization and stabilization. Advanced Drug Delivery Reviews, 48, 27-42.

Zhou,G.X., Ge,Z., Dorwart,J., Izzo,B., Kukura,J., Bicker,G., Wyvratt,J., 2003. Determination and Differentiation of Surfaces and Bound Water in Drug Substances by Near Infrared Spectroscopy. Journal of Pharmaceutical Sciences, 92, 1058-1065.